GEOLOGICAL AND GEOCHEMICAL INVESTIGATION OF THE PETROLEUM SYSTEMS OF THE PERMIAN BASIN OF WEST TEXAS AND SOUTHEAST NEW MEXICO

A Dissertation Presented to
the Faculty of the
Department of Earth and Atmospheric Sciences
University of Houston

In Partial Fulfillment
of the Requirements for the Degree
Doctor of Philosophy

By

Simon Echegu

August 2013

GEOLOGICAL AND GEOCHEMICAL INVESTIGATION OF THE PETROLEUM SYSTEMS OF THE PERMIAN BASIN OF WEST TEXAS AND SOUTHEAST NEW MEXICO

_____

Simon Echegu

APPROVED:

_____

Dr. K. K. (Adry) Bissada, Chairman

_____

Dr. Henry Chafetz

_____

Dr. Regina Capuano

_____

Dr. Louis Elrod

_____

Dr. Dan E. Wells, Dean, College of Natural Sciences and Mathematics

ACKNOWLEDGEMENTS

Special thanks go to Dr. K. K. (Adry) Bissada, PhD Committee Chairman/Advisor for accepting to work with me and allowing me use the laboratory facilities at no cost to me. His guidance throughout this endeavor is highly appreciated. Special thanks also go to my PhD Committee members for their assistance, both at Committee and individual level. Dr. Elrod is especially thanked for being critical on the manuscripts submitted to the AAPG Bulletin.

I would also like to thank Mr. Mike Darnell and Ms. Ewa Szymczyk for introducing me to analytical equipment that I used to undertake analytical work that generated data for this dissertation. Like Dr. Bissada, Mike and Ewa became my good parents.

Special thanks go to my dear wife, Patricia, for always encouraging me at times when I was almost falling apart and most importantly for singlehandedly taking care of the children during the period of this work.

This study was made possible by the scholarship provided by the Fulbright Foundation, through the Fulbright Science and Technology Award. I owe special appreciation to Mr. Vincent Pickett of Department of State (DoS) for coordinating funding and all related administrative work. I would also like to thank Ms. Megan Spillman, Ms. Lori Reynolds, and Ms. Sarah Boeving for administering the Fulbright Science and Technology Award on behalf of the DoS.

I dedicate this work to my beloved children: John, Simon, Maria, and Daniel, and to my father, Mzee Ogoda, a passionate believer in education, who, despite having not entered any classroom in his life time, struggled to see me go to school against all odds.

GEOLOGICAL AND GEOCHEMICAL INVESTIGATION OF THE PETROLEUM SYSTEMS OF THE PERMIAN BASIN OF WEST TEXAS AND SOUTHEAST NEW MEXICO

An Abstract of a Dissertation Presented to
the Faculty of the
Department of Earth and Atmospheric Sciences
University of Houston

In Partial Fulfillment
of the Requirements for the Degree
Doctor of Philosophy

By

Simon Echegu

August 2013

ABSTRACT

Fifty (50) crude oils and nineteen (19) source rock samples from strata ranging in age from Ordovician to Middle Permian, and distributed widely over the Permian Basin, were studied geochemically and chemometrically to identify the petroleum systems within the greater Permian Basin. Variations in the stable carbon isotope and biomarker compositions of the oils, together with chemometric correlations of oils and source rocks, revealed the existence of at least five petroleum systems, involving organic-rich, type II-II/III source rocks of the Simpson Group Shale, the Woodford Shale, the Barnett Shale, the Wolfcamp Shale, and the Bone Spring Marls. The Spraberry source rock is mostly immature with respect to petroleum generation. Geochemical evidence strongly suggests source-rock deposition under suboxic and anoxic-suboxic conditions for all but the Bone Spring and Simpson source beds, in which case the geochemical evidence suggests deposition under anoxic conditions.

Geochemical thermal modeling indicates adequate to advanced maturity for all the source rocks, except for the Spraberry, which is barely entering into the optimum maturation window near the southern end of the Midland Basin. Generation and expulsion from the Wolfcamp Shale begun in Early Triassic, with hydrocarbons migrating laterally, and getting trapped within carbonate aprons encased within the shales of the same stratigraphic age in slope and basinal areas in both the Midland and Delaware basins. Expulsion from the Barnett Shale occurred during Early to Mid-Permian. Migration occurred radially updip from the two depocenters in the Delaware and Midland basins to Pennsylvanian sandstone reservoirs in the Eastern Shelf and Permian carbonate reservoirs

in the Central Basin Platform and the Northwest Shelf. The Woodford shale began expelling petroleum during Early to Late Permian. Migration occurred along vertical pathways to underlying Devonian through Ordovician reservoirs. Expulsion from the Simpson occurred during Early Triassic. Migration followed vertical pathways downwards to Simpson sandstones and Ellenberger carbonates. For all the petroleum systems, traps formed well in advance of generation and expulsion. The petroleum systems are segregated with very limited cross-stratigraphic migration because of alternating reservoir-seal (source rock) facies. This study has established a detailed understanding of the petroleum systems in the Permian Basin and documented the geographic and stratigraphic framework for the inter-relationships between the crude oils and their most likely source rocks in the Permian.

Table of Contents

List of Figures

List of Tables

1.0 GENERAL INTRODUCTION

The Permian Basin of West Texas and Southeastern New Mexico is one of the most prolific petroleum provinces in the United States. It is structurally defined by the Matador Arch to the north, the Marathon-Ouachita Fold belt to the south, the Diablo Platform to the west and the Eastern shelf to the east (Figure 1.1). During its 90+ years exploration history, it has supplied over 35 billion barrels (Bbbl) of oil out of its stock tank original oil in place (STOOIP) of 105 Bbbl (Tyler and Banta, 1989), and several trillion cubic feet of gas, mainly from conventional plays (e.g. Galloway et al., 1983; Dutton et al., 2004; 2005).

In spite of the long production history, the petroleum systems of the Permian Basin remain poorly constrained. The current poor understanding of the Permian Basin petroleum systems is largely due to inadequate geochemical investigation, as most studies have mainly focused on traps/plays, ignoring the shared risk factor, the source rock(s). Stressing the importance of play analysis, Dutton et al. (2004; 2005) urged that exploitation methods which have been proven to be effective in one play set can also be extended to plays of similar type elsewhere. This approach, however, limits other creative ideas on other potential play types (Peters et al., 2005). Demaison and Huizinga (1991) emphasized that volumes of hydrocarbons actually trapped depend on key elements including source, reservoir, and seal rock, and adequate generation, migration, and accumulation factors such as entrapment. This recognition is the backbone to the development and successful utility of the petroleum system as an exploration concept.

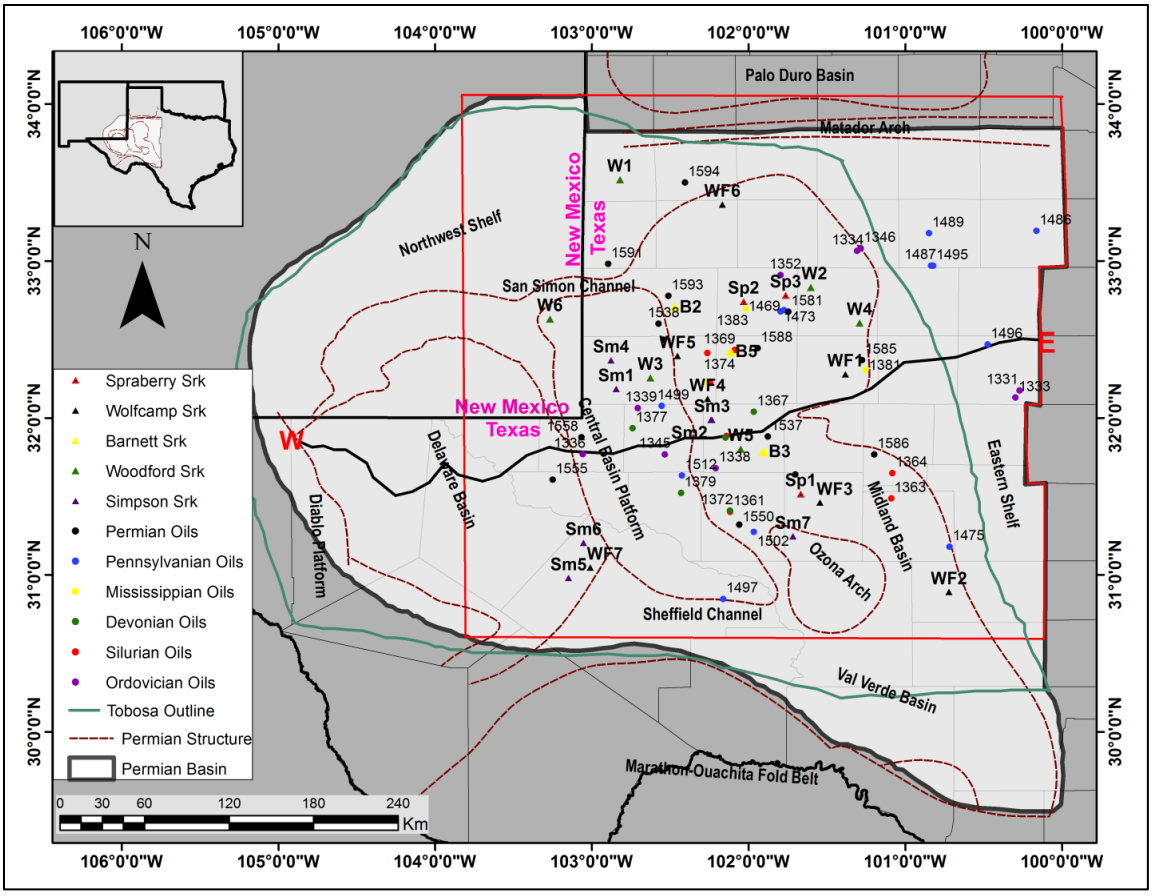

Figure 1.1: Map of the Permian Basin highlighting the study area (red outline) and structural features, and locations of oil and source rock samples used in the study. Base map from Dutton et al. (2004) and Tobosa outline from Frenzel et al. (1988). Srk is an abbreviation for source rock.

Although production has been declining since the late 1970s, the current trend of increasing activity in the Permian Basin, as reflected by the increasing number of operators and new drilling permits as published on the Texas Railroad Commission (Railroad Commission, 2012) website, emphasizes the renewed importance of this petroleum province. A study conducted by the USGS in 2007 (Schenk et al., 2008), indicates that at least 1.3 billion barrels of oil and up to 41 trillion cubic feet (tcf) of natural gas, representing both conventional and continuous (unconventional) gas, remain undiscovered in the Permian Basin. This is an enormous resource by any standard.

Despite the poor understanding of the petroleum systems in this area, the large hydrocarbon endowment suggests the operation of very efficient petroleum system processes such as supercharging, lateral drainage, and high impedance entrapment as described in Demaison and Huizinga (1991). The endowment also suggests parallelism with extremely high quality source rocks and high expulsion and migration efficiencies, as typically observed in source rock-reservoir associated systems. These projections can only be confirmed through geochemical analysis of oils or source rocks where available.

Geochemical analytical data for oils and source rocks are a weak link in the complete understanding of the petroleum systems in the Permian Basin. Even where geochemical analyses have been done on source rocks, such as for the Woodford Shale (e.g. Comer, 1991) and the Barnett Shale (e.g. Kinley, 2008), only screening data are usually available. Although these types of data are adequate enough to confirm a source rock, it is not amenable to oil-source rock correlations, thus cannot identify or define a petroleum system. Although source rocks are known in the Permian Basin, as summarized in Jarvie and Hill (2011), no concerted attempt has been made to put these source rocks in the geological context that allows for determination of stratigraphic and geographic relations with their oils. A few of the Permian Basin petroleum systems reported in the literature are generalized national-grid mentions (e.g. Magoon, 1988a, 1988b, 1992), while others are abstracts (Pawlewicz and Mitchell, 2006; Dow et al., 1990; Jarvie et al., 2001; Corby and Cook, 2003; Hill et al., 2004; Jarvie and Hill, 2011), which only give insight no comprehensive evaluations or detailed discussions, however, can be made, as most of them are either based on geochemistry or modeling independently without the required

integration. A comprehensive petroleum system study by Katz et al. (1994) only covers one petroleum system (the Simpson-Ellenberger) in the Permian Basin.

As discussed by Peters and Cassa (1994), a better understanding of prospects is incomplete without an understanding of types and distribution of effective source rocks and hence the geographic extent of petroleum systems (Magoon and Dow, 1994). The poor understanding of petroleum systems in the Permian Basin provided the impetus to undertake this project with the idea that, understanding the intrinsic geological and geochemical attributes of the petroleum systems of this prolific basin would help: (1) aid exploration in analogous basins by invoking its expulsion/generation and migration models, (2) provide an opportunity to compare and potentially calibrate geochemical data with geological observations, and (3) provide a review of the existing petroleum systems models and develop alternative models for generation, expulsion, and migration in the area.

1.1. The Petroleum System Concept

A petroleum system is a natural geologic system that encompasses a pod of active source rock and all related petroleum and includes all the essential elements and processes necessary for a petroleum accumulation to exist (Magoon and Dow, 1994). Essential geological elements include the source rock, overburden, reservoir rock, migration route, traps, and seals. For a petroleum system to exist, these elements and accompanied processes must be placed in a sequence that allows for an oil/gas accumulation to exist.

Magoon and Beaumont (1999) provide an approach and requirements for defining a petroleum system. The approach essentially includes an identification of elements: source rock, reservoir rock, seal, and overburden rock, and the process of trap formation, generation, migration, and accumulation of hydrocarbons. Of critical importance is the formation of traps prior generation and expulsion of hydrocarbons; otherwise, hydrocarbons will be lost. According to Magoon and Beaumont (1999), a well-defined petroleum system comprises the name of the source rock followed by a hyphen and the principal reservoir formation followed by symbols in parenthesis indicating the degree of certainty of the geochemical correlation; (?), (.) and (!) representing speculative, hypothetical and known genetic relationships, respectively. The exploration advantage of petroleum system studies is its ability to reveal untapped potential in the form of bypassed or unconventional resources (Peters et al., 2013), thus an essential concept in basins considered mature for exploration, such as the Permian Basin.

1.2 The Conceptual Model

As shown above, a source rock is a shared risk factor, whose availability or absence dictates the availability of hydrocarbons in traps. Apart from providing a source of hydrocarbons to the migration route and therefore traps, the source rock, especially its quality and level of thermal maturity plays an important role in determining how reservoirs will actually be charged by controlling expulsion and migration (e.g. Cooles et al, 1986; Quigley et al., 1987; Leythaeuser et al., 1987; Mackenzie and Quigley, 1988; Mackenzie and Quigley, 1988; Leythaeuser et al, 1984; 1987). Expulsion is an important aspect of petroleum system development as it controls how much is expelled by a source

rock, and therefore how much is available for secondary migration, the latter efficient in short migration scenarios as losses are minimized (e,g. Magoon and Valin, 1994; England, 1994).

Despite the potential effects of source rock permeability on expulsion efficiency (Burrus et al., 1993), several geochemical investigations and discussions on expulsion efficiency of source rocks (e.g. Leythaeuser et al, 1984; Cooles et al, 1986; Quigley et al., 1987; Leythaeuser et al., 1987; Mackenzie and Quigley, 1988) indicate a strong relationship between source rock type and expulsion efficiency, with high quality source rocks being generally more efficient than their poorer quality counterparts. The level of thermal maturity and the mechanism of primary migration also exert a strong impact on the expulsion efficiency (e.g. Leythaeuser et al., 1984; 1987). Most workers note in general, that expulsion efficiency depends on initial generation potential; with type I higher, that type II which in turn is higher than type III.

It is hypothesized that, in the Permian Basin, multiple high quality (type II marine) source rocks matured, generated, and expelled hydrocarbons at various times, getting trapped in reservoirs that define short migration distances from candidate source rocks. The adequately mature high quality source rocks are responsible for the rich hydrocarbon endowment because of their favorable generation and expulsion kinetics, with attendant positive impacts on expulsion and migration efficiencies. Generation and expulsion from these source rocks was favorably synchronized with trap formation in such a way that the latter formed well in advance of the former.

1.3 Principal Objectives

The principal objectives include: (1) identify genetically related oils and reconstruct the nature of the depositional environments and organic matter type of their source rocks, (2) characterize the nature, quality, and maturity of potential source rocks in the Permian Basin and undertake correlation of oils to source rocks in order to establish petroleum systems, (3) develop petroleum generation and expulsion models for all identified petroleum systems and put in the timing context that defines probability of entrapment and accumulation and preservation, and (4) map the geographic and stratigraphic extents of the active petroleum systems in Permian Basin to establish a stratigraphic relationship between oils (reservoirs) and their source rocks as a basis to infer migration pathways.

1.4 Project Scope

The project area includes the areas geographically in the eastern Delaware Basin, the Central Basin Platfrom, the Midland Basin and the Eastern Shelf (Figure 1.1). Stratigraphically, the study covers the Cambrian to Lower section of the Upper Permian.

The investigations contains the following components: (1) oil-oil correlations and geochemical inversion, (2) oil-source rock correlations, (3) burial and thermal history modeling, (4) source rock volumetric modeling, (5) petroleum systems maps, (5) petroleum systems events charts, including the critical moment, and (6) an overall petroleum system cross-section for all petroleum systems.

1.5 General Geological Overview- Development of the Permian Basin

1.5.1 General

The structural and stratigraphic development of the Permian Basin is well described in the literature (e.g. Galley, 1958; Adams, 1965; Wright, 1979; Hills, 1984; Hills and Galley, 1988; and Frenzel et al., 1988). An overview is presented below. The generalized west-east cross-section, the tectonic history and stratigraphy are summarized in Figures 1.2, 1.3, 1.4, and 1.5 respectively.

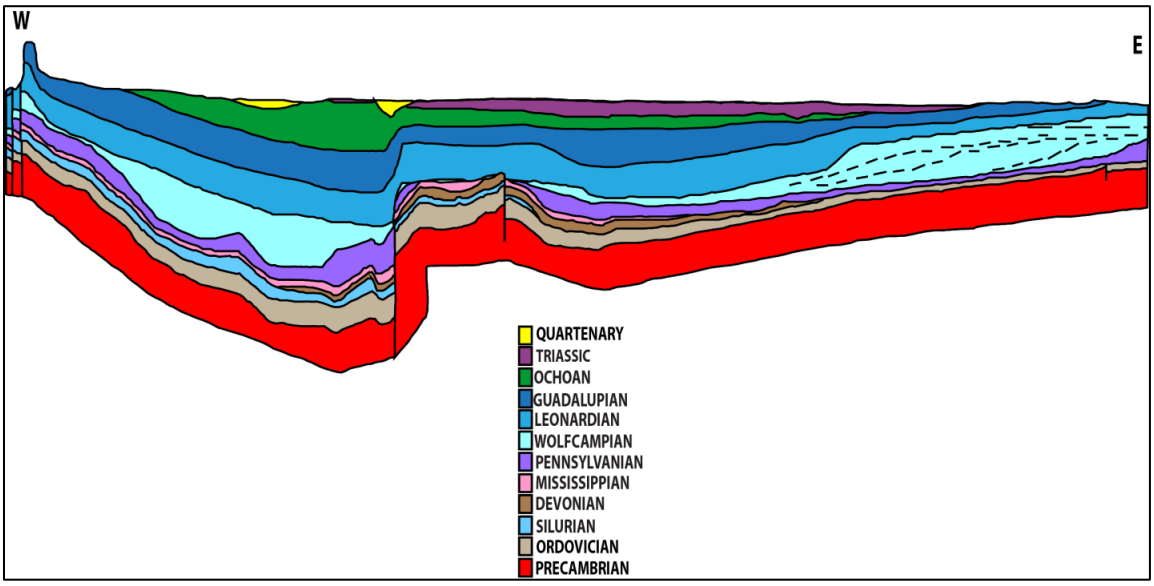

Figure 1.2: Generalized west-east cross-section through the Permian Basin (line of section in Figure 1.1). The Permian Basin achieved this shape by Early Permian. (Redrawn from Lindsay 2012; after Matchus and Jones, 1984).

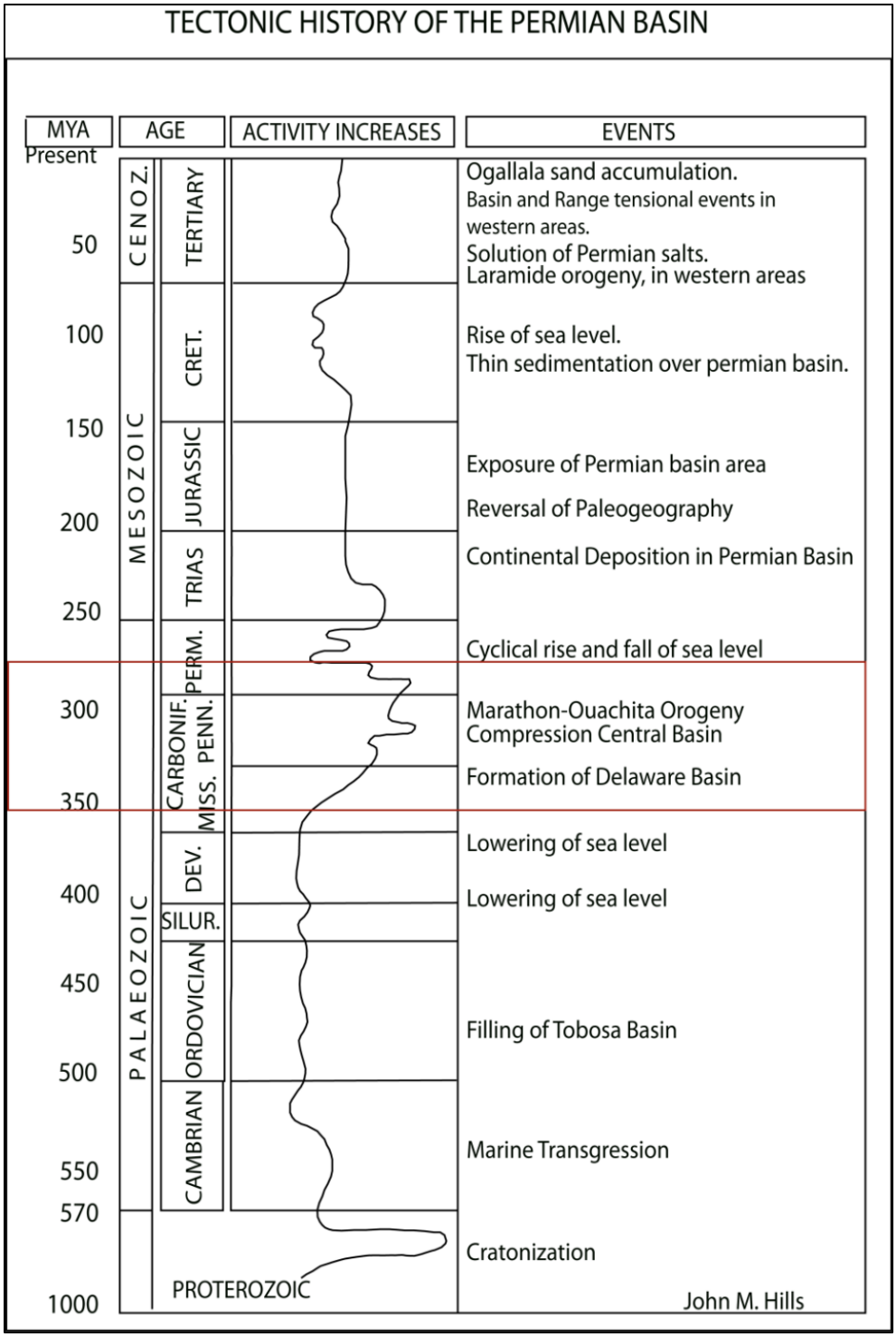

Figure 1.3: Tectonic history of the Permian Basin (Redrawn from Hills and Galley, 1988). The Maroon box highlights a period of major tectonic activity that transformed the Tobosa basin to the current Permian Basin with three major structural subdivisions; the Delaware Basin, Central Basin Platform and Midland Basin (See Figure 1.1). Most structural traps in the Permian Basin also formed during this period.

1.5.2 Pre-Tobosa Stage; Proterozoic to Early Ordovician

During the Proterozoic, the area currently known as the Permian Basin was a passive margin, characterized by weak crustal extension and low subsidence rate with only a veneer of sediments (Hills and Galley, 1988). The low subsidence rate gave birth to a broad, shallow, gently dipping depression, the Tobosa Basin (Galley, 1958). The collapse of the transcontinental arch as a negative feature during the Ordovician caused the transgression of the Early Ordovician Sea, consequently marking the beginning of the sedimentary history in the basin. By the end of this period, only a veneer of sediment existed atop the faulted basement (Galley, 1958; Adams, 1965). The creation of the Tobosa Basin was a major landmark of this period (Figure 1.4A).

1.5.3 The Tobosa Stage; Middle Ordovician to Late Mississippian

The Tobosa basin filled with relatively uniform and widespread shelf carbonates, alternating with thin siliciclastics (Hills, 1984). The associated high subsidence rates during the Late Ordovician to Devonian deepened the axial areas of the Tobosa Basin, causing sediment starvation. Dolomite and chert flourished in the shelves as black shales developed in deeper sections during late Devonian and continuing to the Mississippian (Wright, 1979; Hills and Galley, 1988). Uplift during the Late Devonian exposed the marginal Silurian-Devonian and Upper Ordovician shelf deposits causing their truncation and erosion. This continued until the Late Devonian/Early Mississippian transgression, during which the Woodford black shale was deposited (Adams, 1965; Wright, 1979; Hills, 1984).

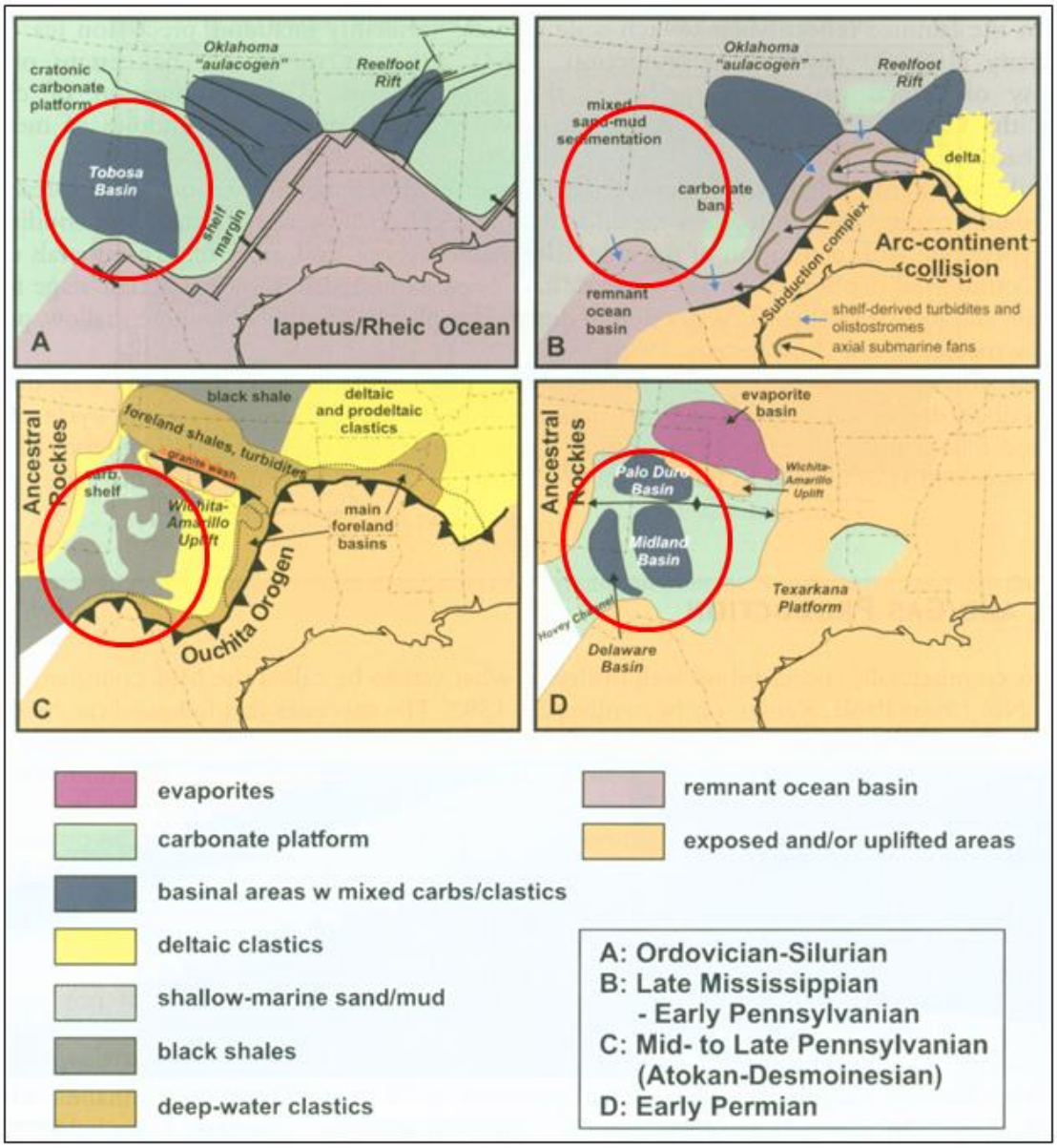

Figure 1.4A-D: The tectonic cycle (A-D) describing the development of the Permian Basin (circled red) from Ordovician to Early Permian (Adapted from Miall, 2008). See also Figure 1.3.

During the Mississippian, the Hercynian/Variscan orogeny, which was initiated by the collision of North America with Gondwana land/South America (Figure 1.4B), gave birth to Ouachita-Marathon fold belt (Figure 1.4C). At this time, compression from the southwest caused the central basin ridge to rise along rejuvenated steeply dipping reverse

faults. The faulting and folding involved the basement and began to deform the basin, creating the central basin uplift, which split the Tobosa Basin into Delaware Basin to the west and the Midland Basin to the East (Figure 1.4D). This tectonic compression also created the Ozona arch and the Val Verde Basin (Figure 1.1). At that point the Permian Basin began to form (Adams, 1965; Wright, 1979; Hills, 1984 and Frenzel et. al., 1988). Vertical movements along Proterozoic weaknesses deepened the eastern portion of the incipient Delaware Basin and tilted it to the east. Shelf margins developed during the Mississippian, and continued to the Pennsylvanian, a period of extensive subsidence. Basins starved and were later buried under shallow carbonates (Hills, 1984).

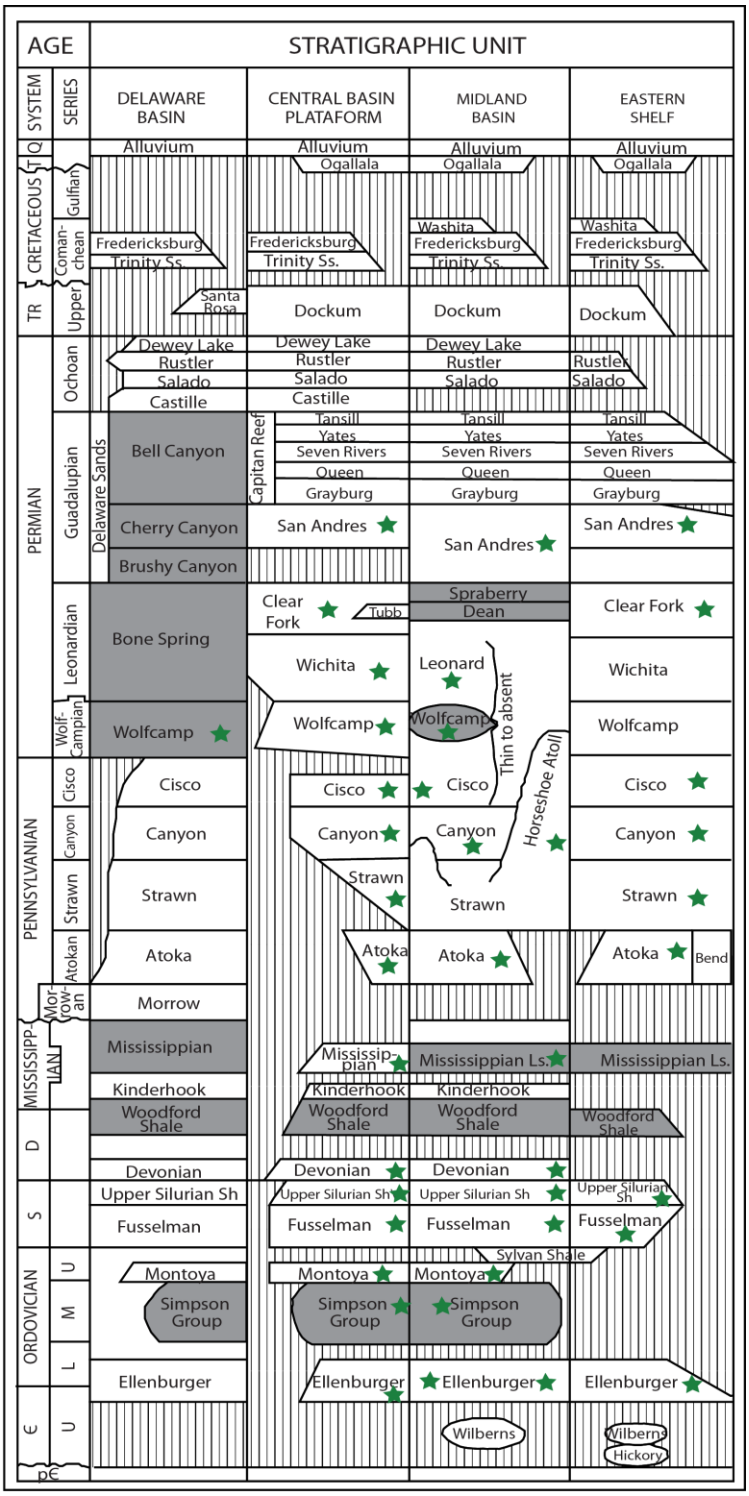

Figure 1.5: Generalized stratigraphy of the Permian Basin of West Texas and Southeast New Mexico (Modified from Galloway et al., 1983). The dark grey shades are siliciclastics, accounting for 25% of the stratigraphy, 75% being carbonates. The green stars represent reservoirs where oil samples were recovered for this study. See Figure 1.1 for basin and sample locations.

1.5.4 The Permian Basin Stage; Late Mississippian to Present

At the beginning of this stage, rapid subsidence continued, albeit at different relative rates; the Central Basin Platform was at its highest ascent during this period as its counterpart, the Diablo Platform on the extreme west was raised to mountainous heights. The uplifting of the Central Basin Platform during the Pennsylvanian and Wolfcamp times were conducive for the growth of reefs and building of shelf margins on the edges of the Delaware and Midland basins, with their respective centers being filled with deep water deposits, mainly siliciclastics while erosion and non-deposition prevailed in the positive features such as the Central Basin Platform (e.g. Hills, 1984). Other than the tilting of the Permian Basin along its edge, the Permian through Early Triassic was a period of general tectonic and structural stability during which the basin fragments filled with enormous amounts of sediments (e.g. Galley, 1958; Ward et al., 1986).

In the Delaware Basin, the associated tectonics during the Early Pennsylvanian supplied clastics into the basin. The clastics were derived mainly from the highland areas in the northwest in central New Mexico and perhaps from the advancing Marathon fold belt. However, due to rapid subsidence then, carbonate banks quickly grew along the basin margins (Hills, 1984). When tectonic activity peaked during Early Permian, the Marathon fold belt provided enormous amounts of clastic sediments into the basin from the southern end and is responsible for the thick shales and minor sandstones in the Delaware Basin. The tectonic quiescence at the end of the Wolfcampian resulted in decreased clastic supply and consequently, carbonate sedimentation returned, but mainly on the basin margins (Hills, 1984). Deposition of clastics (clays and thinner sandstone beds)

continued into Middle Permian (Leonardian), albeit with interruption by numerous carbonate wedges on the basin margins and extending into the basin center as thin limestone (Hills, 1984). The Leonardian is represented by the Bone Spring and Spraberry Formations in the Delaware and Midland basins, respectively. In the Late Permian (Guadalupian) clastics, mainly silts and sands continued to fill the basin as long as accommodation space was constantly being created by compaction and slow tilting of the basin. By the end of the Guadalupian, carbonate reefs and banks on the basin margin substantially reduced the rate of sedimentation in the basin center and restricted circulation, thus the sediments that accumulated (Brushy, Cherry, and Bell Canyons) were rich in organic matter (Hills, 1984). This restriction continued into Latest Permian (Ochoan) resulting in the deposition of Castile evaporite and later Salado and Rustler, all predominantly evaporitic (Hills, 1984).

In the Central Basin Platform, the uplift continued and climaxed during the Pennsylvanian. As a result, Pennsylvanian strata (Morrow, Atokan, Strawn, Canyon, and Cisco) are absent in many places within Central Basin Platform. Within the flanks, interbedded limestone, reef, green/gray shales and scattered conglomerates are reported (Frenzel et al., 1988). The true systematic filling of the central basin uplift with sediment begun during Early Permian. Even then, most of it remained emergent throughout the Wolfcampian, with carbonates developing mainly within its margins (Wright, 1979; Frenzel et al., 1988). Wolfcamp carbonate was deposited during the Early Permian, Abo/Wichita and Clear Fork Group during Leonardian, San Andres, and Artesia Group during the Guadalupian and capped by Salado and Rustler evaporates of Ochoan age.

Apparently, the structural and stratigraphic development, essentially the packaging of the petroleum system elements in the Permian Basin was well synchronized in time and space, making the Permian Basin one of the most classic petroleum provinces in the world.

1.6 Structure of the Dissertation

This dissertation is organized into five major chapters including: Chapter 1 (General Introduction), Chapter 2 (Geochemistry of Oils and Geochemical Inversion), Chapter 2 (Source rock Characterization and Oil-Source Rock Correlations), Chapter 4 (Generation and Expulsion modeling and Migration Analysis), and Chapter 5 (General Conclusions). Chapters 2 through 4 are stand-alone pieces of work, containing abstract through conclusions and ready for publication in peer-reviewed journals.

Chapter 1 covers introductory aspects to the research project and describes the research problem and the overall objectives. This chapter also covers an overview of the structural and stratigraphic development of the Permian Basin.

Chapter 2 describes the geochemistry of oils, chemometric (multivariate statistical analysis) correlations of oils, and geological inferences therefrom. This chapter provided the opportunity to scan through the nature of all the possible contributing source rocks prior to their sampling. The results of this part of the study established play combinations which embrace geochemically similar oils in the Permian Basin. It also provided a fundamental basis for defining potential source rocks to be sampled for further geochemical characterization. At least five potential source rocks were inferred from

these studies, including shales of Ordovician, Devonian, Mississippian, Early Permian (Wolfcampian), and a marl source of Permian Age. This chapter was submitted to the AAPG Bulletin for review and has been accepted for publication under the title "Geochemical characterization and chemometric classification of crude oils of the Permian Basin, West Texas and Southeast New Mexico, USA".

Chapter 3 describes the organic geochemistry of the sampled source rocks and chemometric and stable carbon isotope correlation of oils and source rocks, essentially an identification of petroleum systems. At least four petroleum systems were identified and their stratigraphic extents mapped both geographically and stratigraphically. The identified petroleum systems include; the Simpson petroleum system, the Woodford petroleum system, the Barnett petroleum system and the Wolfcampian petroleum system. The fifth petroleum system, the Bond Spring was inferred from the geochemistry of oils alone. This chapter has been submitted to the AAPG Bulletin for review and publication under the title "Geochemical characteristics of oils and source rocks from the Permian Basin of West Texas and Southeast New Mexico: Implications for petroleum systems".

Chapter 4 contains the results and interpretations from thermal maturity modeling of identified source rocks and describes the process of petroleum generation and expulsion in the Permian Basin. An integration of petroleum systems elements and process was undertaken for each petroleum system identified, including the timing of petroleum generation with respect to trap formation. Distribution of maturity among the source rocks was also mapped for the five source rocks, constraining pods of active source rocks for the petroleum systems identified.

Chapter 5 contains the summary and conclusions from the entire study and includes some recommendations for future work.

1.7 References

Adams, J. E., 1965, Stratigraphic-tectonic development of the Delaware Basin: AAPG Bulletin, v. 49, p. 2140-2148.

Burrus, J., K. Osadetz, J. M. Gaulier, E. Brosse, B. Doligez, G. Choppin de Janvry, J. Barlier and K. Visser, 1993, Source rock permeability and petroleum expulsion efficiency: modeling examples from the Mahakam delta, the Williston Basin and the Paris Basin; Geological Society London, Petroleum Geology Conference series, 1993, v.4, p. 1317-1332.

Comer, J. B., 1991, Stratigraphic analysis of the Upper Devonian Woodford Formation, Permian Basin, West Texas and Southeastern New Mexico, University of Texas, Austin, Bureau of Economic Geology, Report of Investigations No. 201, 63p.

Cooles, G. P., A. S., Mackenzie and T. M. Quingley, 1986, Calculation of petroleum masses generated and expelled from source rocks, Organic geochemistry, v. 10, p. 235-245. Mackenzie, A. S. and T. M. Quigley, 1988, Principles of geochemical prospect appraisal, AAPG Bulletin, 72, p. 399-415

Corby, J. J. and H.E. Cook, 2003, The Permian Basin petroleum systems, Simpson-Ellenberger and Woodford-San Andres-New Insights for exploring a mature petroleum province (Abs), AAPG Annual Convention, Salt Lake City, Utah. May 11-14, 2003.

Demaison, G., and B. J. Huizinga, 1991, Genetic classification of petroleum systems: AAPG Bulletin, v.75, p. 1626-1643.

Dow, W. G., Tulukdar, S. C. and Harmon, L. 1990, Exploration applications of geochemistry in the Midland basin, Texas (abs.), American Association of petroleum Geologists Bulletin, 74, 644-645.

Dutton, S. P., E. M. Kim, R. F. Broadhead, C. L. Breton, W. D. Raatz, S. C. Ruppel, and C. Kerans, 2004, Play analysis and digital portfolio of major oil reservoirs in the Permian basin: Application and transfer of advanced geological and engineering technologies for incremental production opportunities, University of Texas at Austin, Bureau of Economic Geology, Final Report prepared for the U.S. Department of Energy under contract DE-FC26-02NT15131, 408 p.

Dutton, S. P., E. M. Kim, R. F. Broadhead, W. D. Raatz, C. L. Bretton, S. C. Ruppel, and C. Kerans, 2005, Play analysis and leading-edge reservoir development methods in the Permian; increased recovery through advanced technologies: AAPG Bulletin, 89, 55-576.

England, W. A., 1994. Secondary migration and accumulation of hydrocarbons, in L.B. Magoon and W.G. Dow, eds., The Petroleum System-from Source to Trap: AAPG Memoir 60, p. 211-217.

Frenzel, H. N., R. R. Bloomer, R. B. Cline, J. M. Cys, J. E. Galley, W. R. Gibson, J. M. Hills, W. E. King, W. R. Seager, F. E. Kottlowski, S.Thompson III, G. C. Luff, B.

T. Pearson, and D. C. Van Siclen, 1988, The Permian Basin Region, in L. L. Sloss, ed., Sedimentary Cover-North American Craton, US.: Boulder, Colorado, Geological Society of America, The Geology of North America, v. D-2, p. 261-306.

Galley, J. E., 1958, Oil and geology in the Permian Basin of Texas and New Mexico, in Weeks, L. G., ed., Habitat of Oil: American Association of Petroleum Geologists, Tulsa, p. 395-446.

Galloway, W. E., E. T. Ewing, C.M. Garrett, N. Tyler and D. G. Debout, 1983, Atlas of Major Texas Oil Reservoirs, Bureau of Economic Geology, The University of Texas at Austin, 139.

Hill, R. J., D. M. Jarvie, B. L. Claxton, J. D. Burgess, and J. A. Williams, 2004, Petroleum systems of the Permian Basin (abs): AAPG Annual Meeting Program, v. 13. A63.

Hills, J. M. 1984, Sedimentation, tectonism, and hydrocarbon generation in Delaware Basin, west Texas and southeastern New Mexico: AAPG Bulletin, v. 68, p. 250-267.

Hills, J. M., and J. E. Galley, 1988, General Introduction, in Frenzel, H. N., R. R. Bloomer, R. B. Cline, J. M. Cys, J. E. Galley, W. R. Gibson, J. M. Hills, W. E. King, W. R. Seager, F. E. Kottlowski, S.Thompson III, G. C. Luff, B. T. Pearson, and D. C. Van Siclen, 1988, The Permian Basin Region, in L.L. Sloss, ed., Sedimentary Cover-North American Craton, US.: Boulder, Colorado, Geological Society of America, The Geology of North America, v. D-2, p. 261-306.

Hills, J. M., and J. E. Galley, 1988, The Pre-Pennsylvanian Tobosa Basin, in Frenzel, H. N., R. R. Bloomer, R. B. Cline, J. M. Cys, J. E. Galley, W. R. Gibson, J. M. Hills, W. E. King, W. R. Seager, F. E. Kottlowski, S.Thompson III, G. C. Luff, B. T. Pearson, and D. C. Van Siclen, 1988, The Permian Basin Region, in L.L. Sloss, ed., Sedimentary Cover-North American Craton, US.: Boulder, Colorado, Geological Society of America, The Geology of North America, v. D-2, p. 261-306.

Jarvie, D. M., J. D. Burgess, A. Morelos, P. A. Mariotti, and R. Lindsay, 2001, Permian Basin petroleum systems investigations; inferences from oil geochemistry and source rocks (abs). AAPG Bulletin, v. 85, p. 1693-4.

Jarvie, D. M. and R. J. Hill, 2011, Understanding unconventional resource potential by conventional petroleum systems assessment: AAPG Search and Discovery Article #40840. Web accessed 15th February 2013, http://www.searchanddiscovery.com/documents/2011/40840jarvie/ndx_jarvie.pdf.

Katz, B. J., W. C. Dawson, V. D. Robinson, and L.W. Elrod, (1994). Simpson-Ellenberger (.) PS of the Central Basin Platform, West Texas, USA. In Magoon, L. B. and W. G. Dow (eds.). The Petroleum System: From Source to Trap, AAPG Memoir 60, p. 453-461.

Kinley, T. J., L. W. Cook, J. A. Breyer, D. M. Jarvie and A. B. Busbey, 2008, Hydrocarbon potential of the Barnett Shale (Mississippian), Delaware Basin, west Texas and southeastern New Mexico: AAPG Bulletin, v. 92, p. 967-991.

Leythaeuser, D., M. Radke and R.G. Schaefer, 1984, Efficiency of petroleum exploration from shale source rocks: Nature, v. 311, p. 745-748.

Leythaeuser, D., M. Radke and R. G. Schaefer, 1987, On the primary migration of petroleum, 12th World Congr. Proc 2: 227-236

Lindsay, R. F., 2012, West Texas structure, The University of Texas of the Permian Basin http://www.ceed.utpb.edu/geology-resources/west-texas-geology/west-texas-structure> Accessed September 5th, 2012.

Matchus E .J. and T. S. Jones, 1984, East-west cross section through Permian Basin of West Texas, West Texas Geological Society Publication 84-79.

Miall, A. D, 2008; The southern midcontinent, Permian Basin and Ouachitas, Chapter 8, in A.D., Miall, ed., The Sedimentary Basins of the United States and Canada, Elsevier, Amsterdam, The Netherlands, p. 298-329.

Magoon, L. B. and E. A. Beaumont , 1999, Petroleum systems, in E.A Beaumont and N.H. Foster, eds., Handbook of Petroleum Geology: Exploring for Oil and Gas Traps, American Association of petroleum Geologists, Washington D.C., pp 3.1-34.

Magoon, L. B., 1992, Identified petroleum systems in the United States, in Magoon, L. B. (Ed.), The Petroleum Systems-Status of Research and Methods, US Geological Survey Bulletin 2007, p. 2-11.

Magoon, L. B., C.V. Valin, 1994, Overview of petroleum systems case studies, in L. B. Magoon and, W. G. Dow eds. The Petroleum System: From Source to Trap: AAPG Memoir 60, p. 3-24.

Magoon, L. B., and W. G. Dow, 1994, The petroleum system, in L. B. Magoon and, W. G. Dow eds. The Petroleum System: From Source to Trap: AAPG Memoir 60, p. 3-24.

Magoon, L.B., 1988a, The Petroleum Systems of the United States: US Geological Survey Bulletin 1870, 68p.

Magoon, L.B., 1988b, The petroleum system- a classification scheme for research, exploration and resource assessment, in Magoon, L.B. (Ed.), The Petroleum Systems of the United States, US Geological Survey Bulletin 1870, p 2-15.

Pawlewicz, M. and H. Mitchell, 2006, One-D Burial history modeling in the Permian Basin, western Texas and southeastern New Mexico (abs), in Michael A. Raines (Ed.) Southeast New Mexico and West Texas Fall Symposium, West Texas Geological Society; resource plays in the Permian Basin-resource to reserves, p. 87.

Peters, K. E., J. M. Moldowan, and C. C. Walters, 2005, The Biomarker Guide; Biomarkers and Isotopes in Environment and Human History (vol. 1): Cambridge University Press pp. 1-471.

Peters, K. E. and Cassa, M. R., 1994, Applied source rock geochemistry, in, Magoon, L. B. and Dow, W., G., eds., The Petroleum System: From Source to Trap, AAPG Memoir 60, p. 93-120.

Peters, K. E., D. Coutrot, , X. Nouvelle, L. S. Ramos, B.G. Rohrback, L. B. Magoon, and J. E. Zumberge, 2013, Chemometric differentiation of crude oil families in the San Joaquin Basin, Carlifornia: AAPG Bulletin, v. 97, p. 103-143

Quigley, T. M., A. S Mackenzie, and J.R. Gray, 1987, Kinetic theory of petroleum generation, in. Doligez, B., ed., Migration of hydrocarbons in sedimentary basins, Editions technip, Paris, pp. 649-666.

Railroad Commission, 2012, History of Texas initial crude oil, annual production and producing wells, (http://www.rrc.state.tx.us/data/production/oilwellcounts.php), web accessed Jan, 2012.

Schenk, C. J., R. M. Pollastro, T. A. Cook, M. J. Pawlewicz, T. R. Klett, R. R. Charpentier, and H. E. Cook, 2008, Assessment of undiscovered oil and gas resources of the Permian Basin Province of west Texas and southeast New Mexico, 2007, U.S. Geological Survey Fact Sheet 2007–3115, 4p.

Tyler, N., and Banta, N. J., 1989, Oil and gas resources remaining in the Permian Basin: targets for additional hydrocarbon recovery: The University of Texas at Austin, Bureau of Economic Geology, Geological Circular 89-4, 20 p.

Ward, R. F., C.G. ST. C. Kendall and Harris, P. M., 1986, Upper Permian (Guadalupian) facies and their association with hydrocarbons-Permian Basin, West Texas and New Mexico: AAPG Bulletin, v. 70, p. 239-262.

Wright, W. F., 1979, Petroleum Geology of the Permian Basin: West Texas Geological Society Publication 79-71, 98p.

2.0 OIL-OIL CORRELATIONS AND GEOCHEMICAL INVERSION

Abstract

Fifty (50) crude oils from reservoirs ranging in age from Camb-Ordovician to Late Permian, distributed widely over the Permian Basin, were studied geochemically and chemometrically to assess their stratigraphic, regional interrelationships, and provenance. The detailed characterization using stable carbon isotopic composition and biomarker characteristics resulted in recognition of five major genetic groups or petroleum systems. Group I oils originate from Ordovician marine shale (Simpson Group) source rocks having type II kerogen deposited under anoxic conditions. Groups II and III oils are similar in all respects except for a significant terrigenous organic matter input in the latter. This hybrid group (group II/III) oils, sourced from two kitchens, are derived from Devonian marine shale (Woodford) and Mississippian (Barnett) source rocks having type II/III kerogen deposited under sub-oxic environments. Oils of Group IV, sourced from two kitchens, are generated from Early Permian shale (Wolfcamp) source rocks having type II/III kerogen deposited under anoxic-suboxic environments. Group V oils are derived from carbonate-rich shales (marls) of the Middle Permian Bone Spring Formation having type II kerogen deposited under anoxic environments.

Except for Devonian- and Mississippian-sourced oils which occur within a thick stratigraphic interval (Camb-Ordovician to Permian), there is clear reservoir segregation, such that Ordovician-sourced oils are hosted within Ordovician reservoirs, Early Permian-sourced oils are found within Early Permian and underlying Pennsylvanian reservoirs, and Middle-Upper Permian-sourced oils are reservoired within the Middle-

Upper Permian reservoirs. This detailed geochemical study of oils has provided an understanding of the stratigraphic relationships between oils and their source rocks, and thus useful insights into hydrocarbon migration in the Permian Basin.

2.1 Introduction

The Permian Basin of West Texas and Southeastern New Mexico is one of the most prolific petroleum provinces in the United States. It is structurally defined by the Matador Arch to the north, the Marathon-Ouachita Fold belt to the south, the Diablo Platform to the west, and the Eastern shelf to the east (Figure 2.1). During its 90+ years exploration and production history, it has supplied over 35 billion barrels of oil and several trillion cubic feet of gas, mainly from conventional plays (e.g. Galloway et al., 1983; Dutton et al., 2004; 2005). In spite of the long production history, the petroleum systems of the Permian Basin remain poorly constrained. The current poor understanding of the Permian Basin petroleum systems is largely due to inadequate geochemical investigation, as most studies have mainly focused on traps/plays, ignoring the shared risk factor, the source rock(s). Stressing the importance of play analysis, Dutton et al. (2004; 2005) urged that exploitation methods which have been proven to be effective in one play set can also be extended to plays of similar type elsewhere. However, a complete play risk analysis must incorporate all the elements of the petroleum system for without an understanding of the source rocks, prospect evaluation is incomplete (e.g. Peters et al. 1994).

A petroleum system encompasses a pod of active source rock and all related petroleum and includes all the essential geological elements and processes necessary for a petroleum accumulation to exist (Magoon and Dow, 1994). The exploration advantage of petroleum

system studies is its ability to reveal untapped potential in form of bypassed or unconventional resources (Peters et al., 2013). In basins considered mature for exploration, such as the Permian Basin, undertaking petroleum system investigations will undoubtedly add value to the exploration effort. A few of the geochemical investigations of petroleum systems of the Permian Basin (Jarvie et al., 2001, and Hill, et al., 2004) are only available as abstracts.

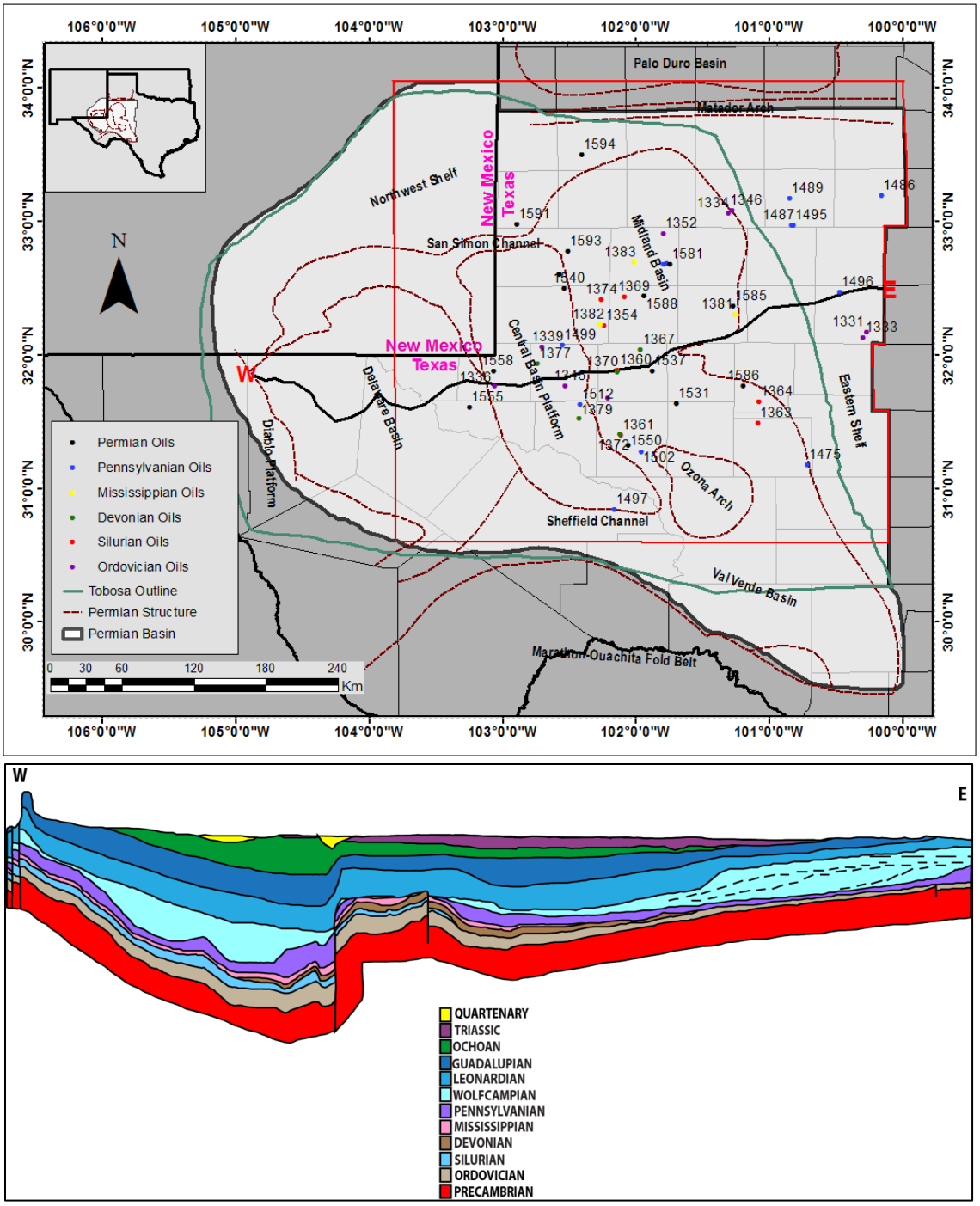

Figure 2.1: Map of the Permian Basin showing stratigraphic and geographic locations of oils used in the study. The green outline is the Tobosa basin from which the Permian basin was derived through large scale structural deformation that eventually formed the Delaware and Midland basins separated by the central basin platform (Modified from Frenzel et al. 1988; Dutton et al., 2004; 2005). The lower image is the generalized East-West cross section of the Permian Basin (Redrawn from Lindsay 2012; after Matchus and Jones, 1984).

Although production has been declining since the late 1970s, the current trend of increasing activity in the Permian Basin, as reflected by the increasing number of operators/new drilling permits as published by the Rail Road Commission (Rail Road Commission, 2012) emphasizes the renewed importance of this petroleum province. A study conducted by the USGS in 2007 (Schenk et al., 2008), indicates that at least 1.3 billion barrels of oil and up to 41 trillion cubic feet (tcf) of natural gas, representing both conventional and continuous (unconventional) gas remain undiscovered in the Permian Basin. This is an enormous resource by any standard.

Despite the poor understanding of the petroleum systems, the large hydrocarbon endowment suggests the operation of very efficient petroleum system processes such as supercharging, lateral drainage and high impedance entrapment as described in Demaison & Huizinga (1991). The endowment also suggests parallelism with extremely high quality source rocks and high expulsion and migration efficiencies, as typically observed in source-rock-reservoir associated or juxtaposed systems. These projections can only be confirmed through geochemical analysis of stratigraphically and geographically well-constrained oils or source rocks where available. Geochemical characteristics of oils provide insights on the nature, genetic character, including organic matter make-up, lithology and maturity of candidate source rocks responsible for the oils, including inferences about the depositional environment and age of source rocks (e.g. Moldowan et al., 1985; Bissada et al., 1993; Dahl et al., 1994).

The objective of this study is, to correlate and infer the provenance of the Permian Basin oils based on their molecular and isotopic compositions focusing on aspects including:

source rock depositional environment, organic matter type, age, and lithology. The results of the study will establish a fundamental basis for defining potential source rocks to be sampled for further geochemical characterization, and develop play combinations which embraces geochemically similar oils, here refered to as hybrid plays. These play hybrids, are assentially petroleum systems.

2.2 Geological Background

The structural and stratigraphic development of the Permian Basin is well outlined in the literature (e.g. Galley, 1958; Adams, 1965; Wright, 1979; Hills et. al., 1984; Hills and Galley, 1988; and Frenzel et al., 1988). The structure and stratigraphy are illustrated in Figures 2.1 and 2.2, respectively.

2.2.1 Pre-Tobosa Stage; Proterozoic to Early Ordovician

During the Proterozoic, the area currently known as the Permian Basin was a passive margin, characterized by weak crustal extension and low subsidence rate with only a veneer of sediments (Hills and Galley, 1988). The low subsidence rate gave birth to a broad, shallow, gently dipping depression, the Tobosa Basin (Galley, 1958). The collapse of the transcontinental arch as a negative feature during the Ordovician caused the transgression of the Early Ordovician Sea, consequently marking the beginning of the sedimentary history in the basin. By the end of this period, only a veneer of sediment existed atop the faulted basement (Galley, 1958; Adams, 1965).

2.2.2 The Tobosa Stage; Middle Ordovician to Late Mississippian

The Tobosa basin filled with relatively uniform and widespread shelf carbonates, alternating with thin siliciclastics (Hills, 1984). The associated high subsidence rates during the Late Ordovician to Devonian deepened the axial areas of the Tobosa basin, causing sediment starvation. Dolomite and chert flourished on the shelves as black shales developed in deeper sections during late Devonian and continuing to the Mississippian (Wright, 1979; Hills and Galley, 1988). Uplifts during the Late Devonian exposed the marginal Silurian-Devonian and Upper Ordovician shelf deposits, causing their truncation and erosion. This continued until the Late Devonian/Early Mississippian transgression, during which the Woodford black shale was deposited (Adams, 1965; Wright, 1979; Hills, 1984).

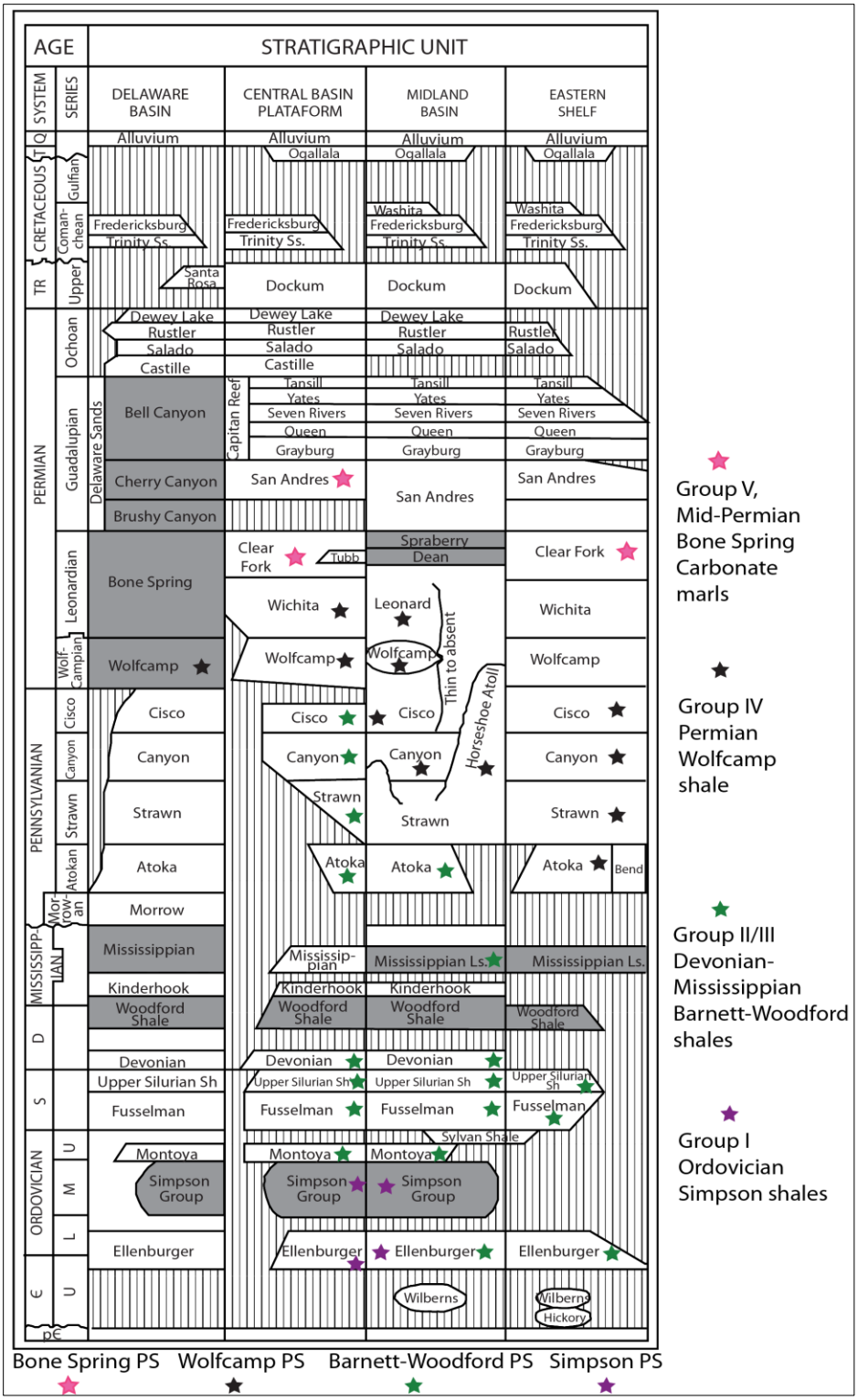

Figure 2.2: Locations of oils samples within the Permian Basin stratigraphic framework (Modified from Galloway et al., 1983). The colors represent inferred petroleum systems from oil-oil correlations by chemometrics and geochemical inversion.

During the Mississippian, the Hercynian/Variscan orogeny, which was initiated by the collision of North America with Gondwana/South America, gave birth to Ouachita-Marathon fold belt. At this time, compression from the southwest caused the central basin ridge to rise along rejuvenated steeply dipping reverse faults. The faulting and folding began to deform the basin, creating the central basin uplift, which split the Tobosa basin into the Delaware Basin to the west and the Midland Basin to the East. This tectonic compression also created the Ozona Arch and the Val Verde basin (Figure 2.1). Since then, the Permian Basin was born (Adams, 1965; Wright, 1979; Hills, 1984 and Frenzel et al., 1988). Vertical movements along Proterozoic weaknesses deepened the eastern portion of the incipient Delaware Basin and tilted it to the east. Shelf margins developed during the Mississippian and continued to the Pennsylvanian, a period of extensive subsidence. Basins starved and were later buried under shallow evaporites and carbonates (Hills, 1984).

2.2.3 The Permian Basin Stage; Late Mississippian to Present

At the beginning of this stage, rapid subsidence continued, albeit at different relative rates; the Central Basin Platform was at its highest ascent during this period, as the Diablo Platform on the extreme west was raised to mountain heights. The uplifting of the Central Basin Platform during the Pennsylvanian and Wolfcamp times was conducive for the growth of reefs and building of shelf margins on the edges of the Delaware and Midland Basins, with their respective centers being filled with deep water siliciclastic deposits, while erosion and non-deposition prevailed in the positive features such as the Central Basin Platform (e.g. Hills, 1984). The structural and stratigraphic development

was well synchronized in time and space, making the Permian Basin one of the most classic petroleum provinces in the world.

2.3 Samples and Methods

The study includes a total of fifty samples (40 crude oil and 10 condensates), sampled from the Texas portion of the Permian Basin, principally the Central Basin Platform, Central Basin Platform, Midland Basin, and Eastern Shelf (Figure 2.1), covering reservoirs ranging from Cambrian (single sample) to Permian and representing a large portion of the Permian Basin play framework. The oil samples were analyzed for API gravity, saturates-aromatics-resins-asphaltenes (SARA) group separation by high performance liquid chromatography (HPLC), hydrocarbon component distribution by gas chromatography (GC), biomarker distribution by gas chromatography-mass spectrometry (GC-MS), and isotopic composition by isotope ratio mass spectrometry (IRMS), as summarized in Figure 2.3 and described in detail below.

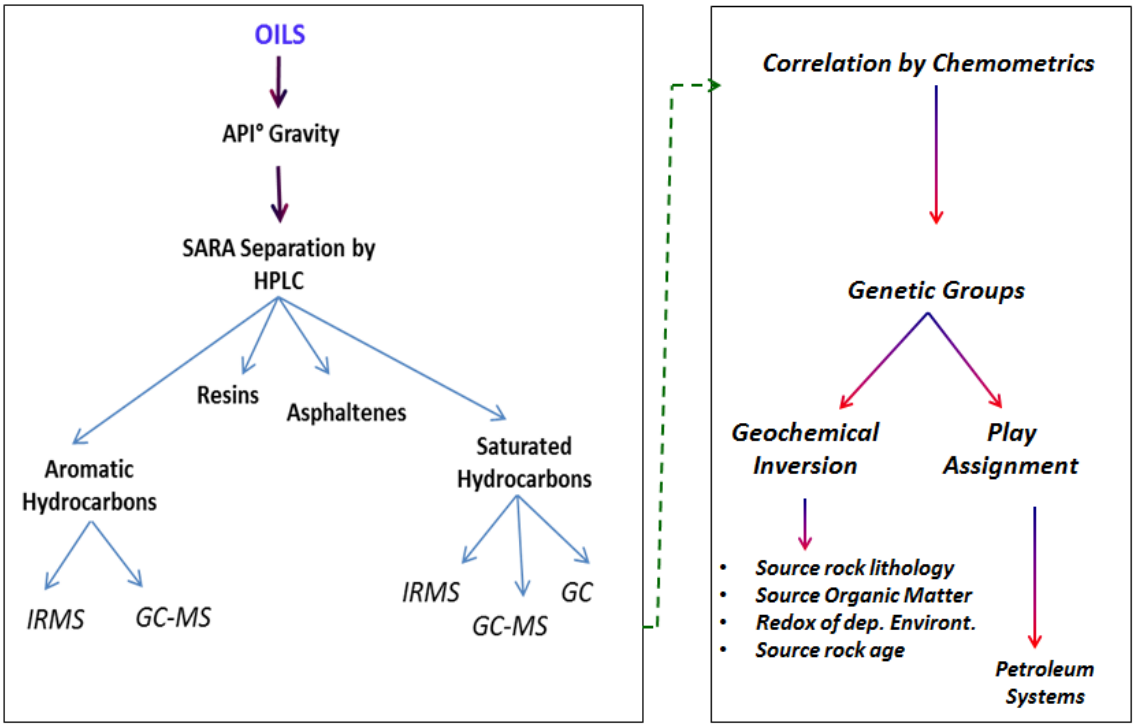

Figure 2.3: Workflow summarizing analyses (after Bissada et al., 1993) and the general research methodology used in this study.

Chemometric techniques of data analyses were utilized to group the oils according to their biomarker and stable carbon isotope compositions. Chemometrics is a collection of multivariate statistical methods for recognizing patterns in large data sets (e.g. Øygard et al., 1984; Zumberge, 1987). For this study, hierarchical cluster analysis (HCA) and principal component analysis (PCA) were used. Thirteen genetically oriented geochemical parameters were selected for use in chemometrics which was executed using XLSTAT software (Addinsoft, 2012).

A detailed analysis of genetic groupings to infer their candidate source rocks was undertaken, mainly utilizing geochemical interpretive charts/plots to arrive at geological inferences from the chemistry of oils (geochemical inversion), including, source lithology, source age, source organic matter type, and source depositional environmental

conditions. Oils were then located within the stratigraphic/play framework of the Permian Basin to establish their stratigraphic relationships with inferred source rocks.

2.3.1 API Gravity

API gravity was determined using a DMA 48 density meter at 60°F according to the specifications defined by ASTM standard method D4052-86.

2.3.2 High Performance Liquid Chromatography, HPLC

Oils were subjected to liquid chromatography using the University of Houston Center for Petroleum Geochemistry HPLC system custom-designed for saturate, aromatics, resins, and asphaltenes (SARA) determinations. The system is a fully automated multidimensional process comprising use of two columns in series through which four solvents are pumped sequentially, in both forward and reverse mode at pre-set times. The four solvents are (i) hexane, (ii) hexane-chloroform (94%:6%), (iii) methanol-acetone-chloroform (15%:15%:70%), and (iv) chloroform. They are used to sequentially elute saturates, resins, asphaltenes, and aromatics, respectively. The column chromatographic process is somewhat similar to other HPLC methods, except for the ability to separate whole oil into its four SARA components without the need to first exclude asphaltenes by precipitation prior to injection. Samples were recovered from the solvents by vacuum-rotary-evaporation.

2.3.3 Gas Chromatography, GC

Gas chromatography of saturated hydrocarbon fractions were run using a Hewlett Packard 6890^{TM} Gas Chromatograph equipped with a flame ionization detector (FID) set at 350°C and a 60m HP-1 capillary GC column, 0.25 mm i.d. with a 0.5 µm coating of methyl siloxane. The oven temperature program comprised: Initial temperature 145°C, hold of 3 minutes; ramp to 250°C at 10°C/min; immediately ramp from 250°C to 310°C @ 2.5°C/min; and hold at 310°C for 42minutes. The total run time was 75.5minutes. Inlet was operated at 325°C with a split mode at a split ratio of 50:1.

2.3.4 Gas Chromatography-Mass Spectrometry, GC-MS

Analysis of the sterane and triterpane biomarkers in the C_{15+} saturated hydrocarbon fraction was accomplished using a Hewlett Packard 5890^{TM} Series II Gas Chromatograph coupled to a Hewlett Packard 5971 series mass spectrometer. Biomarkers in the C_{15+} aromatic fraction were analyzed by the same system. The GC column used was a 60m long x 250µm diameter x 0.25µm methyl siloxane film coat (HP-1). For the saturate fraction, the GC temperature program comprised: initial temperature 145°C, hold time 3 minutes; ramped to 205°C at 6°C/min; final ramp at 2.5°C/min to 320^0C; hold for 17 minute for a total run time of 76 minutes. Injection inlet in split mode, set at 325°C with a split ratio of 100:1. For the aromatic fraction, the column temperature program comprised an initial temperature of 70°C, with hold for 4 minutes; ramp to 145°C at 3°C/minute, no hold time; increase to 320°C at 2°C/minute for a total run time of 116.5minutes. The GC output for both saturate and aromatic

fractions were directed to the mass spectrometer (SIM mode) where the following ions were monitored: m/z 83, 85, 97, 123, 125, 177, 191, 205, 217, 218, 231, and 259 for the saturate fraction, and 92, 128, 133, 142, 154, 156, 166, 168, 170, 178, 180, 182, 184, 191, 192, 198, 206, 212, 230, 231, 234, 245, and 253 for the aromatic fraction. Only selected samples were subjected to aromatics GC-MS.

2.3.5 Isotope Ratio Mass Spectrometry, IRMS

Stable carbon isotope analysis (hydrocarbon fractions) was accomplished using a Finnegan MAT 252 isotope-ratio mass spectrometer (IRMS) system, where the $\delta^{13}C$ is internally calculated according to the equation;

$\delta^{13}C$ (‰) = $[[(^{13}C/^{12}C)_{Sample}\text{-}(^{13}C/^{12}C)_{Std}]/(^{13}C/^{12}C)_{Std}]$ relative to the PDB standard.

NBS 22 standard first prepared by Silverman (1964), supplied by the United States Geological Survey, Reston Stable Isotope Laboratory, was used as a calibration standard. Samples for isotopic analyses were prepared according to the method described by Sofer (1980).

2.3.6 Chemometric (Multivariate Statistics) Analysis

Multivariate statistical analysis of geochemical data to achieve oil-oil correlations (Øygard et al., 1984; Zumberge, 1987) was undertaken using XLSTAT software (Addinsoft, 2012). Owing to the varying maturity amongst samples, only biomarker and stable carbon isotope parameters related to source and depositional environment were selected as input data. At least 13 source and depositional environment parameters

including; $\delta^{13}C$ whole oil, $\delta^{13}C$ saturates, $\delta^{13}C$ aromatics, canonical variable, % tricyclics, % C_{27}-C_{29} Steranes, C_{30} Sterane index, carbon preference index (CPI), Pristane/Phytane ratio, and odd-over even predominance (OEP) were used in the statistical analysis (Table 2.1). Exploratory data analysis, computation and graphical display of patterns were completed by chemometric analysis (Øygard, 1984; Zumberge, 1987) using both agglomerative hierarchical clustering (AHC) and principal component analysis (PCA). In AHC, similarity was based on single linkage and automatic truncation options embedded in XLSTAT version 2012.4 (Addinsoft, 2012). In both cases, the Pearson correlation coefficient was used in auto scaling mode.

2.3.7 Geographic Information Systems, GIS

Maps for combined plays having geochemically related oils were completed using ArcGIS mapping software (ESRI, 2012) and were isolated from a pool of plays as defined in Permian Basin play portfolio (Dutton et al., 2004; 2005).

2.4 Results and Discussion

2.4.1 Bulk Geochemical Characteristics of Oils

The API gravities of the sampled oils range from 25.8° to 69.8°, with majority of the oils between 35° and 55°API. A group of oils reservoired in the Middle-Upper Permian are, however, distinct from the rest by having the lowest API gravities, attributable to either low maturity or possible carbonate sourcing. Moreover, these oils are neither water-washed nor biodegraded, as evidenced by the SARA distribution (Figure 2.4) and *n*-alkane distribution (Figure 2.5, bottom most), respectively. The majority of the oils are

enriched in saturated hydrocarbons relative to aromatics and non-hydrocarbons fractions (Figure 2.4a & b). These observations suggest high thermal maturity, and may explain the occurrence of condensates (API° >50°). Moreover, in general, Permian Basin oils have relatively low biomarker concentrations, a characteristic frequently associated with high levels of maturity (e.g. Van Graas, 1990).

Among the hydrocarbon components, the SARA group separation (Table 2.1 and Figure 2.4a) shows the majority of the Permian Basin oils to be enriched in saturates relative to aromatics, typifying generation from siliciclastic source rocks (e.g. Hughes, 1984; Palacas et al., 1984) and possible accentuation by high maturity. However, as in the API gravity distribution, a sub-group of Permian oils separates from the rest of the oils. These Middle-Upper Permian reservoired oils are relatively enriched in non-hydrocarbons, perhaps explaining their low API gravities. Given that the *n*-alkane distributions of this subgroup of Middle-Upper Permian reservoired oils do not show any evidence of biodegradation, the observed low API gravities and high proportions of non-hydrocarbons could be due to sourcing from carbonate source rocks. Compared to siliciclastic source rocks, which are surface active because of the presence of clay minerals and iron species, carbonate source rocks are not surface active and, therefore, expel hydrocarbon fractions equally. This equal expulsion makes the SARA distribution relatively equal in carbonate-sourced oils compared to siliciclastic sourced oils, where highly polar components of the crude oil (resins and asphaltenes) are preferentially retained due to surface activity (Hughes, 1984; Palacas et al., 1984).

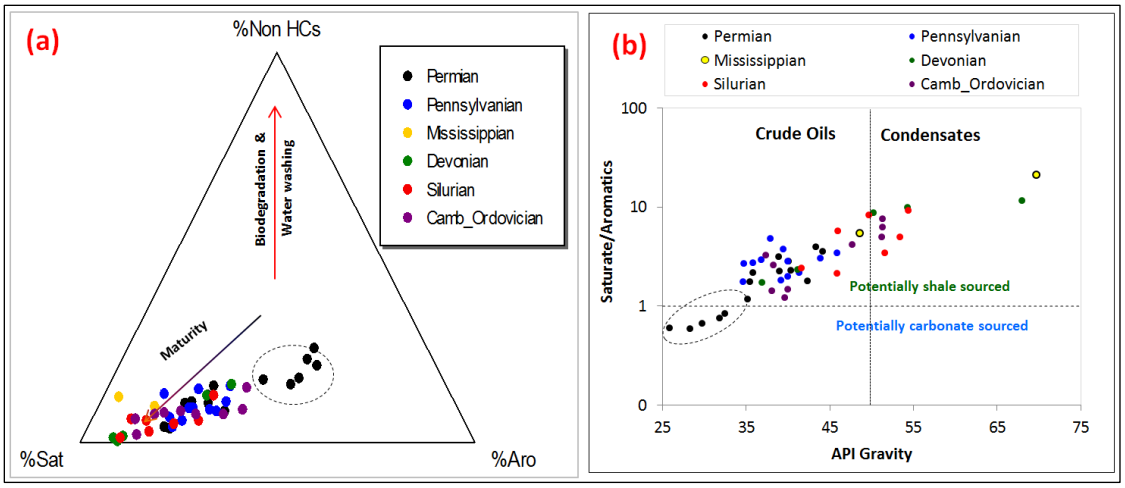

Figure 2.4: Bulk parameters; (a) ternary diagram showing the distribution of crude oil components; saturates, aromatic and non-hydrocarbons (Connan, 1984; Peters et al., 2005), (b) plot of saturate/aromatic ratio versus API gravity potentially indicating Permian Basin oils, except a sub-group from the Permian reservoirs, are derived from silicilastic (shale) source rock (saturate/aromatics line from Palacas et al., 1984; Hughes, 1984).

2.4.2 Gas Chromatographic Fingerprinting and GC-MS Mass Fragmentograms

GC and GC-MS chromatograms for represenetative group samples are shown in Figures 2.5 and 2.6 and their groupings shown in Figure 2.7. Group representative normal alkane distributions (Figure 2.5) show a skew in favor of lighter components, with higher molecular weight *n*-alkanes diminishing rapidly after nC_{20}. This distribution is a characteristic of oils derived from mature marine source rocks (e.g. Bissada et al., 1993; Peters et al., 2005). Oils in Camb-Ordovician reservoirs (group I oils), and some from Devonian, Silurian, and Mississippian reservoirs, however, display a significantly strong odd-over-even predominance (OEP) in the range nC_{15} to nC_{19} (Table 2.1). OEP, which is a measure of abundance of odd relative to even numbered paraffins, in general reflects maturity (Scalan and Smith, 1970). OEP values greater than one are usually attributed to low maturity as values less than 1 suggest, but do not confirm high maturity due to effects of source lithofacies (Peters et al., 2005). However, given that all the oils show

high levels of maturity as indicated (Figure 2.4), and coupled with the isolated OEP range, it is suggested that this OEP may be genetic rather than maturity controlled.

According to Longman & Palmer (1987) oils derived from source rocks of Ordovician age display a significant OEP within the C_{15}-C_{19} range as exemplified by group I oil samples 1339 and 1345. A number of workers investigating Ordovician oils, especially within North America midcontinent basins have reported significant OEP (e.g. Hatch et al., 1987; Jacobson, 1988). The unusual chemistry of these Ordovician sourced oils is caused by their derivation from *Gloeocapsamorpha prisca*, a unicellular prokaryote (Reed et al., 1986), which until recently was only known in Ordovician strata. Although a cautious interpretation of Ordovician derivation based on OEP is advised following a recent discovery of *G. Prisca* in Devonian strata (Fowler et al., 2004), the significant depletion in ^{13}C-isotopes among the group I oils (Table 2.1) supports the interpretation that these oils are Ordovician sourced. This interpretation is supported by empirical observations of significant ^{13}C-isotope depletion among Ordovician-sourced oils (e.g. Reed, 1986; Hatch et al., 1987; Longman and Palmer, 1987).

The Middle-Upper Permian reservoired oils earlier inferred to be derived from carbonate source rocks based on SARA distribution are observed to have low pristane/phytane (Pr/Ph) ratios (Tables 2.1 and 2.2) compared to the rest of the oils. The low Pr/Ph ratio that characterize these oils are consistent with derivation from anoxic depositional environments or carbonate source rocks (e.g. Seifert, 1975; Connan, 1981; Hughes, 1984; Palacas et al., 1984), reinforcing the argument in favor of carbonate sourcing for this sub-group of Permian age oils (group V oils).

Table 2.1: Oils Sample Identities, locations, and geochemical data for the Permian Basin oils studied (1381, 1382, 1363, 1370- group II/III leaning and 1558, 1473, & 1475-group IV leaning excluded). Table continues to next page.

Spl ID.	Top Dep.(ft)	Latitude	Longitude	County	Grp	°API	Sat/ Aro	‰ Oil	‰ Sat	‰ Aro	Can. Var.	CPI	OEP
1336		31.7688	-103.0591	Winkler	I	37.26	3.29	-33.30	-33.65	-32.88	0.52	1.11	1.15
1338	13200	31.6802	-102.2108	Midland	I	51.29	7.67	-33.28	-33.40	-32.21	1.38	1.17	1.17
1339		32.0624	-102.7074	Ector	I	38.25	2.61	-33.23	-33.90	-33.68	-0.62	1.05	1.83
1345		31.7680	-102.5353	Ector	I	47.67	4.23	-32.41	-32.88	-32.32	-0.18	1.28	1.76
1354	12800	32.2232	-102.2452	Andrews	I	49.65	8.38	-33.35	-33.44	-32.10	1.72	1.11	1.16
1334	8100	33.0642	-101.3080	Garza	II	38.05	1.43	-30.44	-30.65	-29.90	-0.45	1.10	1.10
1346	8110	33.0804	-101.2849	Garza	II	39.92	1.48	-30.60	-30.74	-30.22	-0.94	1.15	1.13
1331	5835	32.1755	-100.2713	Nolan	II	51.12	5.01	-29.97	-30.11	-29.53	-1.00	1.11	1.20
1333	6305	32.1296	-100.2984	Nolan	II	51.29	6.29	-29.92	-30.04	-28.82	0.40	1.18	1.14
1352	10381	32.9099	-101.7968	Dawson	II	39.57	1.23	-30.56	-30.69	-29.92	-0.40	1.14	1.08
1369	12237	32.4198	-102.2007	Martin	II	45.93	5.81	-30.04	-30.12	-29.51	-0.93	1.18	1.10
1374	12510	32.3973	-102.3809	Andrews	II	41.58	2.46	-31.48	-31.70	-30.85	0.09	1.13	1.09
1377		31.9342	-102.7413	Ector	II	36.88	1.74	-31.18	-31.31	-30.45	0.00	1.11	1.09
1379		31.5222	-102.4310	Crane	II	41.09	2.36	-31.65	-31.85	-30.83	0.52	1.12	1.12
1489	6630	33.1769	-100.8503	Kent	II	39.15	1.82	-29.56	-29.86	-29.32	-1.16	1.15	1.10
1497	7759	30.8470	-102.1635	Pecos	II	34.60	1.77	-30.82	-31.04	-30.61	-1.04	1.08	1.20
1499	8936	32.0769	-102.5554	Ector	II	39.90	2.86	-30.31	-30.64	-30.48	-1.77	1.20	1.10
1512	9012	31.6328	-102.4261	Crane	II	35.74	2.73	-31.10	-31.46	-31.09	-1.05	1.31	1.09
1591	8274	32.9808	-102.8974	Yoakum	II	42.24	1.81	-29.45	-29.61	-29.30	-1.75	1.13	1.09
1361	11650	31.4021	-102.1182	Upton	III	54.37	9.27	-29.95	-30.61	-28.86	1.75	1.09	1.19
1360	12450	31.8849	-102.1420	Midland	III	53.30	5.02	-30.10	-30.60	-28.88	1.68	1.19	1.35
1364	8651	31.6486	-101.0829	Sterling	III	45.84	2.15	-29.90	-30.29	-28.95	0.74	1.16	1.09
1367	11600	32.0384	-101.9680	Midland	III	54.27	9.90	-30.15	-30.80	-29.10	1.70	1.15	1.15
1372	11200	31.4091	-102.1205	Upton	III	50.16	8.82	-29.65	-29.91	-28.63	0.49	1.09	1.23
1511	6151	31.4965	-103.1958	Ward	IV	40.02	2.84	-28.20	-28.54	-28.01	-1.60	1.14	1.07
1531	8126	31.6394	-101.7025	Reagan	IV	38.84	3.16	-27.91	-28.18	-27.94	-2.35	1.24	1.08
1550	9522	31.3201	-102.0599	Upton	IV	44.12	3.95	-27.50	-27.93	-27.65	-2.34	1.26	1.08
1555	11227	31.6073	-103.2514	Ward	IV	43.25	2.25	-27.88	-27.97	-27.81	-2.59	1.24	1.07
1540	9010	32.4978	-102.5438	Andrews	IV	38.97	3.58	-27.60	-28.06	-27.33	-1.30	1.29	1.05
1581	7033	32.6763	-101.7480	Dawson	IV	40.25	2.29	-28.42	-28.80	-28.57	-2.18	1.24	1.10
1588	7953	32.4456	-101.9429	Martin	IV	35.72	2.19	-28.96	-28.96	-29.69	-4.26	1.24	1.13
1469	8195	32.6861	-101.7758	Dawson	IV	36.74	2.93	-28.46	-28.58	-27.88	-1.21	1.26	1.08
1486	4795	33.1918	-100.1646	Stonewall	IV	41.30	2.18	-29.28	-29.87	-29.53	-1.61	1.16	1.10
1487	6790	32.9700	-100.8364	Kent	IV	37.85	4.85	-29.59	-30.06	-29.94	-2.04	1.15	1.09
1495	6900	32.9692	-100.8228	Kent	IV	39.92	2.01	-30.30	-30.39	-29.91	-1.13	1.20	1.08
1502	9999	31.2743	-101.9669	Upton	IV	43.86	3.49	-27.73	-28.14	-27.51	-1.50	1.27	1.06
1496	6250	32.4680	-100.4756	Nolan	IV	45.82	3.08	-29.57	-29.88	-29.07	-0.56	1.22	1.12
1537	5951	32.5821	-102.7062	Gaines	V	29.68	0.67	-28.48	-29.00	-28.23	-0.92	1.10	1.03
1585	4555	32.3687	-101.2777	Howard	V	25.79	0.61	-28.82	-29.07	-28.56	-1.48	1.04	1.02
1586	5052	31.7669	-101.1985	Sterling	V	32.37	0.85	-27.52	-28.05	-27.26	-1.17	1.11	1.02
1593	5540	32.7785	-102.5126	Gaines	V	35.13	1.18	-28.95	-29.10	-28.73	-1.78	1.08	1.04
1538	9219	32.6003	-102.5754	Gaines	V	31.73	0.76	-27.76	-28.05	-27.40	-1.48	1.09	1.00
1594	7178	33.5000	-102.4068	Hockley	V	28.28	0.59	-28.44	-28.91	-28.61	-1.99	1.09	1.02

**Not measured. °API = API gravity; Sat = Saturated hydrocarbon fraction; Aro = Aromatic hydrocarbons fraction; ‰ Oil = $\delta^{13}C$ of whole oil (bitumen) relative to PDB standard; ‰Sat = $\delta^{13}C$ of Sat relative to PDB standard; ‰Aro = $\delta^{13}C$ of Aro relative to PDB standard; Can. Var. = Canonical Variable (Sofer, 1984) = -2.53 $\delta^{13}C_{Sat}$ + 2.22 $\delta^{13}C_{Aro}$ – 11.65; CPI = carbon preference index = ½*{(C_{25}+C_{27} + C_{29} + C_{31} + C_{33})/(C_{24} + C_{26} + C_{28} + C_{30} + C_{32}) + (C_{25}+C_{27} + C_{29} + C_{31} + C_{33})/(C_{26} + C_{28} + C_{30} + C_{32} + C_{34}); OEP = odd-over-even predominance = 2(C15+C17+C19)/3(C16+C18); Ts = 18α(H)-22, 29, 30-trisnorhopane = trisnorneohopane; Tm = 17α(H)-22, 29, 30 trisnorhopane; Ste.= sterane; Hop =17α(H), 21β(H)-hopane; BNH = Bisnorhopane Index = bisnorhopane/bisnorhopane+hopane;

Ph/ nC18	Pr/ nC17	Pr/ Ph	Ts/ Tm	HHI	BNH Index	Mor. Ratio	Ste./ Hop	Dia/ Ste	% C_{27}	% C_{28}	% C_{29}	C_{30} Ste. Index	DBT/ Phen	20S/ 20(S+R)	22S/ 22(S+R)
0.38	0.40	1.74	2.33	0.47	0.01	0.09	0.21	1.54	40.8	15.6	43.7	0.24	**	0.54	0.60
0.22	0.19	1.76	0.85	0.10	0.03	0.26	0.48	0.90	41.3	18.7	40.1	0.36	0.03	0.42	0.82
0.27	0.12	1.48	1.12	0.53	0.01	0.08	0.31	1.31	30.9	19.4	49.7	0.12	0.05	0.49	0.32
0.28	0.14	1.71	1.25	0.45	0.01	0.14	0.16	1.56	30.4	29.5	40.1	0.11	**	0.46	0.57
0.30	0.40	2.04	0.96	0.10	0.01	0.17	0.23	1.41	66.5	9.1	24.4	0.09	**	0.41	0.66
0.53	0.51	1.32	0.75	0.59	0.01	0.08	0.19	1.51	33.6	16.6	49.9	0.07	**	0.44	0.58
0.46	0.44	1.47	0.77	0.61	0.01	0.06	0.23	1.44	36.3	19.4	44.3	0.06	**	0.47	0.58
0.23	0.30	2.15	3.57	0.40	0.01	0.01	0.32	1.58	44.9	20.0	35.1	0.11	0.16	0.55	0.61
0.22	0.32	2.28	6.67	0.10	0.01	0.07	0.37	1.56	45.1	23.0	31.9	0.10	**	0.57	0.61
0.59	0.67	1.40	0.71	0.36	0.01	0.09	0.27	1.63	34.8	19.1	46.2	0.02	**	0.48	0.63
0.26	0.41	2.13	2.38	0.36	0.01	0.13	0.34	1.56	44.5	12.7	42.8	0.17	**	0.53	0.56
0.47	0.52	1.42	5.56	0.45	0.06	0.17	0.54	1.42	28.9	18.4	52.8	0.07	**	0.43	0.74
0.36	0.44	1.68	1.04	0.10	0.01	0.01	0.14	1.85	40.4	10.2	49.4	0.10	**	0.52	0.75
0.34	0.50	2.08	3.57	0.25	0.01	0.13	0.52	1.36	31.2	20.2	48.6	0.06	**	0.44	0.66
0.44	0.53	1.62	0.97	0.60	0.03	0.06	0.33	1.33	36.8	19.0	44.2	0.06	**	0.48	0.66
0.35	0.30	1.35	0.67	0.10	0.01	0.03	0.34	1.32	32.9	16.2	50.9	0.02	**	0.52	0.63
0.64	0.99	1.89	2.78	0.35	0.01	0.60	0.30	1.53	38.9	20.8	40.3	0.09	0.05	0.54	0.59
0.78	1.16	1.70	3.23	0.10	0.01	0.01	0.29	1.56	34.0	11.1	54.9	0.10	**	0.49	0.76
0.43	0.59	1.87	1.96	0.55	0.02	0.08	0.30	1.39	40.2	17.3	42.5	0.08	**	0.45	0.58
0.15	0.22	2.62	0.69	0.65	0.01	0.05	0.26	1.56	34.5	19.7	45.8	0.07	**	0.49	0.56
0.18	0.22	2.66	1.72	0.65	0.01	0.08	0.25	1.69	34.2	23.8	42.0	0.12	**	0.53	0.56
0.21	0.35	2.29	3.13	0.10	0.01	0.11	0.28	1.66	29.8	29.4	40.7	0.05	**	0.49	0.81
0.31	0.47	2.34	2.17	0.37	0.01	0.09	0.23	1.74	35.2	24.4	40.4	0.10	**	0.48	0.57
0.14	0.20	2.49	0.77	0.73	0.01	0.04	0.38	1.38	32.6	25.9	41.5	0.07	**	0.47	0.45
0.90	1.08	1.39	0.88	0.35	0.02	0.11	0.19	1.21	37.8	20.9	41.2	0.10	**	0.50	0.61
0.74	0.89	1.43	2.00	0.44	0.02	0.11	0.19	1.38	37.5	25.2	37.4	0.12	**	0.52	0.60
0.60	0.76	1.52	0.88	0.10	0.12	0.26	0.28	1.73	30.6	14.0	55.5	0.03	**	0.49	0.55
0.67	0.83	1.54	1.02	0.60	0.01	0.08	0.13	1.61	38.3	17.3	44.4	0.09	0.36	0.46	0.61
0.48	0.80	1.83	2.00	0.50	0.01	0.23	0.38	1.35	43.1	17.0	39.8	0.15	0.24	0.53	0.77
0.84	1.08	1.55	1.69	0.21	0.01	0.10	0.15	1.59	36.6	23.9	39.5	0.06	**	0.49	0.57
1.27	1.40	1.31	0.98	0.45	0.01	0.09	0.15	1.33	38.6	21.3	40.1	0.06	**	0.44	0.57
0.65	1.08	1.85	1.45	0.15	0.01	0.13	0.15	1.50	42.4	19.6	38.1	0.10	**	0.47	0.61
0.73	0.96	1.61	1.06	0.54	0.05	0.16	0.27	1.02	48.3	17.5	34.2	0.07	0.19	0.40	0.59
0.56	0.65	1.44	0.10	0.60	0.03	0.11	0.26	1.42	41.3	19.4	39.4	0.07	0.23	0.44	0.67
0.66	0.75	1.33	0.93	0.56	0.02	0.10	0.26	1.06	44.5	20.6	34.9	0.08	0.2	0.47	0.67
0.41	0.67	1.89	3.57	0.48	0.01	0.09	0.28	1.48	42.5	11.1	46.4	0.13	0.07	0.53	0.70
0.52	0.72	1.82	1.20	0.56	0.01	0.07	0.39	1.32	45.3	22.0	32.7	0.09	0.06	0.55	0.71
0.75	0.50	0.77	0.56	0.63	0.01	0.07	0.09	1.94	39.7	15.7	44.6	0.05	3.43	0.44	0.58
0.96	0.42	0.50	0.88	0.69	0.01	0.07	0.08	2.17	39.2	17.5	43.4	0.03	3.55	0.44	0.55
0.81	0.53	0.73	1.14	0.65	0.01	0.06	0.07	2.50	40.9	13.7	45.4	0.04	7.04	0.44	0.56
0.53	0.49	1.10	0.55	0.64	0.01	0.06	0.11	1.76	36.6	16.1	47.4	0.05	2.22	0.45	0.58
0.77	0.39	0.56	0.66	0.67	0.01	0.06	0.07	2.23	39.3	12.8	47.9	0.04	6.01	0.44	0.55
0.73	0.31	0.50	0.85	0.63	0.01	0.07	0.08	2.16	36.6	14.5	48.9	0.05	4.79	0.44	0.57

Mor.= Moretane = 17β(H), 21α(H)-hopane; DBT = Dibenzothiophene; Phen=Phenanthrene; %C_{27} = C_{27}ααα R/(C_{27}ααα R+ C_{28}ααα R+ C_{29}ααα R); %C_{28} = C_{28}ααα R/(C_{27}ααα R+ C_{28}ααα R+ C_{29}ααα R; %C_{29} = C_{29}ααα R/(C_{27}ααα R+ C_{28}ααα R+ C_{29}ααα R; C_{30} Ste. Index = C_{30}ααα R/(C_{27}ααα R+ C_{28}ααα R+ C_{29}ααα R); HH = Homohopanes = C_{31}-C_{35} hopanes; HHI = Homohopane Index = C_{35}Hop/(C_{35}Hop + C_{34}Hop); Norhop. = Norhopane = C_{29}-hopane; Mor. Ratio = Mor./(Mor. + Hop + Norhop.); Ste./Hop = C_{27}+C_{28} + C_{29} (αββ R +S) Ste./(Norhop. + Hop + HH). Group I = Simpson PS; Group II = Barnett-Woodford PS; Group III = Barnett-Woodoford PS; Group IV = Wolfcamp PS and Group V = Bone Spring PS; PS = petroleum system.

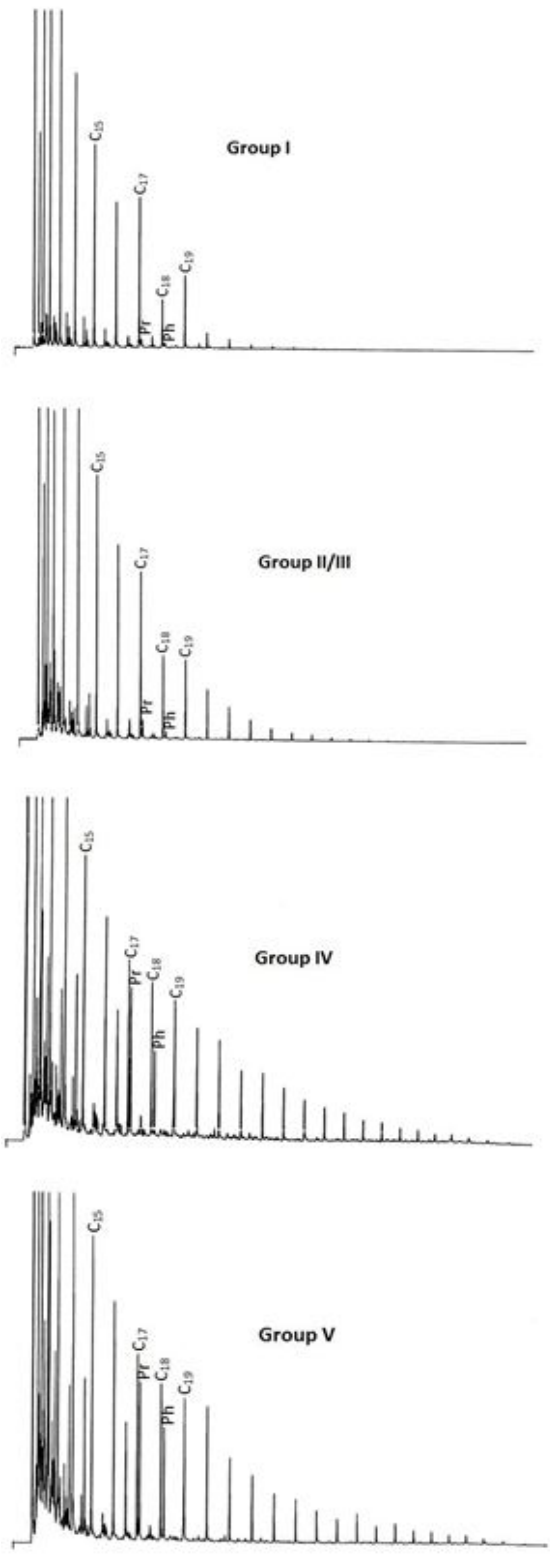

Figure 2.5: Group I-V representative gas chromatograms. Note the OEP within nC_{15} to nC_{19} range and the near absence of isoprenoids (pristane and phytane) in Group I.

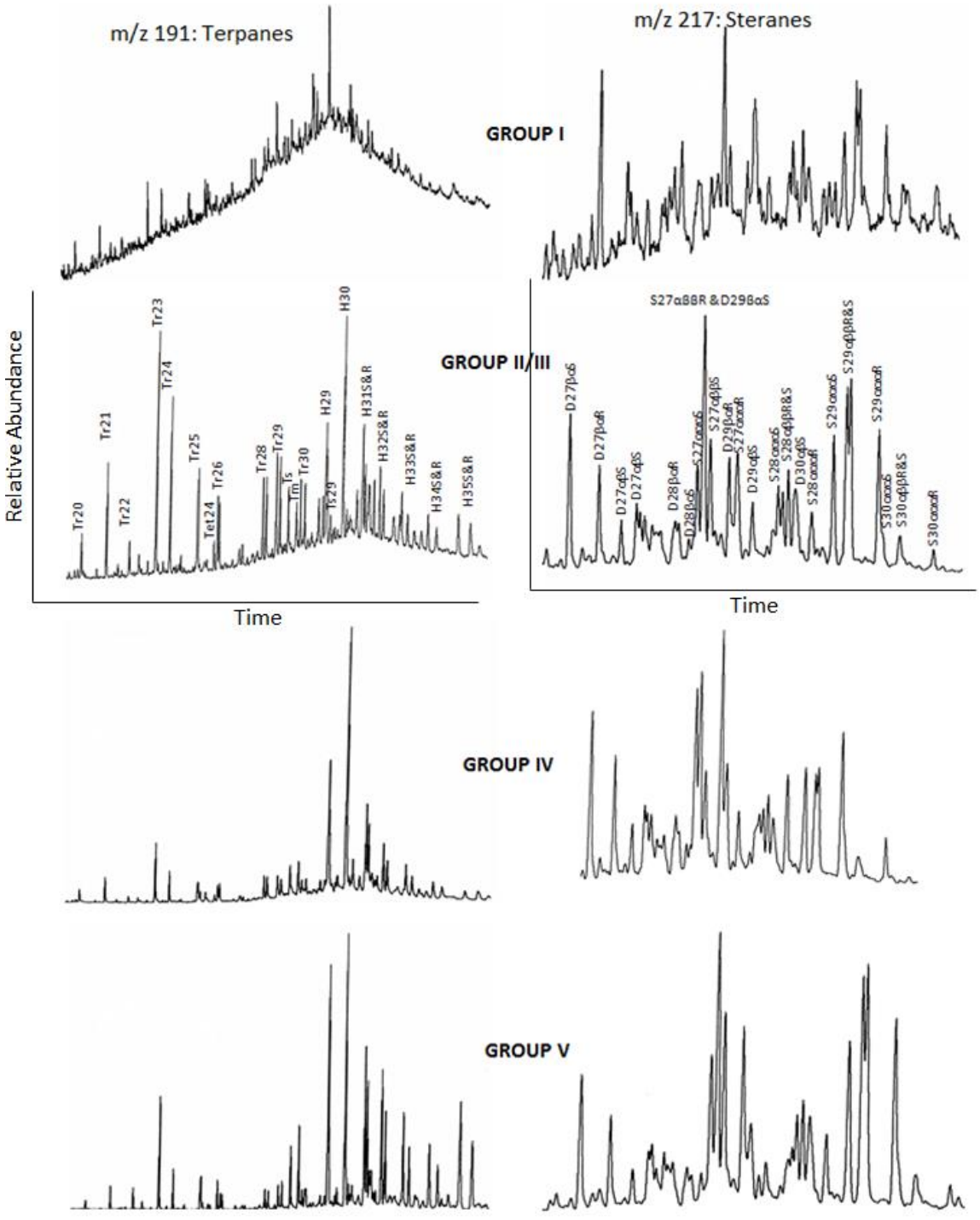

Figure 2.6: Groups I through V oils representative GC-MS ions (m/z 191 for Terpanes and m/z 217 for Steranes) chromatograms for Permian Basin oils studied. Nomenclature as annotated in group II/III apply to the rest of the groups. Note the elevated norhopane (H_{29}) and C_{35} homohopanes (H35S&R) among group V oils. High norhopane and homohopane are typical in highly reducing environments associated with carbonate sourced oils (e.g. Fan Pu et al., 1988; ten Haven et al., 1988).

2.4.3 Chemometrics and Oil-Oil Correlations

One of the most striking characteristics revealed by chemometrics is the high degree of similarity among the Permian Basin oils (Figure 2.7), an artifact that is attributable to significant reduction of biomarkers with increasing maturity (e.g. Peters and Moldowan, 1993). Despite this potential encumbrance, chemometric analysis using source related biomarker and stable carbon isotope data (agglomerative hierarchical clustering (AHC) and principal component analysis (PCA)) discerned five genetic groups (Figure 2.7). Group I oils (not distinct in dendrogram) are distinct in the PCAs (Figure 2.7ii, iii & iv) and are characterized by an extremely negative stable carbon isotopic compositions (Table 2.1).

Oils in the "spurious" category (Figure 2.7i) are interpreted to represent mixed or highly influenced oils. Such evidence is provided, for example, by oils having significant OEP but with heavy isotopic signature. Examples include oil samples 1381, 1382, 1363, and 1370 which share characteristics with groups I, II, and III (note the wandering associations in Figures 2.7ii, iii & iv). This apparent mixing of oils is observable even within well-established groupings as discussed in the following sections. Overall, the groupings suggest, origin of oils from at least five distinct source rocks, suggesting five independent petroleum systems. Observed subgroupings, are interpreted to be due to inherent source rock facies variations, possible oil mixing, and potential imprints associated with varying migration routes.

Besides the mixing possibility, most of the oils in this "spurious" category are condensates. The biomarker signature of condensates is generally low, and may explain

their apparent “unrealistic” correlations. This is also the case of group III oils (all condensates except one, 1364). A low level of confidence is therefore assigned to this genetic group inference.

Conventional geochemical correlations, based on sound understanding of geochemical principles were useful in discerning “accidental” associations in chemometrics. For example, oils 1550 and 1502 appearing within subgroup 2A in Figure 2.7i are actually group IV oils. As discussed in the following section, though all other parameters are consistent with group II, these oils are isotopically too heavy to be part of group II. It would be very difficult to account for 4‰ carbon isotope difference among oils of a single source or genetic group unless these latter oils are cracked. These can only be understood upon thermal modeling.

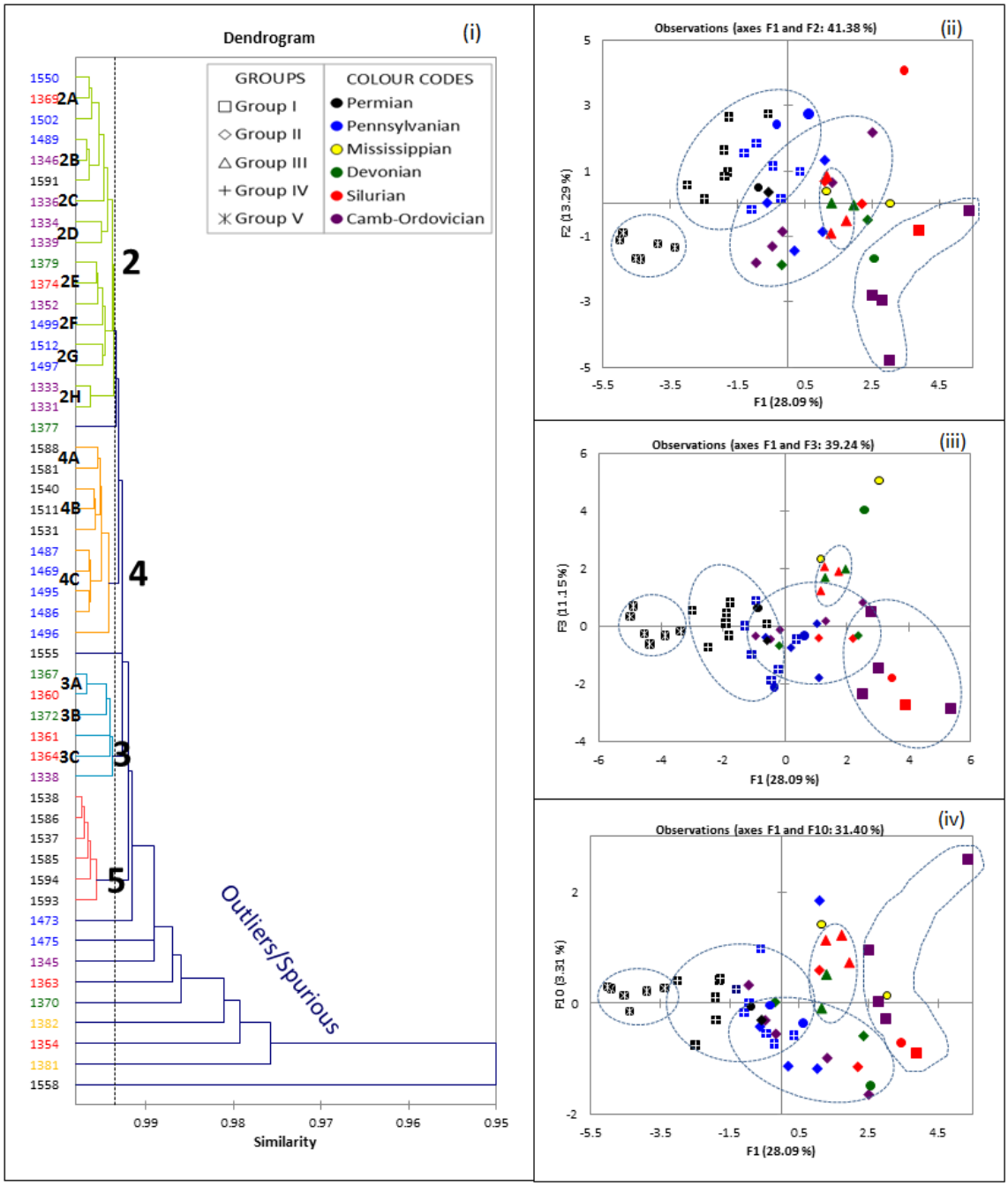

Figure 2.7: Dendrogram (left, i) showing the clustering of oils into genetic groups based on 13 genetically oriented geochemical parameters. Groupings and sub-groupings agree with principal component analyses, PCAs (right, ii, iii, & iv). Group numbering is based on age of projected source rocks, from oldest to youngest. Filled circles in PCAs represent spurious oils in the dendrogram. Note the wandering associations of the spurious oils in the PCAs. In general however, Mississippian reservoired oils 1381 & 1382 and Devonian reservoired oil 1370 are generally associated with group III while 1473 and 1475 are, in general associated with the Pennsylvanian reservoired oils of group IV.

2.4.4 Source Age and Organic Matter Type

Underpinning the geochemical utility of stable carbon isotope composition is the realization of its systematic variation over geologic time (e.g. Degens, 1969; Chung et al. 1992; Andrusevich et al., 1998; Riebesell et al., 2000) and the consistent observation of stable carbon isotope ratios of saturated and aromatic hydrocarbons among terrigenous (waxy oils) and marine sourced oils (Sofer, 1984). Applying these fundamental observations to the Permian oils data set (Table 2.1), we were able to decipher the possible ages and organic matter types responsible for the oils (Figures 2.8 & 2.9). The data depict the oils to be derived from marine Paleozoic source rocks.

Although age interpretation of stable carbon isotope data is not without ambiguities, such as may be caused by stable carbon isotope fractionation during maturation (e.g. Chung et al., 1981; Peters et al., 2005) and fractionation during primary productivity or changes associated with variations in water circulation patterns (e.g. Hayes, et al., 1983; Hatch et al., 1987), the general consistence of groupings as observed in the stable carbon isotope plots (Figures 2.8 and 2.9) versus that in chemometrics (Figure 2.7) suggests minor effects, if any. The oils are sourced from source rocks that range in age from Ordovician to Permian. This inference is also supported by $C_{29} > C_{27}$ steranes (Grantham and Wakefield, 1988). Except group III oils, which show a strong terrigenous affinity as reflected by their relatively high Pr/Ph ratios, and most importantly their positive canonical variable (Table 2.1), the rest of the oils are derived from marine source rocks.

Group I oils (1336, 1338, 1339, 1345 and 1354), hosted in Ordovician and Cambrian reservoirs are characterized by extreme ^{13}C-isotope depletion. Although these oils do not

form a distinct group in the dendrogram in Figure 2.7(i), they plot in distinct regions in the principal component analysis plots (Figures 2.7ii-iv). Their high OEP, low biomarker abundance (Figure 2.6) and the associated extreme ^{13}C isotope depletion are consistent with derivation from Ordovician source rocks (e.g. Longman and Palmer, 1987; Hatch et al., 1987; Jacobson et al., 1988), represented in the Permian Basin by the Simpson Group (Figure 2.2).

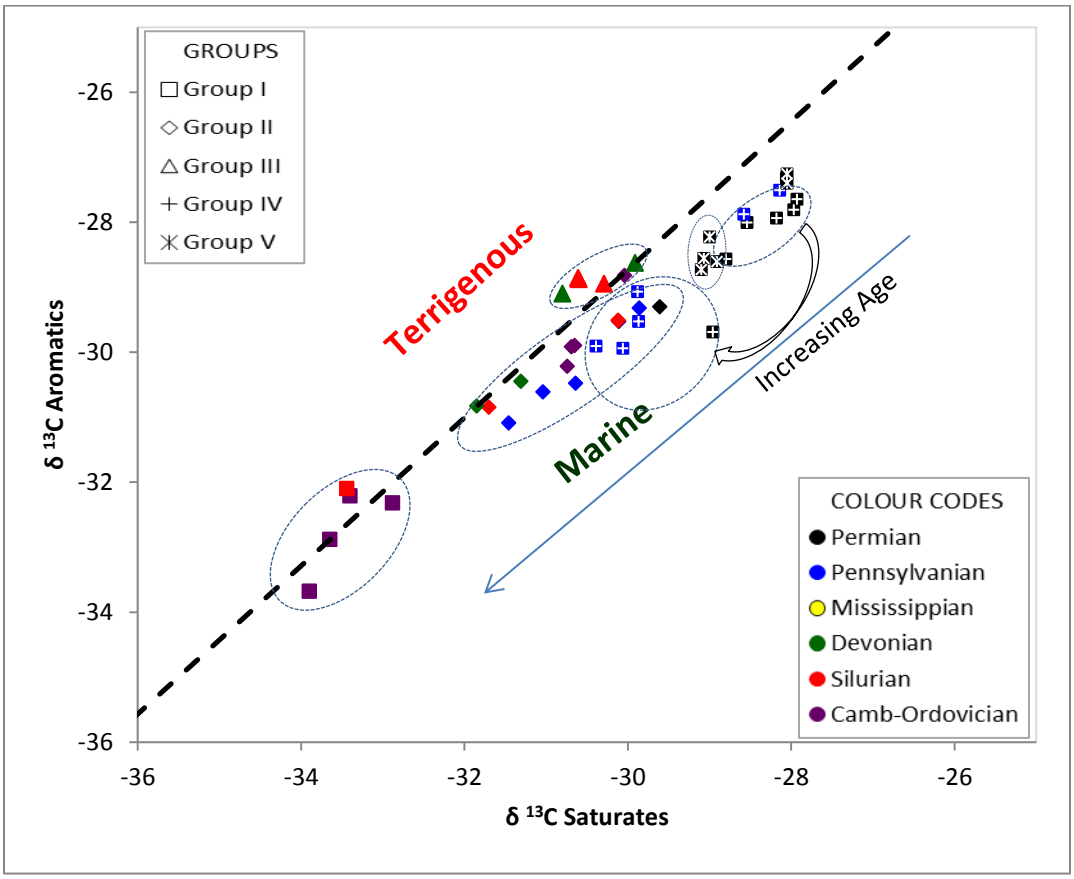

Figure 2.8: Stable carbon isotope ratios in ‰ relative to PDB standard for saturated versus aromatic hydrocarbons. The line separating the terrigenous from marine derived oils is based on statistical analysis of hundreds of known oils (Sofer, 1984). Note the subgroupings among groups II and IV oils.

Groups II and III oils, reservoired in a large stratigraphic extent from Ordovician to Permian have stable carbon isotope compositions from -31.65 to -29.99‰, a range consistent with Devonian-Mississippian age sources (e.g. Mook, 2001; reported in Peters

et al., 2005). Moreover, the Upper Devonian-Lower Mississippian Woodford Shale in the Anardako Basin, Oklahoma is reported to have typical $\delta^{13}C_{saturate}$ values of -30‰ and $\delta^{13}C_{aromatic}$ between -29‰ and -30‰ (Denison, 1990; reported in Wang and Philp, 1997). Closer scrutiny however, indicates that group III oils are different from group II by having higher Pr/Ph ratios and more positive canonical variables. Although Pr/Ph can significantly be affected by maturity, in general, these parameters suggest a significant input of terrigenous organic matter (e.g. Sofer, 1984; Moldowan et al., 1985). Group II oils that are isotopically associated with group III are either due to extreme maturities e.g. 1331, 1333, and 1369 or potentially influenced (1489 & 1591) by the younger group IV oils as indicated in the chemometric projections (Figure 2.7). High maturity levels isotopically displace oils in a positive direction while early generated oils from younger sources have lighter isotopic signatures. However, given that all group III oils and most of group II associated with them are condensates, establishing unambiguous genetic identification based on biomarkers can only be possible upon a thorough study of the source rocks. Until a detailed understanding of source rocks is obtained, group II and group III remain indistinguishable at this point.

Group IV oils are reservoired in Permian and Pennsylvanian reservoirs. Isotopically, the Pennsylvanian reservoired oils are closely associated with group II oils (Table 2.1 and Figure 2.8). However, their lower maturity compared to group II oils (see Section 2.4.6) suggests this as a pseudo association, caused by potential mixing as explained by such a large isotope range of 2.8‰ (Tables 2.1 & 2.2). Despite having a similar group maturity, this subgroup of Pennsylvanian oils is enriched in tricyclics relative to diasteranes. This

relative enrichment is here interpreted to be due to geochromatography (e.g. Seifert et al., 1979) associated with long distance migration, implying that Permian reservoired oils are closer to the source rock than their Pennsylvanian counterparts. This interpretation suggests the Lower Permian (Wolfcamp) as a likely source rock, expelling hydrocarbons to reservoirs within the Permian, as well as the underlying Pennsylvanian reservoirs. As noted earlier, because of having a biomarker semblance with group II oils and stable carbon isotope composition range of 4‰, source rock analysis and thermal modeling is required to understand the actual character of the Wolfcamp, so as to validate the migration interpretation and the possible origin of 1550 and 1502 oils. In particular, it is important to know if some of the source rocks and oils are cracked.

Group V oils, located in the Middle and Upper Permian reservoirs are characterized by isotopic signatures that suggest sourcing from Permian age source rocks (Mook, 2001; reported in Peters et al., 2005). The relative ^{13}C-isotope depletion compared to a majority of other Permian sourced oils, for example, group IV oils, is consistent with their lowest maturity as predicted and confirmed in the maturity section (see Section 2.4.6). The relative ^{13}C-isotope depletion may also be explained by a relatively deeper depositional environment, where limited utilization of atmospheric carbondioxide for photosynthesis was involved (e.g. Holmden et al., 1988; Sigman and Boyle, 2000; Young et al., 2005). The deeper depositional environment for these oils is supported by their low Pr/Ph ratios (Table 2.1). Because, these oils display similar maturities, the observed ^{13}C-isotope enrichment displayed by 1586 and 1538, may suggest possible mixing with group IV.

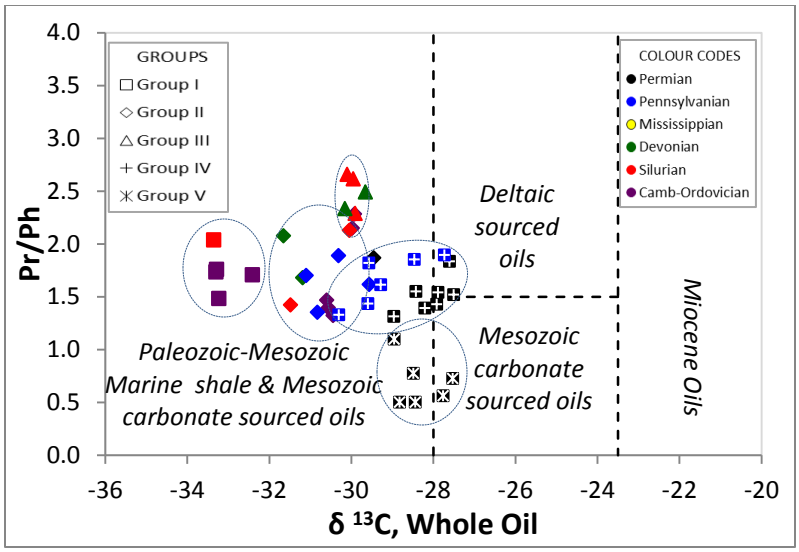

Figure 2.9: Plot of acyclic isoprenoids ratio versus stable carbon isotope (whole oil), illustrating the age of the source rocks responsible for the oils (divisions after Chung et al., 1992). Pr = Pristane; Ph = Phytane.

2.4.5 Source Depositional Environments and Lithology

Since the early recognition of the role of acyclic isoprenoids (pristane and phytane), particularly the Pr/Ph ratio as a proxy for the redox of depositional environments (Powell and McKirdy, 1973), and follow up studies (e.g. Didyk et al., 1978; McKirdy, 1983; ten Haven et al., 1987), Pr/Ph ratio less than one is generally interpreted to mean deposition under anoxia while greater than one implies relative oxicity. Ratios above three represent significant terrestrial organic matter input, typically in proximal, often paludal environments (e.g. Hughes, 1984; Palacas et al., 1984; Tissot & Welte, 1984; Peters et al., 2005). Furthermore, the relative thermal stability of corresponding normal alkane relative to acyclic isoprenoids (ten Haven et al., 1987) and the converse response to biodegradation, due to preferential removal of *n*-alkanes (e.g. Connan, 1984), makes ratios Pr/nC$_{17}$ and Ph/nC$_{18}$ useful proxies for maturity and biodegradation as summarized in the Figure 2.10.

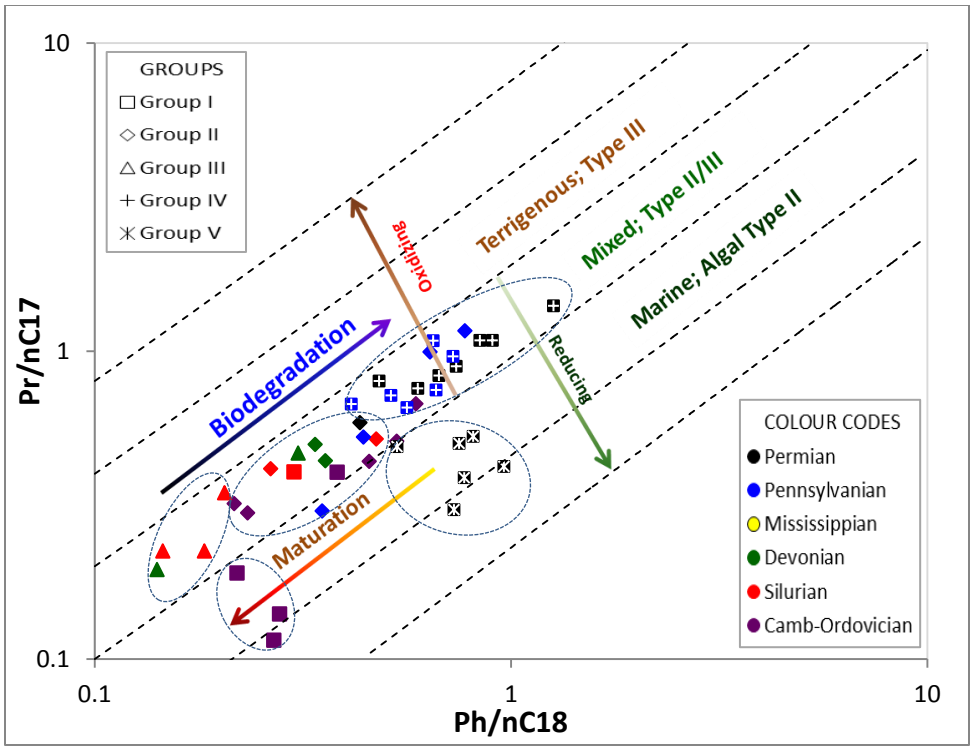

Figure 2.10: Prediction of source organic matter type, redox of depositional environment using a plot of Pristane/nC_{17} versus Phytane/nC_{18} ratios derived from gas chromatograms of saturated hydrocarbon fractions (Template from Peters et al., 1999).

Acyclic isoprenoids and corresponding *n*-alkanes data for oils from the Permian Basin (Figure 2.10), indicates that, except for group I and group V oils which depict derivation from a purely marine type II organic matter, in highly reducing conditions, a majority of the oils are derived from mixed organic matter type II/III. These inferences are also supported by a number of parameters including the homohopane index, pristane/phytane ratios and sterane/hopane ratios (Table 2.1), where group I and, especially group V oils have significant homohopane index accompanied by low Pr/Ph ratios (Figures 2.10 & 2.11), typical ratios found in anoxic marine settings (e.g. Seifert, 1975; Chappe et al., 1980; Peters and Moldowan, 1991).

Demaison and Bourgeois (1985) further noted that such extreme anoxia as reflected by very low pristane/phytane ratio may be associated with carbonate sourcing. Such conditions as well, predict sulfate reduction (e.g. Barbat, 1967) and may result in sulfur-rich oils if the source lithology is carbonate (Peters and Moldowan, 1993).

Plots involving isoprenoids (Figures 2.9, 2.10, 2.11, & 2.12) provide fairly good separation amongst the oil groups. In general, a marine depositional environment for all oils is implied, in agreement with inference from stable carbon isotope data (Figure 2.8). A majority of the oils plot in fields depicting derivation from Paleozoic shale source rocks based on the stable carbon isotope compositions (Figure 2.9). Group V oils stand out from the rest, with highly reducing signatures that suggest possible carbonate sourcing (Figure 2.11). Group V oils also have elevated norhopane as well as an elevated homohopane index (Table 2.1 & Figure 2.6), features typical of carbonate sourced oils (e.g. Hughes, 1984; Fan Pu et al., 1988; ten Haven et al., 1988). Using the dibenzothiophene/phenanthrene ratio as a proxy for sulfur content (Hughes et al., 1995), I was able to further corroborate the carbonate sourcing of group V oils.

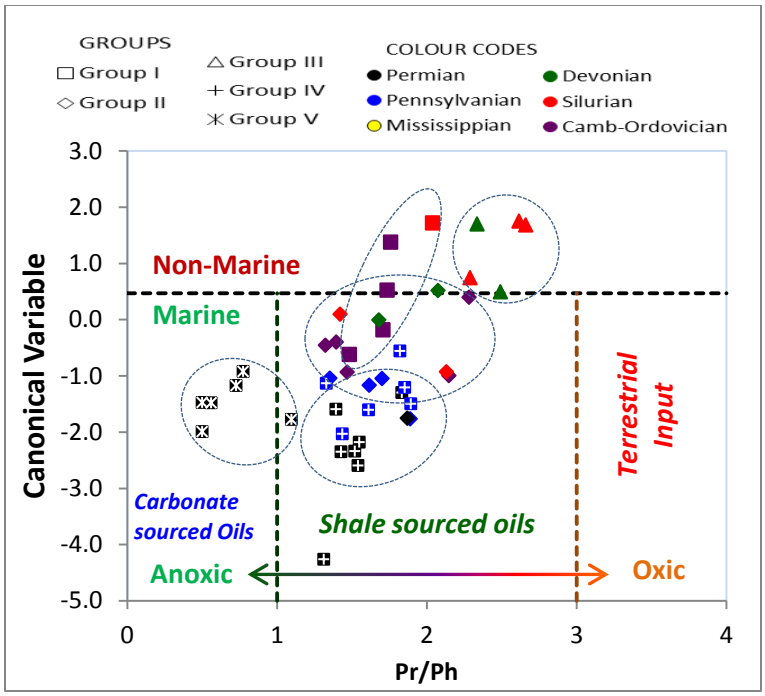

Figure 2.11: Canonical variable, CV (Sofer, 1984) versus acyclic isoprenoids (Pristane/Phytane) ratio, illustrating the depositional conditions, organic Matter type and source lithology. Most of the oils are sourced from marine shale source rocks at sub-oxic conditions. Pr = Pristane; Ph = Phytane.

This additional support for carbonate sourcing also created more questions. For example, in Figure 2.12, the group V oils do not plot in the carbonate zone. The oils have relatively high diasterane/sterane ratios, contrary to expectations from carbonate sourced oils. Moreover, this group is the least mature among the groups. The thermal stability of diasteranes relative to regular steranes may cause high diasterane/sterane ratios in both carbonates and siliciclastics. Clay minerals are required to catalyze the transformation of steranes to diasteranes (Peters and Moldowan, 1993), as such are often enriched in siliciclastic sourced oils or in highly mature oils. The evidence is consistent with the group V oils having originated from source rocks of mixed carbonate-shale facies or possibly having undergone long distance migration or both. Preferential enrichment in diasterane relative to steranes is a documented phenomenon in hydrocarbon migration

(e.g. Peters et al. 1990; Lewan et al., 1986). This interpretation suggests a possible origin of group V oils from the Bone Spring Formation in the Delaware as indicated in Jarvie and Hill (2011), where Pr/Ph and stable carbon isotope ratios are comparable to the findings here. The groups II, III and IV are composed of oils sourced from marine suboxic shale source rocks, with group III oils also containing some non-marine input.

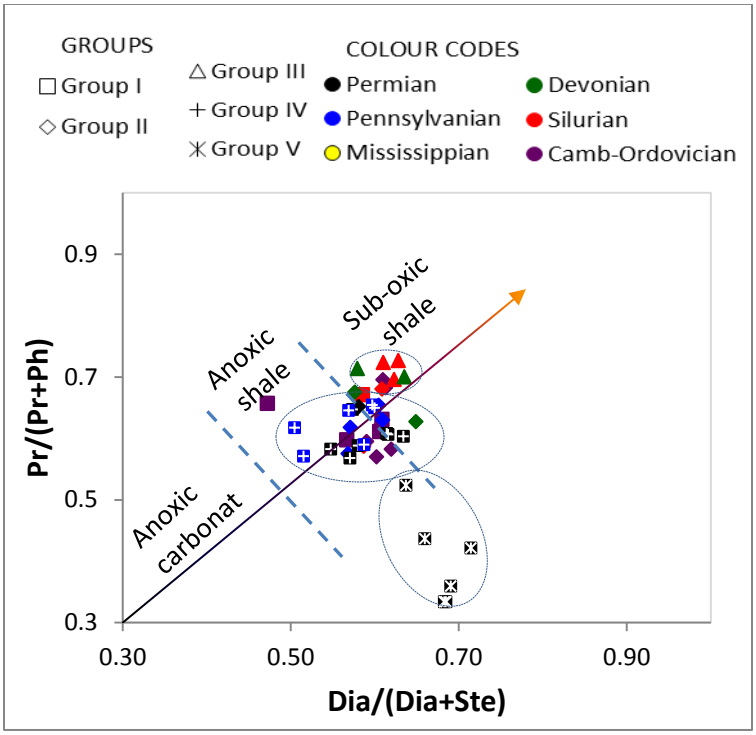

Figure 2.12: The sum ratio of C_{19} and C_{20} acyclic isoprenoids versus the sum ratio of diasteranes and regular steranes indicating the lithology of source rocks responsible for the oils. The line indicates approximate correlation and the arrow indicates direction of change associated with increasing maturity (after Moldowan et al. 1986). Dia = Diasterane; Ste = Steranes as identified and measured in m/z 217 mass fragmentograms (see Figure 2.8).

2.4.6 Source Maturity

A plot of common conventional biomarker maturity parameters, 20S/20[S+R] versus 22S/22[S+R] (Figure 2.13) indicates that nearly all the oils were generated at peak maturity, with a majority currently plotting beyond the bounds for which these isomerization parameters are reliable as maturity indicators (e.g. Mackenzie, 1984;

Moldowan et al., 1992; Waples & Machihara, 1991; Peters et al., 1999). To circumvent this limitation, we chose to use more thermally resilient parameters to decipher maturity variations among the oils and within the oil groups. Specifically we used the percentages of diasteranes and tricyclics (e.g. Van Graas, 1990). Although both tricyclics and diasteranes can be significantly affected by migration, the general consistency of maturity groups (Figure 2.14) with groupings established by chemometrics (Figure 2.7) suggests that, migration and lithology effects, if any, are very minimal. Moreover, there is a general maturity consistency as shown by both CPI and to some extent Ts/Tm data (Tables 2.1 and 2.2) except for group V oils, where there is interference due to carbonate sourcing.

As shown in Figure 2.14, the oils and oil groups show a range of maturities, reflecting the different thermal zonation associated with the structural make-up of the Permian Basin. Groups V and II represent extreme maturities, the least mature Group V on one end and the most mature group II on the other; with groups IV, I, and III, in order of increasing maturity lying in between. Except for oils projected to be sourced from Ordovician age, the rest of the oil groups show maturities consistent with the projected ages of their source rocks. The deviation of group I oils is deemed to be a consequence of the structural make-up of the Permian Basin. The data suggest that, the Ordovician-sourced oils may have originated from the uplifted portion of the Permian Basin, where, thermal stress is significantly lower due to its shallow depth (Figure 2.1).

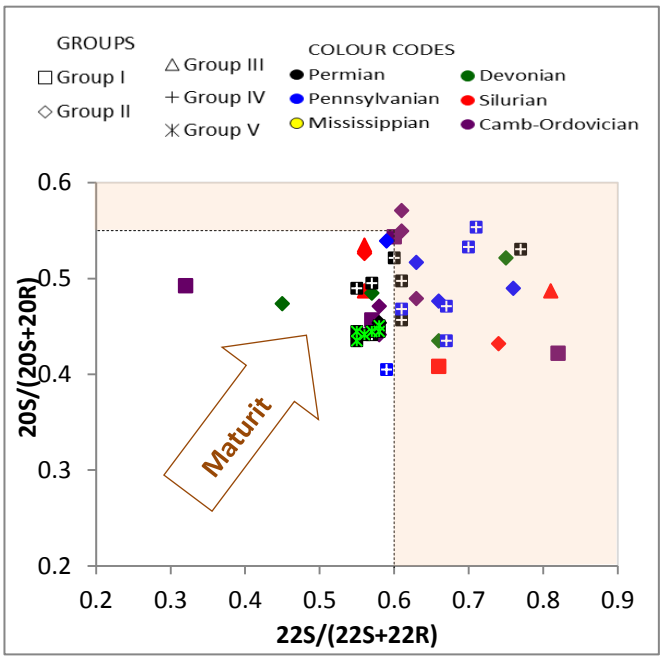

Figure 2.13: Sterane (20S/(20S+20R)) and Hopane (22S/(22S+22R)) biomarker isomerization type maturity parameters showing maturity of the oils. Oils generally show peak maturity, with most of the oils plotting in the shaded region where further maturation does not significantly increase ratios or are unreliable (e.g. Peters et al. 1999).

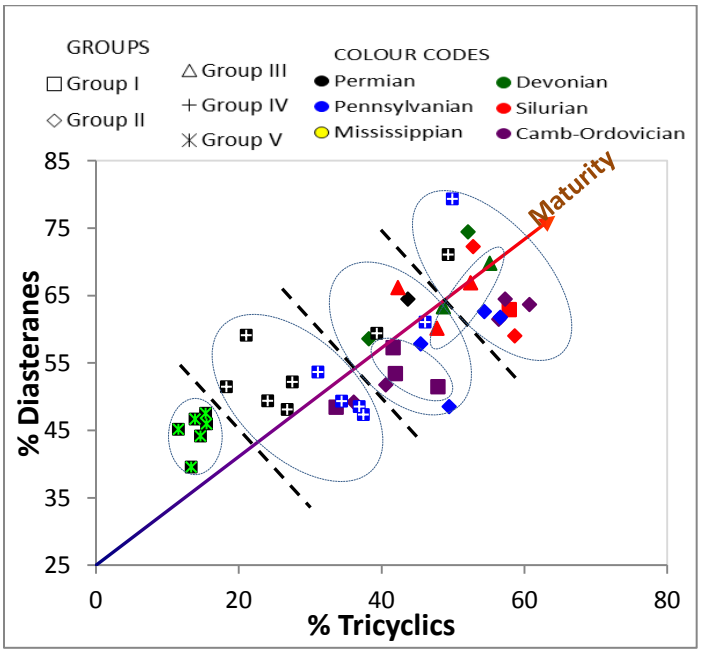

Figure 2.14: Percent diasteranes (measured as percentage of total components in the m/z 217 'sterane' fragmentogram) versus percent tricyclics (C_{19} through C_{29} tricyclis as percent of total identified m/z 191 fragmentogram). Both diasteranes and tricyclics increase with maturity (Seifert and Moldowan, 1978; Peters et al., 1986; Peters and Moldowan, 1991) as indicated by the arrowed line. Transverse dotted lines are maturity demarcations suggested by the data.

The two maturity clusters displayed by groups II and III oils can also be explained by evoking the structure of the Permian Basin. In general, the high maturity cluster (1331, 1333, 1352, 1369, 1374, 1379, 1499, & 1512) is geographically associated with the Midland Basin while the lower maturity cluster (1377, 1346, 1497, 1499, 1591, & 1489) is geographically in close proximity with the shallower Central Basin Platform and Eastern shelf. These observations are consistent with generation from two major kitchens for which the deeper Delaware Basin on the west is not represented, implying effectively sealing platform boundary faults.

Excluding the oils influenced by group II (1550 & 1502), group IV oils cluster into two thermal regimes, represented by 1555 on one end and 1581, 1588, 1540, 1511, 1531, 1487, 1469, 1495, & 1486 on the other end. An apparent third thermal regime, represented by 1496, is likely an artifact of enrichment of both diasteranes and tricyclics during migration. The two kitchens responsible for the group IV oils are in the Delaware and Midland basins. The absence of a third thermal regime is consistent with the geological development of the Permian Basin, which dictated the absence by non-deposition and erosion in the Central Basin Platform during the Early Permian (Wright, 1979; Hills and Galley, 1988), supporting the Early Permian as the source rock for group IV oils. Group V oils represent one thermal regime, thus a single source kitchen.

Table 2.2: Inferred source rock characteristics from oil properties

	Group I		Group II		Group III		Group IV		Group V	
	Range	Avg.	Range	Avg.	Range	Avg.	Range	Avg.	Range	Avg.
°API	37.3 - 51.3	44.8	34.6 - 51.3	41.22	45.8 - 54.4	51.6	35.7 - 45.8	40.55	25.8 - 35.1	30.5
OEP	1.2 - 1.8	1.4	1.1 – 1.2	1.12	1.1-1.3	1.2	1.1	1.1	1.0	1.0
CPI	1.1 - 1.3	1.1	1.1 – 1.3	1.15	1.1-1.2	1.14	1.2 - 1.3	1.23	1.0 – 1.1	1.09
Pr/ Ph	1.5 - 2.0	1.8	1.4 – 2.3	1.74	2.3 - 2.7	2.48	1.3 – 1.9	1.59	0.5 – 1.1	0.69
$\delta^{13}C$	-33.4- -32.4	-33.5	-31.6- -29.5	-30.5	-30.8-29.9	-29.9	-30.3- -27.5	-28.6	-28.9- -27.5	-28.3
Can. Var.	-0.6 - 1.7	0.56	-1.8 - 0.52	-0.68	0.49 1.75	1.28	-4.3 - -0.6	-1.92	-2.0 - -0.9	-1.47
Ste/ Hop.	0.16 - 0.48	0.28	0.14 – 0.54	0.32	0.23 – 0.38	0.28	0.13 – 0.39	0.24	0.07 – 0.11	0.08
Ts/ Tm	0.9 – 2.3	1.3	0.7 – 6.7	2.5	0.7 – 3.1	1.7	0.1 – 3.6	1.4	0.6 – 1.1	0.8
Inferred Source Rocks Characteristics										
Kerogen Type	Type II		Type II/III		Type II/III		Type II		Type II	
Source Lithology	Mar. Shale		Mar. Shale		Mar. Shale (Hi. Terr. o.m)		Mar. shale		Mar. Marl	
Dep. Env. Redox	Anoxic		Sub-oxic		Sub-oxic		Sub-oxic		Anoxic	
Source Age	Ordovician		Devonian		Mississippian		L-M Permian		M-U Permian	
Source Maturity	Peak		Past Peak		Past peak		Peak		Oil-Window	

Mar. = Marine; Dep. Env. = Depositional Enviornment

2.5 Inferred Petroleum Systems

2.5.1 Petroleum System I

This petroleum system comprises Ordovician-sourced group I oils; 1336, 1338, 1339, 1345, and 1354. According to depth and geographic locations of these oils vis-à-vis the Permian Basin play framework (Dutton et al., 2004; 2005), the Cambrian-Ordovician reservoired oils of this group belong to two plays; the Simpson cratonic sandstone play and Ellenberger karst modified restricted ramp carbonate play, both geographically located within the Central Basin Platform. The Ellenberger play extends to the Midland

Basin (Figure 2.15). The Silurian oil (sample 1354) resides in the lowest part of Silurian Fusselman shallow platform carbonate play in Midland Basin. However, we believe that this accumulation actually belongs to Ordovician Simpson cratonic sandstone play. This re-assignment considers three likely scenarios, including; possible poor constraint on the upper limits of Ordovician strata, potential poor sealing, and the likelihood of the Ordovician seal being an effective source rock.

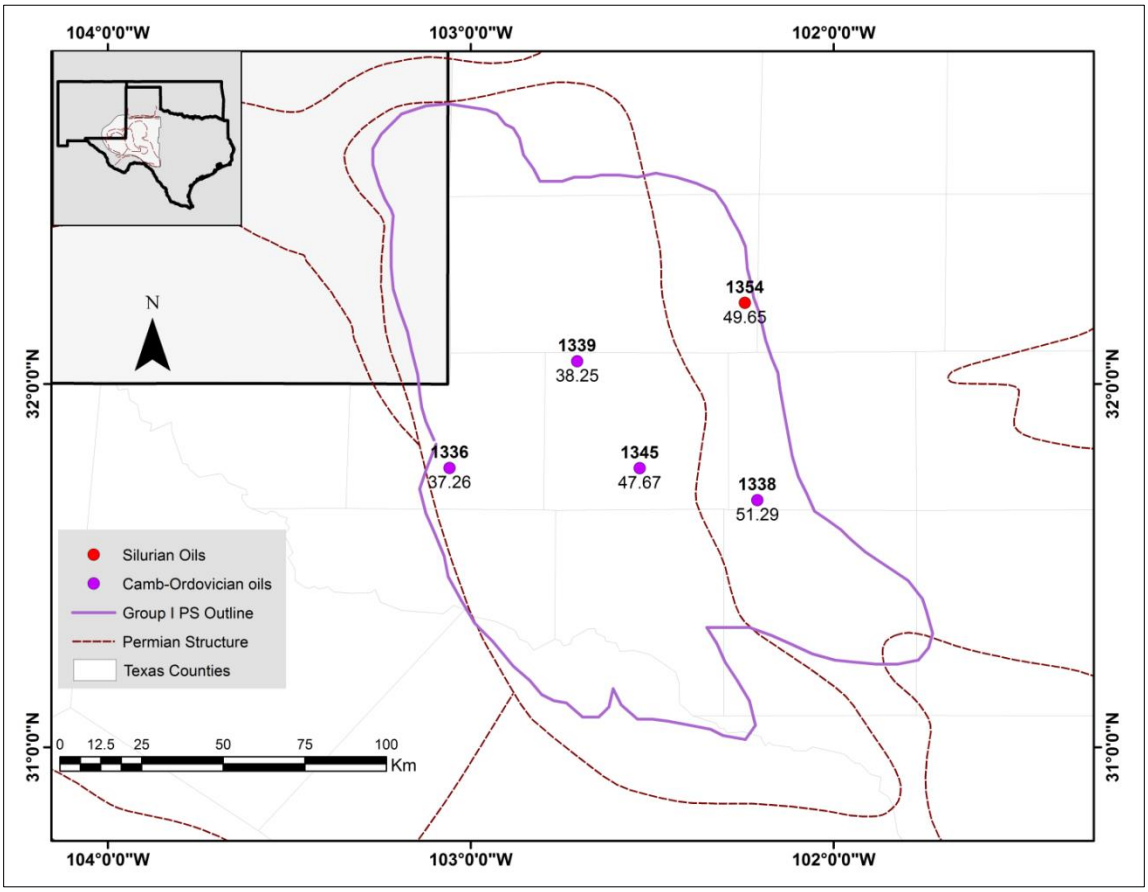

Figure 2.15: Geographic extent of Petroleum System I in the Permian Basin as defined by two plays; the Simpson cratonic sandstone play and Ellenberger karst modified restricted ramp carbonate play. Stratigraphic extent of this petroleum system is Cambrian to Upper Ordovician. (Modified from Permian Basin Play framework of Dutton et al., 2004; 2005). Top and bottom labels represent sample Id and API gravity respectively. See Appendix 1 for detailed play combinations.

2.5.2 Hybrid Petroleum System II/III

The oils belonging to this hybrid petroleum system are listed in Table 2.1. These two groups occur in reservoirs of similar plays, perhaps explaining the high number of spurious (mixed) oils closely related to these two groups. Consequently, the concept of a hybrid petroleum system as defined by Cao et al. (2005) was evoked to combine the two groups as one hybrid petroleum system.

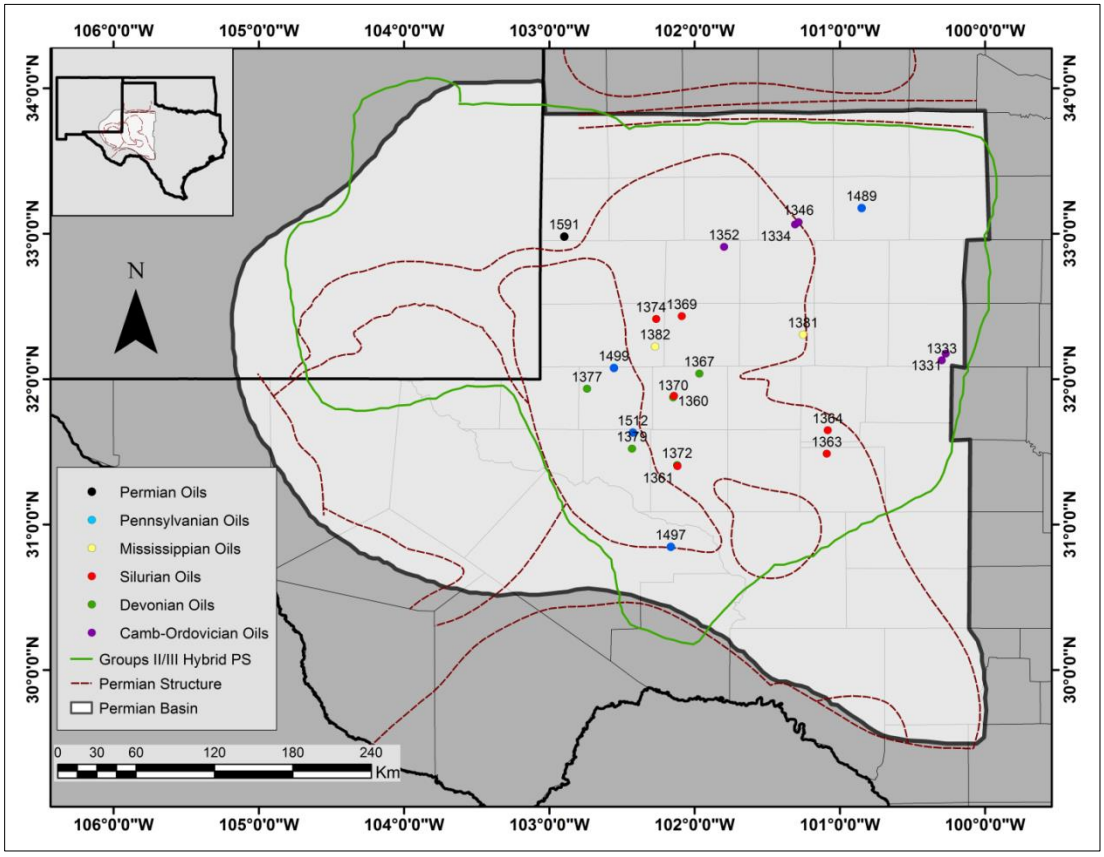

Figure 2.16: Geographic extent of Hybrid Petroleum System II/III in the Permian Basin. Stratigraphic extent of this hybrid petroleum system ranges from Ordovician to Upper Pennsylvanian (Modified from Permian Basin Play framework of Dutton et al., 2004; 2005). See Appendix 1 for detailed play combinations.

According to the Permian Basin play framework (Dutton et al., 2004; 2005), oils 1331, 1333 1334, 1352, and 1346 are hosted in Ordovician reservoirs located in Ellenberger selectively dolomitized ramp carbonate play; Silurian oils 1360, 1361, 1363, 1364, 1369, and 1374 are hosted by reservoirs belonging to Fusselman shallow platform carbonate play. Devonian oils 1367 and 1370 belong to the Devonian Thirtyone deep-water chert play while 1372, 1377, and 1379 are hosted by Devonian Thirtyone ramp carbonate play. All these plays are largely located in the Central Basin Platform and partly in Midland Basin. The only two Mississippian oils, 1381 and 1382, are hosted in the Mississippian Platform carbonate play, the only play in the Mississippian. Pennsylvanian oils 1497, 1499 and 1512 are hosted in the Pennsylvanian platform carbonate play located mainly in the Central Basin Platform, while 1489 and 1591 are hosted in the Upper Pennsylvanian-Lower Permian slope basinal sandstone play, located mainly on the Eastern shelf and Wolfcamp platform carbonate located mainly in the Northern Shelf (Figure 2.16).

2.5.3 Petroleum System IV

This petroleum system comprises a total of sixteen (16) Early Permian-sourced oils geochemically designated as group IV oils (Table 2.1). According to the Permian Basin play framework of Dutton et al. (2004; 2005), group IV oils are reservoired in Pennsylvanian play in Midland Basin, Wolfcampian Platform play and Wolfcamp-Leonardian play in Midland and Delaware basins (Figure 2.17).

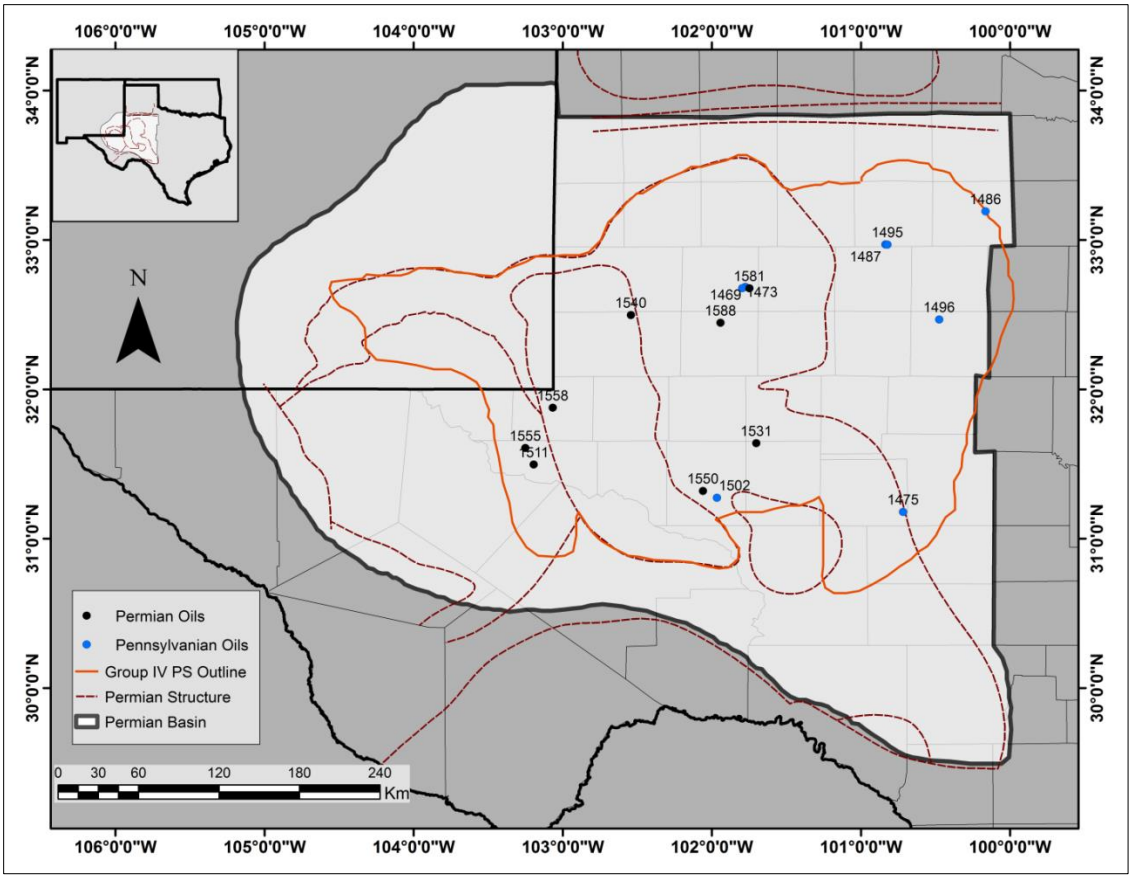

Figure 2.17: Geographic extent of the Petroleum System IV in the Permian Basin. Stratigraphic extent of this play hybrid ranges from Pennsylvanian to Leonardian/Permian (Modified from Permian Basin Play framework of Dutton et al., 2004; 2005). See Appendix 1 for detailed play combinations.

2.5.4 Petroleum System V

This petroleum system comprises Permian-sourced oils geochemically designated as genetic group V oils, which are located mainly in the Upper Permian Reservoirs. These include oil samples 1537, 1538, 1585, 1586, 1593, and 1594 (Figure 2.18). According to the play framework of Dutton et al. (2004; 2005), the plays include San Andres/Grayburg Lowstand carbonate play, Eastern Shelf San Andres platform carbonate play, Northwest Shelf San Andres Platform carbonate play, Queen tidal flat sandstone play and and San Andres platform carbonate (See Appendix 1).

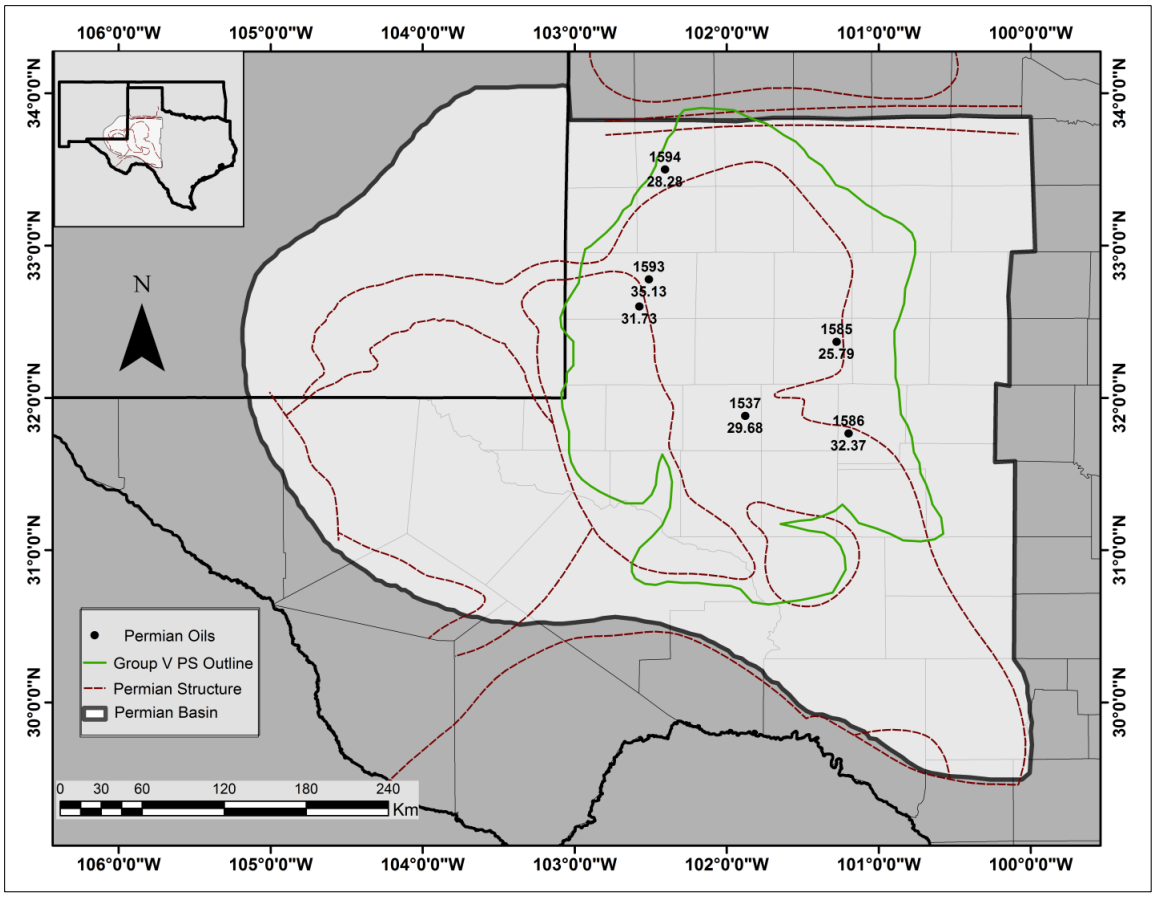

Figure 2.18: Geographic extent of the Petroleum System V in the Permian Basin. Stratigraphic extent of this play hybrid ranges from Leonardian to Upper Permian. Top and bottom labels represent sample Id and API gravity respectively (Modified from Permian Basin Play framework of Dutton et al., 2004; 2005). See Appendix 1 for detailed play combinations.

2.6 Conclusions

A comprehensive study of oils located in the Texas portion of the Permian Basin, mainly the Central Basin Platform, Midland Basin, and Eastern Shelf (Figure 2.1), using geochemical, and chemometric approaches provide insights into the petroleum systems operating within the Permian Basin. Despite the high level of maturity and wide-spread mixing, analysis of biomarker and isotopic data for 50 samples indicates the presence of at least five petroleum systems, ranging from Ordovician to Permian and reservoired in

the Cambrian to Permian. With the exceptions of low maturity group V, whose oils show evidence of a strong carbonate affinity and deposition under anoxia, the rest of the oils were generated at peak maturities from predominantly marine type II, and II/III shale source rocks deposited under predominantly sub-oxic environments. Group III with overwhelming evidence of terrestrial input is strongly related to group II and thus group II/III hybrid petroleum system.

Petroleum System I (group I oils) is geochemically characterized by high OEP, extreme isoprenoids deficiency, high ^{13}C-isotope depletion and very low biomarker concentrations; characteristics associated with Ordovician-sourced oils, represented in the Permian Basin stratigraphy by the Simpson Group. This Ordovician petroleum system is constituted from the amalgamation of the Simpson cratonic sandstone play and Ellenberger karst modified restricted ramp carbonate play, both Ordovician in age and geographically located within the Central Basin Platform. The Ellenberger play extends to the Midland Basin.

Hybrid Petroleum System II/III comprises groups II & III oils. Except for the elevated Pr/Ph ratios, highly positive canonical variable and high API gravities among group III oils, the two groups are generally geochemically similar. Their stable carbon signatures range from -31.6 to -29.9‰, a Devonian-Mississippian age bracket. The Devonian and Mississippian-sourced oils occupy shared plays, and represent not only the most mixed oils but also occupy the largest stratigraphic and geographic extents in the Permian Basin. The hybrid petroleum system is constituted from the amalgamation of eight plays; from Cambrian to Permian.

Petroleum System IV (group IV oils) is characterized by average Pr/Ph ratios and intermediate isotopic signatures (-30.3 to -27.5‰). These Early Permian (Wolfcamp)-sourced oils are highly influenced (especially the Pennsylvanian reservoired oils) by the underlying Devonian-Mississippian oils. The oils are hosted in amalgamated plays comprising one Wolfcamp/Leonardian play and three Pennsylvanian plays.

Petroleum System V (group V oils) is characterized by a complete absence of OEP, lowest API among the oils, very low CPI, extremely low Pr/Ph and sterane/hopane ratios and average stable carbon isotope signatures in the range -28.9 to -27.5‰. These characteristics make this youngest petroleum system unique. These Permian, marl-sourced oils are located mainly in the four plays of Upper Permian, including, San Andres/Grayburg Lowstand carbonate play, Eastern Shelf San Andres platform carbonate play, Northwest Shelf San Andres Platform carbonate play, Queen tidal flat sandstone play, and and San Andres platform carbonate (See Appendix 1).

Within the context of the Permian Basin play framework, in all projected petroleum systems, the oils are generally located in close proximity to their source rocks, for example, Ordovician-sourced oils are found within Ordovician reservoirs and Early Permian oils are found within Early Permian and underlying Pennsylvanian reservoirs. Such systems depict relatively short migration distances, are highly efficient with very limited migration loses, and could explain the petroleum endowment in the Permian Basin.

2.7 References

Adams, J. E., 1965, Stratigraphic-tectonic development of the Delaware Basin: AAPG Bulletin, v. 49, p. 2140-2148.

Addinsoft, 2011, XLSTAT analytical solutions for MS Excel: 28 West 27th Street, Suite 503, New York, NY 10001, United States.

Andrusevich, V. E., M. H. Engel, J. E. Zumberge, and L. A. Brothers, 1998, Secular, episodic changes in stable carbon composition of crude oils: Chemical Geology, v. 152, p. 59-72.

Barbat, W. N., 1967, Crude-oil correlations and their role in exploration: AAPG Bulletin, v. 51, p. 1255-1292.

Bissada, K. K., L. W. Elrod, L. M. Darnell, H. M. Szymczyk, and , J. L. Trostle, 1993, Geochemical inversion-a modern approach to inferring source-rock identity from characteristics of accumulated oils and gas: Energy Exploration and Exploitation 11, 295-328.

Bray, E. E., and E. D. Evans, 1961, Distribution of *n*-paraffins as a clue to recognition of source beds: Geochimica et Cosmochimica Acta, v. 22, p. 2-15.

Cao, J., Y. Zhang, W. Hu, S. Yao, X. Wang, Y. Zhang, and Y. Tang, 2005, The Permian hybrid petroleum system of the Junggar Basin, northwest China: Marine and Petroleum Geology, v. 22, p. 331-349.

Chappe, B., W. Michaelis, and P. Abrecht, 1980, Molecular fossils of Archea bacteria as selective degradation products of kerogen, in A. G., Douglas and J. R. Maxwell, eds., Advances in Organic Geochemistry, 1979, Oxford, England, Pergamon Press, p. 265-274.

Chung, H. M., M. A. Rooney, M. B. Toon, and G. E. Claypool, 1992, Carbon isotope composition of marine crude oils: AAPG Bulletin, v. 76, p. 1000-1007.

Chung, H. M., S. W. Brand, and P. L. Grizzle, 1981, Carbon isotope geochemistry of Paleozoic oils from Big Horn Basin: Geochemica et Cosmochemica Acta, v. 45, p. 1803-1815.

Connan, J., 1981, Biological markers in crude oils, in, J. F. Mason, ed., Petroleum Geology in China, Penn Well, Tulsa, Ok, p. 48-70.

Connan, J., 1984, Biodegradation of hydrocarbons in reservoirs, in J. Brooks and D. H. Welte, eds., Advances in Petroleum Geochemistry, vol. 1, Academic Press London, p. 299-335.

Dahl, J. E., J. M. Moldowan, S. C. Teerman, M. A. McCaffrey, P. Sundaraman, M. Pena, and C. E. Stelting, 1994, Source rock quality determination from oil biomarkers: a new geochemical technique: AAPG Bulletin, v.78, p. 1507-1526.

Demaison, G., and B. J. Huizinga, 1991, Genetic classification of petroleum systems: AAPG Bulettin, v.75, p. 1626-1643

Demaison, G., and F. T. Bourgeois, 1985, Environment of deposition of Middle Miocene, Alcanar, carbonate source beds, Casablanca field, Tarragona basin, Spain, in J.G., Palacas, ed., Petroleum Geochemistry and Source Rock Potential of Carbonate Rocks: AAPG Studies in Geology #18, p. 151-161.

Degens, E. T., 1969, Biogeochemistry of stable carbon isotopes, in G. Eglinton and M. T. J. Murphy, eds., Organic Geochemistry: New York, Springler-Verlag, p. 306-329.

Didyk, B. M., B. R. T. Simoneit, S. C. Brassell, and G. Eglinton, 1978, Organic geochemical indicators of paleoenvironmental conditions of sedimentation: Nature, 272, 216-222.

Dutton, S. P., E. M. Kim, R. F. Broadhead, C. L. Breton, W. D. Raatz, S. C. Ruppel, and C. Kerans, 2004, Play analysis and digital portfolio of major oil reservoirs in the Permian basin: Application and transfer of advanced geological and engineering technologies for incremental production opportunities, University of Texas at Austin, Bureau of Economic Geology, Final Report prepared for the U.S. Department of Energy under contract DE-FC26-02NT15131, 408 p.

Dutton, S. P., E. M. Kim, R. F. Broadhead, W. D. Raatz, C. L. Bretton, S. C. Ruppel, and C. Kerans, 2005, Play analysis and leading-edge reservoir development methods in the Permian; increased recovery through advanced technologies: AAPG Bulletin, 89, 55-576.

ESRI, 2012, ArcMap Version 10.1, Environmental Systems Research Institute Inc., 380 New York Street, Redlands, CA 92373-8100.

Fan Pu, J. D. King, and G. E. Claypool, 1988, Characteristics of biomarker compounds in Chinese crude oils, in R. K. Kumar, P. Dwivedi and V. Banerjie and V. Gupta, eds., Petroleum Geochemistry and Exploration in the Afro-Asian Region; Proceedings of the First International Conference on Petroleum Geochemistry and Exploration in the Afro-Asian Region, Dehradun, 25-27 November 1985: Balkema Rotterdam, p. 197-202.

Fowler, M. G., L. D. Stasiuk, M. Hearn, and M. Obermajer, 2004, Evidence for *Gloeocapsomorpha prisca* in Late Devonian source rocks from southern Alberta, Canada: Organic Geochemistry, v. 35, p.425-441.

Frenzel, H. N., R. R. Bloomer, R. B. Cline, J. M. Cys, J. E. Galley, W. R. Gibson, J. M. Hills, W. E. King, W. R. Seager, F. E. Kottlowski, S.Thompson III, G. C. Luff, B. T. Pearson, and D. C. Van Siclen, 1988, The Permian Basin Region, in L. L. Sloss, ed., Sedimentary Cover-North American craton, US.: Boulder, Colorado, Geological Society of America, The geology of North America, v. D-2, p. 261-306.

Galley, J. E., 1958, Oil and geology in the Permian Basin of Texas and New Mexico, in Weeks, L. G., ed., Habitat of Oil: American Association of Petroleum Geologists, Tulsa, p. 395-446.

Grantham, P. J., and L. L. Wakefield, 1988, Variations in the sterane carbon number distributions of marine source rock derived crude oils through geological time: Organic Geochemistry, v. 12, p. 61-73.

Van Graas, G. W., 1990, Biomarker maturity parameters for high maturities; calibration of the working range up to the oil/condensate threshold: Organic Geochemistry, v. 16, p. 1025-1032.

Handford, C. R., 1981, Sedimentology and genetic stratigraphy of Dean and Spraberry Formations (Permian), Midland Basin, Texas, AAPG Bulletin, v. 65, p. 1602-1616.

Hatch, J. R., S. R. Jacobson, B. J. Witzke, J. B. Risatti, D. E. Abders, W. L. Watbet, K. D. Nowell, and A. K. Vuletich, 1987, Possible Late-Middle Ordovician organic carbon isotope excursion; evidence from Ordovician oils and hydrocarbon source rocks, mid-continent and east central United States: AAPG Bulletin, v. 71, p. 1342-1354.

Hayes, J. M., I. R. Kaplan, and K. M. Wedeking, 1983, Precambrian organic geochemistry, preservation of record, in J. W. Schopf, ed., Earth's Earliest Biosphere, Its Origin and Evolution, Princeton University Press, NJ, pp. 93-134.

Hill, R. J., D. M. Jarvie, B. L. Claxton, J. D. Burgess, and J.A. Williams, 2004, Petroleum systems of the Permian Basin (abs): AAPG Annual Meeting Program, v. 13. A63.

Hills, J. M. 1984, Sedimentation, tectonism, and hydrocarbon generation in Delaware Basin, west Texas and southeastern New Mexico: AAPG Bulletin, v. 68, p. 250-267.

Hills, J. M., and J. E. Galley, 1988, The Pre-Pennsylvanian Tobosa Basin, in Frenzel et al., 1988, The Permian Basin Region, in L.L. Sloss, ed., Sedimentary Cover-North American Craton, US.: Boulder, Colorado, Geological Society of America, The Geology of North America, v. D-2, p. 261-306.

Holmden, C., R. A. Creaser, K. Muehlenbachs, S. A. Leslie, S. M. Bergström, 1988, Isotopic evidence for geochemical decoupling between ancient epeiric seas and bordering oceans: implications for secular curves: Geology, v. 26, p. 567-570.

Hughes, W. B., 1984, Use of thiophenic organosulphur compounds in characterizing crude oils derived from carbonate versus siliciclastic sources, in J. G., Palacas ed., Petroleum Geochemistry and Source Rock Potential of Carbonate Rocks: AAPG Studies in Geology, #18, p.181-196.

Hughes, W. B., A. G. Holba, and L .I .P. Dzou, 1995, The ratios of dibenzothiophene to phenanthrene and pristane to phytane as indicators of depositional environment and lithology of petroleum source rocks. Geochimica et Cosmochimica Acta, v. 59, p. 3581-3598.

Jacobson, S. R., J. R. Hatch, S. C. Teerman, and R. A. Askin, 1988, Middle Ordovician organic matter assemblages and their effect on Ordovician-derived oils: AAPG Bulletin, v. 72, p. 1090-1100.

Jarvie, D. M., J. D. Burgess, A. Morelos, P. A. Mariotti, and R. Lindsay, 2001, Permian Basin petroleum systems investigations; inferences from oil geochemistry and source rocks (abs). AAPG Bulletin, v. 85, p. 1693-4.

Lewan, M. D., M. Bjoroy and D. L. Dolcater, 1986, Effects of thermal maturation on steroid hydrocarbons as determined by hydrous pyrolysis of Phosphoria Retort Shale: Geochemica et Cosmochimica Acta, v. 50, p. 1977-1987- the group

Lindsay, R. F., 2012, West Texas structure, The University of Texas of the Permian Basin http://www.ceed.utpb.edu/geology-resources/west-texas-geology/west-texas-structure> Accessed September 5th, 2012.

Longman, M. W., and S. E. Palmer, 1987, Organic geochemistry of Mid-Continent Middle and Late Ordovician Oils: AAPG Bulletin, v. 71, p.938-950.

Mackenzie, A. S., 1984, Applications of biological markers in petroleum geochemistry, in J. Brooks and D. Welte, eds., Advances in Petroleum Geochemistry, Volume 1, London, Academic Press, p. 115-214.

Magoon, L. B., and W. G. Dow, 1994, The petroleum system, in L. B. Magoon and, W. G. Dow eds. The Petroleum System: From Source to Trap: AAPG Memoir 60, p. 3-24.

Matchus E .J. and T. S. Jones, 1984, East-west cross section through Permian Basin of West Texas, West Texas geological Society Publication 84-79.

McKirdy, D. M., A. K. Aldridge, and P. J. M. Ypma, 1983, A geochemical comparison of some crude oils from pre-Ordovician carbonate rocks, in M. Bjorøy, C. Albrecht, C. Conford, eds., Advances in Organic Geochemistry 1981, John Willey and Sons, p. 99-107.

Moldowan, J. M., C. Y. Lee, P. Sundararaman, P. Salvatori, A. Alajbeg, B. Gjukic, G. J. Demaison, N. E. Slougui, and D. S. Watt, 1992, Source correlation and maturity assessment of select oils and rocks from the Central Adriatic basin (Italy and Yugoslavia), in. J. M. Moldowan, P. Albrecht, and R. P. Philp, eds., Biological Markers in Sediments and Petroleum: Englewood Cliffs, New Jersey, Prentice Hall, p. 370-401.

Moldowan, J. M., W. K. Seifert, and E. J. Gallegos, 1985, Relationship between petroleum composition and depositional environment of petroleum source rocks: AAPG Bulletin, v. 69, p. 1255-1268.

Øygard, K., O. Grahl-Nielsen, and S. Ulvøen, 1984, Oil/oil correlation by aid of chemometrics, Organic Geochemistry v. 6, p. 561-567.

Palacas, J. G., D. E. Anders, and J. D. King, 1984, South Florida Basin-a prime example of carbonate source rocks of petroleum, in J. G. Palacas, ed., Geochemistry and

Source Rock Potential of Carbonate Rocks, AAPG Studies in Geology #18: Tulsa, American Association of Petroleum geologists, p. 71-96.

Peters, K. E., J. M. Moldowan, M. Schoell, and W. B. Hempkins, 1986, Petroleum isotopic and biomarkers composition related to source rock organic matter and depositional environment, Organic Geochemistry, v. 10, p. 17-27.

Peters, K. E., and J. M. Moldowan, 1991, Effects of source, thermal maturity and biodegradation on the distribution and isomerization of homohopanes in petroleum, Organic Geochemistry, v. 17, p. 47-61.

Peters, K. E., and J. M. Moldowan, 1993, The Biomarker Guide, Interpreting Molecular fossils in Petroleum and Ancient Sediments: Englewood Cliffs, New Jersey, Prentice Hall, 363p.

Peters, K. E., T. H. Fraser, W.Amris, B. Rustanto and E. Hermanto, 1999, Geochemistry of crude oils from Eastern Indonesia: AAPG Bulletin, v. 83, p. 1927-1942.

Peters, K. E., J. M. Moldowan, and C. C. Walters, 2005a, The Biomarker Guide; Biomarkers and Isotopes in Environment and Human History (vol. 1): Cambridge University Press pp. 1-471.

Peters, K. E., J. M. Moldowan and C.C. Walters, 2005b, The Biomarker Guide; Biomarkers and Isotopes in Petroleum Exploration and Earth History (vol. 2): Cambridge University Press pp. 475-1155.

Peters, K. E., J. M. Moldowan and P. Sundararaman, Effects of hydrous pyrolysis on biomarker thermal maturity parameters: Monterey phosphatic and siliceous Members: Organic Geochemistry, v. 15, p. 249-265.

Peters, K. E., D. Coutrot, , X. Nouvelle, L. S. Ramos, B.G. Rohrback, L. B. Magoon, and J. E. Zumberge, 2013, Chemometric differentiation of crude oil families in the San Joaquin Basin, Carlifornia: AAPG Bulletin, v. 97, p. 103-143

Powell, T. G., and D. M. McKirdy, 1973, Relationship between ratio of pristane to phytane, crude oil composition and geological environment in Australia: Nature, v. 243, p. 37-39.

Rail Road Commission, 2012, History of Texas initial crude oil, annual production, and producing wells, (http://www.rrc.state.tx.us/data/production/oilwellcounts.php), web accessed Jan, 2012.

Reed, J. D., H. A. Illich, and B. Horsfield, 1986, Biochemical evolutionary significance of Ordovician oils and their sources: Organic Geochemistry, v. 10, p. 347-358.

Riebesell, U., A. T. Revil, D. G. Holdsworth, and J. K. Volkman, 2000, The effect of varying CO_2 concentration on lipid composition and carbon isotope fractionation in *Emiliania huxleyi*, Geochimica et Cosmichimica Acta, v. 64, p. 4179-4192.

Scalan, R. S., and J. E. Smith, 1970, An improved measure of the odd-to-even predominance in the normal alkanes of sediment extracts and petroleum, Geochimica et Cosmochimica Acta, v. 34, p. 611-620.

Schenk, C. J., R. M. Pollastro, T. A. Cook, M. J. Pawlewicz, T. R. Klett, R. R. Charpentier, and H. E. Cook, 2008, Assessment of undiscovered oil and gas resources of the Permian Basin Province of west Texas and southeast New Mexico, 2007, U.S. Geological Survey Fact Sheet 2007–3115, 4p.

Seifert, W. K., 1975, Carboxylic acids in petroleum and sediments, in W. Herz, H. Grisebach, and G.W. Kirby, eds., Progress in Chemistry of Organic Natural Products, v. 32, New York, Springer-Verlag, pp. 1-49.

Sigman, D. M. and Boyle, E. A., 2000, Glacial/interglacial variation in atmospheric carbon dioxide: Nature, v. 407, p. 859-869.

Silverman, S. R., 1964, Investigations of petroleum origin and evolution mechanisms by carbon isotope studies. In: Craig H., Miller, S. L., Wasserburg, G. J., eds., Isotopic and Cosmic Chemistry, North Holland, 92-102.

Sofer, Z., 1980, Preparation of Carbon dioxide for stable carbon isotope analysis of petroleum fractions: Analytical Chemistry, v. 52, p. 1389-1391.

Sofer, Z., 1984, Stable carbon isotope compositions of crude oils; application to source depositional environments and petroleum alteration: AAPG Bulletin, v. 68, p. 31-49.

ten Haven, H. L., J. W. de Leeuw, J. S. Sinnighe Damste, P. A. Schenck, S. E. Palmer, and J. E. Zumberge, 1988, Application of biological markers in the recognition of palaeo-hypersaline environments, in K. Kelts, A. Fleet, and M. Tablot, eds., Lacustrine Petroleum Source Rocks, Special Publication, v. 40: Blackwell, Geological Society, p. 123-130.

ten Haven, H. L., J. W. de Leeuw, J. Rullkotter, and J. S. Sinninghe Damste, 1987, Restricted utility of the pristane/phytane ratio as a paleoenvironmental indicator, Nature, v. 330, p. 641-643.

Tissot, B. P., and D. H. Welte, 1984, Petroleum Formation and Occurrence: Springer-Verlag, New York, 699p.

Wang, H. D., and R. P. Philp, 1997, Geochemical study of potential source rocks and crude oils from the Anardako Basin, Oklahoma: AAPG Bulletin, v.81, p. 249-275.

Waples, D. W., and T. Machihara, 1991, Biomarkers for Geologists-A pratical Guide to the Application of Steranes and Triterpanes in Petroleum Geology: AAPG Methods in Exploration, No.9, p.1-91.

Wright, W.F., 1979, Petroleum Geology of the Permian Basin: West Texas Geological Society Publication 79-71, 98p.

Young, S. A., Saltzman, M. R., and Bergström, S. M., 2005, Upper Ordovician (Mohawkian) carbonate isotope ($\delta^{13}C$) stratigraphy in eastern and central North America: regional expression of a perturbation of the global carbon cycle: Palaogeography, Palaeoclimatology, Palaeoecology, v. 222, p. 53-76.

Zumberge, J. E. 1987, Prediction of source rock characteristics based on terpane biomarkers in crude oils: a multivariate statistical approach. Geochemica et Cosmochimica Acta, v. 51, p. 1625-1637.

3.0 SOURCE-ROCK CHARACTERIZATION AND OIL-SOURCE ROCK CORRELATIONS

Abstract

Chemometric analysis and an independent stable carbon isotope correlation constrained by thermal maturity analysis were undertaken on data for 50 oils and 19 source rock samples from strata ranging from Ordovician to Mid-Permian and distributed over much of the Permian Basin. Biomarker maturity indicates very high maturity for most of the oils while individual organic-rich, marine type II-II/III source rocks: Simpson, Woodford, Barnett, Wolfcamp, and Spraberry shales are markedly varied in organofacies. Geochemical evidence suggests deposition under suboxic and anoxic-suboxic conditions, except Bone Spring- and Simpson-derived oils where deposition under anoxia is inferred.

Correlations demonstrate the existence of five petroleum systems involving the shales of the Simpson, Woodford, Barnett, Wolfcamp, and Bone Spring marl. The petroleum systems are segregated with very limited cross-stratigraphic migration due to the presence of pervasive seals/source rocks. Entrapment in the Pre-Pennsylvanian systems is dominantly structural and migration is vertical, both upwards (Barnett) and downwards (Woodford and Simpson) against buoyancy. To the contrary, entrapment in the Post-Pennsylvanian systems is dominantly stratigraphic and lateral migration is a norm. This study has established a detailed understanding of the petroleum systems in the Permian Basin, documenting the geographic and stratigraphic relationships between oils and their candidate source rocks and providing useful insights into hydrocarbon migration in the basin.

3.1 Introduction

The Permian Basin of west Texas and Southeast New Mexico, structurally defined by the Matador Arch to the north, the Marathon-Ouachita fold belt to the south, the Diablo platform to the west and the Eastern shelf to the east (Figure 3.1), is one of the most endowed petroleum provinces in the United States. Over 35 billion barrels of oil and several trillion cubic feet of gas have come from this province since 1920s, mainly from conventional plays (Galloway et al., 1983; Dutton et al., 2004; 2005). Despite the long history, however, the petroleum systems studies are not widely published, and therefore are not available in the public domain. A few of the Permian Basin petroleum systems reported in literature are generalized national-grid mentions (e.g. Magoon, 1988a & b; Magoon, 1992) while others are abstracts (Dow et al., 1990; Jarvie et al., 2001; Corby and Cook, 2003; Hill et al., 2004; Jarvie and Hill, 2011), which only give insight but no evaluations or detailed discussions can be made. A comprehensive petroleum system study by Katz et al. (1994) only covers one petroleum system (the Simpson-Ellenberger) in the Permian Basin.

A petroleum system is a natural geologic system that encompasses an active source rock and all related petroleum and includes all the essential elements and processes necessary for a petroleum accumulation to exist (Magoon and Dow, 1994; Magoon and Beaumont, 1999). Essential geological elements include the source rock, overburden, reservoir rock, migration route, traps and seals. As discussed by Peters and Cassa (1994), a better evaluation of prospects is incomplete without an understanding of types and distribution

of effective source rocks and hence the geographic extent of petroleum systems (Magoon and Dow, 1994).

Oil-source rock correlation is an established geochemical methodology used to identify candidate source rocks for oil accumulations (Curiale, 1994; Waples and Curiale, 1999; Peters et al., 2005). A positive correlation between an oil and source rock implies and defines the existence of a petroleum system (e.g. Magoon and Dow, 1994; Magoon and Beaumont, 1999). The fundamental basis for the utility of oil-source rock correlations to define petroleum systems is premised on the understanding that certain compositional parameters of migrated oils, especially biomarkers and stable carbon isotope ratios, do not differ substantially from that of extractable bitumen remaining in the source rock (e.g. Peters et al., 2005).

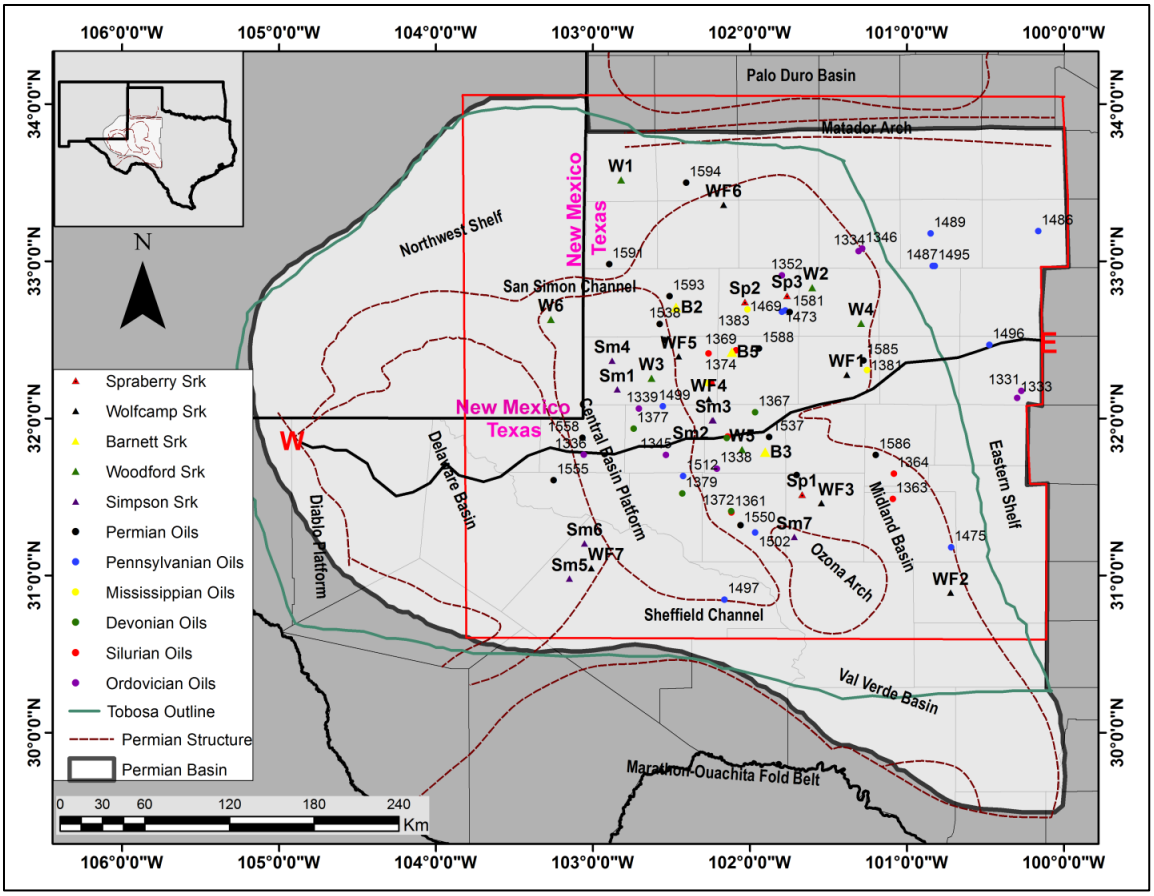

Figure 3.1: The Permian Basin of West Texas and Southeast New Mexico showing the location of oil and source rock samples used in the study. Sm, W, B, WF, Sp represent samples from Simpson Group, Woodford, Barnett, Wolfcamp and Spraberry respectively. Permian Basin outline and definition from Dutton et al. (2004; 2005 and references therein). Red outline indicates the actual focus area of study.

In a bid to understand the petroleum systems operative in the Permian Basin, 50 oil samples stratigraphically recovered from Ordovician to Middle Permian (Leonardian), covering a large extent of the Permian Basin play framework were geochemically characterized and classified (Chapter 2). Five petroleum systems were inferred. The inferred source rocks included the Simpson shales, the Woodford-Barnett shales, the Wolfcamp shales and a marl, which, according to literature points to the Bone Spring Formation (e.g. Jarvie and Hill, 2011). In this part of the study, in addition to the oils used in Chapter 2, inferred potential source rocks were sampled, geochemically analyzed

for biomarker and stable carbon isotopes, and then correlated with oils. The principal objective is to verify the petroleum systems inferred in Chapter 2 so as to accurately delineate them geographically and stratigraphically.

3.2 Structure and Stratigraphy

A detailed structural and stratigraphic development of the Permian Basin is outlined in Chapter 1.

3.3 Samples and Methods

Samples used in this study encompassed oils and source rocks. The source rock samples are mainly cuttings, including the Ordovician Simpson Group shales, the Upper Devonian Woodford shale, the Mississippian Barnett shale, the Early Permian (Wolfcampian) shale, and the Middle Permian (Leonardian) Spraberry shale. However, due to extremely limited amount of sample size, Ordovician Simpson Group shales were not extracted and therefore not part of the biomarker and stable carbon isotope correlations. In defining the petroleum systems however, oils constrained in Chapter 2 to be derived from Ordovician source rocks were considered to be sourced from the Simpson Group shales, the only shale of Ordovician age in the Permian Basin.

Because of low biomarker concentrations inherent in condensates, they were not included in chemometric correlations but were constrained using stable carbon isotopic compositions. Source rock extracts were subjected to analytical approaches similar to oils. Detailed analytical (experimental) procedures for oils are described in Chapter 2. Oil

samples are presented within a stratigraphic framework in Figure 3.12 and summarized in Table 3.2. Detailed oil sample identification and locations are contained in Appendix 2 and shown in Figure 3.1. Source rock sample locations are listed in Appendices 3 through 5.

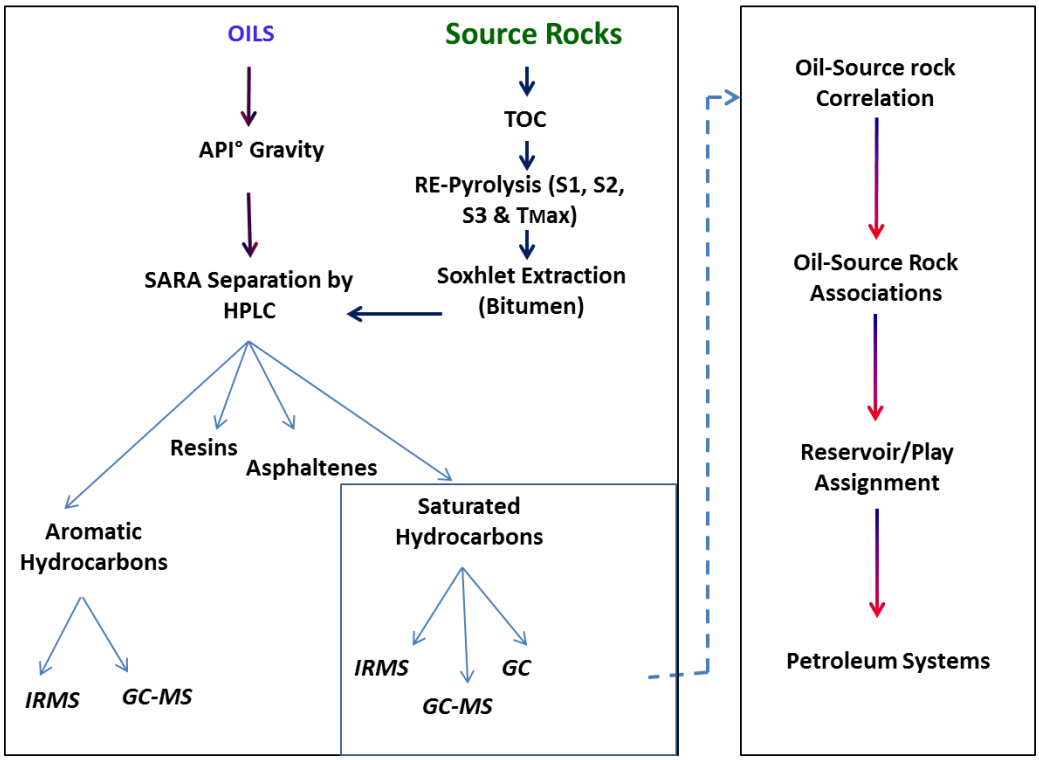

Figure 3.2: Analytical work program undertaken on potential source rock samples and oils. TOC=total organic carbon; RE = Rock-Eval; GC=gas chromatography; HPLC=high performance liquid chromatography; GC-MS=gas chromatography-mass spectrometry; and IRMS=isotope ratio mass spectrometry as described in Bissada et al. (1993). Saturated biomarkers and stable carbon isotopes were mainly used in correlations.

Source rock samples from the Simpson, the Woodford, the Barnett, the Wolfcamp, and the Spraberry were crushed and pulverized to 60-mesh. Approximately 100g of pulverized rock sample was weighed into porous crucibles placed on a glass tray. Any inorganic carbon in the samples was neutralized with excess hydrochloric acid (3N) poured onto a tray containing the crucibles with their samples. After an overnight

reaction, the acid was drained from the tray and the crucibles by aspiration. The acid was then washed away from the samples by repeated flood-drain cycles with distilled water. Washed samples were then dried in an oven at 70°C overnight before subjecting to carbon analysis using Leco^{R} CS Analyzer to measure total organic carbon content (TOC).

Rock Eval pyrolysis was accomplished using Rock-Eval 2 equipment. Approximately 100mg of sample was weighed into the crucibles and directly subjected to pyrolysis in Rock-Eval 2. The pyrolysis oven temperature program comprised an initial temperature of 300°C with a hold of 3 minutes. The temperature was then ramped to 550°C at a rate of 25°C per minute for a total run time, including CO_2 trapping, of about 20 minutes. At 300°C, hydrocarbons already generated by the source rock and trapped within the mineral surfaces are released and registered by equipment as S1. Between 300°C and 550°C, cracking of the kerogen in the source rock sample takes place, generating hydrocarbons, registered by the equipment as S2. The equipment also registers a temperature at which maximum evolution of S2 occurs and displays it as T_{Max}. During the entire cycle from 0°C to 550°C, any carbondioxide produced is trapped and measured at the end of the cycle. This is registered as S3. From these TOC and Rock-Eval pyrolysis parameters, secondary parameters are derived, including Hydrogen Index (HI) and Transformation Ratio (TR) as described in detail in Peters and Cassa (1994) and shown in Figure 3.3.

Petroleum systems were defined using oil-source rock associations in two steps. The first step involved use of chemometric analysis (Øygard, 1984; Zumberge, 1987) using agglomerative hierarchical clustering, AHC. Similarity was based on the Pearson correlation coefficient utilizing complete linkage and automatic truncation options

embedded in XLSTAT version 2012.4 (Addinsoft, 2012). However, because of potential effects of varying maturity on stable carbons isotope compositions, with source rocks usually heavier than their oils (e.g. Chung et al., 1981; Peters et al., 2005), a second approach using stable carbon isotope compositions in conjunction with maturity assessment was used to confirm oil-source rock correlations established by chemometrics. In addition to validating correlations, maturity analysis was used to confirm if a source rock truly generated oils and to also determine the source area (Delaware, Central Basin Platform or Midland sub basins) of an oil for a given established petroleum system. Oil-source rock correlations were further supported by modeling thermal maturity and hydrocarbon generation modeling in a later chapter.

As reported in Chapter 2, oils from the Permian Basin are geochemically closely related, an artifact they attributed to high maturity, possible oil cracking associated with downward migration, and charge integration over a long period of time. Therefore, in order to get a clear understanding of the petroleum systems, source rock extracts were geochemically characterized separately prior to oil-source rock correlations by chemometrics. Because not all reservoirs in the Permian Basin were sampled, unsampled reservoirs were assumed to have formed at the same time, as sampled reservoirs in the same play and therefore must have received charge from a similar source rock. This assumption is supported by the play definition of White (1980) and depends to a large extent on the amount of charge from the source rock as determined by its TOC, HI, and level of maturity.

3.4 Results and Discussion

3.4.1. Source Rock Screening

TOC and Rock-Eval data for all source rock samples studied are presented in Appendix 5 and for composite source rock samples presented in Figure 3.3a-c and in Table 3.1. This selection was obtained by combining and homogenizing cuttings samples of a given source rock recovered from the same well. This was necessitated in order to get adequate amount for stable carbon isotope and biomarker characterizations. The average TOCs for these source rocks puts Woodford shale on top with 3.05%, Barnett shale 2.47%, Wolfcamp 2.32% while Simpson and Spraberry tie at 1.6%.

A comprehensive TOC distribution for the Woodford shale (Comer, 1991) indicates that it is up to 6%, with an average of 2-4%. The TOC values for Barnett correspond as well to those measured by Kinley (2008) in the Barnett in Delaware Basin. Jarvie and Hill (2011) indicate average TOC value of about 1.5%, a little lower than the average measured here. However, the number and location of samples is not provided in Jarvie and Hill (2011), therefore, no comparative evaluation can be made. This applies to all the source rock samples listed by Jarvie and Hill (2011). The differences in TOCs between those presented here and those for example in Kinley (2008) and Comer (1991) for the Barnett and the Woodford respectively, could be attributed to many factors including differences in maturities of the samples, and also the varying nature of the organofacies among the source rocks. The effect of maturity on TOC and Rock-Eval pyrolysis S1 and S2 is demonstrated by the immature Barnett shale sample, B5 which plots in a distinct

region of high S2, TOC and HI compared to its mature counterparts B2 and B3 (Figure 3.3a).

Based on the grading guidelines of Peters and Cassa (1994), the Woodford, the Barnett, and the Wolfcamp shales are considered excellent source rocks, while the Simpson, and the Spraberry are good source rocks, based on their total organic carbon contents (TOCs) which are greater than 1% (Figure 3.3a).

Table 3.1: TOC and Rock-Eval pyrolysis data for selected representative potential source rock samples

Sample Id	TOC %	S1 (mg/g)	S2 (mg/g)	S3 (mg/g)	T_{Max} (°C)	S1+S2 (mg/g)	S2/ S3	NOC	HI	OI	TR or PI	HI_o
Sp1	1.56	1.04	2.49	0.12	443	3.53	21	67	160	8	0.29	202
Sp2	1.06	0.20	2.98	0.01	427	3.18	298	19	281	1	0.06	n.c.
Sp3	2.15	0.44	6.14	0.33	427	6.58	19	20	286	15	0.07	n.c
WF1	3.63	1.95	5.81	0.20	438	7.76	30	54	160	5	0.25	176
WF2	0.91	0.09	0.30	0.04	469	0.39	9	10	33	4	0.23	71
WF3	5.65	1.92	13.77	0.16	436	15.69	84	34	244	3	0.12	252
WF4	0.94	0.13	0.21	0.02	414	0.34	14	14	22	2	0.38	n.c
WF5	1.61	1.20	2.00	0.08	439	3.20	26	74	124	5	0.37	139
WF6	2.03	0.52	4.97	0.09	434	5.49	58	26	244	4	0.10	238
WF7	1.50	0.29	0.69	0.02	456	0.98	35	19	46	1	0.29	78
B2	1.52	0.18	0.83	0.16	438	1.02	5	12	47	14	0.21	51
B3	1.56	0.28	1.43	0.10	437	1.71	14	16	80	7	0.16	85
B5	5.92	2.32	28.24	0.45	431	30.56	63	39	477	8	0.08	n.c
W1	3.12	1.38	7.01	0.03	448	8.39	280	44	225	1	0.16	322
W2	1.57	0.09	2.22	0.06	441	2.31	37	6	141	4	0.04	170
W3	3.10	1.02	6.13	0.09	440	7.15	71	33	198	3	0.14	233
W4	2.93	0.81	8.63	0.12	434	9.43	72	27	294	4	0.09	286
W5	2.52	1.07	1.68	0.10	448	2.75	17	42	67	4	0.39	95
W6	5.09	0.63	1.44	0.01	470	2.07	144	12	28	0	0.30	62
Sm1	1.58	0.54	1.69	0.08	442	2.23	23	33	104	5	0. 24	127
Sm2	1.60	0.53	1.12	0.14	456	1.65	8	34	70	9	0.33	118
Sm3	1.98	1.04	1.84	0.11	435	2.88	15	49	85	6	0.37	85

Sp = Spraberry; BS = Bone Spring; WF = Wolfcamp; B = Barnett; W = Woodford; and Sm = Simpson). TOC = total organic carbon content; S1 = free hydrocarbons already generated by source rock; S2 = hydrocarbons from source rock cracking during pyrolysis or remaining potential; S3 = organic carbon dioxide released from source rock; T_{Max} = temperature at peak evolution of S2 hydrocarbons; HI (Hydrogen Index) = (S2/TOC)*100; OI (Oxygen Index) = (S3/TOC)*100; (S1/TOC)*100 = normalized oil content (NOC); PI (Production Index) = S1/(S1+S2), also called Transformation Ratio (TR); HI_o as defined in the text. n.c = not calculated.

Kerogen type was assessed based on hydrogen indices (HIs) as obtained from the relation HI = (S2/TOC)*100. The HI data is indicated in Table 3.1 and Figure 3.3a. However, because most samples are adequately mature, measured HI values could be lower than the original. Corrected HI, was obtained using the relationship established by Barnejee et al. (1998; 2000), thus,

$$HI_m = 1/[a^{b(Tmax-435)}]+1/HI_o$$

where HI_m and HI_o are measured and original HI respectively, a and b are constants that relate to the kerogen type. Type II values, $a = 1.91*10^{-4}$ and b = 0.1925 were used in this study. HI_o values as averaged for each source rock are the basis for volumetric calculations in Chapter 4. The averaged values are; Simpson Shale, 110; Woodford Shale, 195; Barnett, 201; Wolfcamp, 140; and Spraberry, 256. The data for all the five source rocks (HI and HI_o) suggest mixed oil/gas-prone, predominantly type II to II/III (Figures 3.3a and b), essentially, good quality source rocks according to grading guidelines of Peters and Cassa (1994).

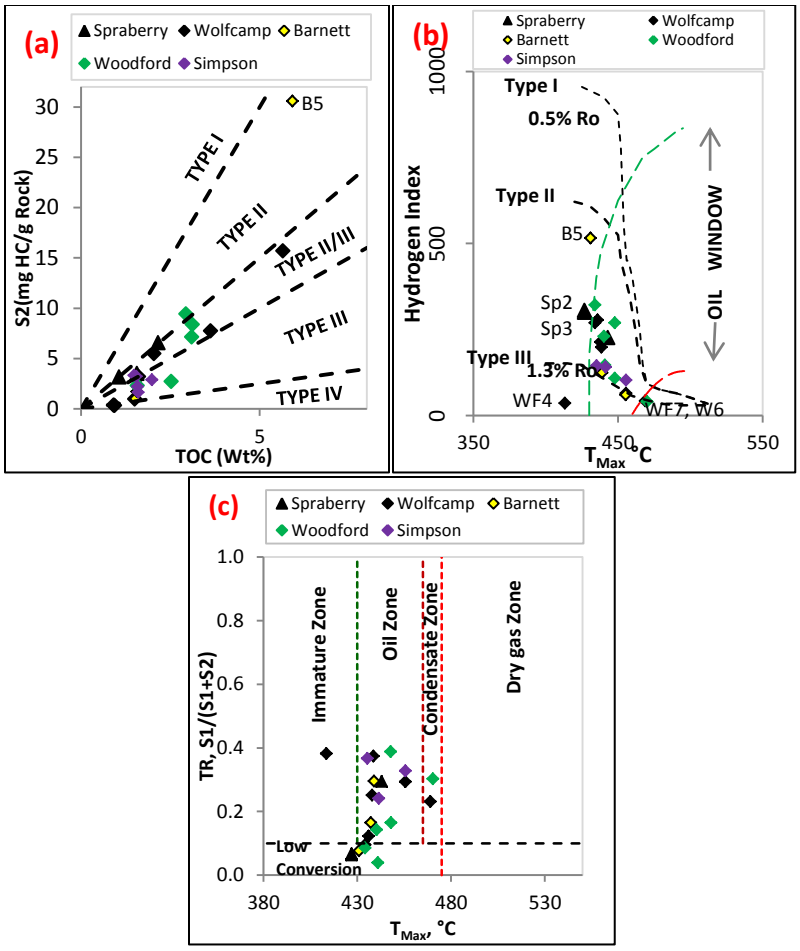

Figure 3.3: (a). S2 versus TOC defining Hydrogen Index (HI) and kerogen types for selected representative potential source rocks. Maturity shifts the samples towards the bottom-left corner (Jarvie and Hill, 2011). The slopes of the demarcating dashed black lines represent hydrogen indices 600, 300, 200 and 50 (after Peters and Cassa, 1994). (b) Kerogen typing based on HI and T_{Max} and (c) Maturity of source rock based on T_{Max} and TR (see Table 3.1 for definition of terms).

A majority of the samples are within the oil window except for a couple of samples from the Spraberry and one sample each from Wolfcamp and Barnett shales which are approaching oil window maturity. One Woodford shale and one Wolfcamp shale are well beyond the beyond oil-window maturity.

3.4.2. Source Rocks Stable Carbon Isotope Data

Stable carbon isotope compositions of source rock samples are listed together with oils in Table 3.2 and plotted in Figure 3.10. Jarvie and Hill (2011) reported stable carbon isotope compositions of $\delta^{13}C_{Sat.}$ -30.5 to -29.5‰ and $\delta^{13}C_{Aro}$ -29.9 to -28.5‰ for oils sourced from the Woodford shale. These values are isotopically heavier than the Woodford-sourced oils from this study and overlap with the Woodford-sourced condensates (Figure 3.10). For oils from the Barnett of the Permian Basin, Jarvie and Hill (2011) reported stable isotope compositions of $\delta^{13}C_{Sat}$ -30.0 to -29.0‰ and $\delta^{13}C_{Aro}$ -28.5 to -29.5‰ which overlap with the Barnett-sourced oils in this study (Figure 3.10). This overlap supports the source rock correlation for these oils. Jarvie and Hills (2011) Woodford oils $\delta^{13}C$ are heavier than both the Woodford oil samples and source rock $\delta^{13}C$ from this study. This is questionable as source rock $\delta^{13}C$ should be isotopically heavier than its oils (e.g. Peters et al. 2005). Even though the condensates under study are isotopically heavier than Woodford oils and source rocks, the three are correlative, with condensates acceptably isotopically heavier by virtue of their higher maturity.

The average stable carbon isotopic compositions for the Wolfcamp are $\delta^{13}C_{Sat.}$-28.19 and $\delta^{13}C_{Aro.}$-27.89 while that for the Spraberry are $\delta^{13}C_{Sat.}$ -28.83 and $\delta^{13}C_{Aro.}$ -27.53. The results suggest a general isotopic change in a positive direction from Devonian Woodford to Permian Wolfcamp and Spraberry samples. This trend of change in stable carbon isotope composition over time is extensively discussed in the literature (e.g. Degens, 1969; Chung et al. 1992; Andrusevich et al., 1998; Riebesell et al., 2000) and is thought to be linked to changes in carbon dioxide concentration over time (e.g. Andrusevich,

1998), though some variation may be due to fractionation during maturation (e.g. Chung et al., 1981; Peters et al., 2005) and primary productivity or associated with water circulation patterns (e.g. Hayes, et al., 1983; Hatch et al., 1987). Based on stable carbon isotope data, specifically with reference to the negative canonical variables (Sofer, 1984), marine organic matter is dominant in all the source rocks studied as indicated in Figure 3.10. The highly positive canonical variable exhibited by the Spraberry (Sp2), the Barnett (B5), and Woodford (W6) however, suggests terrigenous organic matter input in these samples, signifying variability in depositional conditions during the deposition of these source rocks.

3.4.3 N-Alkanes and Acyclic Biomarker Distributions of Source Rocks

The *n*-alkane distributions in gas chromatograms for representative source rock extracts are shown in Figure 3.4 and measured data depicted in Table 3.2. Despite the differences among the source rock extracts, the abundance of higher homologs above nC_{25} is significantly diminished in all the samples, suggesting non-waxiness (e.g. Bissada et al., 1993) and therefore promoting a marine origin for all the shale samples studied, in conformity with their stable carbon isotope compositions as discussed under stable carbon isotope compositions above.

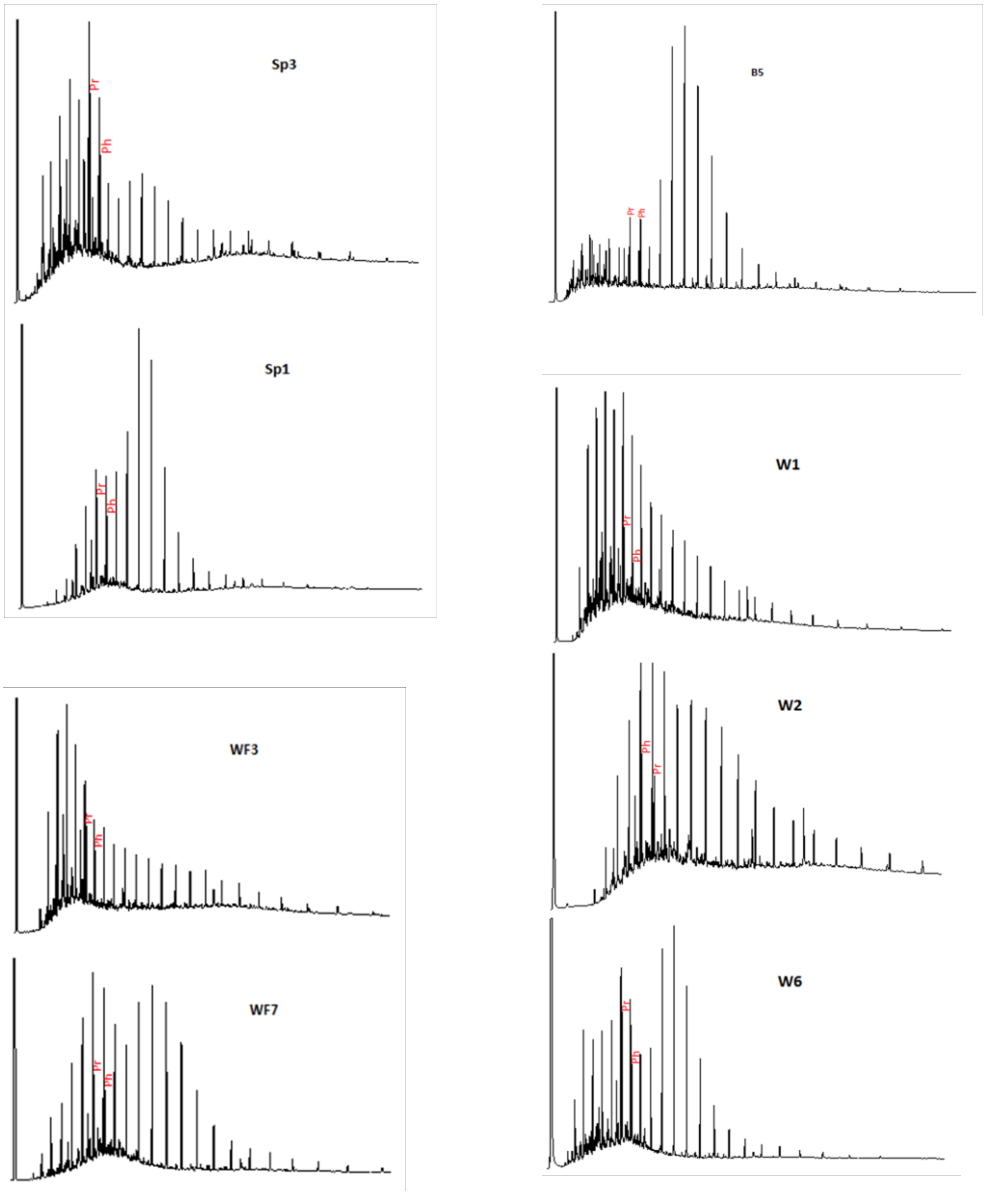

Figure 3.4: Gas chromatograms showing *n*-alkane and isoprenoid distributions among selected representative samples from Spraberry (Sp1 and Sp3), Wolfcamp (WF3 and WF7), Barnett (B5) and Woodford (W1, W2 and W6) shale source rocks. Each regularly spaced peak represents a normal paraffin, where pristane (Pr) and phytane (Ph) stand immediately (almost co-eluting) after nC_{17} and nC_{18} respectively. Note the abundance of pristane and phytane isoprenoids relative to corresponding *n*-alkanes in sample B5, a reflection of its low maturity.

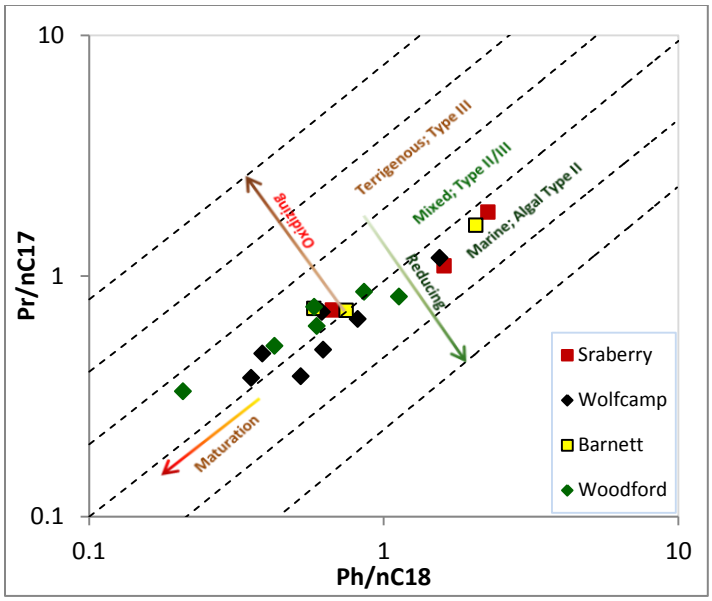

Figure 3.5: Plot of ratio of isoprenoids (represented by pristane and phytane) to the corresponding n-alkane ratios, defining the kerogen type, redox of depositional environments and maturities for potential source rocks. Template from Peters et al. (1999). Throughout this manuscript, n-alkanes and *n*-paraffins are used synonymously. Srks = source rocks.

3.4.3.1 The Spraberry

The *n*-paraffin distributions exhibited by the three Spraberry source rock extracts indicate that Sp1 is slightly different from both Sp2 (not shown) and Sp3 which appear similar. In Sp1, the n-alkane distribution can best be described as unimodal (Figure 3.4) while both Sp2 and Sp3 show slight bimodal distributions with maxima at nC_{17} and nC_{22}. Bimodal *n*-paraffin distribution essentially represents contribution of organic matter from two dominant source organisms, frequently observed in environments where more than one type of algae are involved (e.g. Bissada et al., 1993) or where wax-rich organic matter is involved (e.g. McKirdy et al., 1983; Peters et al., 2005). Both OEP (Scalan and Smith, 1970) and CPI (Bray and Evans, 1961) are generally low for the Spraberry samples (Table 3.2), with differences attributed to maturity contrasts among the samples as

reflected in the Pr/nC$_{17}$ and Ph/nC$_{18}$ plot (Figure 3.5). Sp1 depicts high maturity, mixed type II/III organic matter deposited under sub-oxic conditions, while Sp2 and Sp3 depict relatively less mature marine algal type II organic matter deposited under anoxic environments. These interpretations of organic matter type, redox of depositional environments, and maturity are consistent with inferences from source rock screening data and suggest varied geological settings (e.g. Shanmugan, 1985) for the Spraberry.

3.4.3.2 The Wolfcamp

Based on the *n*-paraffin distributions, the Wolfcamp source rocks can be divided into two subgroups. Subgroup I shows unimodal distribution and comprises WF1, WF2, and WF3. Subgroup II shows bimodal distribution and comprises WF4, WF5, WF6, and WF7. Similar interpretations, where involvement of algae is suggested for bimodal distributions apply as discussed under Spraberry above. Despite the visual differences in the chromatograms (Figure 3.4), CPI, OEP, and pr/ph ratio for all Wolfcamp shale samples are virtually identical, and may suggest similarity in organofacies. CPI and OEP are approximately 1, indicating mature samples except WF6 which has a high OEP, commensurate with inference from source rock screening data. As seen in Figure 3.5, Pr/Ph ratio for the Wolfcamp samples are within a range that suggest anoxic to sub-oxic depositional conditions. Samples WF1, WF2, WF4, and WF5 plot in the zone that depicts marine algal type II organic matter deposited under anoxic conditions while the second category, comprising WF3, WF6, and WF7 infer a mixed type II/III organic matter deposited under sub-oxic conditions. This divide in redox of depositional environment

suggests variability in depositional conditions ranging from deep and shallow waters during the Wolfcampian.

3.4.3.3 The Barnett shale

All the Barnett shale samples studied display a unimodal *n*-paraffin distribution with maxima around nC$_{21}$-nC$_{24}$ (Figure 3.4). This suggests contribution of organic matter predominantly from one type organic matter precursor. CPI for the Barnett shale samples is slightly higher than one. Although this could be attributed to relatively low maturity (e.g. Bray and Evans, 1961), the least mature sample B5 has a lower CPI, thus dispelling the maturity interpretation or suggesting factors other than maturity control. The low maturity of the Barnett, B5 sample is clearly manifested in Ph/nC$_{18}$ versus Pr/nC$_{17}$ plot (Figure 3.5) where it plots against the direction of increasing maturity. Pr/Ph ratios for all these samples are less than one, suggesting deposition under anoxic conditions (e.g. ten Haven et al., 1987). However, with the exception of sample B5, Pr/nC$_{17}$, and Ph/nC$_{18}$ for the Barnett source rock extracts infer mature mixed type II/III organic matter deposited under sub-oxic conditions.

3.4.3.4 The Woodford shale

Three typical *n*-alkane envelopes of the Woodford shale samples are displayed in Figure 3.4. The Woodford shale samples have CPI values typical of thermally mature siliciclastic source rocks (e.g. Bray and Evans, 1961). The pristane/phytane ratios (Table 3.2) for all Woodford samples, with the exception of W5 are greater than one. The Pr/Ph ratios together with Pr/nC$_{17}$ and Ph/nC$_{18}$ (Figure 3.5), suggest that the Woodford shale

kerogen is enriched in mixed type II/III organic matter deposited under predominantly sub-oxic conditions and thus imply deposition under relatively shallow waters.

Table 3.2: Geochemical data for oils and source rocks; parameters used in chemometrics are indicated with an asterisk. For a given petroleum system, oils and source rocks samples are enclosed. There are no oils associated with the Spraberry source rock samples. Oil samples 1475, 1502 and 1550 have abnormal maturities and stable carbon isotopes and are apparently interpreted as to be cracked oils of the Woodford. These three oils are separated from the rest of Woodford by a dotted line in the Table (Table splits to the next page).

PS Name	Spl No.	Spl Type	OEP	Ph/ nC18	Pr/ nC17	Pr/ Ph*	‰ Sat*	‰ Aro*	C.V*	% Tri.*	HHI*	BNI*	Mor. Ratio
Bone Spring	1537	O	1.03	0.75	0.50	0.77	-29.00	-28.23	-0.92	14.66	0.63	0.01	0.07
	1585	O	1.02	0.96	0.42	0.50	-29.07	-28.56	-1.48	15.52	0.69	0.01	0.07
	1586	O	1.02	0.81	0.53	0.73	-28.05	-27.26	-1.17	13.90	0.65	0.01	0.06
	1593	O	1.04	0.53	0.49	1.10	-29.10	-28.73	-1.78	15.41	0.64	0.01	0.06
	1538	O	1.00	0.77	0.39	0.56	-28.05	-27.40	-1.48	13.37	0.67	0.01	0.06
	1594	O	1.02	0.73	0.31	0.50	-28.91	-28.61	-1.99	11.59	0.63	0.01	0.07
Wolf-camp	WF1	S	1.19	0.62	0.49	1.14	-27.32	-27.20	-2.89	24.79	0.40	0.12	0.20
	WF2	S	1.10	0.52	0.38	1.06	-27.64	-27.35	-2.41	24.29	0.00	0.03	0.20
	WF3	S	1.18	0.62	0.71	1.73	-27.40	-26.89	-1.98	32.92	0.30	0.05	0.12
	WF4	S	1.10	0.39	0.48	1.68	-28.05	-27.20	-1.03	64.42	0.52	0.01	0.08
	WF5	S	1.14	0.82	0.66	0.89	-28.61	-28.05	-1.50	29.91	0.55	0.04	0.07
	WF6	S	1.30	1.55	1.19	1.10	-28.35	-27.70	-1.37	36.43	0.54	0.04	0.12
	WF7	S	1.01	0.36	0.38	1.19	-26.49	-25.91	-2.11	81.23	0.20	0.16	0.20
	1511	O	1.07	0.90	1.08	1.39	-28.54	-28.01	-1.60	26.84	0.35	0.02	0.11
	1581	O	1.10	0.84	1.08	1.55	-28.80	-28.57	-2.18	21.09	0.21	0.01	0.10
	1588	O	1.13	1.27	1.40	1.31	-28.96	-29.69	-4.26	18.29	0.45	0.01	0.09
	1469	O	1.08	0.65	1.08	1.85	-28.58	-27.88	-1.21	34.46	0.15	0.01	0.13
	1531	O	1.08	0.74	0.89	1.43	-28.18	-27.94	-2.35	27.56	0.44	0.02	0.11
	1540	O	1.07	0.67	0.83	1.54	-27.97	-27.81	-2.59	24.07	0.60	0.01	0.08
	1555	O	1.08	0.60	0.76	1.52	-27.93	-27.65	-2.34	39.37	0.10	0.12	0.26
Barnett	B2	S	1.88	0.58	0.73	0.98	-30.00	-28.77	0.40	72.07	0.57	0.03	0.15
	B3	S	1.23	0.75	0.72	0.87	-30.16	-29.51	-0.83	47.24	nm	0.04	0.13
	B5	S	1.12	2.05	1.62	0.90	-30.55	-28.52	2.36	69.71	0.36	0.02	0.14
	1473	O	1.11	0.92	1.42	1.71	-29.31	-28.66	-1.09	38.38	0.10	0.05	0.07
	1489	O	1.10	0.44	0.53	1.62	-29.86	-29.32	-1.16	45.49	0.60	0.03	0.06
	1486	O	1.10	0.73	0.96	1.61	-29.87	-29.53	-1.61	36.92	0.54	0.05	0.16
	1487	O	1.09	0.56	0.65	1.44	-30.06	-29.94	-2.04	31.11	0.60	0.03	0.11
	1495	O	1.08	0.66	0.75	1.33	-30.39	-29.91	-1.13	37.47	0.56	0.02	0.10
	1496	O	1.12	0.52	0.72	1.82	-29.88	-29.07	-0.56	46.15	0.56	0.01	0.07
	1591	O	1.09	0.43	0.59	1.87	-29.61	-29.30	-1.75	43.71	0.55	0.02	0.08
Wood-ford	W1	S	1.16	0.21	0.33	2.26	-30.89	-30.55	-1.28	81.18	0.50	0.06	0.39
	W2	S	1.08	0.43	0.51	1.31	-31.32	-30.19	0.61	49.71	0.32	0.02	0.19
	W3	S	1.14	0.86	0.86	1.43	-31.00	-30.01	0.19	45.16	0.49	0.02	0.11
	W4	S	1.08	1.13	0.82	1.18	-30.54	-29.73	-0.38	56.31	0.41	0.01	0.10
	W5	S	1.13	0.59	0.62	0.95	-31.17	-30.17	0.25	57.20	0.43	0.02	0.15
	W6	S	1.12	0.58	0.74	1.68	-30.86	-28.11	4.04	31.98	nm	0.07	0.14
	1346	O	1.13	0.46	0.44	1.47	-30.74	-30.22	-0.94	40.61	0.61	0.01	0.06
	1352	O	1.08	0.59	0.67	1.40	-30.69	-29.92	-0.40	56.42	0.36	0.01	0.09
	1369	O	1.10	0.26	0.41	2.13	-30.12	-29.51	-0.93	52.84	0.36	0.01	0.13

* Data used for chemometrics; - nm = not measurable; O = Oil; C = Condensate; S = Source rock; OEP = odd-over-even predominance = 2(C15+C17+C19)/3(C16+C18); Pr = Pristane; Ph = Phytane; ‰Sat = $\delta^{13}C$ of Saturated hydrocarbon fraction relative to PDB standard; ‰Aro = $\delta^{13}C$ of Aromatic hydrocarbon fraction relative to PDB standard; C.V = canonical variable = -2.53 $\delta^{13}C_{Sat}$ + 2.22 $\delta^{13}C_{Aro}$ – 11.65; Tri = Tricyclic terpanes; HHI = Homohopane index = $C_{35}/(C_{34}+ C_{35})$; BNI = Bisnorhopane Index = bisnorhopane/bisnorhopane+hopane; Mor = Moretane;

Ster/ Hop*	% Diaste	Steranes C27*	C28*	C29*	C30 Ste. Index*	C27/ C29*	C28/ C29*	Ts/ Tm	Hop/ Ste*	Pr/ (Pr+Ph)	C19 Tri/ C23 Tri.*	Norho/ Hop.*
0.09	44.17	39.70	15.66	44.64	0.05	0.89	0.35	0.56	11.11	0.44	nm	nm
0.08	45.96	39.16	17.46	43.38	0.03	0.90	0.40	0.88	12.50	0.33	nm	nm
0.07	46.66	40.91	13.74	45.35	0.04	0.90	0.30	1.14	14.29	0.42	nm	nm
0.11	47.56	36.55	16.08	47.37	0.05	0.77	0.34	0.55	9.09	0.52	nm	nm
0.07	39.57	39.28	12.79	47.93	0.04	0.82	0.27	0.66	14.29	0.36	nm	nm
0.08	45.16	36.63	14.45	48.92	0.05	0.75	0.30	0.85	12.50	0.33	nm	nm
0.50	48.07	38.07	22.63	39.31	0.05	0.97	0.58	1.26	2.00	0.53	0.69	0.44
0.29	44.63	29.99	21.49	48.52	0.00	0.62	0.44	1.30	3.45	0.51	0.50	0.59
0.46	47.03	30.50	23.29	46.20	0.10	0.66	0.50	1.28	2.17	0.63	0.12	0.85
0.31	57.78	43.99	17.21	38.80	0.06	1.13	0.44	0.89	3.23	0.63	0.03	1.11
0.17	40.12	36.08	13.01	50.91	0.07	0.71	0.26	0.94	5.88	0.47	0.09	1.40
0.62	53.23	46.24	19.50	34.26	0.02	1.35	0.57	0.73	1.61	0.52	0.08	0.52
0.86	47.26	45.86	24.08	30.06	0.17	1.53	0.80	0.63	1.16	0.54	0.23	0.81
0.19	48.11	37.83	20.93	41.24	0.10	0.92	0.51	0.88	5.26	0.58	nm	nm
0.15	59.14	36.59	23.93	39.48	0.06	0.93	0.61	1.69	6.67	0.61	nm	nm
0.15	51.48	38.60	21.31	40.09	0.06	0.96	0.53	0.98	6.67	0.57	nm	nm
0.15	49.35	42.39	19.55	38.06	0.10	1.11	0.51	1.45	6.67	0.65	nm	nm
0.19	52.17	37.45	25.17	37.38	0.12	1.00	0.67	2.00	5.26	0.59	nm	nm
0.13	49.37	38.26	17.34	44.40	0.09	0.86	0.39	1.02	7.69	0.61	nm	nm
0.28	59.38	30.56	13.96	55.48	0.03	0.55	0.25	0.88	3.57	0.60	nm	nm
0.55	56.73	50.84	39.16	10.00	0.06	5.08	3.92	1.00	1.82	0.50	0.32	0.79
0.53	55.75	40.42	27.55	32.03	0.00	1.26	0.86	0.85	1.89	0.46	0.22	0.66
1.25	34.66	47.31	8.26	44.43	0.02	1.06	0.19	0.36	0.80	0.47	0.01	0.73
0.16	36.00	53.48	18.57	27.95	0.19	1.91	0.66	0.18	6.25	0.63	nm	nm
0.33	57.86	36.82	18.97	44.21	0.06	0.83	0.43	0.97	3.03	0.62	nm	nm
0.27	48.53	48.26	17.50	34.24	0.07	1.41	0.51	1.06	3.70	0.62	nm	nm
0.26	53.66	41.26	19.35	39.39	0.07	1.05	0.49	0.10	3.85	0.59	nm	nm
0.26	47.37	44.54	20.60	34.86	0.08	1.28	0.59	0.93	3.85	0.57	nm	nm
0.39	61.06	45.26	22.03	32.71	0.09	1.38	0.67	1.20	2.56	0.65	nm	nm
0.30	64.47	40.17	17.29	42.54	0.08	0.94	0.41	1.96	3.33	0.65	nm	nm
1.50	54.90	54.81	15.29	29.90	0.08	1.83	0.51	0.56	0.67	0.69	0.11	nm
1.33	66.29	49.27	22.91	27.82	0.06	1.77	0.82	0.88	0.75	0.57	0.17	0.62
0.52	55.92	45.93	20.96	33.11	0.04	1.39	0.63	0.81	1.92	0.59	0.38	0.73
0.42	42.93	46.89	18.69	34.43	0.03	1.36	0.54	0.53	2.38	0.54	0.21	0.66
0.53	51.49	40.19	31.40	28.41	0.06	1.41	1.11	1.00	1.89	0.49	2.68	0.91
0.66	55.03	34.00	22.75	43.25	0.10	0.79	0.53	0.76	1.52	0.63	0.27	0.81
0.23	51.78	36.33	19.39	44.28	0.06	0.82	0.44	0.77	4.35	0.59	nm	nm
0.27	61.47	34.78	19.07	46.15	0.02	0.75	0.41	0.71	3.70	0.58	nm	nm
0.34	72.26	44.45	12.74	42.81	0.17	1.04	0.30	2.38	2.94	0.68	nm	nm
0.54	59.01	28.88	18.35	52.77	0.07	0.55	0.35	5.56	1.85	0.59	nm	nm
0.52	74.44	31.24	20.17	48.59	0.06	0.64	0.42	3.57	1.92	0.67	nm	nm
0.34	48.54	32.88	16.23	50.89	0.02	0.65	0.32	0.67	2.94	0.58	nm	nm

Ste.= sterane; Hop =17α(H), 21β(H)-hopane; Dia = Diasteranes; Ts = 18α(H)-22, 29, 30-trisnorhopane = trisnorneohopane; Tm = 17α(H)-22, 29, 30 trisnorhopane ; Norhop. = Norhopane = C29 Hopane; Mor. Ratio = Mor./(Mor. + Hop + Norhop.); $\%C_{27} = C_{27}\alpha\alpha\alpha R/(C_{27}\alpha\alpha\alpha R + C_{28}\alpha\alpha\alpha R + C_{29}\alpha\alpha\alpha R)$; $\%C_{28} = C_{28}\alpha\alpha\alpha R/(C_{27}\alpha\alpha\alpha R + C_{28}\alpha\alpha\alpha R + C_{29}\alpha\alpha\alpha R$; $\%C_{29} = C_{29}\alpha\alpha\alpha R/(C_{27}\alpha\alpha\alpha R + C_{28}\alpha\alpha\alpha R + C_{29}\alpha\alpha\alpha R$; C_{30} Ste. Index = $C_{30}\alpha\alpha\alpha R/(C_{27}\alpha\alpha\alpha R + C_{28}\alpha\alpha\alpha R + C_{29}\alpha\alpha\alpha R)$.

Table 3.2 Continued (Table splits to the next page)

PS N	Spl	Spl Type	OEP	Ph/ nC18	Pr/ nC17	Pr/ Ph*	‰ Sat*	‰ Aro*	C.V*	% Tri.*	HHI*	BNI*	Mor. Ratio
	1379	O	1.12	0.34	0.50	2.08	-31.85	-30.83	0.52	52.14	0.25	0.01	0.13
	1497	O	1.20	0.35	0.30	1.35	-31.04	-30.61	-1.04	49.48	0.10	0.01	0.03
	1499	O	1.10	0.64	0.99	1.89	-30.64	-30.48	-1.77	54.43	0.35	0.01	0.60
	1512	O	1.09	0.78	1.16	1.70	-31.46	-31.09	-1.05	56.68	0.10	0.01	0.01
	1364	O	1.09	0.21	0.35	2.29	-30.29	-28.95	0.74	52.49	0.10	0.01	0.11
	1334	O	1.10	0.53	0.51	1.32	-30.65	-29.90	-0.45	36.16	0.59	0.01	0.08
	1377	O	1.09	0.36	0.44	1.68	-31.31	-30.45	0.00	38.26	0.10	0.01	0.01
	1381	O	1.09	0.30	0.40	1.72	-30.86	-29.88	0.12	66.81	0.10	0.14	0.24
	1331	C	1.20	0.23	0.30	2.15	-30.11	-29.53	-1.00	57.33	0.40	0.01	0.01
	1333	C	1.14	0.22	0.32	2.28	-30.04	-28.82	0.40	60.73	0.10	0.01	0.07
	1361	C	1.19	0.15	0.22	2.62	-30.61	-28.86	1.75	42.32	0.65	0.01	0.05
	1360	C	1.35	0.18	0.22	2.66	-30.60	-28.88	1.68	47.80	0.65	0.01	0.08
	1367	C	1.15	0.31	0.47	2.34	-30.80	-29.10	1.70	48.67	0.37	0.01	0.09
	1372	C	1.23	0.14	0.20	2.49	-29.91	-28.63	0.49	55.19	0.73	0.01	0.04
	1370	C	1.38	0.42	0.61	2.93	-30.41	-28.89	1.18	56.71	0.10	0.01	0.01
	1382	C	1.38	0.36	0.38	0.00	-31.55	-30.10	1.38	34.35	0.61	0.01	0.09
	1336	C	1.15	0.38	0.40	1.74	-33.65	-32.88	0.52	41.65	0.47	0.01	0.09
	1338	C	1.17	0.22	0.19	1.76	-33.40	-32.21	1.38	47.94	0.10	0.03	0.26
	1339	O	1.83	0.27	0.12	1.48	-33.90	-33.68	-0.62	41.96	0.53	0.01	0.08
	1345	O	1.76	0.28	0.14	1.71	-32.88	-32.32	-0.18	33.67	0.45	0.01	0.14
	1354	O	1.16	0.30	0.40	2.04	-33.44	-32.10	1.72	57.91	0.10	0.01	0.17
	1558	O	1.05	0.37	0.49	1.69	-29.89	-29.58	-1.67	22.24	0.45	0.01	0.14
	1475	O	1.10	0.42	0.64	2.00	-28.49	-28.00	-1.70	68.71	0.10	0.01	0.01
	1502	O	1.06	0.41	0.67	1.89	-28.14	-27.51	-1.50	49.96	0.48	0.01	0.09
	1550	O	1.05	0.48	0.80	1.83	-28.06	-27.33	-1.30	49.36	0.50	0.01	0.23
	SP1	S	1.08	0.67	0.72	1.24	-28.80	-27.56	0.07	57.83	0.31	0.02	0.10
	SP2	S	1.11	1.60	1.10	0.98	-29.24	-27.26	1.84	34.06	0.45	0.03	0.11
	SP3	S	1.12	2.26	1.84	1.27	-28.45	-27.76	-1.28	21.13	0.24	0.03	0.16

Ster/ Hop*	% Diaste	Steranes C27*	C28*	C29*	C30 Ste. Index*	C27/ C29*	C28/ C29*	Ts/ Tm	Hop/ Ste*	Pr/ (Pr+Ph)	C19 Tri/ C23 Tri.*	Norho/ Hop.*
0.29	61.77	33.98	11.11	54.91	0.10	0.62	0.20	3.23	3.45	0.63	nm	nm
0.28	66.90	29.83	29.44	40.73	0.05	0.73	0.72	3.13	3.57	0.70	nm	nm
0.19	49.22	33.58	16.57	49.85	0.07	0.67	0.33	0.75	5.26	0.57	nm	nm
0.14	58.59	40.43	10.21	49.36	0.10	0.82	0.21	1.04	7.14	0.63	nm	nm
0.67	57.59	40.54	40.00	19.46	0.10	2.08	2.06	0.76	1.49	0.63	nm	nm
0.32	64.49	44.89	20.01	35.10	0.11	1.28	0.57	3.57	3.13	0.68	nm	nm
0.37	63.67	45.09	23.00	31.91	0.10	1.41	0.72	6.67	2.70	0.70	nm	nm
0.26	66.18	34.45	19.74	45.81	0.07	0.75	0.43	0.69	3.85	0.72	nm	nm
0.25	60.17	34.15	23.83	42.02	0.12	0.81	0.57	1.72	4.00	0.73	nm	nm
0.23	63.32	35.17	24.40	40.43	0.10	0.87	0.60	2.17	4.35	0.70	nm	nm
0.38	69.80	32.63	25.91	41.46	0.07	0.79	0.62	0.77	2.63	0.71	nm	nm
0.25	72.84	23.89	25.46	50.65	0.05	0.47	0.50	2.78	4.00	0.75	nm	nm
0.21	52.68	36.32	18.17	45.51	0.04	0.80	0.40	0.68	4.76	1.00	nm	nm
0.21	57.28	40.76	15.55	43.69	0.24	0.93	0.36	2.33	4.76	0.61	nm	nm
0.48	51.50	41.26	18.65	40.09	0.36	1.03	0.47	0.85	2.08	0.66	nm	nm
0.31	53.40	30.88	19.44	49.68	0.12	0.62	0.39	1.12	3.23	0.60	nm	nm
0.16	48.46	30.43	29.45	40.12	0.11	0.76	0.73	1.25	6.25	0.63	nm	nm
0.23	62.90	66.48	9.13	24.39	0.09	2.73	0.37	0.96	4.35	0.67	nm	nm
0.19	59.10	17.28	49.40	33.32	0.01	0.52	1.48	0.94	5.26	0.63	nm	nm
0.52	64.93	42.58	19.96	37.46	0.18	1.14	0.53	1.89	1.92	0.67	nm	nm
0.28	79.36	42.49	11.10	46.41	0.13	0.92	0.24	3.57	3.57	0.65	nm	nm
0.38	71.09	43.12	17.04	39.84	0.15	1.08	0.43	2.00	2.63	0.65	nm	nm
0.31	46.27	39.55	22.46	37.99	0.09	1.04	0.59	1.04	3.23	0.55	0.05	0.49
1.93	49.31	59.19	22.66	18.15	0.08	3.26	1.25	0.43	0.52	0.50	0.07	0.59
1.09	47.92	43.83	14.63	41.55	0.04	1.05	0.35	0.25	0.92	0.56	0.15	0.87

3.4.4 Cyclic Biomarker Characteristics of Source Rocks

Cyclic biomarkers, mainly steranes and terpanes determined by GC-MS through single ion monitoring of molecular ions with m/z 217 and m/z 191, respectively, were used in this study to characterize organic matter in source rock extracts and oils. Peak identification in steranes and terpanes fragmentograms is illustrated by Woodford sample W3 (Figure 3.6). The data for all source rock samples are listed together with oils in Table 3.2.

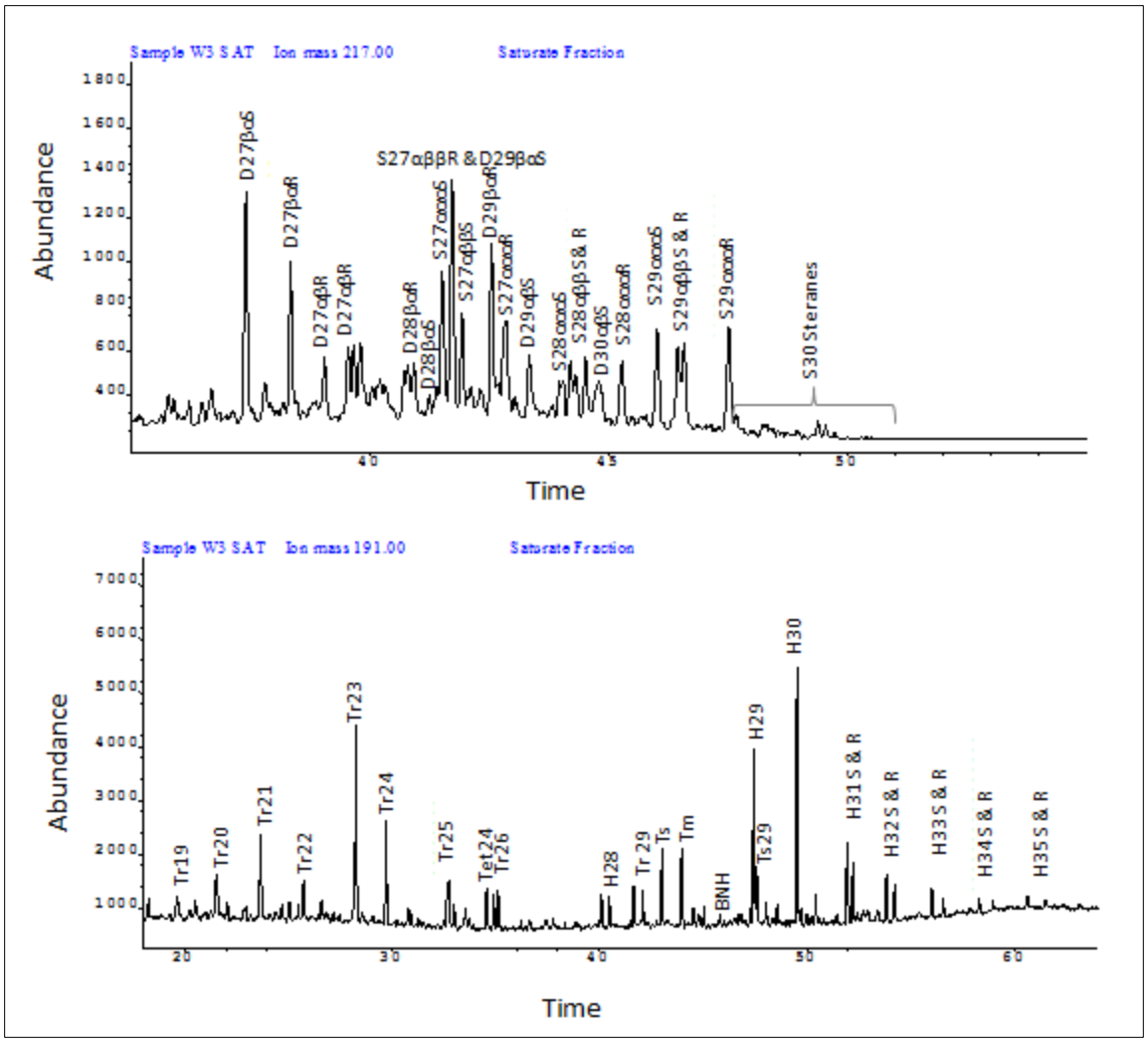

Figure 3.6: GC-MS m/z 191 (Terpanes) and m/z 217 (Steranes) mass fragmentograms for Woodford (W3) source rock sample. D, S, Tr, and H represents Diasterane, Sterane, Tricyclic terpane, and Hopane respectively.

3.4.4.1 Organic Matter Type

The occurence of C_{30} steranes, a marine marker (Moldowan et al., 1985), sterane/hopane ratios (Moldowan et al., 1985), C_{19}/C_{23} tricyclic ratios and pristane/phytane ratios (McKirdy et al., 1983) were used to constrain the nature and type of organic matter in source rocks. The use of sterane/hopane ratios in inferring organic matter type in

sediment extracts and oils is premised on the realization that hopanes are derived from prokaryotic bacteria while steranes are derived from eukaryotes, including plankton and benthic algae. Consequently, in environments where organic matter reworking by bacteria does occur, such as in most non-marine environments, hopanes will be more abundant compared to steranes (Moldowan et al., 1985; Mello et al., 1988).

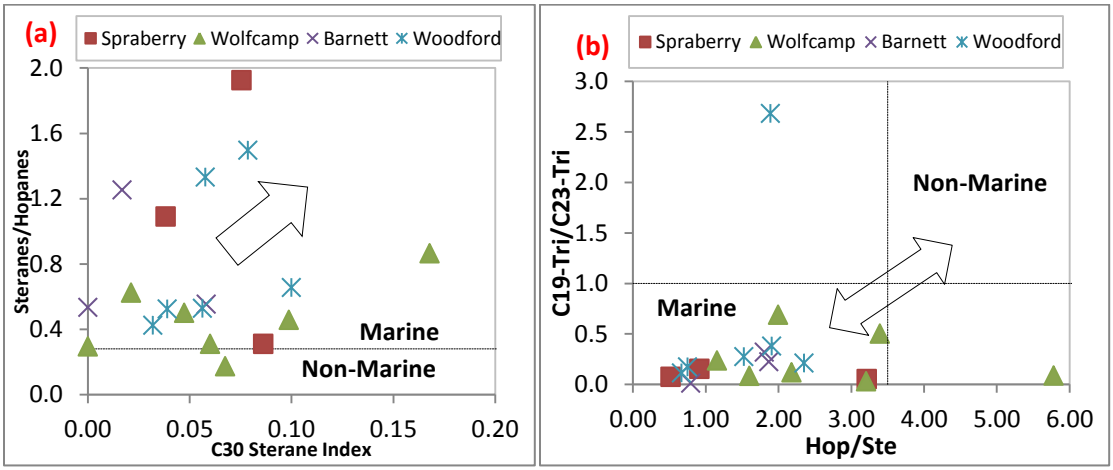

Figure 3.7: Depiction of organic matter type among the source rocks studied. (a) Plot of steranes/hopanes versus C_{30} sterane index inferring the nature of organic matter in source rocks. The arrow indicates direction of increasing marineness (Moldowan et al., 1985). (b). Plot of C_{19}/C_{23} tricyclic ratio versus hopane/sterane ratio illustrating the organic matter type. Note the variance in organic matter among the samples of a given source rock. See Table 3.2 for data and definition of terms

Some of the biomarker parameters that depict the nature of organic matter are plotted in Figure 3.7. Like their oils (Chapter 2), there are no clear-cut contrasts within the biomarker data of the different source rock extracts. Although all the source rocks are comprised of marine organic matter, there is a high variance among the samples of an individual source rock. These observations of marine and varied organic matter are also supported by the distribution of C_{27}, $C_{28,}$ and C_{29} steranes (Table 3.2), which generally show higher C_{27} compared to C_{29}. High C_{27} relative C_{29} steranes is an attribute consistent

with autochthonous organic matter, predominantly marine algal/phytoplankton/bacterial precursors as opposed to higher plant organic matter which is usually associated with enrichment in C_{29} steranes (Huang and Meinschein, 1979; Shanmugam, 1985; Moldowan et al., 1985; Volkman, 1986). A C_{27}-C_{28}-C_{29} sterane ternary plot (not included) did not uniquely differentiate samples.

The Wolfcamp source rock extracts, however, show special characteristic in that they are mostly enriched in enriched in C_{29} steranes relative to C_{27} steranes (Table 3.2). Exceptions to this are Wolfcamp extract samples WF4 and WF7. Although these observations suggest enrichment in higher plant organic matter, *n*-alkanes, and isoprenoids data (Figures 3.4 and 3.5), stable carbon isotope compositions (Figure 3.10), and other biomarker data (Figure 3.7a & b) suggest dominance of marine algal/phytoplankton organic matter. The dominance in C_{29} steranes relative to C_{27} and C_{28} steranes in contradiction with abundant evidence of algal and phytoplankton organic matter may imply contribution of C_{29} steranes from a specific type (red and green) of algae (e.g Volkman, 2003; Schwark and Empt, 2005; Kodner et al., 2008).

Although not significantly rich in C_{30} steranes (Figure 3.7a), a marker of marine organic matter (Moldowan et al., 1985; Mello et al., 1988), their sterane/hopane ratios, Pr/Ph and C_{19}/C_{23} tricyclic ratios (Figure 3.7b and Table 3.2) support a predominance of marine algal/phytoplankton/bacterial organic matter for all source rocks studied. The observed variance among extracts from individual source rocks is interpreted as a reflection of variability in organic matter, and by default depositional environments. Although this

variability could be enhanced by the scale of the sampling, it gives an idea of how variable shales can be.

3.4.4.2 Depositional Environmental Conditions

The redox conditions during the deposition of organic matter in the source rocks were inferred using established biomarker redox parameters including bisnorhopane, gammacerane, homohopane, norhopane (C_{29} hopane), and Pr/Ph among others. Bisnorhopane is a known biomarker in anoxic environments (Tornabene et al., 1979; Katz and Elrod, 1983; Moldowan et al., 1984) while gammacerane is known in hypersaline/stratified, usually anoxic water columns where Pr/Ph ratio is usually less than 0.5 due to contribution of phytane from halophilic bacteria (ten Haven et al., 1987; 1988; Moldowan et al., 1985; Sinninghe Damsté et al., 1995). Both Bisnorhopane and gammacerane are extremely low in the source rock extracts as well as in the oils under study. Although this could be interpreted to be associated with deposition under non-reducing conditions, these biomarkers are not universally available in all reducing environments in marine settings. For example bisnorhopane is generally known to be low in marine siliciclastics (Mello, 1988). Moreover, it is highly affected by maturity, significantly reducing at high maturities (Moldowan et al., 1984; McDade et al., 1993). As for gammacerane, not all highly reducing environments have gammacerane (ten Haven et al., 1987; 1988; Sinninghe Damsté et al., 1995). Because of these limitations, most of the redox interpretations discussed here are based mostly on acyclic biomarkers (isoprenoids), homohopanes (Peters and Moldowan, 1991; Dahl, 1994) and norhopanes,

the latter also a known biomarker in carbonate source rocks (Fan Pu et al., 1988 and ten Haven et al., 1988).

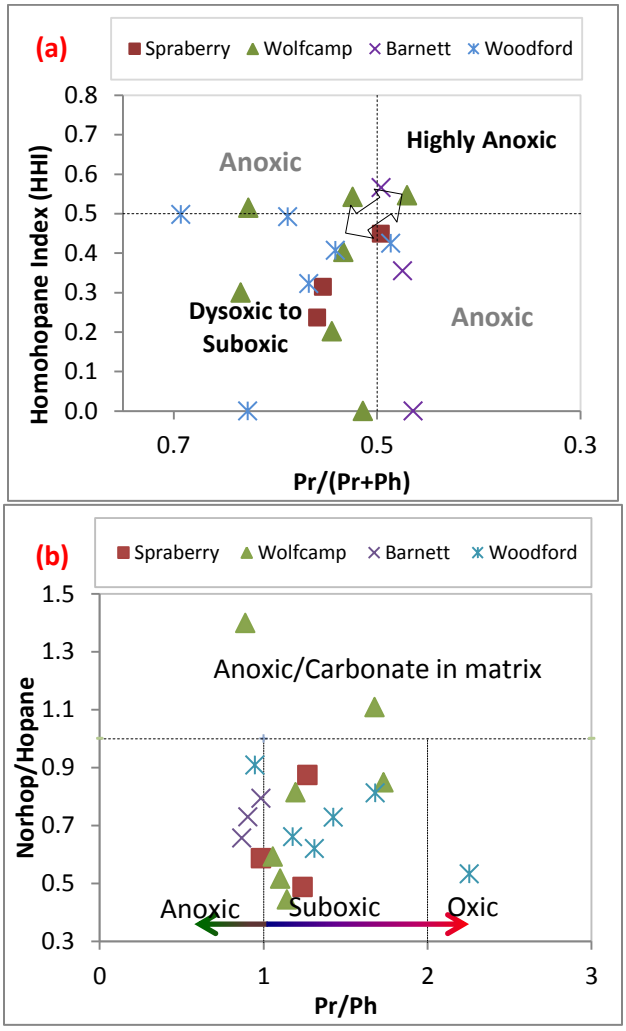

Figure 3.8: Depiction of redox of the depositional environment during the deposition of source rocks studied. (a). Plot of Homohopane index versus the sum ratio of pristane and phytane. (b). Norhopane/Hopane versus Pristane/Phytane ratio illustrating the redox of the depositional environment, potential lithology and organic matter type. Note the anoxic and potentially carbonate presence in the Barnett samples. See Table 3.2 for definition of terms. HHI line from Dahl et al. (1994), Norhopane/Hopane line from Fan Pu et al. (1988); Pr/Ph and Pr/(Pr+Ph) lines from several sources (e.g. Hughes et al., 1984; Palacas et al., 1984).

Apart from the Barnett extract samples which consistently plot in area indicating deposition under marginally anoxic conditions, the rest of the studied source rocks plot in regions that indicate deposition under sub-oxic conditions (Figures 3.5, 3.8a & b). The

scatter among the samples of a given source rock is consistent with varied depositional conditions as discussed earlier.

The stable carbon isotopes ratios, the C_{27}-C_{28}-C_{29} sterane distributions and sterane/hopane ratios for all these source rock extracts support a marine organic matter and or depositional setting. The homohopane index, Pr/Ph, Pr/nC_{17}, Ph/nC_{18}, (Table 3.2 and Figure 3.5) all suggest predominance of sub-oxic or shallow water depositional conditions for all these source rocks. The Barnett shale is however an exception, with Pr/Ph ratios depicting anoxia. Deep-water conditions for the Barnett are also supported by geological investigations of Loucks and Ruppel (2007). Shallow water conditions during the deposition of the Woodford shale is consistent with geological interpretations of Johnson et al. (1985) in which they report several regressions and transgressions episodes during the Devonian.

3.5. Oil-Source Rock Correlations

3.5.1 Chemometrics

The biomarker and stable carbon isotope data used in chemometrics are listed in Table 3.2. The choice of chemometric approach was based of its aptness in handling large data (Øygard, 1987; Zumberge, 1987; Peters et al., 2007; Peters et al., 2013) compared to forensic-type correlation approaches. In fact, correlation attempts using x/y-type plots did not yield unambiguous results. Although several reasons for non-correlation could be enumerated (e.g Curiale, 2002; 2008), for this data set, individual source rock samples are highly varied in organofacies. Secondly, most of the oils are highly mature, and are

likely to be cracked based on the definitions of Dahl et al. (1999) and Schoell and Carlson (1999). It could as well be due to the fact that oil is a composite fluid generated from various horizons of the source rock (Peters et al., 2005; Curiale, 2008). A multi-variate statistical correlation or chemometric approach using biomarker however resulted in the identification of reliable oil-source rock associations or probable petroleum systems (Figure 3.9).

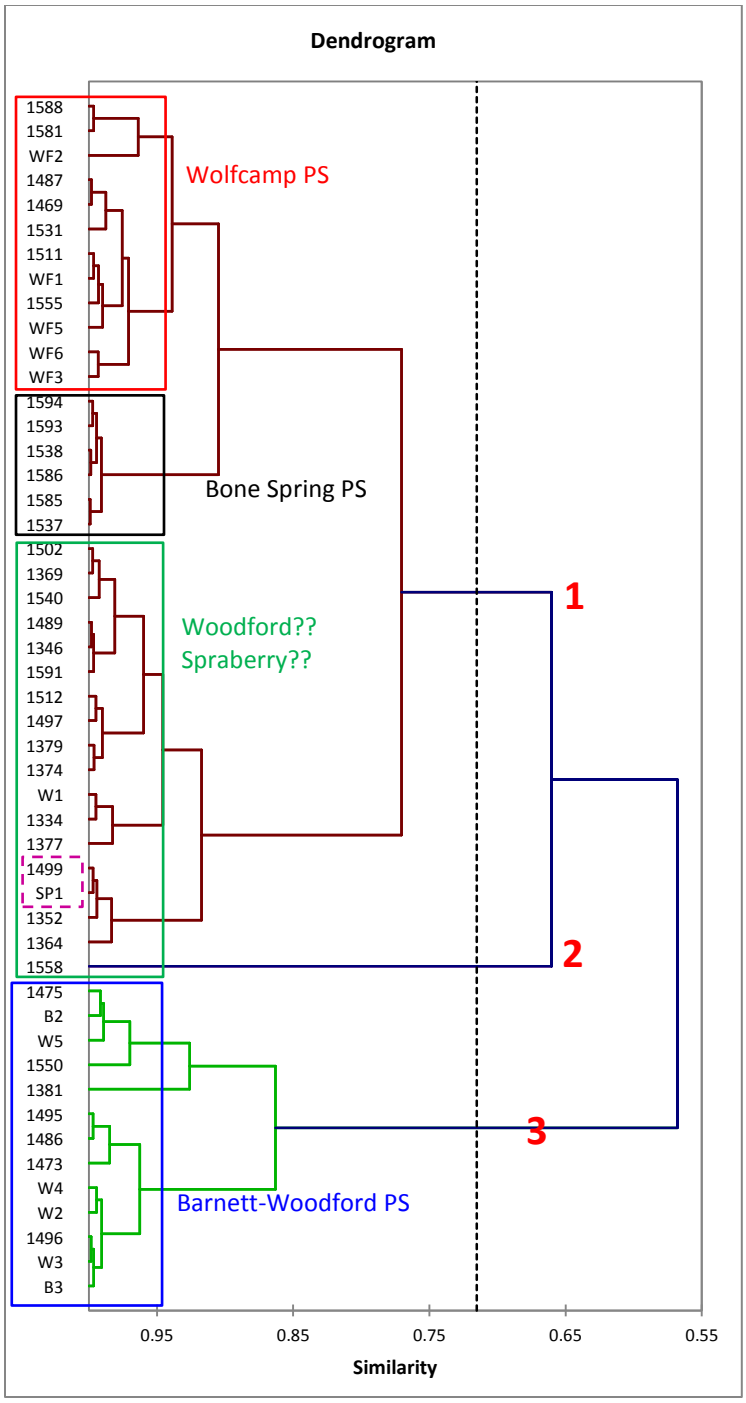

Figure 3.9: Chemometric correlation using source related biomarker and stable carbon isotope data. Calculated using Pearson correlation, auto truncation and complete linkage options embedded in XLSAT (Addinsoft, 2012). Condensates, Simpson oils, and obviously immature source rock samples; Sp2, Sp3, WF4 and B5 excluded. This classification leaves the oils inferred as Bone Spring sourced (Chapter 2) intact, implying no source rock association in the data set. The correlation divides the samples into pre-Pennsylvanian and Post-Pennsylvanian systems. Group 2 cluster of one sample (1558) is certainly highly mixed. Simpson oils were separated from the Barnett-Woodford-Simpson by virtue of their extremely low stable carbon isotopic compositions and strong OEP within nC$_{15}$-nC$_{19}$ range as discussed in detail in Chapter 2.

3.5.1.1 Analysis of Chemometric Groupings (oils and source rocks)

A striking observation is that oils and source rocks are generally closely related as reflected by the division into only two major clusters in all the dendrograms (Figure 3.9). Oil sample 1558 which forms an independent group or "cluster of one" is interpreted as highly mixed oil. The two major clusters appear to separate the samples into pre-Pennsylvanian and Post-Pennsylvanian. Increasing the degree of similarity to 95% resulted into 4 major distinct groupings of oils and source rocks (Figure 3.9). The new clustering (enhanced by color boxes) allows for definition of Wolfcamp and the Bone Spring (marl) petroleum systems. The remaining oils associate with the Barnett, Woodford, and Spraberry in two clusters and therefore imply a mixed Barnett-Woodford-Spraberry petroleum system. These latter oils were inferred by geochemical inversion (Chapter 2) to be sourced from Woodford-Barnett source rocks.

Oil sample 1499 located in the Pennsylvanian platform carbonate play in the Central Basin Platform is intimately related to the Spraberry source rock sample Sp1. Stable carbon isotope data indicate that oil sample 1499 has $\delta^{13}C_{Sat}$ of -30.64 and $\delta^{13}C_{Aro}$ of -30.48. As discussed earlier, this range is typical of Woodford and/or Barnett extracts. In addition, Ts/Tm ratio for this oil is 2.78, which is too high for the maturity of the Spraberry even at its deepest occurrence based on thermal modeling (Chapter 4). Finally, it would be hard to explain the Spraberry-generated oil in the Pennsylvanian carbonate reservoirs at Central Basin Platform. This is premised on the fact that the Spraberry started generating, long after generation from Woodford, Barnett, and Wolfcamp

(Chapter 4), all of which have pathways into this play and are still actively generating. This association is therefore considered spurious.

Of the remaining oils, most of which were interpreted to be sourced from either the Barnett or the Woodford, only oil samples 1473, 1475, 1381, 1486, 1495, and 1496 intimately cluster with Barnett and Woodford shale samples at a similarity degree of 96% (Figure 3.9). These oils are therefore considered genuine for the Barnett-Woodford system while oil samples 1512, 1374, 1497, 1379, 1369, 1502, 1499, 1352, 1364, 1334, 1346, 1591, 1489, 1364, and 1377 with only one Woodford sample, may be genuine for Woodford as further explained under section 3.5.2 below. The apparent hazy relationship of these oils with the Woodford-Barnett source rock samples is attributed to maturity contrasts between oils and source rocks. The oils are higher in maturity than most of the source rock samples used in this study. Moreover, the source rock samples are highly varied in organofacies. This does not however rule out the possibility of influence by other oils sourced from other systems as well. This is especially likely in oils hosted in the Central Basin Platform reservoirs, where, because of the Pennsylvanian uplift and erosion that affected as deep as Ordovician (Wright, 1979; Hills, 1984), all the pre-Pennsylvanian source rocks have a potential pathway to reservoirs there.

3.5.2 Stable Carbon Isotope Compositions

Utilization of stable carbon isotopes in correlations, including associated limitations is widely discussed in the geochemical literature (e.g. Chung et al., 1981; Hatch et al., 1987; Riebesell et al. 2000). Peters et al. (2005) indicated that for equivalent levels of maturity,

bitumens are approximately 0.5-1.5‰ depleted in ^{13}C compared to their kerogens. In addition to differences caused by generation fractionation, maturity contrast between the source rocks and oils also cause differences in isotopic compositions, where source rocks are generally heavier than their oils (Chung et al., 1981; Peters et al., 2005). $\delta^{13}C$ data were used to refine the oil-source rock associations established by chemometrics above.

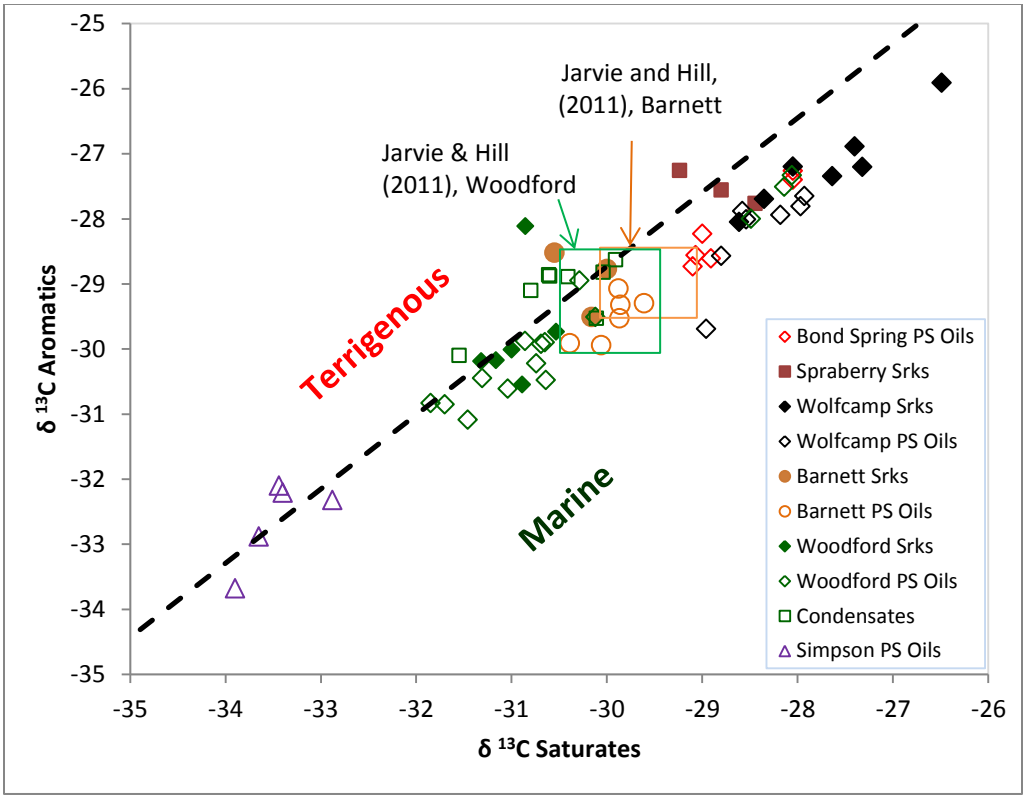

Figure 3.10: Stable carbon isotope ratios in ‰ relative to Pee Dee Belemnite (PDB) standard for saturated versus aromatic hydrocarbons showing relationship between oils and source rock extracts. The line separating the terrigenous from marine derived oils is based on statistical analysis of hundreds of known oils (Sofer, 1984). Srks = Source rocks; PS = petroleum system.

As seen from Figure 3.10, the Simpson oils are distinct with ^{13}C-stable carbon isotope depletion, a characteristic that is associated with Ordovician sourcing (e.g. Reed et al., 1986; Longman and Palmer, 1987; Hatch et al., 1987; Jacobson et al., 1988). Although

source rocks for these oils were not included in the correlations due to extremely low amount of sample size, the characteristic nature of Ordovician sourcing, especially ^{13}C depletion is clearly evident. This group of oils was discussed in detail in Chapter 2, where, it was noted that, in addition to isotopic depletion and very low isoprenoid (Pr and Ph) abundance, these oils also have significant odd-over-even predominance (OEP), a characteristic which, for mature oils, typify Ordovician sourcing (e.g. Longman and Palmer, 1987; Hatch et al., 1987; Jacobson et al., 1988). This uniqueness, establishes a justification for an Ordovician petroleum system, which according to their geochemical characteristics (Chapter 2), points to shales of the Simpson Group, an already established petroleum system (Simpson-Ellenberger) in the Permian Basin (Katz et al., 1994). For this study, because of the presence of oils in both Simpson and Ellenberger reservoirs, the descriptive name Simpson-Simpson-Ellenberger is deemed desirable.

Although the Barnett and Woodford systems couldn't be separated in the dendrogram (Figure 3.9), isotopically, oil samples; 1475, 1486, 1489, 1495, 1496, 1591, and all but one condensate, 1382 are closely associated with the Barnett. The condensates in this category include samples 1331, 1333, 1360, 1361, 1367, 1370, and 1372. Oil samples 1334, 1352, 1377, 1364, 1369, 1374, 1379, 1381, 1497, and 1512 are isotopically closely associated with Woodford and include one condensate sample 1382. Excluding the condensates, the most striking distinction created by this isotopic divide is that oils isotopically associated with the Woodford are found in reservoirs which are stratgraphically in the Mississippian and below while the oils isotopically associated with the Barnett are stratigraphically in reservoirs above the Mississippian. This divide also

separates the oils in such a way that Mississippian sourced oils are lower in maturity than the higher maturity Woodford oils (Figure 3.11). A limitation of this distinction is that stable carbon isotope values for Woodford and Barnett are very close and therefore difficult to distinguish unequivocally. This is especially so, considering the phenomenon of "migration of stable carbon isotope composition values with maturity" as discussed earlier. In other words, the stable carbon isotope data migration associated with maturity contrasts is such that Woodford and Barnett would be indistinguishable isotopically.

However, although the data do not unambiguously separate the two petroleum systems, maturity contrasts between the oils from the two supposedly petroleum systems, together with the distinction in stratigraphic locations of the respective oils suggest that the difference could be geologically realistic. The geological explanation for this occurrence is that the Mississippian acted as a perfect seal, preventing upward migration of Woodford generated oils. This is supported by the observation of Woodford-generated oils (1499, 1497, and 1512) in the Pennsylvanian in the Central Basin Platform where the Barnett is absent by erosion.

Except for one, the condensates are isotopically associated with the Barnett and reservoired in stratigraphically lower reservoirs of the Devonian, Silurian, and Ordovician and are actually more mature than the Barnett source rocks analyzed (Figure 3.11). The observed isotopic association with the Barnett is therefore interpreted to be due to enrichment with increasing maturity of the condensates, implying an origin other than the Barnett. One condensate, sample 1382, which is relatively low in maturity, is isotopically associated with the Woodford source rock samples and is reservoired in the

Lower Mississippian. This insinuates a possibility of the Woodford being a source for all condensates. The relatively low maturity of condensate sample 1382 associated with Woodford source rock samples, suggests that some condensates may be genetic rather than due to thermal alteration, further supporting a strongly varied organofacies for the Woodford. These sub types of condensates are distinguishable based on their stable carbon isotope compositions, with thermally generated condensates isotopically heavier than their genetically derived counterparts.

The assignment of the condensates to Woodford sourcing is also supported by the work of Broadhead (2005; 2010) where he tracked changes in the gas-oil-ratio (GOR) of oils in the underlying Wristen reservoirs of New Mexico and found it to be related to changes in Woodford organofacies (kerogen types) and maturity. In his observations, he noted a change in Woodford organofacies from marine in the center of the basin to terrestrial in the northern reaches in New Mexico where he also observed a corresponding increase in the GOR and API gravity of the oils, depicting sourcing from terrestrial organic matter sources. This also explains the observed terrestrial affinity in Figure 3.10.

3.5.3 Biomarker Maturity of Oils and Source Rocks

Attempts to evaluate maturity using common conventional biomarker maturity parameters 20S/[20(S+R)] and 22S/[22(S+R)] showed that nearly all the oils and source rocks are at advanced maturities. A majority of the samples plotted beyond the bounds for which these isomerization parameters are reliable as maturity indicators (e.g. Mackenzie, 1984; Moldowan et al., 1992; Waples & Machihara, 1991; Peters et al.,

1999). Only the low maturity Spraberry source rock samples, and the oils inferred to be sourced from the Bone Spring marl source rock, could adequately be interpreted using these conventional biomarker maturity parameters. Therefore, thermally more resilient maturity parameters, specifically the percentages of diasteranes and tricyclics (e.g. Van Graas, 1990), were opted to evaluate the maturities of oils and source rocks to validate correlations or petroleum systems assignments. As indicated in Figure 3.11, oils and source rock samples show a range of maturities. Of particular significance is the separation of samples into four maturity clusters (Figure 3.11). Oils inferred to be sourced from the Bone Spring source rock are extremely low in maturity and define a separate cluster on their own (<1.0% R_o).

The next cluster in the maturity ladder comprises mainly Spraberry source rock and Wolfcamp petroleum system samples, both oil and source rocks. One Ordovician reservoired oil, inferred to be derived from the Simpson by virtue of its extremely low isotope signatures, and one condensate sample also belong to this maturity cluster. In addition, four oils from the Barnett petroleum system are part of this maturity cluster. The next higher maturity cluster includes the remaining three oil samples from the Barnett petroleum system, three samples from the Simpson petroleum system, six samples including condensates from the Woodford petroleum system, one oil sample from the Wolfcamp petroleum system, three Woodford source rock samples, one Spraberry source rock sample, and two Barnett source rock sample all belong to this maturity cluster. The most mature cluster comprises oil samples derived from the Woodford shale and includes most of the condensates. One oil sample from the Simpson petroleum system, two source

rock samples from the Woodford and one from the Barnett belong here. Despite the varied maturity, the presence of oils of a given inferred petroleum system together with their source rocks is an indication for the existence of that petroleum system as supported by modeling (Chapter 4). In general, high maturity, especially of the oils, is a major constraint in the clear definition of petroleum systems within the Permian Basin.

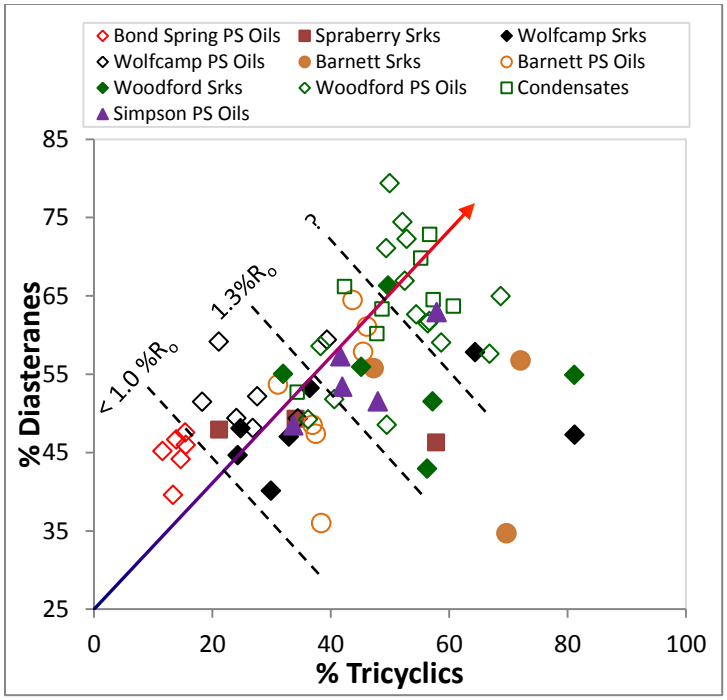

Figure 3.11: Percent diasteranes (measured as percentage of total components in the m/z 217 'sterane' fragmentogram) versus percent tricyclics (C_{19} through C_{29} tricyclis as percent of total identified m/z 191 fragmentogram. Both Diasteranes and tricyclics increase with maturity (Seifert and Moldowan, 1978; Peters et al., 1986; Peters and Moldowan, 1991) as indicated by the arrowed line. Transverse dotted lines are approximate $\%R_o$ maturity equivalents (Peters et al., 2005). Again, oils inferred to be sourced from the Bone Spring (Chapter 2) stand alone, without any source rock associations. Srks = Source rocks; PS = petroleum system.

3.6. Petroleum Systems Distributions

Based on chemometrics, stable carbon isotope compositions and maturity of oils and source rock samples, as well as the inference from geochemical inversion (Chapter 2), five stratigraphically segregated petroleum systems (Figure 3.12) are recognizable within the scope of the study. Oils are listed in association with their respective source rocks in Table 3.2. A detailed description of the petroleum systems elements and process, including trap formation, generation, and expulsion timing and migration are contained in Chapter 4.

Table 3.3: Oil Samples within a stratigraphic/Play framework. The dominant entrapment style is indicated in parenthesis-most structural traps formed during the Mississippian-Pennsylvanian tectonism. Sample colors correspond with the petroleum system colors as used in Figure 3.12). Based on several sources (Frenzel et. al., 1988; Dutton et al., 2004). See Chapter 4 for a detailed listing of sources.

Reservoir Age/Entrapment	**Play Name and Associated Oil Samples**	**Location**
Upper Permian	San Andres Platform Carbonate Play: 1593	Eastern CBP
Early/Middle Permian (Stratigraphic)	Leonardian Restricted Carbonate Play: 1537, 1538, 1594 & 1585	CBP and Shelf areas
	Wolfcamp/Leonardian Slope & Basinal Carbonate Play: 1511, 1531, (1550), 1555, 1581, 1586 & 1588	Slope and basin areas of MLD & DLW
	Wolfcamp Platform Carbonate Play: 1540, {1558} & 1591	CBP edges & NWS
Pennsylvanian (Stratigraphic & Structural)	Pennsylvanian Platform Carbonate Play: 1497, 1499 (1502) & 1512	CBP and MLD
	The Horseshoe Atoll: 1469, 1473, 1487 & 1489	Northern MLD
	Upper Pennsylvanian/Lower Permian Slope/Basinal Sandstone Play: (1475), 1486, 1495 & 1496	Eastern Shelf
Mississippian (Structural)	The Mississippian Platform Carbonate Play: 1381 & 1382	Most of the northern PB
Devonian (Structural)	Thirtyone Deep-water Chert: 1377 & 1379	South and Central CBP
	Thirtyone Ramp Carbonate Play: 1367, 1370 & 1372	Central CBP
Silurian (Structural)	Fussellman Shallow Platform Carbonate Play: 1360, 1361, 1363 & 1364	CBP, NW Shelf & MLD
	Wristen Buildups and Platform Carbonate Play: 1369 & 1374	North of Central Basin Platform & NW Shelf
Ordovician (Structural)	Ellenberger Selectively Dolomitized Ramp Carbonate Play: 1331 & 1333	Eastern Shelf
	Simpson Cratonic Sandstone Play: 1336, 1339 & 1354	CBP
	Ellenberger Karst-modified Play: 1334, 1338, 1345, 1346 & 1352	CBP/MLD

DLW = Delaware, CBP = Central Basin Platform, MLD = Midland and PB= Permian Basin; NWS = Northwest Shelf.

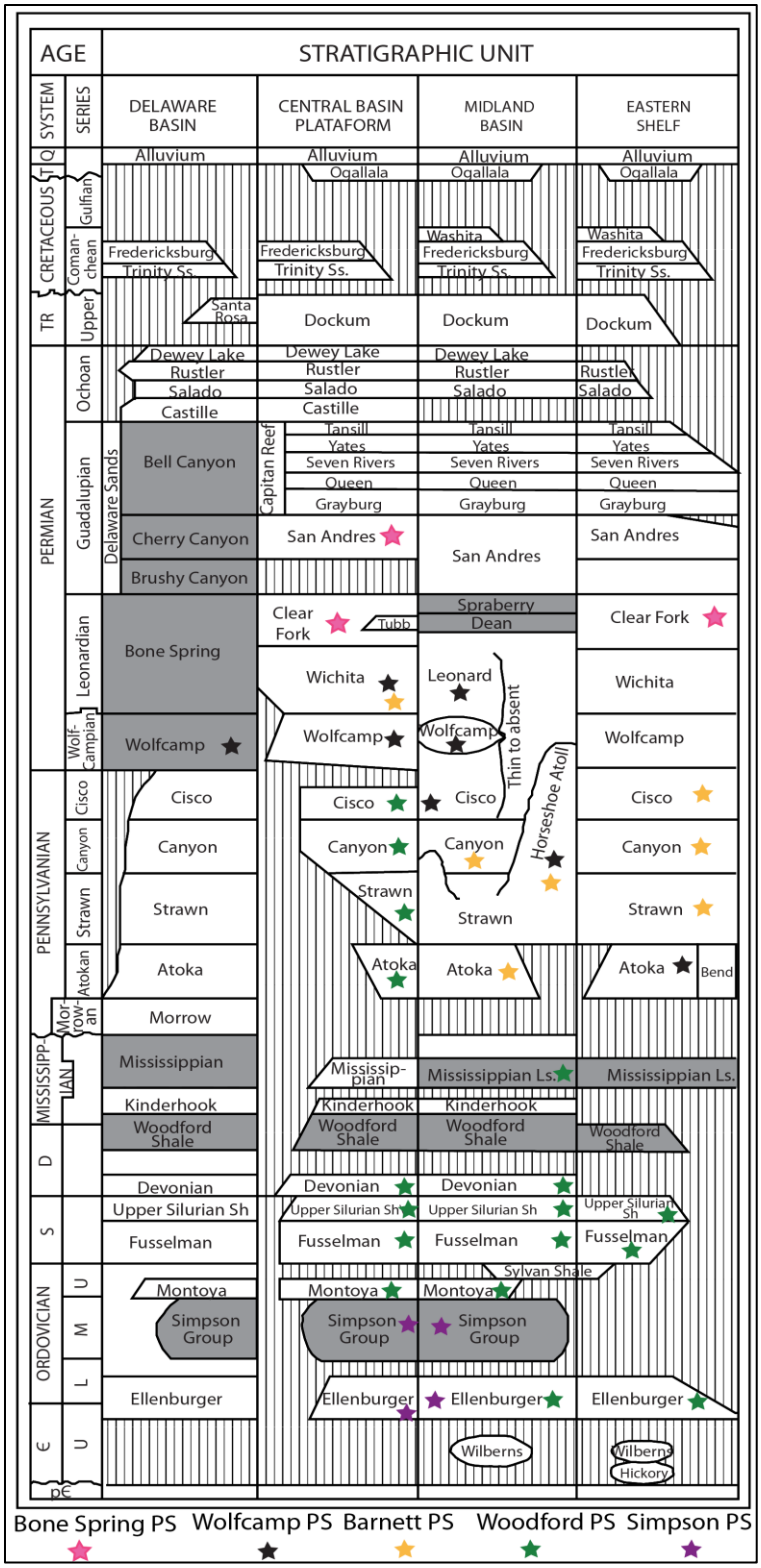

Figure 3.12: Stratigraphic distribution of petroleum systems in the Permian Basin based on oil-source rock correlations. Stratigraphy as modified from Galloway et al. (1983).

3.7 Conclusions

Despite the high thermal maturity of the oils and the internal organofacies variability among individual source rocks, geochemical correlations by chemometrics and independently using stable carbon isotope compositions constrained by thermal maturity analysis, reveal the existence of at least five petroleum systems between Ordovician and Leonardian in the Permian Basin. An apparent geochemical divide exists among the petroleum systems; the PrePennsylvanian-Post Pennsylvanian systems, coinciding with the structural evolution of the Permian Basin; Pre-Pennsylvanian Tabosa and the Post-Pennsylvanian Permian Basin.

The Post-Pennsylvanian petroleum systems include the Wolfcamp and the Bone Spring source rocks. Most of the Spraberry is thermally immature and is not considered significant in the petroleum systems dynamics of the Permian Basin. These petroleum systems are characterized by relatively low maturity oils deposited in anoxic (Bone Spring) and anoxic-suboxic (Wolfcamp) depositional settings. Although not overly rich in organic matter, their present TOCs and HIs are sufficient enough to characterize them as good to very good source rocks (Wolfcamp and Spraberry). The Bone Spring source rock was not geochemically analyzed but could be richer given the inferred highly reducing conditions during its deposition. Based on the stratigraphic relationship between the source rocks and reservoirs, these petroleum systems are inferred to be dominantly laterally drained.

The Pre-Pennsylvanian petroleum systems include the Barnett, the Woodford, and the Simpson source rocks. These petroleum systems have experienced vertical movement of

their oils in both upwards (Barnett) and downwards against buoyancy (Simpson and Woodford). In terms of entrapment of hydrocarbons, these Pre-Pennsylvanian petroleum systems are dominantly structurally controlled. This structural control created by the Pennsylvanian tectonics could potentially have control on migration as well, in these petroleum systems. With TOCs mostly above 3%, and HI above 300, the Woodford and Barnett shale source rocks are exceptionally rich in good quality organic matter.

The petroleum systems are, in general, stratigraphically segregated except in areas around the Central Basin Platform where seals are not interlayered with reservoirs. This stratigraphic segregation strongly suggests high integrity seals and short distance migration, which by default implies minimum migration losses. Together with high organic richness, high quality source rocks and adequate thermal maturity and well-timed generation/expulsion relative to trap formation, these factors, are responsible in part for the high hydrocarbon endowment of the Permian Basin.

3.8 References

Addinsoft, 2012, XLSTAT Analytical Solutions for MS Excel (2012 Release): 28 West 27th Street, Suite 503, New York, NY 10001, United States.

Andrusevich, V. E., M. H. Engel, J. E. Zumberge, and L. A. Brothers, 1998, Secular, episodic changes in stable carbon composition of crude oils: Chemical Geology, v. 152, p. 59-72.

Banerjee, A., A. K. Sinha, A.K. Jain, N. J. Thomas, K. N. Misra, and K. Chandra, 1998, A mathematical representation of Rock-Eval Hydrogen Index vs. Tmax profile, Organic Geochemistry, v. 28, p. 43-55.

Banerjee, A., M. Jha, A.K., Mittal, N. J. Thomas, and K.N. Misra, 2000, Effective source rocks in the north Cambay Basin, India, Marine and Petroleum Geology, v. 17, p. 1111-1130.

Bissada, K. K., L. W. Elrod, L. M. Darnell, H. M. Szymczyk, and , J. L. Trostle, 1993, Geochemical inversion-a modern approach to inferring source-rock identity from characteristics of accumulated oils and gas: Energy Exploration and Exploitation v. 11, 295-328.

Bray, E. E., and E. D. Evans, 1961, Distribution of n-paraffins as a clue to recognition of source beds: Geochemica et Cosmochemica Acta, v. 22, p. 2-15.

Broadhead, R. F., 2005, Regional Aspects of the Wristen Petroleum System in Southeast New Mexico, New Mexico Bureau of Geology and Mineral Resources, a Division of New Mexico Tech, Open File report No 485, 43pp.

Broadhead, R. F., 2010, Woodford in Southeastern New Mexico: Distribution and source rock characteristics, New Mexico Bureau of Geology and Mineral Resources, New Mexico Institute of Mining and Technology, v. 32, p. 79-90.

Chung, H. M., M. A. Rooney, M. B. Toon, and G. E. Claypool, 1992, Carbon isotope composition of marine crude oils: AAPG Bulletin, v. 76, p. 1000-1007.

Chung, H. M., S. W. Brand, and P. L. Grizzle, 1981, Carbon isotope geochemistry of Paleozoic oils from Big Horn Basin: Geochemica et Cosmochemica Acta, v. 45, p. 1803-1815.

Comer, J. B., 1991, Stratigraphic Analysis of the Upper Devonian Woodford Formation, Permian Basin, West Texas and Southeastern New Mexico, University of Texas, Austin, Bureau of Economic Geology, Report of Investigations No. 201, 63p.

Corby, J. J. and H. E. Cook, 2003, The Permian Basin petroleum systems, Simpson-Ellenberger and Woodford-San Andres-New Insights for exploring a mature petroleum province (Abs), AAPG Annual Convention, Salt Lake City, Utah. May 11-14, 2003.

Curiale, J., 1994, Correlation of oils and source rocks- a conceptual and historical perspective: in Magoon, L.B. and W. G. Dow, eds., The Petroleum System: From Source to Trap, AAPG Memoir 60, p. 251-260.

Curiale, J. A., 2008, Oil-source rock correlations-limitations and recommendations, Organic Geochemistry, v. 39, p. 1150-1161.

Curiale, J. A., 2002, A review of the occurrences and causes of migration–contamination in crude oil. Organic Geochemistry, v. 33, p. 1389–1400.

Dahl, J. E., J. M. Moldowan, S. C. Teerman, M. A. McCaffrey, P. Sundaraman, M. Pena, and C. E. Stelting, 1994, Source rock quality determination from oil biomarkers I: a new Geochemical technique: AAPG Bulletin, v.78, p. 1507-1526.

Dahl, J. E., J. M. Moldowan, K. E , Peters, G. E. Claypool, G. E. Rooney, G. E. Michael, M. R. Mello and M. L. Kohnen, 1999, Diamondoid hydrocarbons as indicators of natural oil cracking: Nature, v. 3999, p. 54-57.

Degens, E. T., 1969, Biogeochemistry of stable carbon isotopes, in G. Eglinton and M. T. J. Murphy, eds., Organic Geochemistry: New York, Springler-Verlag, p. 306-329.

Dow, W. G., Tulukdar, S. C. and Harmon, L. 1990, Exploration applications of geochemistry in the Midland basin, Texas (abs.), American Association of petroleum Geologists Bulletin, 74, 644-645.

du Rouchet, J., 1981, Stress fields, a key to oil migration, AAPG Bulletin, v. 65, p. 74-85.

Dutton, S. P., E. M. Kim, R. F. Broadhead, C. L. Breton, W. D. Raatz, S. C. Ruppel, and C. Kerans, 2004, Play analysis and digital portfolio of major oil reservoirs in the Permian basin: Application and transfer of advanced geological and engineering technologies for incremental production opportunities, University of Texas at Austin, Bureau of Economic Geology, Final Report prepared for the U.S. Department of Energy under contract DE-FC26-02NT15131, 408 p.

Dutton, S. P., E. M. Kim, R. F. Broadhead, W. D. Raatz, C. L. Bretton, S. C. Ruppel, and C. Kerans, 2005, Play analysis and leading-edge reservoir development methods in the Permian; increased recovery through advanced technologies: AAPG Bulletin, 89, 55-576.

England, W. A., 1994. Secondary migration and accumulation of hydrocarbons, in L.B. Magoon and W.G. Dow, eds., The Petroleum System-from source to trap: AAPG Memoir 60, p. 211-217.

Espitalie, J. and L. Joubert, 1987, Use of Tmax as a maturation index in petroleum exploration, in Proceedings of Meeting: First International Conference on Petroleum Geochemistry and Exploration in the Afro-Asian Region, Dehra Dun, India, November 25–27, 1985, eds. R.K. Kumar, P. Dwivedi, V. Banerjie and V. Gupta, pp.67–73. Rotterdam, Netherlands.

ESRI, 2012, ArcMap Version 10.1, Environmental Systems Research Institute Inc., 380 New York Street, Redlands, CA 92373-8100.

Fan Pu, J. D. King, and G. E. Claypool, 1988, Characteristics of biomarker compounds in Chinese crude oils, in R. K. Kumar, P. Dwivedi and V. Banerjie and V. Gupta, eds., Petroleum Geochemistry and Exploration in the Afro-Asian Region; Proceedings of the First International Conference on Petroleum Geochemistry and Exploration in the Afro-Asian Region, Dehradun, 25-27 November 1985: Balkema Rotterdam, p. 197-202.

Frenzel, H. N., R. R. Bloomer, R. B. Cline, J. M. Cys, J. E. Galley, W. R. Gibson, J. M. Hills, W. E. King, W. R. Seager, F. E. Kottlowski, S.Thompson III, G. C. Luff, B. T. Pearson, and D. C. Van Siclen, 1988, The Permian Basin Region, in L. L. Sloss, ed., Sedimentary Cover- North American craton, US, The Geology of North America, v. D-2: Boulder, Colorado, Geological Society of America, p. 261-306.

Galloway, W. E., E. T. Ewing, C.M. Garrett, N. Tyler and D. G. Debout, 1983, Atlas of Major Texas Oil Reservoirs, Bureau of Economic Geology, The University of Texas at Austin, Austin, Texas, 139p.

Hatch, J. R., S. R. Jacobson, B. J. Witzke, J. B. Risatti, D. E. Abders, W. L. Watbet, K. D. Nowell, and A. K. Vuletich, 1987, Possible Late-Middle Ordovician organic carbon isotope excursion; evidence from Ordovician oils and hydrocarbon source rocks, mid-continent and east central United States: AAPG Bulletin, v. 71, p. 1342-1354.

Hayes, J. M., I. R. Kaplan, and K. M. Wedeking, 1983, Precambrian organic geochemistry, preservation of record, in: J. W. Schopf, ed., Earth's Earliest Biosphere, Its Origin and Evolution, Princeton University Press, NJ, pp. 93-134.

Hill, R. J., D. M. Jarvie, B. L. Claxton, J. D. Burgess, and J. A. Williams, 2004, Petroleum systems of the Permian Basin (abs): AAPG Annual Meeting Program, v. 13. A63.

Hills, J. M. 1984, Sedimentation, tectonism, and hydrocarbon generation in Delaware Basin, west Texas and southeastern New Mexico: AAPG Bulletin, v. 68, p. 250-267.

Hills, J. M., and J. E. Galley, 1988, The Pre-Pennsylvanian Tobosa Basin, in Frenzel et al., 1988, The Permian Basin Region, in L.L. Sloss, ed., Sedimentary Cover-North American Craton, US, The Geology of North America, v. D-2: Boulder, Colorado, Geological Society of America, p. 261-306.

Hindle, A. D, 1997, Petroleum migration pathways and charge concentration: a three-dimensional model, AAPG Bulletin, v.81, p. 1451-1481.

Huang and Meinschein, 1979, Sterols as ecological indicators, Geochemica et Cosmochemica Acta, v. 43, p. 739-745

Jacobson, S. R., J. R. Hatch, S. C. Teerman, and R. A. Askin, 1988, Middle Ordovician organic matter assemblages and their effect on Ordovician-derived oils: AAPG Bulletin, v. 72, p. 1090-1100.

Jarvie, D. M., B. L. Claxton, F. Henk, and J. T. Breyer, 2001a, Oil and gas from the Barnett shale, Fort Worth Basin, Texas (abs.): AAPG Annual Meeting Abstracts, p. A100.

Jarvie, D. M., J. D. Burgess, A. Morelos, P. A. Mariotti, and R. Lindsay, 2001b, Permian Basin petroleum systems investigations; inferences from oil geochemistry and source rocks (abs). AAPG Bulletin, v. 85, p. 1693-4.

Jarvie, D. M. and R. J. Hill, 2011, Understanding unconventional resource potential by conventional petroleum systems assessment: AAPG Search and Discovery Article #40840. Web accessed 15th February 2013, http://www.searchanddiscovery.com/documents/2011/40840jarvie/ndx_jarvie.pdf.

Johnson, J. G., G. Klapper, and Sandberg, C. A., 1985, Devonian eustatic fluctuations in Euramerica: Geological Society of America Bulletin, v. 96, p. 567-587.

Katz, B. J. and L.W. Elrod, 1983, Organic geochemistry of DSP site 467, offshore California, Middle Miocene to Lower Pliocene strata, Geochemica et Cosmochemica Acta, v. 47, p. 389-396.

Katz, B. J., Dawson, W. C., Robinson, V. D., and Elrod, L. W. (1994). Simpson-Ellernberger(.) PS of the Central Basin Platform, West Texas, USA, in Magoon, L.B. and W. G. Dow, eds., The Petroleum System: From Source to Trap, AAPG Memoir 60, p. 453-461.

Kinley, T. J., L. W. Cook, J. A. Breyer, D. M. Jarvie and A. B. Busbey, 2008, Hydrocarbon potential of the Barnett Shale (Mississippian), Delaware Basin, west Texas and southeastern New Mexico: AAPG Bulletin, v. 92, p. 967-991.

Kodner, R. B., A. Pearson, R. E. Summons and A. H. Knoll, 2008, Sterols in red and green algae: quantification, phylogeny, and relevance for the interpretation of geologic steranes, Geobiology, v. 6, p. 411-420.

Littke, R., D. R. Barker, D. Leythaeuser, 1988, Microscopic and sedimentologic evidence for the generation and migration of hydrocarbons in Toarcian source rocks of different maturities, Organic Geochemistry, v. 13, p. 549-560.

Longman, M. W., and S. E. Palmer, 1987, Organic geochemistry of Mid-Continent Middle and Late Ordovician Oils: AAPG Bulletin, v. 71, p.938-950.

Loucks, R. G. and S. C. Ruppel, 2007, Mississippian Barnett Shale: lithofacies and depositional setting of a deep-water shale-gas succession in the Fort Worth Basin, Texas, AAPG Bulletin, v. 91, p. 579-601.

Mackenzie, A. S., 1984, Applications of biological markers in petroleum geochemistry, in J. Brooks and D. Welte, eds., Advances in Petroleum Geochemistry, Volume 1, London, Academic Press, p. 115-214.

Magoon, L.B., 1988a, The Petroleum Systems of the United States: US Geological Survey Bulletin 1870, 68p.

Magoon, L.B., 1988b, The petroleum system-a classification scheme for research, exploration and resource assessment, in Magoon, L.B. (Ed.), The Petroleum Systems of the United States, US Geological Survey Bulletin 1870, p 2-15.

Magoon, L. B., 1992, Identified petroleum systems in the United States, in Magoon, L.B. (Ed.), The petroleum systems-status of research and methods, US Geological Survey Bulletin 2007, p. 2-11.

Magoon, L. B. and E. A. Beaumont , 1999, Petroleum Systems, in E.A Beaumont and N.H. Foster, eds., Handbook of Petroleum Geology: Exploring for Oil and Gas Traps, American Association of petroleum Geologists, Washington D.C., pp 3.1-34.

Magoon, L. B., and W. G. Dow, 1994, The petroleum system, in L. B. Magoon and, W. G. Dow eds. The Petroleum System: From source to trap: AAPG Memoir 60, p. 3-24.

McDade, E.C., R. Sassen, L. Wenger, and G. A. Cole, 1993, Identification of organic-rich Lower tertiary shales as petroleum source rocks, South Louisiana, Transactions Gulf Coast Association of Geological Societies, v. 43, p. 257-267.

McKirdy, D. M., A. K. Aldridge, and P. J. M. Ypma, 1983, A Geochemical comparison of some crude oils from pre-Ordovician carbonate rocks, in M. Bjorøy, C. Albrecht, C. Conford, eds., Advances in Organic Geochemistry 1981, John Willey and Sons, p. 99-107.

Mello, M. R., N. Telnaes, P.C. Galianone, M.I. Chicarelli, C.S. Brassel, and J.R., Maxwell, 1988, Organic Geochemical characterization of depositional environments of source rocks and oils in Brazilian marginal basins, Organic Geochemistry, v. 13, p. 31-45.

Moldowan, J. M., C. Y. Lee, P. Sundararaman, P. Salvatori, A. Alajbeg, B. Gjukic, G. J. Demaison, N. E. Slougui, and D. S. Watt, 1992, Source correlation and maturity assessment of select oils and rocks from the Central Adriatic basin (Italy and Yugoslavia), in. J. M. Moldowan, P. Albrecht, and R. P. Philp, eds., Biological Markers in Sediments and Petroleum: Englewood Cliffs, New Jersey, Prentice Hall, p. 370-401.

Moldowan, J. M., W. K. Seifert, E. Arnold, and J. Clardy, 1984, Structure proof and significance of stereoisomeric 28,30 bisnorhopane in petroleum and petroleum source rocks, Geochemica et Cosmochemica Acta, v. 48, p. 1651-1661.

Moldowan, J. M., W. K. Seifert, and E. J. Gallegos, 1985, Relationship between petroleum composition and depositional environment of petroleum source rocks: AAPG Bulletin, v. 69, p. 1255-1268.

Øygard, K., Grahl-Nielsen, O. and Ulvøen, S. *(*1984). Oil/oil correlation by aid of chemometrics. Organic Geochemistry 6, 561-567.

Peters, K. E. and Cassa, M. R., 1994, Applied source rock geochemistry, in, Magoon, L. B. and Dow, W., G., eds., The Petroleum system-from source to trap, AAPG Memoir 60, p. 93-120.

Peters, K. E., D. Coutrot, , X. Nouvelle, L. S. Ramos, B.G. Rohrback, L. B. Magoon, and J. E. Zumberge, 2013, Chemometric differentiation of crude oil families in the San Joaquin Basin, Carlifornia: AAPG Bulletin, v. 97, p. 103-143

Peters, K. E., T. H. Fraser, W. Amris, B. Rustanto and E. Hermanto, 1999, Geochemistry of crude oils from Eastern Indonesia: AAPG Bulletin, v. 83, p. 1927-1942.

Peters, K. E., J. M. Moldowan, M. Schoell, and W. B. Hempkins, 1986, Petroleum isotopic and biomarkers composition related to source rock organic matter and depositional environment, Organic Geochemistry, v. 10, p. 17-27.

Peters, K. E., and J. M. Moldowan, 1991, Effects of source, thermal maturity and biodegradation on the distribution and isomerization of homohopanes in petroleum, Organic Geochemistry, v. 17, p. 47-61.

Peters, K. E., J. M. Moldowan, and C. C. Walters, 2005a, The Biomarker Guide; Biomarkers and Isotopes in Environment and Human History (vol. 1): Cambridge University Press pp. 1-471.

Peters, K. E., J. M. Moldowan and C.C. Walters, 2005b, The Biomarker Guide; Biomarkers and Isotopes in Petroleum Exploration and Earth History (vol. 2): Cambridge University Press pp. 475-1155.

Peters, K. E, L. S. Ramos, J. E. Zumberge, Z.C. Valin, C.R. Scotese and D.L. Gautier, 2007, Circum-Arctic petroleum systems identified using decision-tree chemometrics: AAPG Bulletin, v. 91, p. 877-913.

Powell, T. G., and D. M. McKirdy, 1973, Relationship between ratio of pristane to phytane, crude oil composition and geological environment in Australia: Nature, v. 243, p. 37-39.

Pratsch, J. C., 1983, Gasfields, NW German basin: secondary gas migration as a major geologic parameter, Journal of Petroleum Geology, v. 5, p. 229-244.

Reed, J. D., H. A. Illich, and B. Horsfield, 1986, Biochemical evolutionary significance of Ordovician oils and their sources: Organic Geochemistry, v. 10, p. 347-358.

Riebesell, U., A. T. Revil, D. G. Holdsworth, and J. K. Volkman, 2000, The effect of varying CO_2 concentration on lipid composition and carbon isotope fractionation in *Emiliania huxleyi*, Geochemica et Cosmochemica Acta, v. 64, p. 4179-4192.

Scalan, R. S., and J. E. Smith, 1970, An improved measure of the odd-to-even predominance in the normal alkanes of sediment extracts and petroleum, Geochimica et Cosmochemica Acta, v. 34, p. 611-620.

Schoell, M., and R. M. K Carlson, 1999, Diamondoids and oil are not forever: Nature, v. 399, p. 15-16.

Schwark, L. and Empt, P. T., 2006, Sterane biomarkers as indicators palaeozoic algal evolution and extinction events, Palaeogeography, Palaeoclimatology, and Palaeoecology, v. 240, p. 225–236.

Seifert, W. K., and J. M. Moldowan, 1978, Applications of steranes, triterpanes and monoaromatics to the maturation, migration and the source of crude oils, Geochemica et Cosmochemica Acta, v. 42, p. 77-95.

Shanmugam, G. 1985, Significance of coniferous rain forests and related organic matter in generating commercial quantities of oil, Gippsland Basin, Australia, AAPG Bulletin, v. 69, p. 1241-1254.

Shumaker, R. C., 1992, Paleozoic structure of the central basin uplift and adjacent Delaware basin, West Texas: AAPG Bulletin, v. 76, p. 1804-1824.

Sinninghe Damste, J.S., Kenig, F., Koopmans, M.P., Koster, J., Hayes, J. M., and Leeuw, J. W.1995, Evidence for gammacerane as an indicator of water column stratification, Geochemica et Cosmochemica Acta, v. 59, p. 1985-1900.

Sofer, Z., 1984, Stable carbon isotope compositions of crude oils; application to source depositional environments and petroleum alteration: AAPG Bulletin, v. 68, p. 31-49.

ten Haven, H. L., J. W. De Leeuw, J.S. Sinnighe Damste, P. A. Schenck, S. E. Palmer, and J. E. Zumberge, 1988, Application of biological markers in the recognition of palaeo-hypersaline environments, in K. Kelts, A. Fleet, and M. Tablot, eds., Lacustrine Petroleum Source Rocks, Special Publication, v. 40: Blackwell, Geological Society, p. 123-130.

ten Haven, H. L., J. W. de Leeuw, J. Rullkotter, and J. S. Sinninghe Damste, 1987, Restricted utility of the pristane/phytane ratio as a paleoenvironmental indicator, Nature, v. 330, p. 641-643.

Tornabene, T.G., T.A., Langworthy, G. Holzer, J. Oró, 1979, Squalenes, phytanes and other isoprenoids as major neutral lipids of methanogenic and thermoacidic "archaebacteria", Journal of Molecular Evolution, v. 13, p. 73-83.

Van Graas, G. W., 1990, Biomarker maturity parameters for high maturities; calibration of the working range up to the oil/condensate threshold: Organic Geochemistry, v. 16, p. 1025-1032.

Volkman, J. K, 1986, A review of sterol markers for marine and terrigenous organic matter. Organic Geochemistry, v. 9, p. 83–99.

Volkman J. K., 2003, Sterols in microorganisms, Applied Microbiology and Biotechnology, v. 60, p. 495–506.

Waples, D. W., and T. Machihara, 1991, Biomarkers for Geologists-A Practical Guide to the Application of Steranes and Triterpanes in Petroleum Geology: AAPG Methods in Exploration, No.9, p.1-91.

Waples, D. W. and J. A. Curiale, 1999, Oil-oil and oil-source rock correlations: in Beaumont, E.A. and N.H. Foster, eds., Exploring for Oil and Gas Traps, AAPG Treatise of Petroleum Geology, p. 8.1-8.71.

White, D. A., 1980, Assessing oil and gas plays in facies cycle wedges: American AAPG Bulletin, v. 64, p. 1158–1178.

Wright, W. F., 1979, Petroleum geology of the Permian Basin: West Texas Geological Society Publication 79-71, 98p.

Zumberge, J. E. 1987, Prediction of source rock characteristics based on terpane biomarkers in crude oils: a multivariate statistical approach. Geocheimica et Cosmochemica Acta, v. 51, p. 1625-1637.

4.0 ONE-DIMENSIONAL THERMAL MATURITY AND PETROLEUM GENERATION MODELING

Abstract

Thermal maturity, petroleum generation, and source rock volumetrics have been modeled for five organic-rich, high-quality (type II and II/III) oil-prone source rocks from the Permian Basin. The source rocks include the shales of the Spraberry, Wolfcamp, Barnett, Woodford, and Simpson. Calibrated numerical 1-D models indicate that, for each of these source rocks, burial history, thermal maturity, and timing of petroleum generation vary within the basin. With maturity increasing from south to north, the Simpson, the Woodford, and Barnett have reached maximum generation in most parts. The Wolfcamp in the Delaware Basin is at condensate to dry gas generation and is immature to oil-window in the Midland Basin. The Spraberry is mostly immature with respect to petroleum generation.

Generation and expulsion from the Wolfcamp shale began in the Early Triassic, with hydrocarbons migrating laterally, and then trapped within carbonate aprons encased within the shales of the same stratigraphic interval. Expulsion from the Barnett shale occurred during Early to Mid-Permian, where migration occurred radially updip from the two depocenters in the Delaware and Midland basins to Pennsylvanian sandstone reservoirs in the Eastern Shelf and Permian carbonate reservoirs in Central Basin Platform and Northwest Shelf. The Woodford shale started expelling during Early-Late Permian, where migration occurred along vertical pathways against buoyancy to underlying reservoirs, Devonian through Ordovician. Expulsion from the Simpson occurred during Early Triassic and migration, followed vertical pathways downwards to

Simpson sandstones and Ellenberger carbonates. This study has provided a detailed delineation of areas of petroleum generation and an assessment of petroleum resource potential for the source rocks in the Permian Basin. Adequate thermal maturity coupled with organic-rich high-quality relatively thick source rocks, are key factors in the hydrocarbon endowment in the basin.

4.1 Introduction

The principal constraint to the petroleum endowment of any basin is the adequacy of the charge factor, defined by Sluijk and Nederlof (1984) as hydrocarbons available for entrapment. Generation of petroleum from source rocks occurs when a source rock reaches a maturity threshold, usually above vitrinite reflectance (R_o) 0.55% with the oil window achieved at 0.68%, varying with kerogen type. For example, type I kerogen usually begins at $\%R_o$ of 0.50 (Dow, 1977). For type II kerogen source rocks, Waples (1985) indicated that the onset of petroleum generation occurs at $\%R_o$ between 0.45- 0.50 and 0.60 for sulphur-rich kerogen. Inspite of the variations with kerogen types, and R_o scales, in general, < 0.55% R_o 0.55-0.70%, 0.7-1.3%, and 1.3-2.0%R_o for immature, early mature, mature (also known as oil-window), and over mature (also known as condensate and gas generation zones), respectively. This scale is used throughout in this chapter.

Once hydrocarbon generation has begun, expulsion follows upon satisfaction of two fundamental conditions: (1) generation of enough hydrocarbons to exceed the retention capacity of source rocks, and (2) development of adequate pore pressure to exceed the lithostatic pressure to induce fracturing in the otherwise impermeable source rocks (e.g.

du Rouchet, 1981; Littke et al., 1988; England, 1994). The implications of this is that at late stages of generation, when generation is no longer able to adequately increase pore pressure, expulsion and hence migration will stop (e.g. England, 1994), with the remnant hydrocarbons only removable as unconventional resource.

A source rock is a rock with adequate organic matter and capable of generating hydrocarbons under adequate thermal maturity (Tissot and Welte, 1984). The amount of organic matter, referred as organic richness, is usually expressed by its total organic carbon content (TOC) and sometimes expressed as genetic potential (S1+ S2) obtained from total organic carbon analyzer and Rock-Eval pyrolysis, respectively. Organic matter type on the other hand is expressed using hydrogen index (HI) obtained from the expression (S2/TOC*100). Guidelines for assessment of source rock richness, source rock type, and source rock maturity are discussed in detail in Peters and Cassa (1994) and Jarvie (2001). These parameters of source rocks are linked together through a series of reactions, collectively referred to as source rock kinetics (e.g. Cooles et al., 1986; Tissot et al., 1987; Mackenzie and Quingley, 1988, Welte et al., 1997; Behar, 1997). The source rock kinetics is controlled by the kerogen type and determines the timing of petroleum generation, the volumes of hydrocarbons generated from the source rock at a given level of maturity, and hence the expulsion and migration rates (e.g. England et al., 1987). The kinetic basis for volumetric estimation is the change in HI immature (initial (HI_o) and mature (present (HI_p) as a direct measure of volume of hydrocarbons generated (e.g. Schmoker, 1994). As important as thermal maturity, petroleum generation and volumetric modeling is, only one comprehensive study is adequately described in the literature for the Permian Basin. This is the Simpson–Ellenberger petroleum system (Katz et al., 1994).

Other modeling works are only available as abstracts (Dow et al., 1990; Corby and Cook, 2003; and Pawlewicz and Mitchell, 2006). Though insightful, no adequate evaluations and discussions can be made based on these abstracts.

The principal objectives of this part of the study include, but not limited to; (1) delineate thermal maturity or pods of active source rocks, (2) determine the timing of petroleum generation for each petroleum system identified, (3) estimate amount of hydrocarbon charge from each of the source rocks, and, together with information obtained from geochemical correlations (Chapters 2 and 3), and (4) infer migration pathways for each of the petroleum systems. The overall outcome is generation of petroleum systems maps and events charts that define the relationship between petroleum systems elements and processes.

4.2 One-Dimensional Models Development Methodology

Thermal maturation, petroleum generation and expulsion modeling was undertaken using PetroMod® software (Schlumberger, 2012). Because most of the source rocks span a wide geographic extent, from Delaware to Midland, with a potential for varying thermal regimes, models were created in locations such that potential variability associated with the three sub divisions of the Permian Basin are captured. Prior to modeling, potential source rock samples were screened by TOC and Rock-Eval pyrolysis techniques as described in Chapter 3.

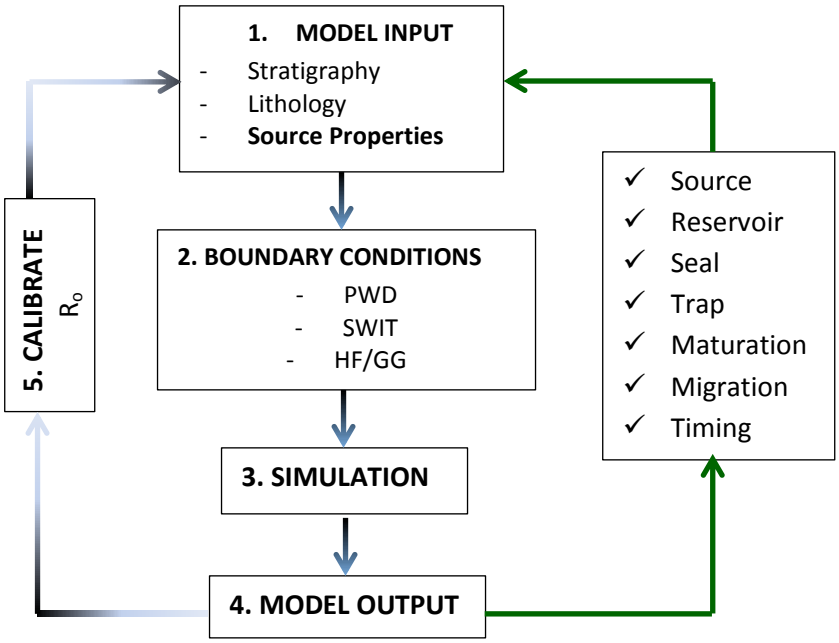

Figure 4.1: 1-D Modeling Workflow used in this study (Adapted from Introduction to PetroMod® training and exercise guide, Schlumberger, 2012).

4.2.1 Model(s) Input Parameters

Input parameters used in building the models included chronostratigraphic units, and boundary conditions including paleobathymetry or paleo-water depth (PWD), sediment-water interface temperature (SWIT) and Heat Flow (HF). Chronostratigraphic age assignment was based on published dates from AAPG-Correlation of Stratigraphic Units of North America, COSUNA, 1983 chart for the Southwest/Southwest-Midcontinent described in Salvador (1985). Thickness of strata was based on isopachs maps from several sources including Galley (1958), Wright (1979), Comer (1991) and Frenzel (1988). Assignment of unconformities (erosional and hiatuses) was also based on the COSUNA (1983) chart. Section of strata lost to erosion was estimated using the method suggested by Dow (1977), which is based on displacement of vitrinite reflectance

profiles. Despite potential effects of vitrinite annealing with time (e.g. Katz, 1988), the observed displacements in R_o profiles in Central Basin Platform and Midland basins meant that annealing was minimal if any.

Due to lack of adequately published sources for paleobathymetry based on benthic foraminifera within the Permian Basin, PWD was estimated from the sea-level curves of Haq et al. (1987) and Haq and Schutter, (2008) together with the global palaeogeographic reconstructions of the earth by Blakely (2008) available through Google Earth. The SWIT through time was calculated using Wygrala's (1989) approach which relates geologic age and mean surface paleo-temperature based on plate tectonic reconstructions to present-day latitudes (Figure 4.2), available as a select-option in PetroMod® (Schlumberger, 2012).

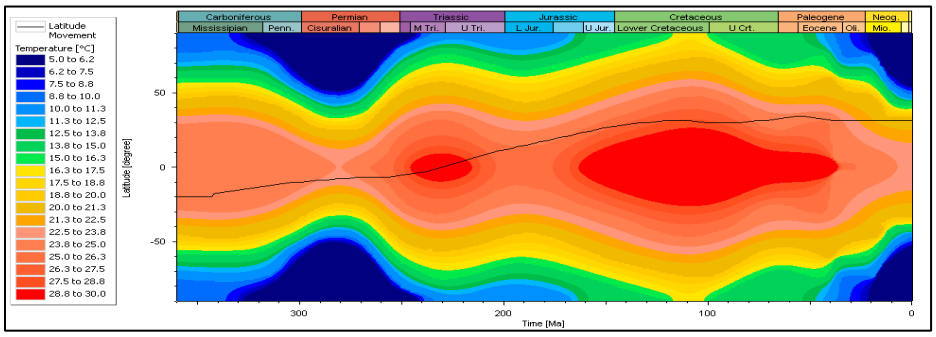

Figure 4.2: Determination of sediment-water interface temperature (SWIT) using Wygrala (1989) curve embedded in PetroMod (Schlumberger, 2012). In this example for model location in the Central Basin Platform at latitude 31°, the black line indicates variation in SWIT over geologic time.

Modeling was based on assumed constant heat flow over geological time. Present heat flow was obtained from a database from which the regional geothermal map of North America (Blackwell and Richards, 2004) is published. The data were also compared with

the geothermal gradient (Ruppel et al., 2005) as indicated in the Southeast portion (Figure 4.3). Thermal history was constrained using measured R_o data.

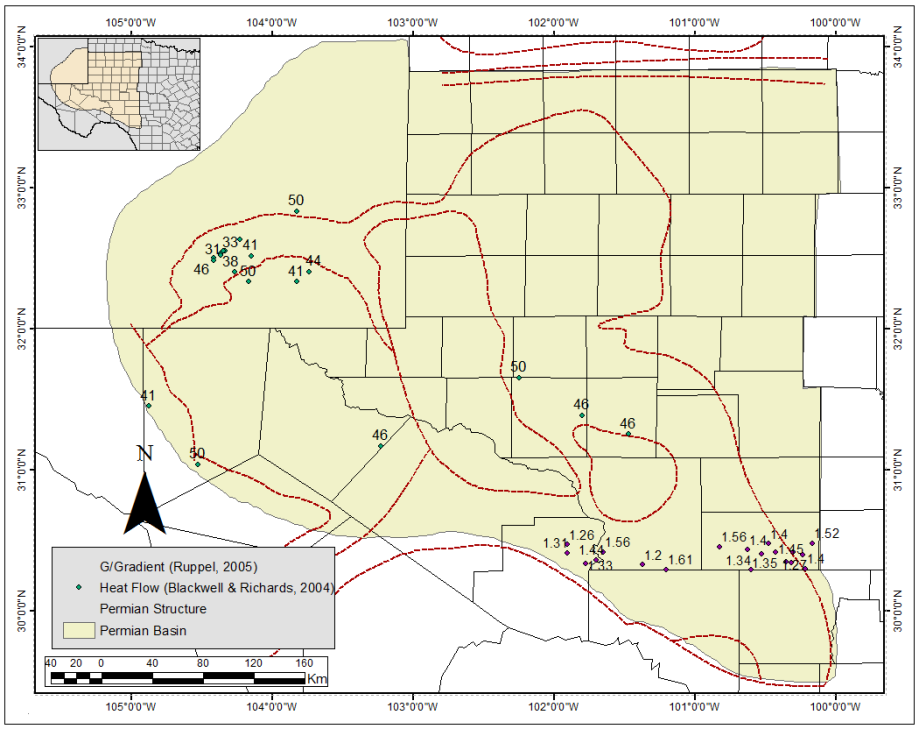

Figure 4.3: Present-day heat-flow (mW/m^2) map and geothermal gradient (°C/100ft) map of the Permian Basin. Heat flow from Blackwell and Richards (2004) and geothermal gradient from Ruppel et al. (2005). Base map from Dutton et al. (2004).

4.2.2 Petroleum Generation Kinetics

Source rock kerogen type was used to assign appropriate petroleum generation kinetics from a list of kinetics embedded in PetroMod® Software (Schlumberger, 2012). All model calculations employed type II kerogen kinetics of Behar et al. (1997). Calibration was accomplished by comparing measured vitrinite reflectance data with modeled vitrinite reflectance determined using Easy $\%R_o$ method of Sweeney and Burnham (1990) embedded in the PetroMod® (Schlumberger, 2012). For this purpose, measured vitrinite

reflectance (Pawlewicz, 2005) was used. Volumes of hydrocarbons generated by source rocks were calculated based on modeled results that indicates bulk yield of hydrocarbons expelled by a volume of source rock under one square kilometer. This value was then multiplied by the volume of the pod of active source rock to get the total bulk hydrocarbons expelled by the source rock. Source rock volumes were calculated using the spatial analyst statistical tools available in ArcGIS (ESRI, 2012). Original (immature) HI was used in the estimation of expelled hydrocarbons and was based on the method Barnejee (1998; 2000) as discussed in Chapter 3.

4.3 Results and Discussions

4.3.1 Thermal Maturity Modeling

Thermal maturity was modeled in 14 locations spread over the Permian Basin, producing R_o profiles (Figures 4.5-4.7) and R_o distribution atop source rocks of interest: the Leonardian Spraberry, the Lower Permian Wolfcamp, the Mississippian Barnett, the Upper Devonian Woodford, and the Ordovician Simpson shales (Figures 4.8-4.12, respectively).

4.3.2.1 Delaware Basin

Burial and thermal history of the Permian Basin in the Delaware is illustrated in Figure 4.5. Three candidate source rocks under investigation in this model location are Woodford, Barnett, and Wolfcamp. The Simpson was excluded as its TOC and HI data indicated non-source facies in Delaware and Midland. The burial curve and calibrated maturity profile indicate that the base and top of Woodford is currently at maturity zone

five (%R_o above 2.0%) where organic matter has completely been metamorphosed. This also applies to the Barnett shale. The top of Wolfcamp shale is at maturity 1.28% R_o, just shy of 1.3%, the limit for liquid hydrocarbon generation. Its base is at 2.0% R_o, the beginning of maturity zone five or the end of the dry gas zone. The geochemical implications of these observations are that, Barnett and Woodford shales at this location are overcooked (reached maximum generation) as far as hydrocarbon potential is concerned. The Wolfcamp on the other hand is at a level which makes it a favorable target for unconventional gas as discussed in detail in section 4.3.3.2. The model also suggests abundant condensate generation from the Wolfcamp in the Delaware.

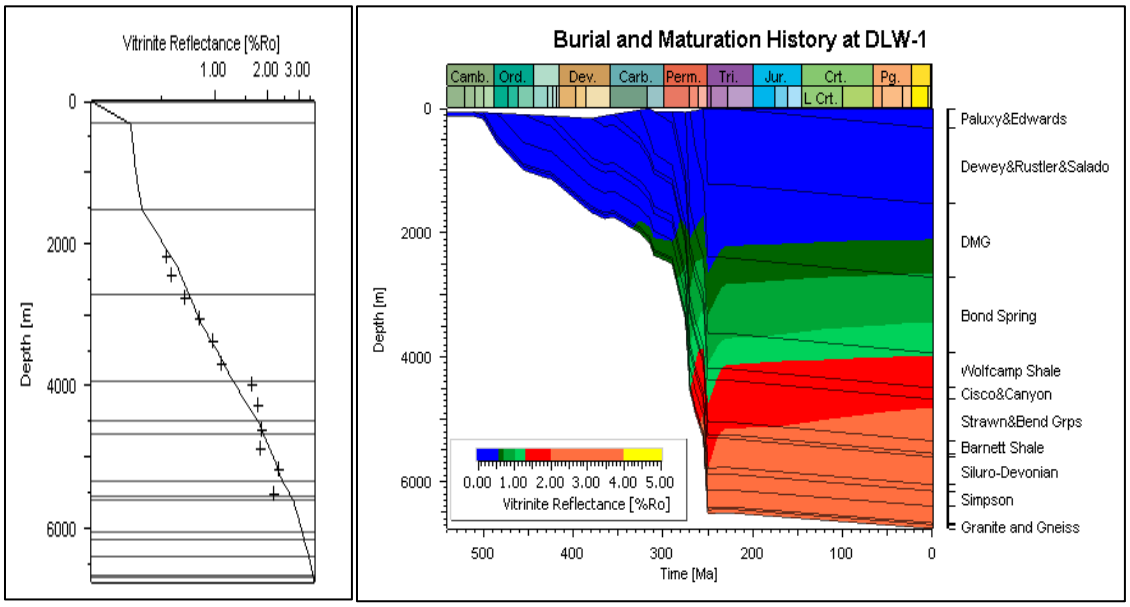

Figure 4.5: Selected burial and maturation history for Permian Basin strata in the Delaware as calculated using PetroMod (Schlumberger, 2012). Left is the calibrated %R_o profile at the same location. Thickness of strata from Galley (1958), Wright (1979) and Frenzel et al. (1988). Measured %R_o used for calibration from Pawlewicz (2005). Detailed model parameters used are listed in Appendix 6.

4.3.2.2 Central Basin Platform

The burial and thermal history through the Central Basin Platform is displayed in Figure 4.6. The candidate source rocks under investigation at this location are the Simpson and

the Woodford shales. The Wolfcamp in the Central Basin Platform is non-source facies while the Barnett is missing by erosion (e.g. Wright, 1979). Both the top and base of Woodford are currently at the oil-window. The top of Simpson shale is currently at $\%R_o$ = 1.5 and the base at $\%R_o$ = 1.7, all passed the oil window.

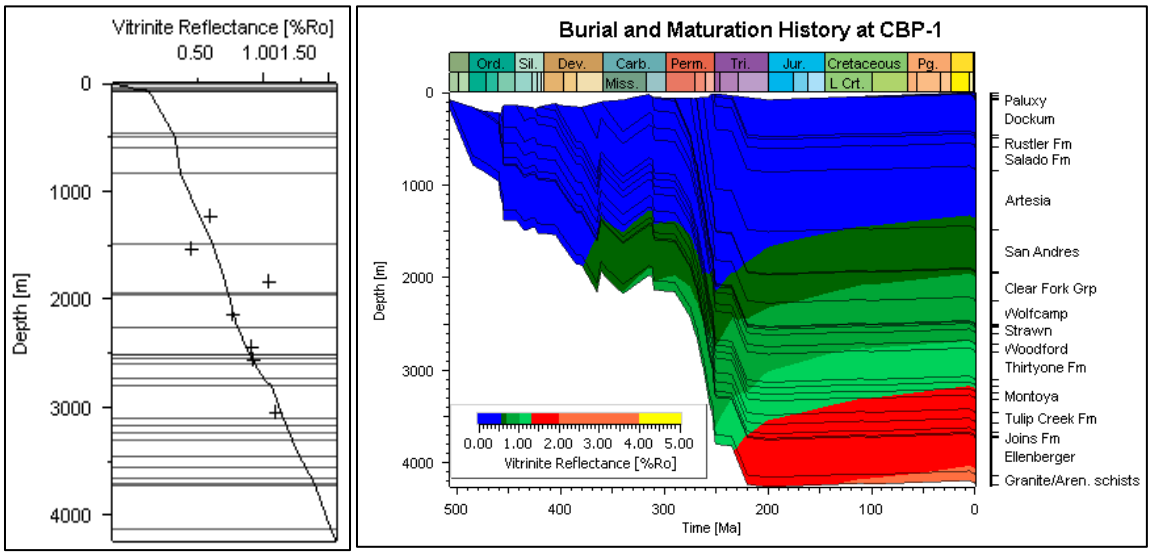

Figure 4.6: Selected burial and maturation history for Permian Basin strata in the Central Basin Platform as calculated using PetroMod (Schlumberger, 2012). Left is the calibrated $\%R_o$ profile. Thickness of strata from Galley (1958), Wright (1979) and Frenzel et al. (1988). Measured R_o used for calibration from Pawlewicz (2005). Detailed model parameters used are listed in Appendix 6.

4.3.2.3 Midland Basin

The burial and thermal histories through two locations in the Midland are illustrated in Figure 4.7a and b. The candidate source rocks in the path of model MLD-2 include the Spraberry, the Wolfcamp, the Barnett, and the Woodford shales. The source rocks in the MLD-3 model path are Woodford, Barnett, and Wolfcamp. The burial curve at MLD-2 indicates that the base of Spraberry is at 1.2% R_o and the top is at approximately 0.55% R_o. The base of Wolfcamp is at the oil window and its top is at $\%R_o$ of 0.7). Top of Barnett is currently at $\%R_o$ of 1.4 while the base is at $\%R_o$ of 1.5. This suggests that the

entire Barnett at the model location is within the condensate zone. The Woodford is currently at $\%R_o$ of 1.5, a zone of intense condensate generation.

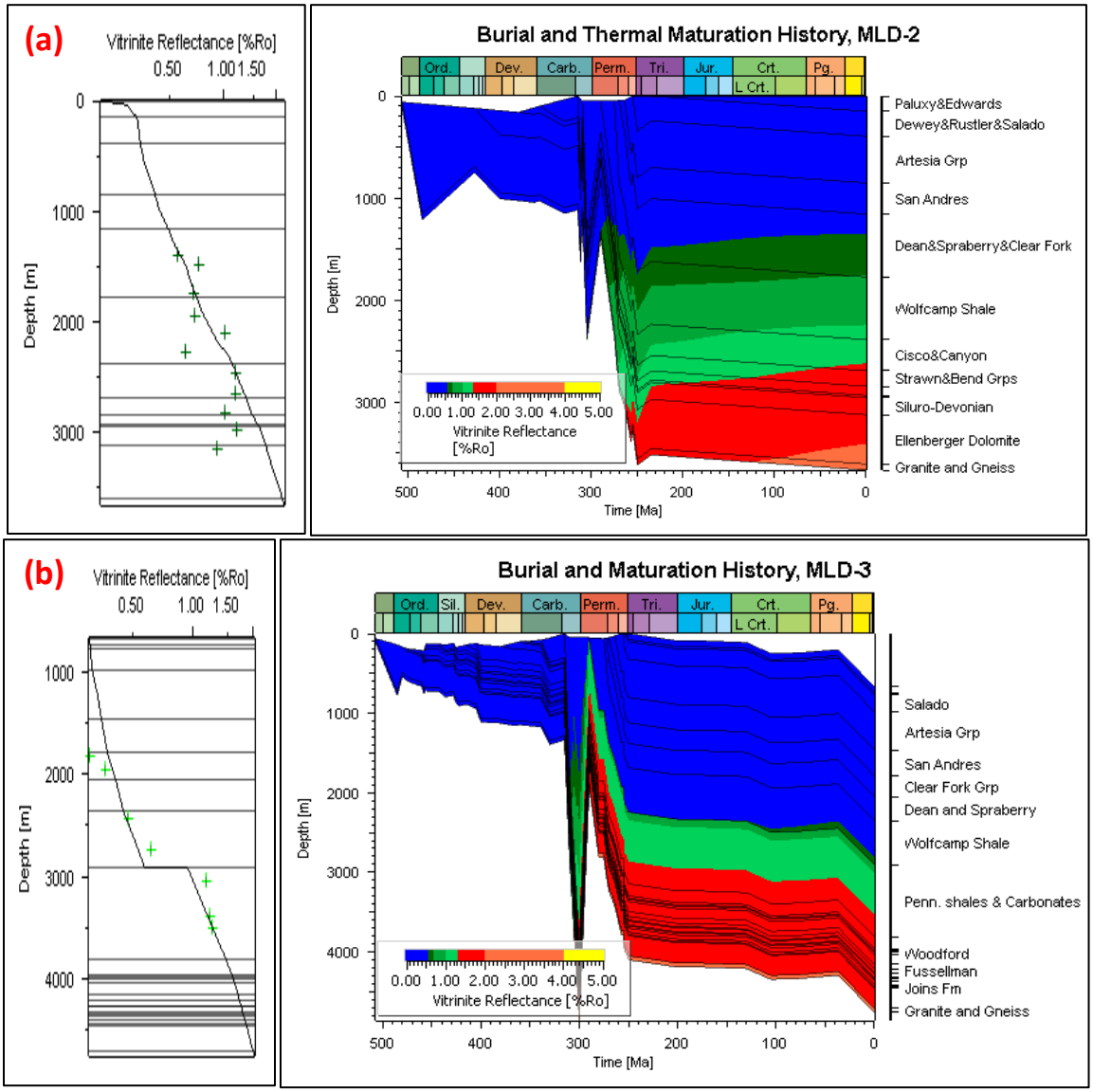

Figure 4.7a-b: Selected burial and maturation histories for Permian Basin strata in two locations in the Midland Basin illustrating variation in depositional and erosional conditions as calculated using PetroMod (Schlumberger, 2012). Left is the calibrated $\%R_o$ profile in respective locations. Thickness of strata from Galley (1958), Wright (1979) and Frenzel et al. (1988). Measured R_o used for calibration from Pawlewicz (2005). Detailed model parameters used are listed in Appendix 6.

Based on the modeled maturity profiles, the top of the Spraberry in most part is considered generally immature with respect to petroleum generation (Figure 4.8). This

observation is in agreement with actual measured maturity based on T_{Max} and TR (Figure 4.4c) where the Spraberry samples Sp2 and Sp3 plot in the region of low kerogen conversion or low thermal maturity compared to Sp1. The implications of these maturity distribution as confirmed by measured maturities is that, any hydrocarbons related to the Spraberry source rocks, must come from the south, where it is thermally mature for hydrocarbon generation. However, it is likely to be volumetrically insignificant given the thin nature of the shales as discussed in Handford (1981).

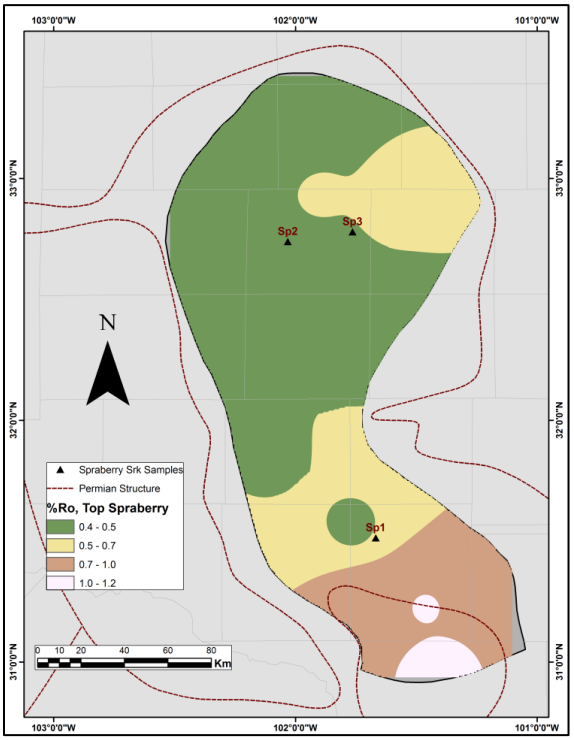

Figure 4.8: Distribution of the modelled thermal maturity atop Spraberry in the Permian Basin as calculated by interpolation using IDW option available in ArcGIS (ESRI, 2012). Spraberry outline from USGS Permian Basin geospatial data (USGS, 2012).

Unlike the Spraberry, modeled thermal maturity and overburden distributions atop Wolfcamp, Barnett, Woodford, and Simpson source rocks (Figures 4.9-4.12) indicate adequate thermal maturity for hydrocarbon generation. The Wolfcamp shale is however,

immature with respect to petroleum generation in the northeast and northern Midland Basin. The northeast is generally a low maturity area for all the source rocks under study.

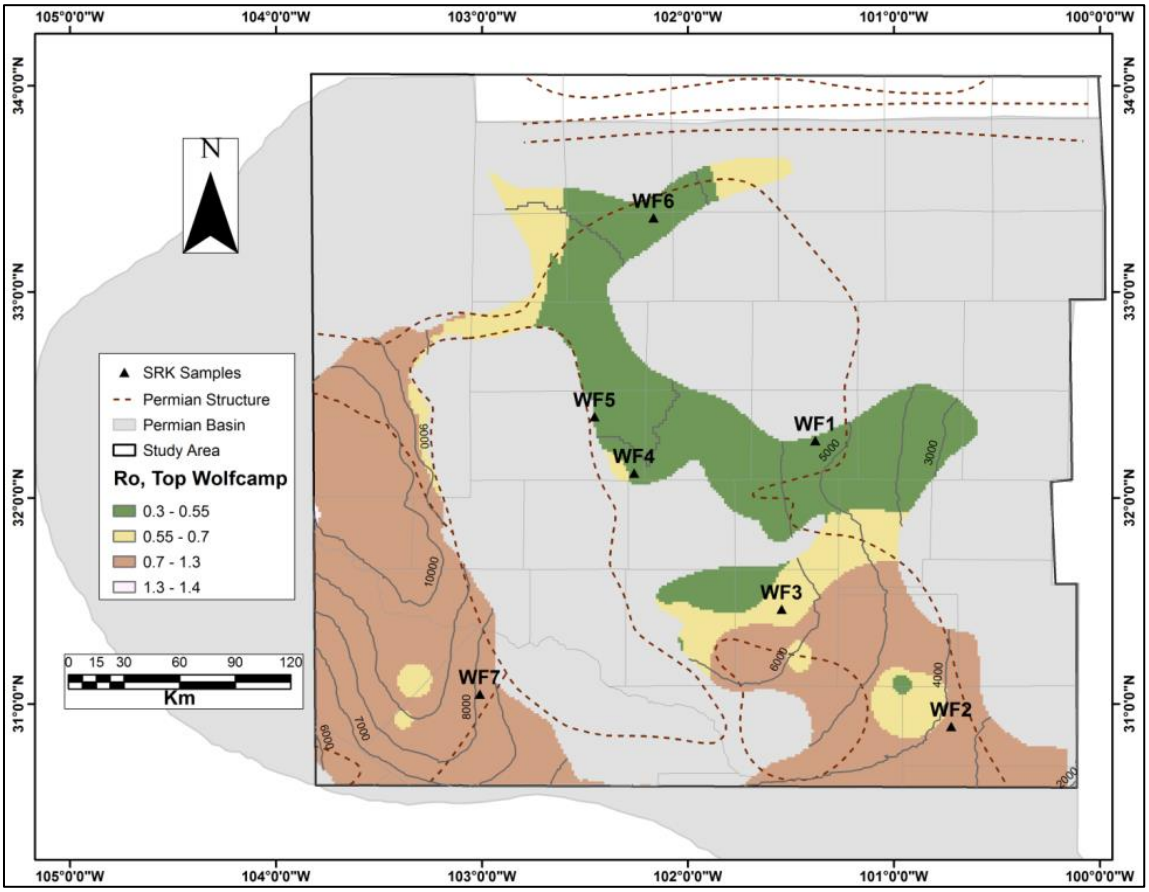

Figure 4.9: Distribution of the overburden and modelled thermal maturity atop Wolfcamp shale in the Permian Basin as calculated by interpolation using IDW option available in ArcGIS (ESRI, 2012). Wolfcamp Shale outline from USGS Permian Basin geospatial data (USGS, 2012).

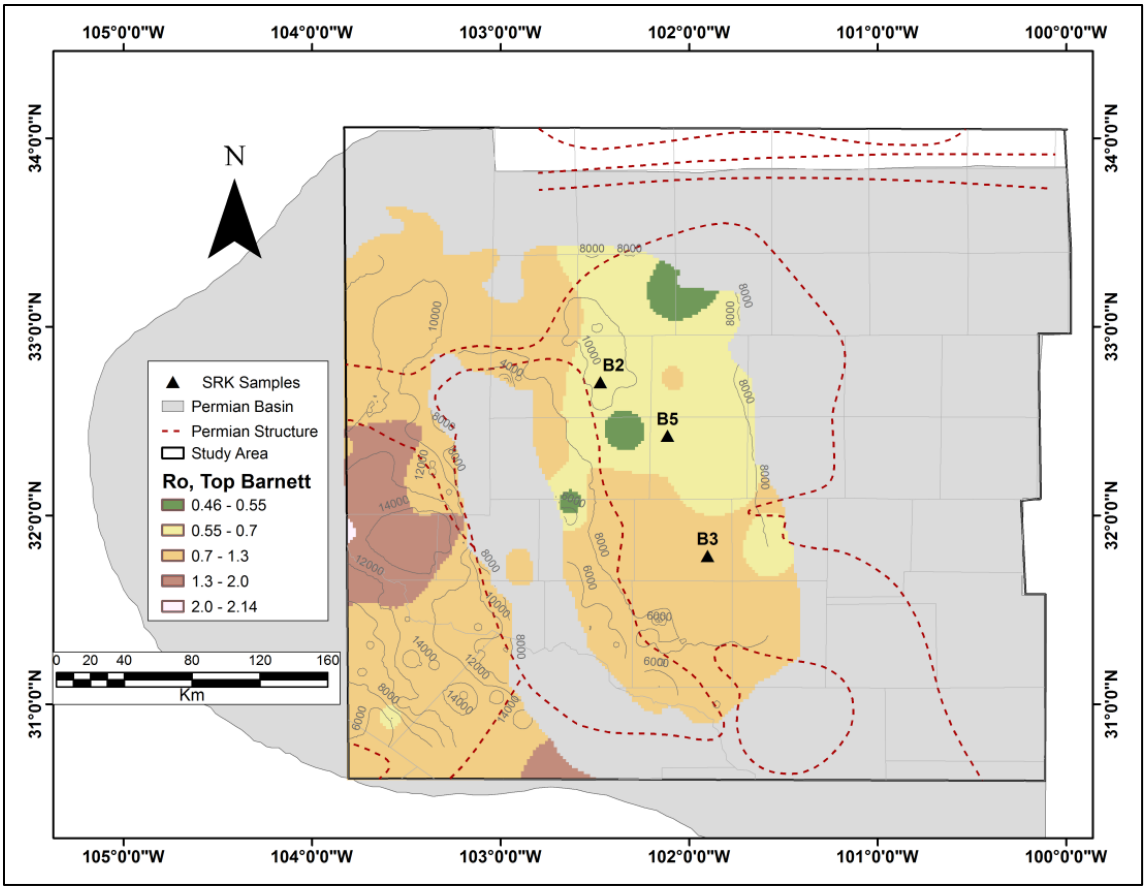

Figure 4.10: Distribution of the overburden and modelled thermal maturity atop Barnett shale in the Permian Basin as calculated by interpolation using IDW option available in ArcGIS (ESRI, 2012). The Barnett is adequately mature for hydrocarbon generation throughout the Permian Basin, except small patches in northern Midland Basin where it is below the oil window. Barnett outline digitized from Frenzel et al. (1988).

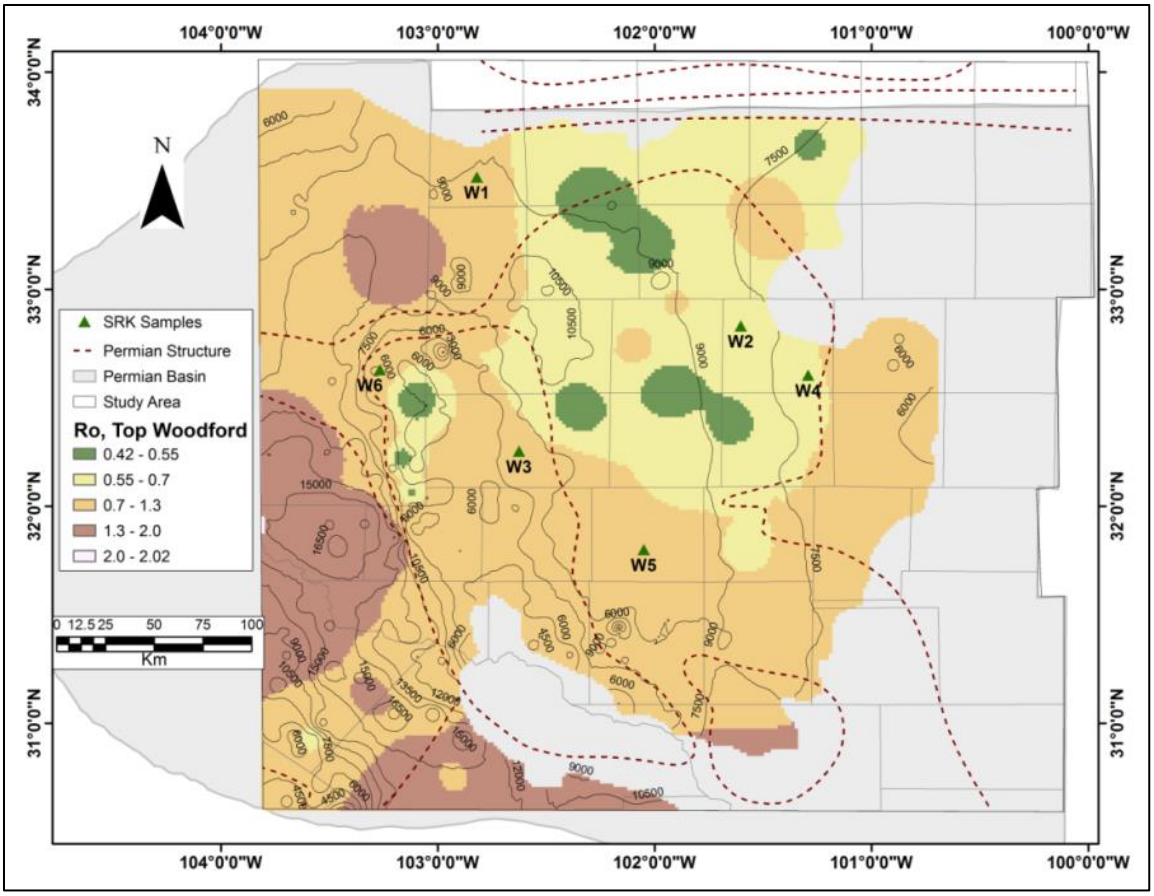

Figure 4.11: Distribution of the overburden and modelled thermal maturity atop Woodford shale in the Permian Basin as calculated by interpolation using IDW option available in ArcGIS (ESRI, 2012). The Woodford is adequately mature for hydrocarbon generation throughout the Permian Basin, except small patches in northern Midland Basin where it is below the oil window. Woodford outline and depth to digitized from Comer (1991).

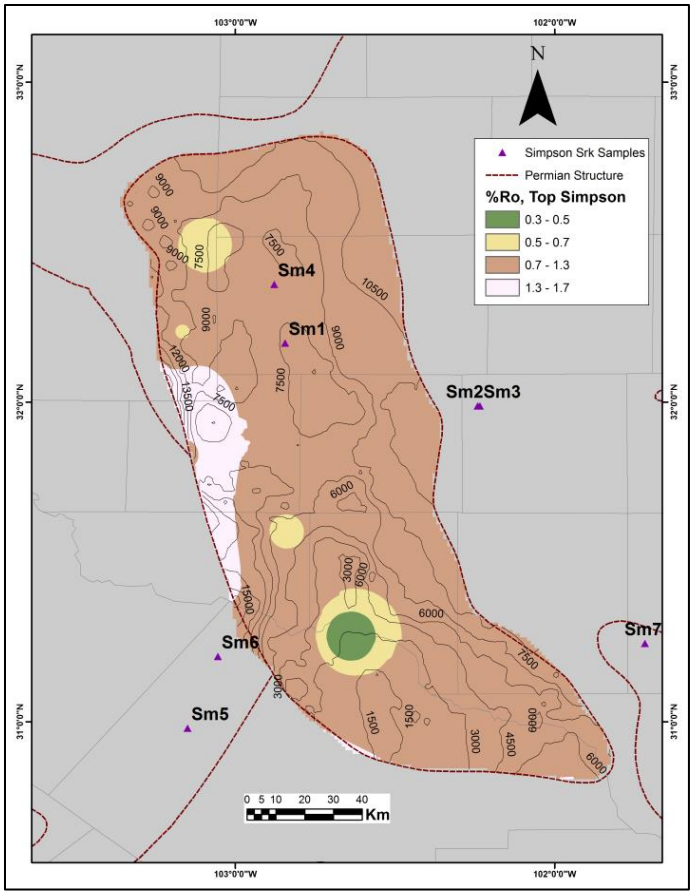

Figure 4.12: Distribution of the overburden and modelled thermal maturity atop Simpson shale in the Permian Basin as calculated by interpolation using IDW option available in ArcGIS (ESRI, 2012). The Simpson is adequately mature for hydrocarbon generation throughout the Permian Basin, except small patches in the south where it is below the oil window. Depth to Simpson calculated using the raster calculator in ArcGIS by addition of Simpson isopach (Galley, 1958; Wright, 1979; Frenzel et al., 1988) to the Ellenberger structure digitized from Frenzel et al. (1988).

4.3.3 Petroleum Generation and Expulsion Timing

4.3.3.1 The Spraberry

Modeling indicates that incipient generation from the Spraberry, mainly from the southern portion started during Early Triassic. However, only 6% kerogen conversion has occurred in the deepest part of the Spraberry (Figure 4.13a). Given the requirement to first satisfy the retention capacity (equivalent to 10% TR in PetroMod) of the source rock

before any expulsion can begin (e.g. du Rouchet, 1981; Littke et al., 1988; England, 1994) the 6% kerogen conversion translates to no expulsion as indicated in Figure 4.13b. This inference contradicts findings of Guevara and Mukhopadhyay (1987) which indicated adequate thermal maturities for hydrocarbon generation for the Spraberry shales. However, no tangible discussions can be made based on an abstract.

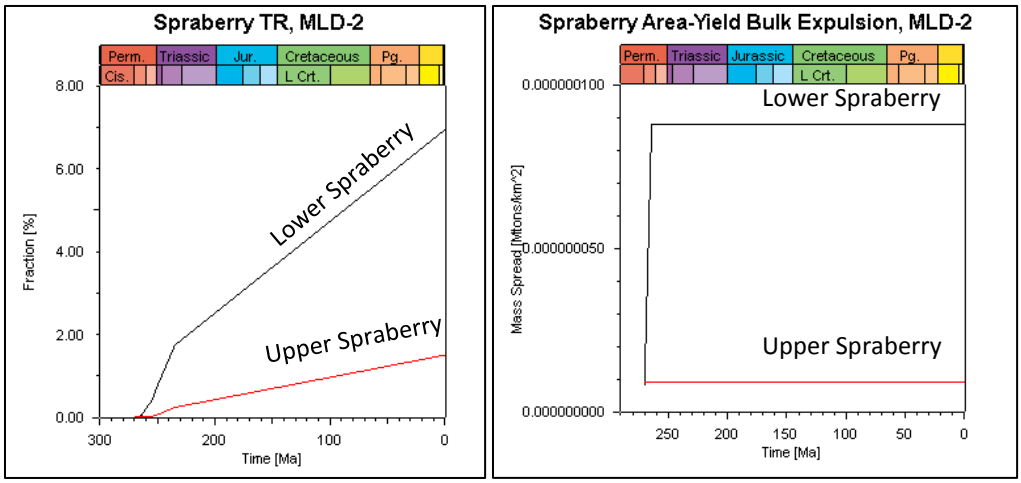

Figure 4.13: (a) Timing of generation and expulsion from upper (bottom curve) and lower (top curve) portions of the Spraberry. (b) Bulk petroleum mass spread for the Spraberry-based on total thickness of the Spraberry which includes sandstones and siltstones (Handford, 1981). TR = Transformation Ratio = percentage of kerogen transformed into hydrocarbons. Mass spread is hydrocartbons in metric tonnes/km^2 generated over time. Calculated using PetroMod (Schulumbeger, 2012). Model parameters in Appendix 6.

Galloway et al. (1983) described the Spraberry as a self-contained system by virtue of the presence of shales (source rocks) juxtaposed with sandstones (reservoirs). Assuming effective sourcing, secondary migration in this "petroleum system" is inferred to be largely through lateral and vertical pathways by virtue of the juxtaposed nature of the source and reservoirs. The natural fractures in the Spraberry trend (e.g. Lorenz, 2002) justify the existence of vertical migration pathways. However, considering the thin nature of the shales within the Spraberry (Hanford, 1981), together with the generation and

expulsion modeling results (Figures 4.8 and 4.13), there is virtually no expulsion from Spraberry. Moreover, geochemical correlations (Chapter 4) did not show any oils related to the Spraberry source rocks. Based on this observations, the "Spraberry petroleum system" is not considered a quantitatively significant petroleum system in the Permian Basin and is not discussed any further.

4.3.3.2 The Wolfcamp

Petroleum generation and onset of expulsion from the Wolfcamp shale occurred in Early Triassic, about the same time in both the Delaware and the Midland basins (Figure 4.14 a-c). As indicated by maturity distribution (Figure 4.9) and generation profiles (Figure 4.14a-c), a big portion of the Wolfcamp is still at early stages of generation, and therefore suggests an ongoing process, especially on the stratigraphically upper portions of the Wolfcamp in the Midland Basin. To illustrate this, at the location where model MLD-3 was taken in the Midland Basin (Figure 4.14c), present kerogen conversion is as low as 2%, indicating no expulsion. In the Delaware Basin however, the Wolfcamp is at late generation (65-90% kerogen conversion) where expulsion is inefficient leading to a lot of hydrocarbons remaining within the source rock, implying significant unconventional gas potential for the Wolfcamp strata in the Delaware Basin.

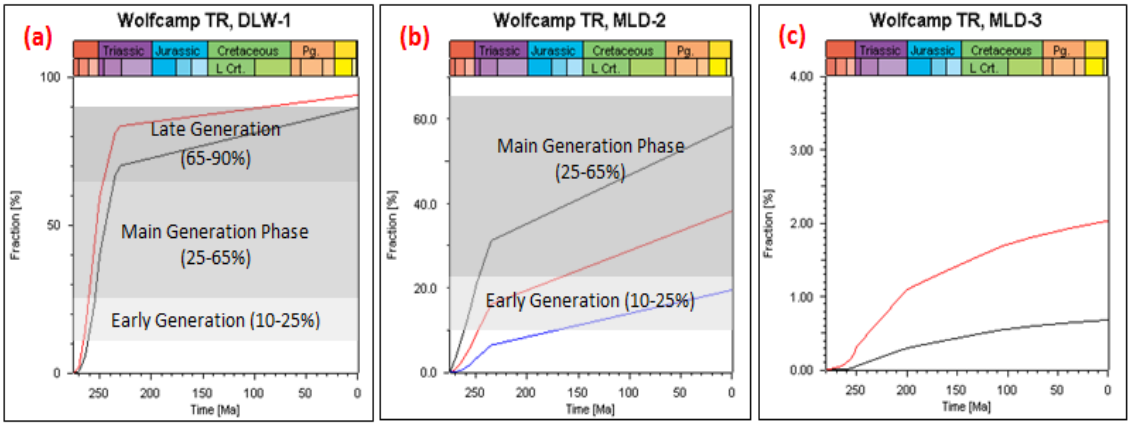

Figure 4.14 a-c: The timing and levels of generation and expulsion from the Wolfcamp shale in the Permian Basin; top curve represents the lower portion while bottom curve represents top portion of the shale. TR = Transformation Ratio = percentage of kerogen transformed into hydrocarbons. Calculated using PetroMod (Schulumbeger, 2012). Model parameters in Appendix 4. 1. The Wolfcamp is currently at main phase or peak generation in some parts of the Midland (MLD-2 and MLD-3) and at late generation in the Delaware (DLW-1). In some parts of the Midland, the Wolfcamp is thermally immature, and consequently, there is no generation at all. Model parameters in Appendix 6.

4.3.3.3 The Barnett Shale

Modeling indicates that petroleum generation from the Barnett shale, in both Delaware and Midland basins begun from Early- to Mid-Permian. Expulsion did not occur until the Leonardian, peaking during the Early Triassic. The Barnett in the Delaware and some parts of the Midland basins is currently beyond the maturity stage for oil generation (Figure 4.15a & c). In some parts of the Midland Basin however, as represented by model at location MLD-2 in the Midland Basin, the Barnett is at late generation, implying possible unconventional gas potential as discussed under the Wolfcamp in Delaware Basin above. At location of model MLD-3, generation occurred during the Pennsylvanian, peaking and ending in Late Pennsylvanian.

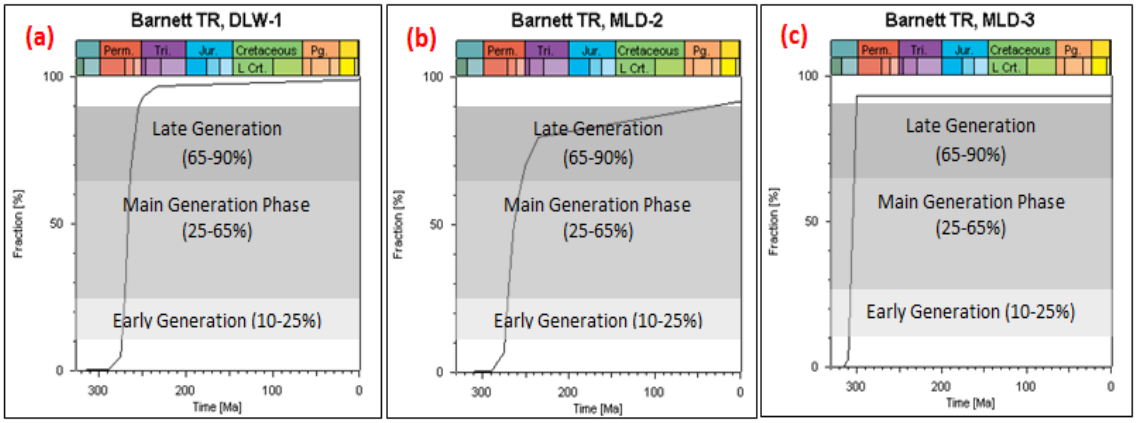

Figure 4.15 a-c: The timing and levels of generation and expulsion from the Barnett shale in the Permian Basin; Midland (MLD-2 and MLD-3) and Delaware (DLW-1), basins respectively. TR = Transformation Ratio = percentage of kerogen transformed into hydrocarbons. Calculated using PetroMod (Schulumbeger, 2012). Model parameters in Appendix 6. Barnett is absent in the Central Basin Platform. The Barnett has reached maximum generation in all these modal locations.

4.3.3.4 The Woodford

Generation from this source rock occurred at various times in the Delaware, Central Basin Platform, and Midland Basins (Figure 4.16a-d). In the Delaware, generation occurred during the Early-Mid Permian, peaking at Early Gudalupian. In the Central Basin Platform, generation from the Woodford Shale begun during Early Triassic and peaked in Mid-Triassic. In the Midland Basin, as indicated by model MLD-2, generation begun during Mid-Permian and peaked by Late Leonardian. However, at MLD-3, also in the Midland Basin, generation occurred rapidly, starting by Mid-Pennsylvanian and ending in Late Pennsylvanian. Except in the Central Basin Platform where the Woodford is actively expelling, there is currently no active generation and expulsion from the Woodford in the Delaware and Midland basins. In these basins, the Woodford is coked or reached maximum generation, except in some areas in the Midland Basin where the

Woodford is at late generation and where unconventional gas potential is implied. Having said that, there are, however, some patches in the northeast where the Woodford is actually immature with respect to petroleum generation (Figure 4.11).

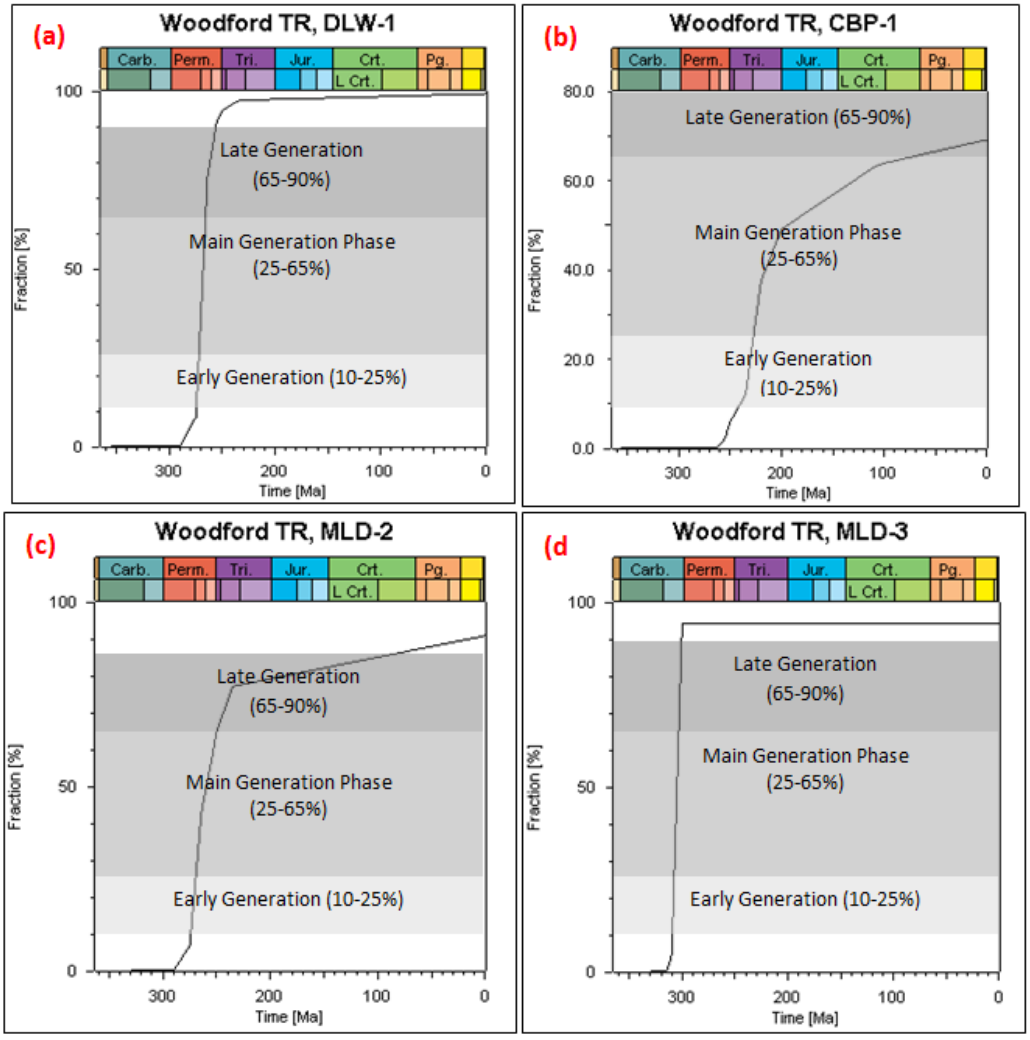

Figure 4.16 a-d: The timing and levels of generation and expulsion from Woodford shale in the Permian Basin; from top to bottom, Delaware (DLW-1), Central Basin Platform (CBP-1) and Midland (MLD-2 and MLD-3) basins respectively. TR = Transformation Ratio = percentage of kerogen transformed into hydrocarbons. Calculated using PetroMod (Schulumbeger, 2012). Model parameters in Appendix 6. The Woodford shale has reached maximum generation in Midland and Delaware basins.

4.3.3.5 The Simpson

The distribution of the overburden and maturity atop Simpson source rock over the Central Basin Platform is shown in Figure 4.12. Simpson shales begun generating hydrocarbons in Early Triassic and peaked at Mid-Triassic (Figure 4.17a). At this model location, the Simpson has just ended generation/expulsion and has therefore exhausted its hydrocarbon potential.

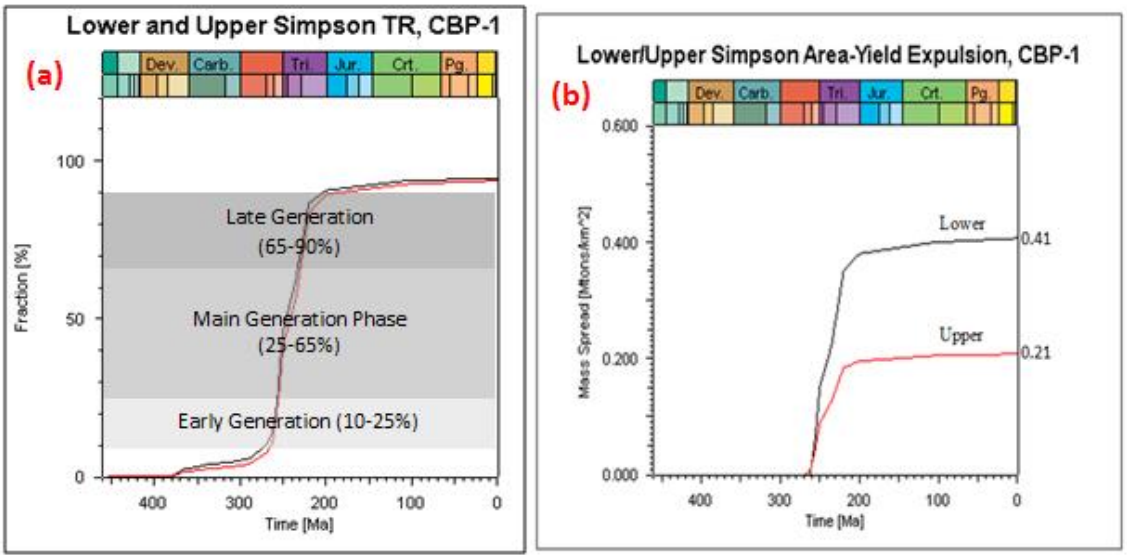

Figure 4.17: (a) The timing and levels of generation and expulsion from Simpson shale in the Central Basin Platform (CBP-1) in Permian Basin. TR = Transformation Ratio = percentage of kerogen transformed into hydrocarbons. TR = Transformation Ratio = percentage of kerogen transformed into hydrocarbons. Mass spread is hydrocartbons in metric tonnes/km^2 generated over time. Calculated using PetroMod (Schulumbeger, 2012). The Simpson has reached maximum generation in the Central Basin Platform. (b) Volumes of hydrocarbons under one square kilometer, generated by the upper (red) and lower (gray) Simpson Shales in the Central Basin Platform.

4.3.4 Source Rock Volumetrics

Source rock isopach maps highlighting pods of active source rocks as well as modeled bulk mass of hydrocarbons expelled by a volume of source rock under a square kilometer

based on the thickness at the location of the model are presented in Figures 5.18 through 5.21 and final volumetrics summarized in Table 4.1. As discussed in Chapter 3, all source rocks are of high quality (type II and II/III), organic-rich (TOC > 1.0%) and adequately mature (> 0.75R_o) as confirmed by the modeling above. Generated or expelled hydrocarbons from source rocks vary depending on the size of the source rock, with the Wolfcamp and Barnett having the highest hydrocarbons expelled. However, because of poor sample coverage especially for the Barnett, where the actual effective source facies hasn't been constrained, and the volume could be lower. Effective source rock coverage is a major source of uncertainty in the Barnett petroleum system volumetrics. For the Wolfcamp, uncertainties are associated with the sedimentation cyclicity involving shale and carbonates (e.g. Silver and Todd, 1969; Mazzullo, 1998) and complete cyclicity involving shale, carbonate and sandstone reported in the southern regions in the Val Verde Basin (e.g. Hamlin, 2009). The resedimented carbonate facies encased in the shale (e.g. Frenzel et al., 1988; Dutton et al., 2004) which define major reservoirs for this petroleum system is a manifestation of this phenomenon and could significantly reduce the actual volumetrics of the source facies.

Table 4.1: Summary of modeled source rock volumetrics

Model Loc.	Thick-ness (m)	H/C Mtons/ Km2)	Thickness Vol. (Km3)	Pod Vol. (Km3)	H/C Mass/ Metric tons	Expelled Bbbl	Avg. Expelled (Bbbl)
WOLFCAMP*		**(HI_o = 140**	**TOC 2.3)**				
DLW-1	549	4.579	0.549	14908.2	1.2E+10	91.1439	73.9
MLD-2	610	3.166	0.61	14908.2	7.7E+9	56.7166	
BARNETT*		**(HI_o = 201**	**TOC 3.0)**				
DLW-1	198	2.791	0.198	6058.48	8.5E+9	62.5983	80.9
MLD-2	90	2.413	0.09	6058.48	1.6E+10	119.064	
MLD-3	150	2.06	0.15	6058.48	8.3E+9	60.9879	
WOODFORD		**(HI_o = 195**	**TOC = 2.6)**				
DLW-1	61	0.724	0.061	1627.8	1.9E+9	14.1613	13.3
MLD-2	22	0.233	0.022	1627.8	1.7E+9	12.6365	
MLD-3	30	0.332	0.03	1627.8	1.8E+9	13.2042	
CBP-1	80	0.575	0.08	1627.8	1.16E+9	857.58[¥]	
SIMPSON		**(HI_o = 110**	**TOC 1.73)**				
CBP-1	150	0.623	0.15	396.0	1.6E+8	1.20	1.20

CBP, MLD, DLW represent model location in the Central Basin Platform, Midland and Delaware respectively. *Source poorly constrained. HI_o determined using the method of Barnejee et al., 1998; 2000) as described in Chapter 3. [¥] Not included in average.

Given the entire Permian Basin STOOIP of only 105Bbbl (Tyler and Banta, 1989), the conservative volumetrics from the source rocks suggest that generation and expulsion from the source rocks is not a constraint to hydrocarbon endowment in the Permian Basin. Moreover, the source rocks considered here are just a fraction of the source rock pool of the Permian Basin (Chapter 3, Figure 3.12).

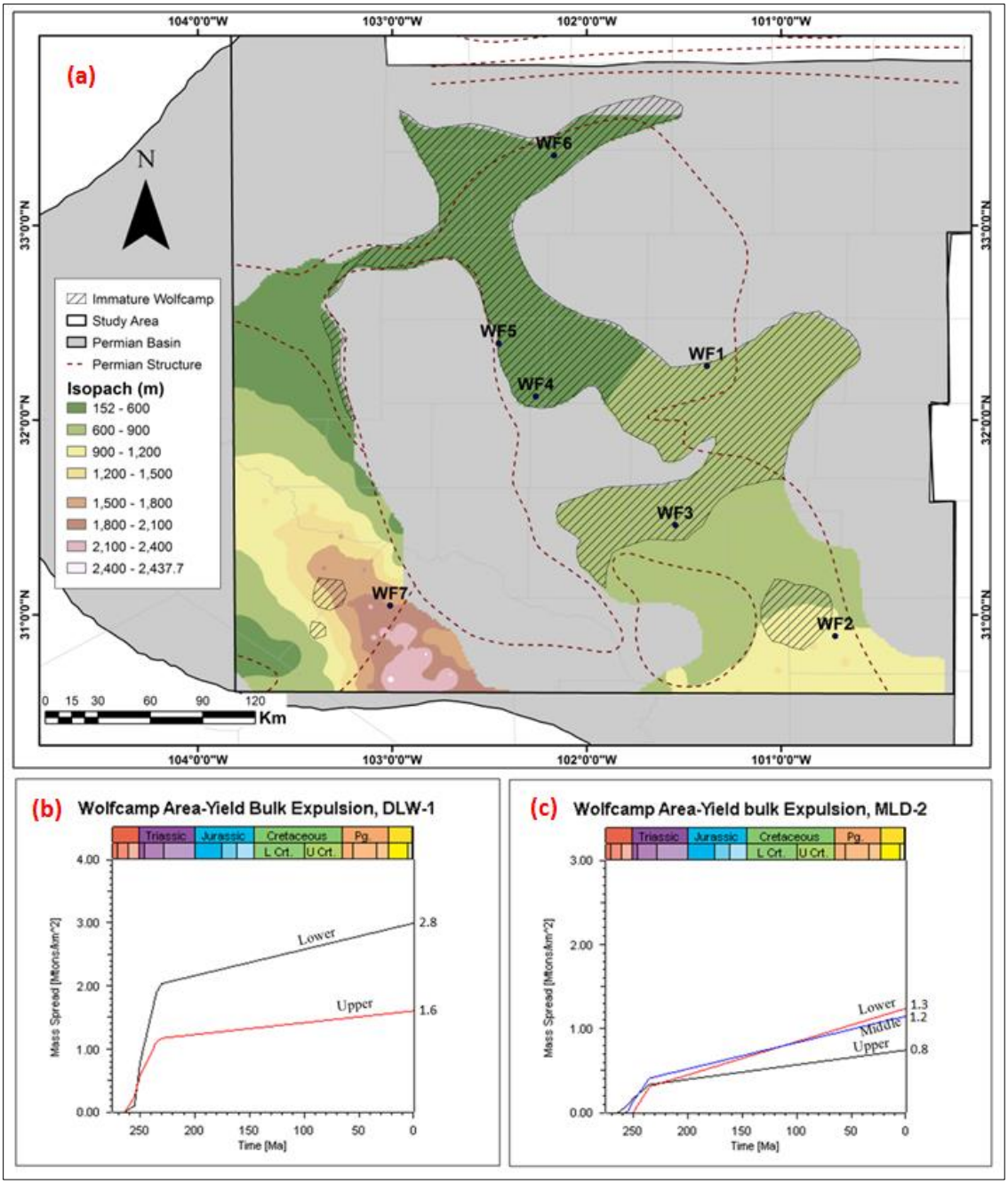

Figure 4.18 (a) Wolfcamp shale isopach in the Permian Basin (from Galley, 1958, Frenzel et al., 1988). Immature portions of the Wolfcamp shaded. Modeled volumetric in Delaware, DLW-1 (b) and Midland, MLD-2 (c). Calculated using PetroMod (Schulumbeger, 2012). Model parameters are listed in Appendix 6 (See Table 4.1 for summary of volumetrics). Base map from Dutton et al. (2004).

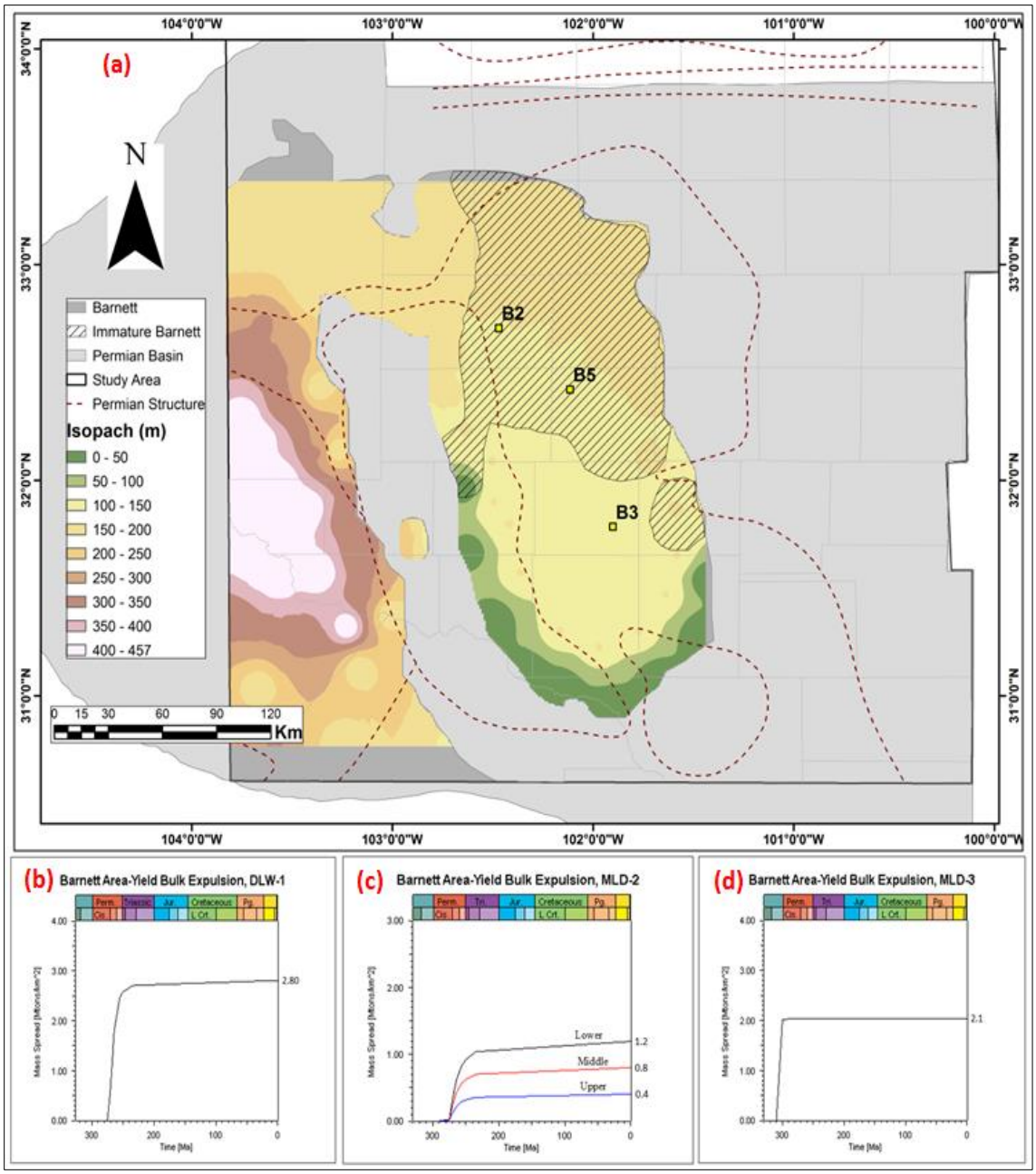

Figure 4.19 a-d: Barnett Shale Isopach in the Permian Basin, includes the carbonate (from Galley, 1958, Frenzel et al., 1988). Immature portions of the Barnett source rock shaded. The lower Figures indicate modeled volumetrics in two locations. Mass spread is hydrocartbons in metric tonnes/km^2 generated over time. Calculated using PetroMod (Schulumbeger, 2012). Model parameters are listed in Appendix 6 (See Table 4.1 for summary of volumetrics). Base map from Dutton et al. (2004).

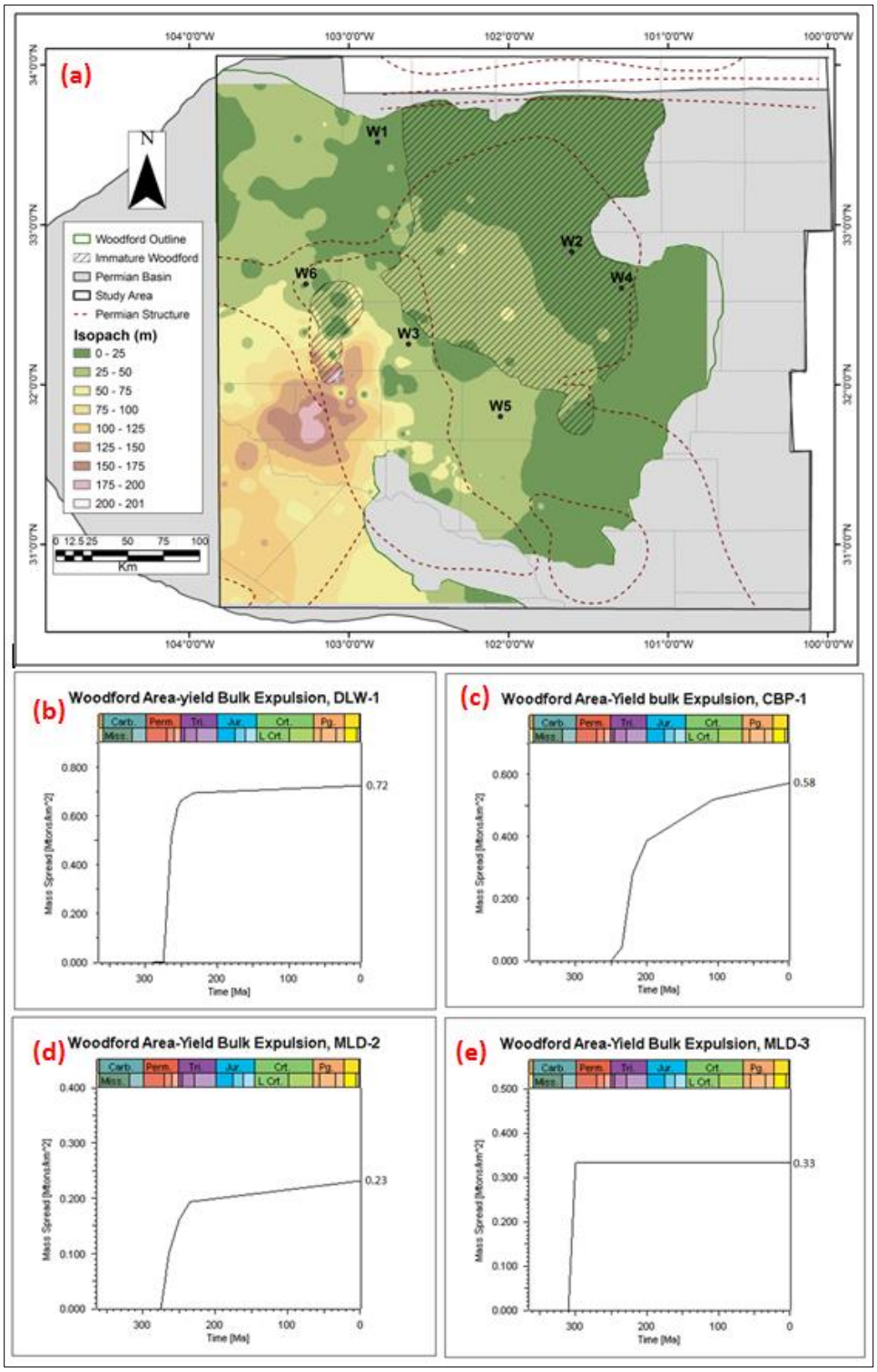

Figure 4.20 a-e: Woodford Shale isopach in the Permian Basin (from Galley, 1958, Frenzel et al., 1988 and Comer, 1991). b-e indicate modeled volumetrics in two locations. Mass spread is hydrocarbons in metric tonnes/km^2 generated over time. Immature portions of the Woodford shaded. Calculated using PetroMod (Schulumbeger, 2012). Model parameters are listed in Appendix 6 (See Table 4.1 for summary of volumetrics). Base map from Dutton et al. (2004).

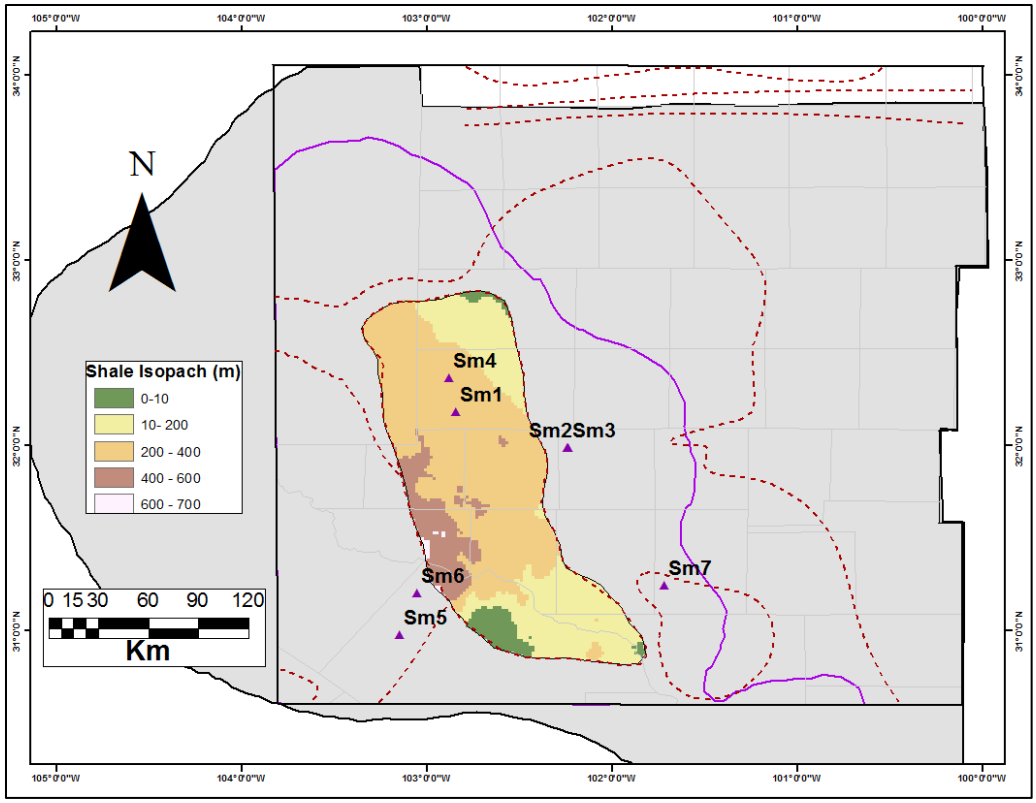

Figure 4.21: Simpson shale isopach in the Permian Basin (from Galley, 1958, Frenzel et al., 1988). Net shale obtained by subtracting the Simpson carbonate and sandstone units using raster calculator available in ArcGIS. Modeled volumetrics is shown in Figure 4.19 (b). Model parameters are listed in Appendix 6 (See Table 4.1 for summary of volumetrics). Base map from Dutton et al. (2004).

Because of the uncertainties discussed above, and the poor constraints on the actual stratigraphic limits of the petroleum systems, especially occasioned by migration and possible mixing over the Central Basin Platform as discussed in detail in Section 4.4 below, estimation of generation-accumulation efficiency for petroleum systems was deemed untenable so it was not done. In all, the large volumetrics suggest that the petroleum systems are supercharged according to the definition of Demaison and Huizinga (1991), thus generation from source rocks is not a constraint to hydrocarbon endowment in the Permian Basin.

4.4 Migration and Entrapment

4.4.1 The Wolfcamp Petroleum System

The geographic extent of the Wolfcamp petroleum system is depicted in Figure 4.22. The petroleum systems elements and processes for this petroleum system are summarized in the events chart in Figure 4.23 and migration illustrated in Figure 4.30. According to geochemical correlations (Chapters 2 and 3), the oils generated from the Wolfcamp shale are found in reservoirs that collectively define the Wolfcamp/Leonardian slope and basinal carbonate play and in reservoirs that define the Wolfcamp platform carbonate play located in the Central Basin Platform (Dutton et al., 2004; 2005). Reservoirs of these plays are variously described (e.g. Loucks, 1999; Mazzullo, 1997; Mazzullo, 1998). Traps are largely stratigraphic, with reservoirs encased in dark-gray to black basinal Wolfcampian shales, which acts both as seal and source rock (e.g. Frenzel et. al., 1988; Dutton et al., 2004).

Evoking Pratsch (1983) and Hindle (1997) models of expulsion and primary migration, where hydrocarbons begin migration from the zone of highest maturity and pushing hydrocarbons to zones of low maturity where pressure is low, the area of focusing of petroleum from the Wolfcampian source rocks are the Central Basin Platform and the northern reaches of the Midland Basin including the Horseshoe Atoll (Figure 4.22). This is in agreement with the distribution of oils geochemically constrained to be sourced from the Wolfcamp source rock. From the stratigraphic framework view point, oils generated from the Wolfcamp source rock, could potentially be within the Upper Permian

reservoirs as well. This is because of lack of seal rocks until the Ochoan evaporite stratigraphic horizon (Chapter 3, Figure 3.12).

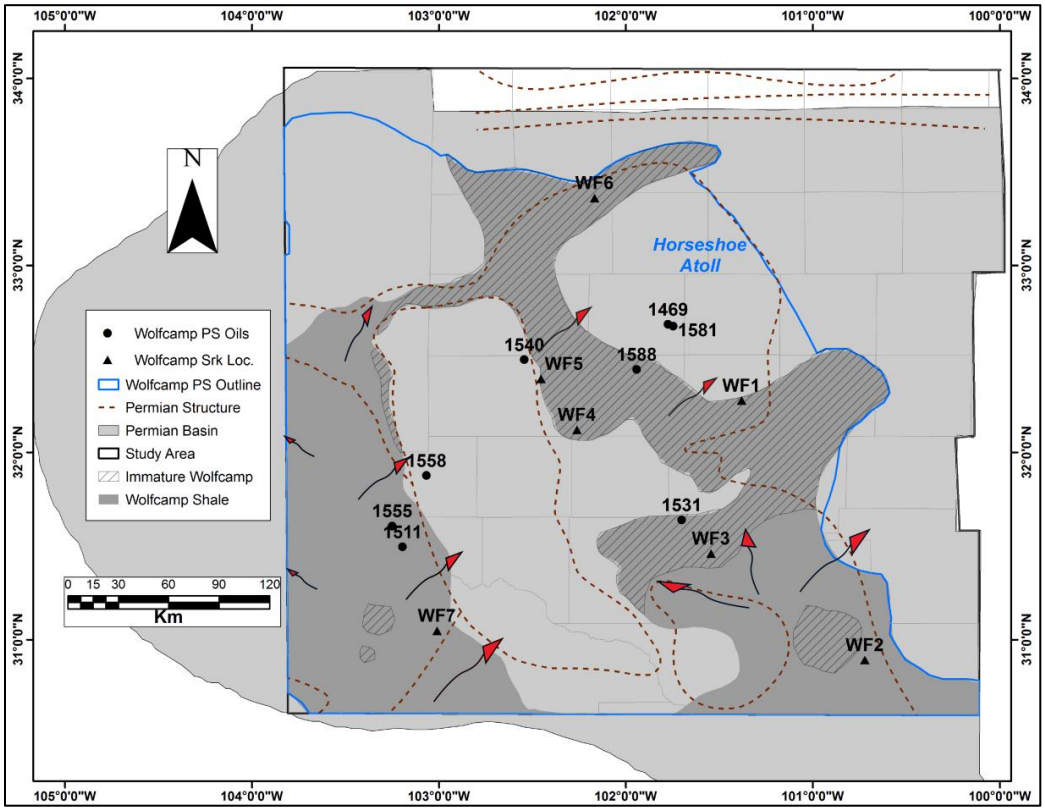

Figure 4.22: The geographic extent of the Wolfcamp petroleum system showing the potential migration paths based on the basin configuration. Oils and source rock samples used to constrain this petroleum system are indicated. Shaded area are places were top Wolfcamp is immature.

Given the juxtaposed source-reservoir relationship, secondary migration in this petroleum system is inferred to be dominantly lateral (Figure 4.30), with short migration distances. This petroleum system presents a unique scenario in the petroleum system elements context. The Wolfcamp is a source rock as well as a seal. The re-sedimented or detrital carbonates, which are reservoirs, are encased within the Wolfcamp shales. This means that the source rock, the reservoirs, and the seals are all Wolfcampian.

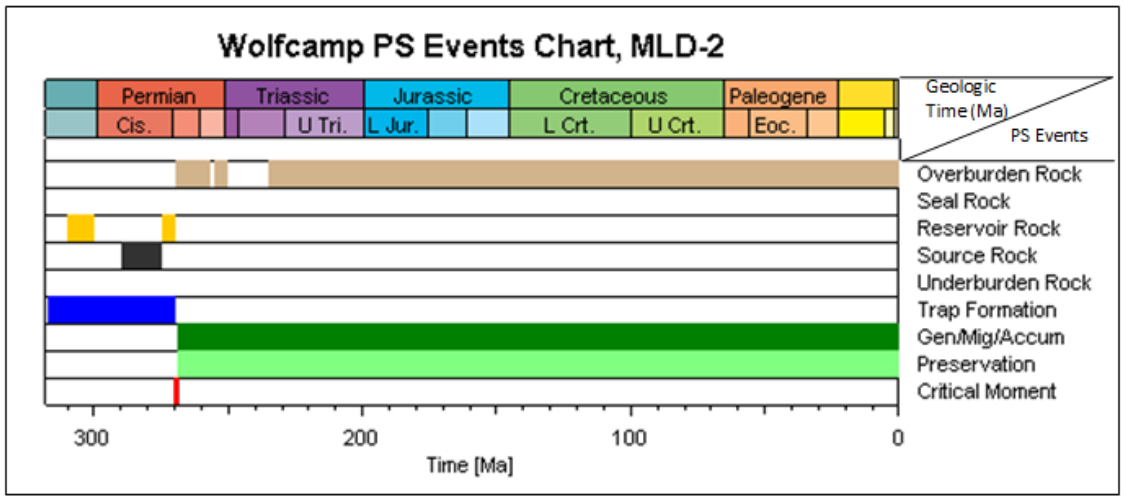

Figure 4.23: Events chart for the Wolfcamp Petroleum Systems in the Permian Basin. Timing of expulsion relative to trap formation not a constraint. Reservoirs, traps, seals from several sources (Dutton et al., 2004; 2005; Loucks, 1999; Mazzullo, 1997; Mazzullo, 1998). See text for detailed listing of sources. Calculated using PetroMod (Schulumbeger, 2012). Model parameters in Appendix 6. PS = Petroleum System.

Although there are slight variations, depending on the location of the model location, in general, generation from the Wolfcamp begun during Leonardian but only became significant during the Triassic. By the time of generation and expulsion, the reservoirs, traps, and seals had already formed, thus justifying the existence of the Wolfcamp petroleum system.

4.4.2 The Barnett Petroleum System

The geographic extent of the Barnett petroleum system is depicted in Figure 4.24. The events chart in Figure 4.25 summarizes the elements and process related to this petroleum system. Migration from the Barnett shale is illustrated in Figure 4.30. Geochemical correlations (Chapters 2 and 3) indicate that oils from the Barnett shale source rock are hosted, mainly in reservoirs that define the Pennsylvanian plays and the Permian platform

carbonate play located in the Central Basin Platform and Northwest Shelf regions. These reservoirs are summarized in Dutton et al., (2004) and Galloway et al. (1983) and discussed in detail in primary sources, including Heckel (1986), Saller et al. (1999), and Dickson and Saller (1995). Entrapment in these reservoirs is derived from updip pinch-outs of sandstone bodies, low relief anticlines and a combination of traps formed by facies change and partial structural closure (Galloway et al., 1983). Though no oil samples were recovered from the Pennsylvanian platform carbonate reservoirs located in the Central Basin Platform, the occurrence of oils, interpreted to be sourced from the Barnett shale in the Permian reservoirs above this play implies that Barnett oils could be present in the Permian plays as well. The reservoirs of this play are discussed under Woodford petroleum system.

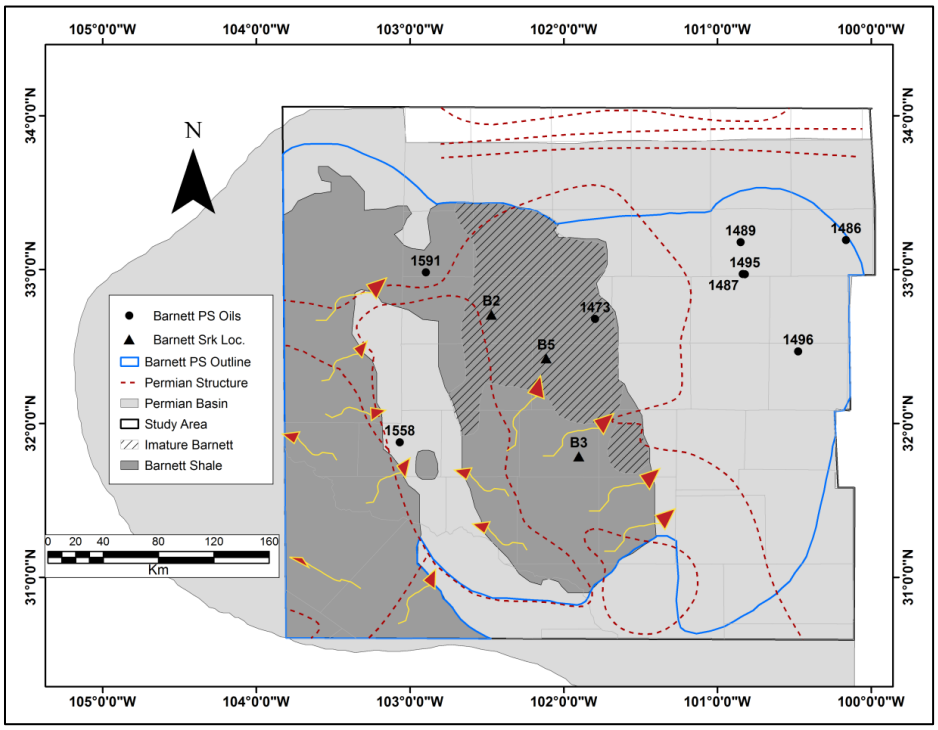

Figure 4.24: The geographic extent of the Barnett petroleum system showing potential migration pathways based on the basin geometry as discussed using the migration models of Pratsch (1983 and Hindle (1997). Shaded area are places were top Barnett is immature. Oils and source rock samples used to constrain this petroleum system are indicated.

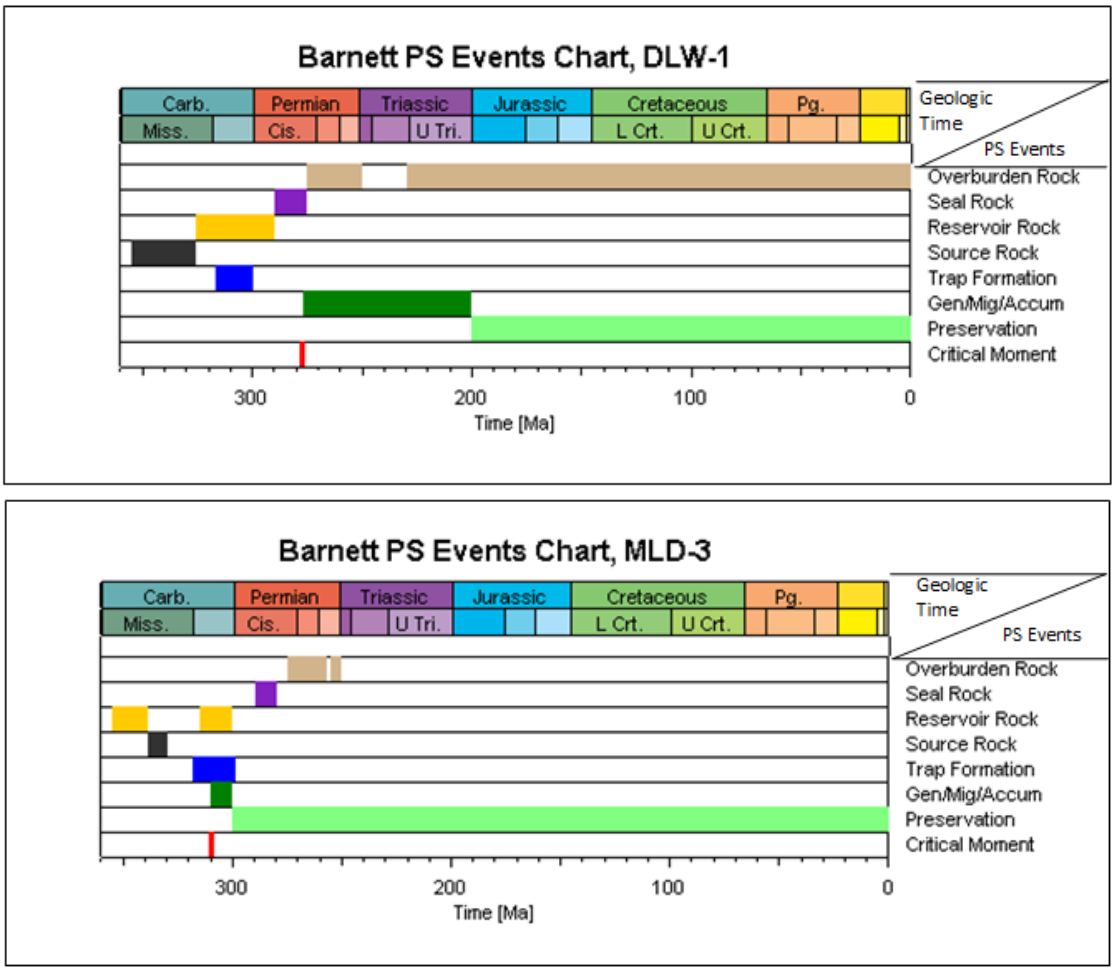

Figure 4.25a-b: Events chart for the Barnett petroleum system in the Permian Basin: from top to bottom; Delaware (DLW-1) and Midland (MLD-3) basins respectively. Timing of expulsion relative to trap formation not a constraint. Reservoirs, traps and seals from several sources (Heckel (1986; Saller et al. (1999; Dickson and Saller, 1995). See text for detailed listing of sources. Calculated using PetroMod (Schulumbeger, 2012). Model parameters in Appendix 6. PS = Petroleum System.

The reservoirs hosting the Barnett oils are largely controlled by the Pennsylvanian structural deformation that transformed the Tobosa Basin into the Permian Basin (e.g Galloway et al., 1983). These vertical structures or discontinuities inevitably distort the migration pattern associated with the basin geometry as suggested by Pratsch (1983) and Hindle (1997) models. These vertical fractures could be potential avenues for vertical migration. In additional to the Pennsylvanian vertical faults, a distortion of migration

associated with basin geometry can be visualized in areas around the Central Basin Platform where the Barnett is completely eroded (Figure 4.24). Given that the Pennsylvanian erosion affected the entire stratigraphy including the Ordovician Ellenberger (Galley, 1958; Wright, 1979), this region of the Central Basin Platform is a potential mixing chamber, not only for the Barnett-derived oils but all source rocks active in the intervening Delaware and Midland basins and thus a degree of uncertainty on the stratigraphic limits of this petroleum system.

4.4.3 The Woodford Petroleum System

The geographic extent of the Woodford petroleum system is depicted in Figure 4.26. The events chart for the Woodford petroleum system is shown in Figure 4.27 and migration illustrated in a model in Figure 4.30. Geochemical correlations (chapters 2 and 3) indicate that oil from the Woodford shale migrated mainly to the underlying carbonate and cherty-carbonate reservoirs of the Devonian, Silurian, and Ordovician. This observation suggests effective sealing by the overlying Barnett Formation. The only exception to this are the oils reservoired in the Pennsylvanian platform carbonate in the Central Basin Platform where upward migration is depicted.

The Devonian, Silurian, and Ordovician reservoirs are described in detail by various workers including Saller et al. (1991; 2001), Ruppel and Hovorka (1995), Ruppel and Barnaby (2001), Ruppel and Holtz (2001), and Mazzullo (1997). Traps are dominantly anticlinal, mainly simple and faulted anticlines (Galloway et al., 1983) associated with structural uplifts as evidenced by bounding by basement reverse faults that formed during

the Pennsylvanian (Montgomery, 1998). Woodford shale acts as a source rock and, where it directly overlies the Silurian, it acts as a seal (Comer, 1991).

Reservoirs belonging to the Pennsylvanian platform carbonate play are described by Saller et al. (1999), Dickson and Saller (1995), and Heckel (1986) and generally comprise simple anticlinal closures. As discussed under Barnett and Wolfcamp petroleum systems above, the oils from the Woodford shale could be present in Permian reservoirs over the Central Basin Platform, thus a degree of uncertainty on the stratigraphic limits of this petroleum system.

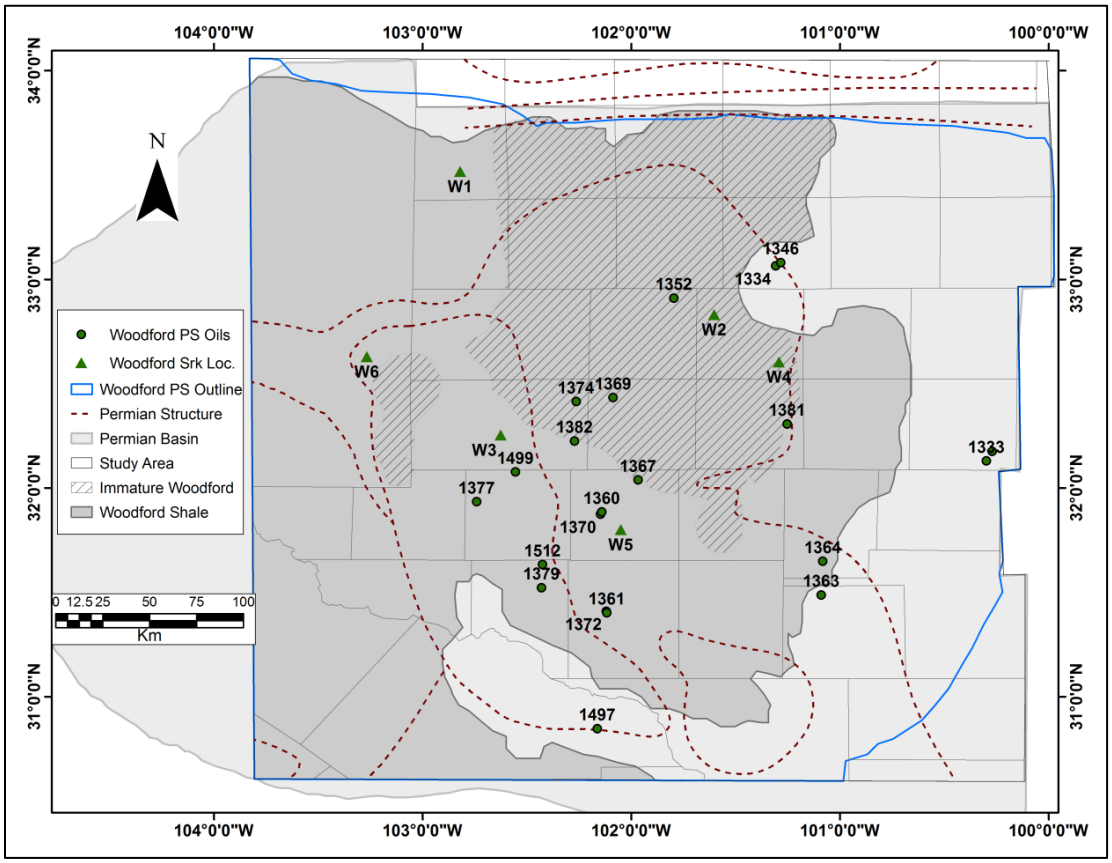

Figure 4.26: Geographic extent of the Woodford petroleum system in the Permian Basin. Migration from the Woodford source rock took a downward direction against buoyancy, to underlying reservoirs ranging in age from Devonian to Ordovician. Shaded area are places were top Woodford is immature.

As discussed above, migration from the Woodford predominantly took a downward direction against buoyancy, to the underlying Devonian, Silurian, and Ellenberger reservoirs. Although not a common phenomenon, downward migration is possible under high pressure conditions (e.g. Mann et al., 1997). For the Woodford Shale, it is suggested that high pressures must have been occasioned by enormous generation of hydrocarbons. This interpretation is arrived at based on its high TOC and HI as well as high maturity and is premised on the fundamental observations of Meissner (1978), Hunt (1990), and du Rouchet (1981). It could as well be due to the fact that the buoyancy force was thwarted by the presence of a thick Barnett shale Formation atop the Woodford which prevented the buoyant advance of Woodford generated hydrocarbons. This is supported by the presence of Woodford generated hydrocarbons in the Pennsylvanian in the Central Basin Platform where the Barnett is absent due to Pennsylvanian uplift and erosion.

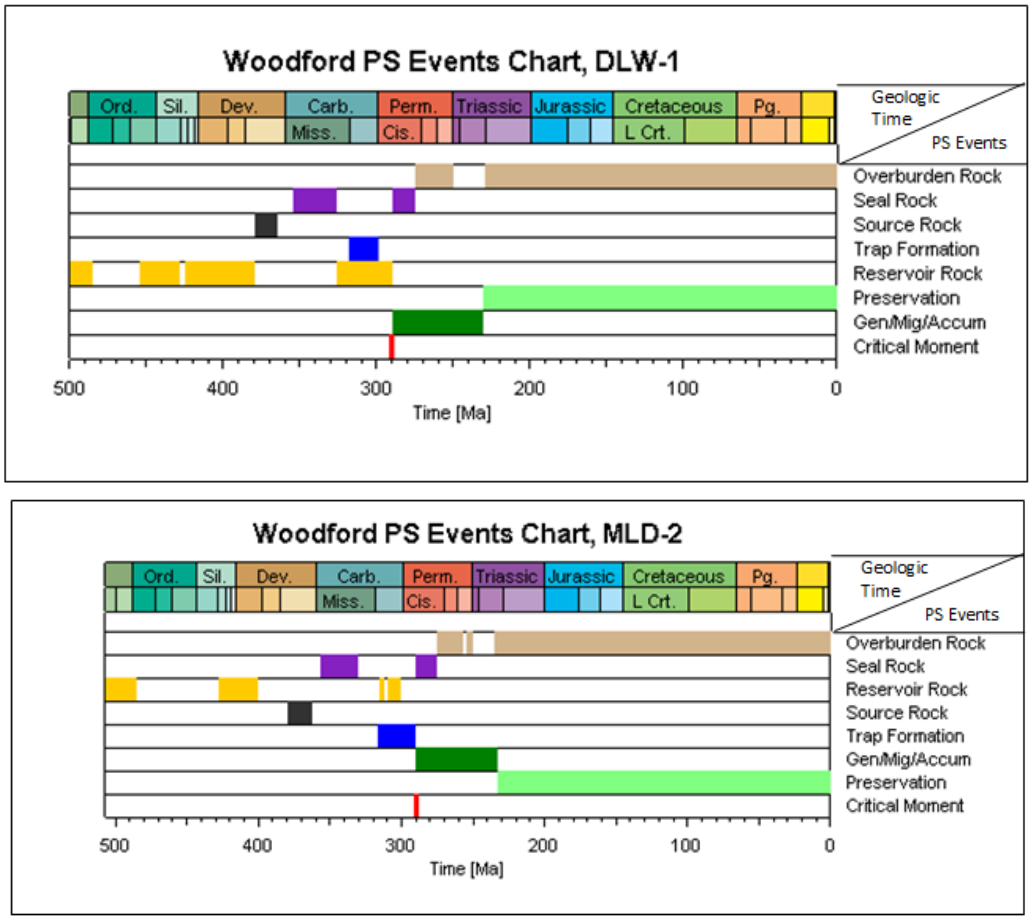

Figure 4.27a-b: Events chart for the Woodford petroleum system in the Permian Basin: from top to bottom, Delaware, Central Basin Platform and Midland basins respectively. Timing of expulsion relative to trap formation is not a constraint. Reservoirs, Traps and seals from several sources (Saller et al. (1991; 2001; Ruppel and Hovorka, 1995; Ruppel and Barnaby, 2001; Ruppel and Holtz, 2001; Mazzullo, 1997; Galloway et al., 1983; Montgomery, 1998; Comer, 1991). See text for detailed listing of sources. Calculated using PetroMod (Schulumbeger, 2012). Model parameters in Appendix 6. PS = Petroleum System.

Although no direct evidence exists to decipher whether migration occurred through faults, or unconformities, or through tortuous networks, the definition of traps by the Pennsylvanian vertical structures which traverse both the source rocks (Barnett, Woodford and Simpson) and their reservoirs may suggest involvement of faults in the migration process. Migration through faults is a documented process (e.g. Price, 1980; Sluijk and Nederlof, 1984; Karlsen et al. 2004).

4.4.4 The Simpson Petroleum System

The geographic extent of the Simpson petroleum system is depicted in Figure 4.28. Petroleum systems and process events chart for this system is summarized in Figure 4.29 and migration illustrated in Figure 4.30. Geochemical correlations (Chapters 2 and 3) indicate that oils from the Simpson shales are hosted in reservoirs segregated into two plays, Ellenberger karst-modified restricted ramp carbonate play and the Simpson cratonic sandstone plays where entrapment is mainly by simple and faulted anticlines (Galloway et al., 1983; Kerans, 1988; Dutton et al., 2004). The relationship between the source and reservoirs suggests vertical migration in a downward direction for this system.

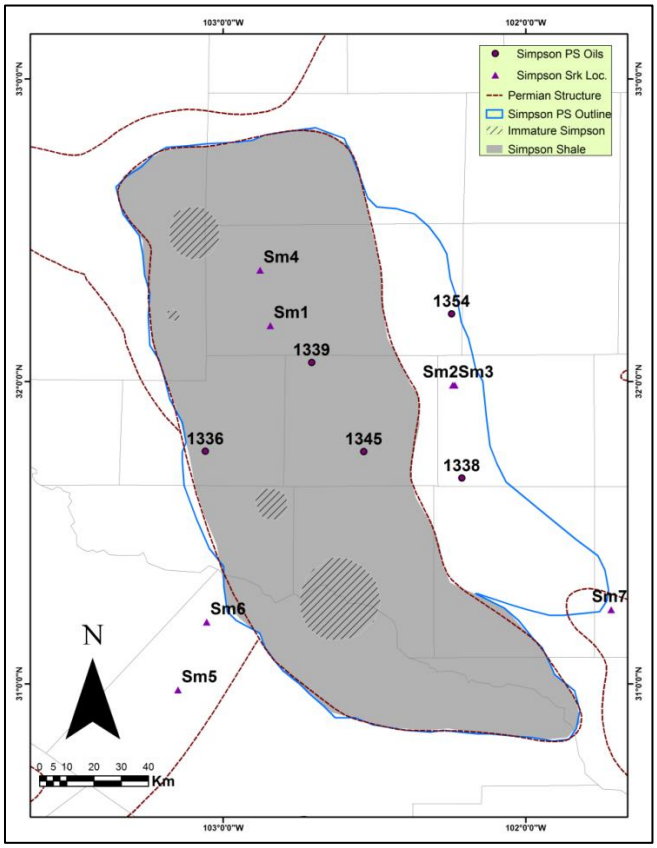

Figure 4.28: Geographic extent of the Simpson petroleum system in the Permian Basin. Migration from the Simpson took a downward direction against buoyancy to the underlying Ordovician Ellenberger and internally within the Simpson sandstones. Shaded area are places were top Simpson is immature.

Like in the Woodford, vertical faults could have provided feeder routes to traps in both the underlying Ellenberger and the intra-Simpson sandstones. However, direct contact between the source rocks and the reservoirs could be a major factor in the accumulations in this petroleum system. The hydrocarbon generation must have caused overpressure to overcome buoyancy and therefore allow for downward migration.

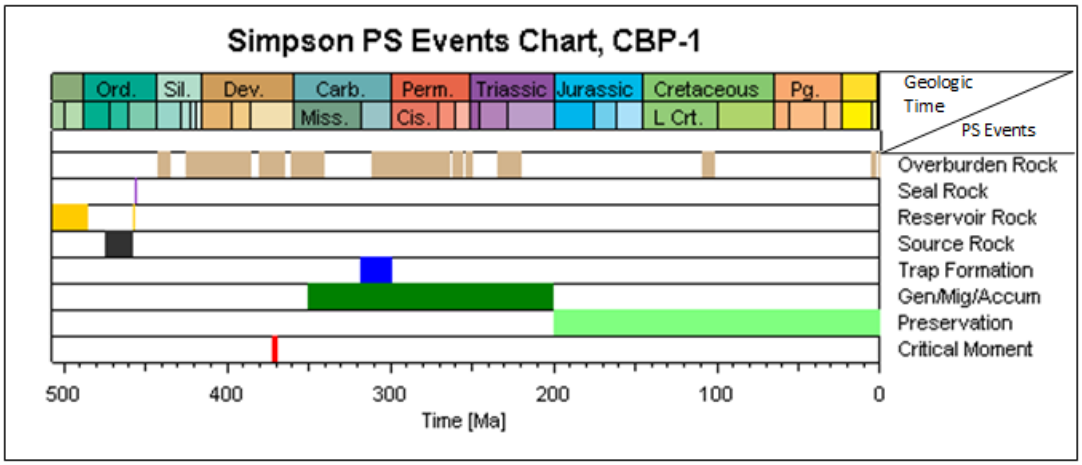

Figure 4.29: Events chart for the Simpson petroleum system in the Central Basin Platform of the Permian Basin. Timing of expulsion relative to trap formation not a constraint in the Simpson petroleum system. Reservoirs, traps and seals from several sources (Galloway et al., 1983; Kerans, 1988; Dutton et al., 2004). See text for detailed listing of sources. Calculated using PetroMod (Schulumbeger, 2012). Model parameters in Appendix 4. 1. PS = Petroleum System.

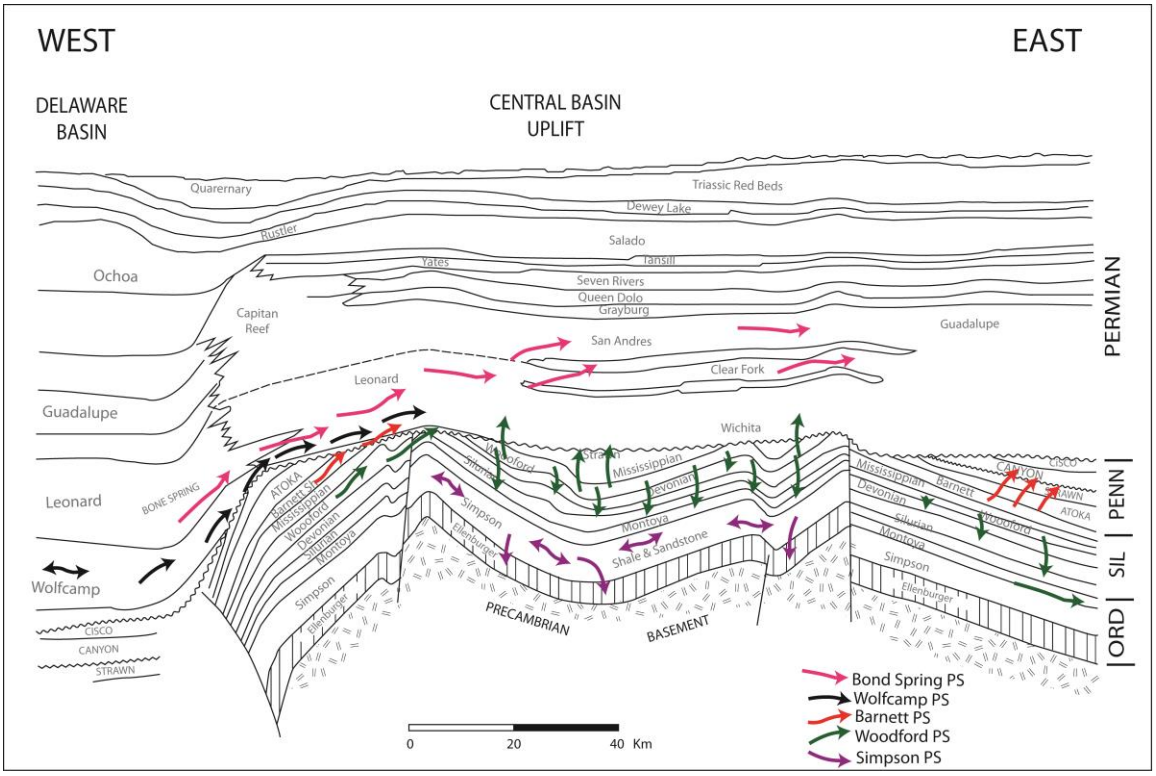

Figure 4.30: A model illustrating generation, expulsion and migration from the five major source rocks/petroleum systems investigated. Cross-section from Shumaker (1992). The Bone Spring petroleum system is inferred. Note how the Central Basin Platform is a potential mixing chamber for all oils from all the source rocks. The absence of potential sealing rocks above the Central Basin Platform until Ochoan (Salado, Rustler and Dewey) could imply mixed oils from all the source rocks except Simpson, in the Upper Permian reservoirs of the Grayburg, Queen, Seven Rivers and Tansill. Apart from the Central Basin Platform where oils show potential extensive vertical migration, in the Midland and possibly in the Delaware, because of extensive lateral seals, which also double as source rocks, the petroleum systems are in general stratigraphically segregated. This stratigraphic segregation is also interpreted to imply exceptional seal integrity in the Permian Basin.

4.5 Conclusions

Maturation, hydrocarbon generation, and expulsion modeling indicates that most of the source rocks suggested by geochemical correlations are adequately mature for hydrocarbon generation and therefore confirm petroleum systems. The petroleum systems involve the Simpson, the Woodford, the Barnett, and the Wolfcamp shales. The Spraberry source rock is thermally immature in most part and considered insignificant in the petroleum dynamics of the Permian Basin. Besides the fairly thick source strata as is

the case in the Wolfcamp, Simpson and to some extent the Barnett, kerogen type, organic richness, and maturity of source rocks were important factors in the development of the Permian Basin as a rich petroleum province. The high maturity and quality of the kerogen meant high expulsion and migration efficiencies for all these petroleum systems. In addition, stratigraphic segregation of petroleum systems illustrates the importance of seal integrity and relatively short migration distances for most of the petroleum systems in the basin. This also implies limited loses enroute the traps. The unusual downward migration as noted in the Woodford and Simpson petroleum systems is particularly worthy of note in this regard. Based on these two scenarios, it appears that downward hydrocarbon migration might be a more common phenomenon in geological systems than previously thought. Perhaps, the last and most important, timing of trap formation relative to petroleum generation for all petroleum systems was well synchronized, with former happening well in advance of the former.

4.6 References

Banerjee, A., A. K. Sinha, A.K. Jain, N. J. Thomas, K. N. Misra, and K. Chandra, 1998, A mathematical representation of Rock-Eval hydrogen Index vs. Tmax profile, Organic Geochemistry, v. 28, p. 43-55.

Banerjee, A., M. Jha, A.K., Mittal, N. J. Thomas, and K.N. Misra, 2000, Effective source rocks in the north Cambay Basin, India, Marine and Petroleum Geology, v. 17, p. 1111-1130.

Behar, F., M. Vandenbroucke, Y. Tang, and F. Marquis and J. Espitalie, 1997, Thermal cracking of kerogen in open and closed systems: determination of kinetic parameters and stoichiometric coefficients for oil and gas generation, Organic Geochemistry, v. 26, p. 321-339.

Blakely, R.C., 2008, Paleogeography and geologic evolution of North America, Department of Geology, Northern Arizona University, Web accessed 2nd Jan, 2013, http://www.geology.nau.edu/

Blackwell, D. D., and Richards, M., eds., 2004, Geothermal Map of North America: American Association of Petroleum Geologists, Tulsa, Oklahoma.

Comer, J. B., 1991, Stratigraphic analysis of the Upper Devonian Woodford Formation, Permian Basin, West Texas and Southeastern New Mexico, University of Texas, Austin, Bureau of Economic Geology, Report of Investigations No. 201, 63p.

Cooles, G. P., A. S., Mackenzie and T. M. Quingley, 1986, Calculation of petroleum masses generated and expelled from source rocks, Organic geochemistry, v. 10, p. 235-245.

Corby, J. J. and H. E. Cook, 2003, The Permian Basin petroleum systems, Simpson-Ellenberger and Woodford-San Andres-New Insights for exploring a mature petroleum province (abs), AAPG Annual Convention, Salt Lake City, Utah. May 11-14, 2003.

COSUNA 1983, Southwest/Southwest-Mid-continent Region: AAPG Correlation of Stratigraphic Units of North America Project, 1 Sheet.

Demaison, G., and B. J. Huizinga, 1991, Genetic classification of petroleum systems: AAPG Bulletin, v.75, p. 1626-1643.

Dickson, J. A. D. and Saller, A. H., 1995, Identification of subaerial exposure surfaces and porosity preservation in Pennsylvanian and lower Permian shelf limestones, eastern Central Basin Platform Texas, in Budd, D. A., Saller, A. H., and Harris, P. M., eds., Unconformities in Carbonate Shelf Strata—Their Recognition and the Significance of Associated Porosity: AAPG Memoir 57, p. 239–257.

Dow, W. G., 1977, Kerogen studies and geological interpretations: Journal of Geochemical Exploration, v. 7, p. 77-79.

Dow, W. G., S. C. Tulukdar, and L. Harmon, 1990, Exploration applications of geochemistry in the Midland basin, Texas (abs.), AAPG Bulletin, 74, 644-645.

du Rouchet, J., 1981, Stress fields, a key to oil migration, AAPG Bulletin, v. 65, p. 74-85.

Dutton, S. P., E. M. Kim, R. F. Broadhead, C. L. Breton, W. D. Raatz, S. C. Ruppel, and C. Kerans, 2004, Play analysis and digital portfolio of major oil reservoirs in the Permian basin: Application and transfer of advanced geological and engineering technologies for incremental production opportunities, University of Texas at Austin, Bureau of Economic Geology, Final Report prepared for the U.S. Department of Energy under contract DE-FC26-02NT15131, 408 p.

England, W. A., 1994. Secondary migration and accumulation of hydrocarbons, in L.B. Magoon and W.G. Dow, eds., The Petroleum System: From Source to Trap, AAPG Memoir 60, p. 211-217.

England, W. A., A. S. Mackenzie, D. M. Mann, and T. M. Quigley, 1987, The movement and entrapment of petroleum fluids in the subsurface: Journal of Geological Society, London, v. 144, p. 327-347.

Espitalie, J. and L. Joubert, 1987, Use of Tmax as a maturation index in petroleum exploration, in R.K. Kumar, P. Dwivedi, V. Banerjie and V. Gupta, eds., Proceedings of Meeting: First International Conference on Petroleum Geochemistry and Exploration in the Afro-Asian Region, Dehra Dun, India, November 25–27, 1985, , pp.67–73. Rotterdam, Netherlands.

ESRI, 2012, ArcMap Version 10.1, Environmental Systems Research Institute Inc., 380 New York Street, Redlands, CA 92373-8100.

Frenzel, H. N., R. R. Bloomer, R. B. Cline, J. M. Cys, J. E. Galley, W. R. Gibson, J. M. Hills, W. E. King, W. R. Seager, F. E. Kottlowski, S.Thompson III, G. C. Luff, B. T. Pearson, and D. C. Van Siclen, 1988, The Permian Basin Region, in L. L. Sloss, ed., Sedimentary Cover-North American Craton, US, Boulder, Colorado, Geological Society of America, The Geology of North America, v. D-2, p. 261-306.

Galley, J. E., 1958, Oil and geology in the Permian Basin of Texas and New Mexico, in Weeks, L. G., ed., Habitat of Oil: AAPG, Tulsa, p. 395-446.

Galloway, W. E., E. T. Ewing, C.M. Garrett, N. Tyler and D. G. Debout, 1983, Atlas of Major Texas Oil Reservoirs, Bureau of Economic Geology, The University of Texas at Austin, Texas, 139.

Guevara E. H. and Mukhopadhyay P. K. 1987. Source rock potential and oil source correlation, Permian (Leonardian) strata, central Spraberry trend, Midland basin, Texas-preliminary study (abs), AAPG Bulletin, v. 71, p. 561-562.

Hamlin, H. S., 2009, Ozona sandstone, Val Verde Basin, Texas: Synorogenic stratigraphy and depositional history in a Permian foredeep basin, AAPG Bulletin, v.93. p. 573-594.

Handford, C. R., 1981, Sedimentology and genetic stratigraphy of Dean and Spraberry Formations (Permian), Midland Basin, Texas, AAPG Bulletin, v. 65, p. 1602-1616.

Haq, B.U., J. Hardenbol and P. Vail, 1987, Chronology of fluctuating sea levels since the Triassic, Science, v. 235, p. 1156-1167.

Haq, B. U., and S. R. Schutter, 2008, A chronology of Paleozoic sea-level changes; Science, v. 322, p. 64-68.

Heckel, P. H., 1986, Sea-level curve for Pennsylvanian eustatic marine transgressive-regressive depositional cycles along the Midcontinent outcrop belt, North America, Geology, v. 14, p. 330–334.

Hindle, A. D, 1997, Petroleum Migration Pathways and Charge Concentration: A Three-Dimensional Model, AAPG Bulletin, v.81, p. 1451-1481.

Hunt, J. M., 1990, Generation and migration of petroleum from abnormally pressured fluid compartments: AAPG Bulletin, v. 74, p. 1-12.

Jarvie, D. M., B. L. Claxton, F. Henk, and J. T. Breyer, 2001, Oil and gas from the Barnett shale, Fort Worth Basin, Texas (abs.): AAPG Annual Meeting Abstracts, p. A100.

Jarvie, D. M. and R. J. Hill, 2011, Understanding unconventional resource potential by conventional petroleum systems assessment: AAPG Search and Discovery Article #40840. Web accessed 15th February 2013, http://www.searchanddiscovery.com/documents/2011/40840jarvie/ndx_jarvie.pdf.

Karlsen, D. A., J. E. Skeie, K. Backer-Owe, K. Bjorlykke, R. Olstad, K. Berge, M. Cecchi, E. Vik and R.G. Schaefer, 2004, Petroleum migration , faults and overpressure, Part II. Case history: The Haltenbanken petroleum province, offshore Norway, in Cubit, J. M., and W. A., England, eds. Understanding Petroleum Reservoirs: Towards an Integrated Reservoir and Geochemical Approach, Geological Society, London, Special Publications, v. 237, p. 305-372.

Katz, B. J., Dawson, W. C., Robinson, V. D., and Elrod, L.W. (1994). Simpson-Ellernberger(.) PS of the Central Basin Platform, West Texas, USA. In Magoon, L.B. and W. G. Dow (eds.). The Petroleum System: From Source to Trap, AAPG Memoir 60, p. 453-461.

Katz, B. J., R. N. Pheifer, D. J. Schunk, 1988, Interpretation of discontinuous vitrinite reflectance profiles, AAPG Bulletin, v. 72, p. 926-931.

Kerans, C., 1988, Karst-controlled reservoir heterogeneity in Ellenberger Group carbonates of West Texas: AAPG Bulletin, v. 72, p. 1160-1183.

Kinley, T. J., L. W. Cook, J. A. Breyer, D. M. Jarvie and A. B. Busbey, 2008, Hydrocarbon potential of the Barnett Shale (Mississippian), Delaware Basin, west Texas and southeastern New Mexico: AAPG Bulletin, v. 92, p. 967-991.

Littke, R., D. R. Barker, D. Leythaeuser, 1988, Microscopic and sedimentologic evidence for the generation and migration of hydrocarbons in Toarcian source rocks of different maturities, Organic Geochemistry, v. 13, p. 549-560.

Lorenz, J. C., J. L. Sterling, D.S. Scheicheter, C. L. Whigam and J. L. Jensen, 2002, Natural fractures in the Spraberry Formation, Midland Basin, Texas: The effects of mechanical stratigraphy on fracture variability and reservoir behavior, AAPG Bulletin, 86, p. 505-524.

Loucks, R. G., 1999, Paleocave carbonate reservoirs: origins, burial-depth modifications, spatial complexity, and reservoir implications: AAPG Bulletin, v. 83, p. 1795–1834.

Mackenzie, A. S. and T. M. Quigley, 1988, Principles of geochemical prospect appraisal, AAPG Bulletin, 72, p. 399-415.

Mann, U., T. Hantschel, R.G. Schaefer, B. Krooss, D. Leythaeser, R. Littke and R. F. Sachsenhofer, 1997, Petroleum migration: mechanisms, pathways, efficiencies and numerical simulations, in, D.H. Welte, B. Horsfield and D. R. Barker (eds.), Petroleum and Basin Evolution, Insights from Petroleum Geochemistry, Geology and Basin Modeling, Chapter 7, p 403-509.

Mazzullo, S. J., 1997, Stratigraphic exploration plays in Ordovician to Lower Permian strata in the Midland Basin and on the Eastern Shelf, in DeMis, W. D., ed., Permian Basin Oil and Gas Fields: Turning Ideas into Production: West Texas Geological Society, Publication No. 97-102, p. 1–37.

Mazzullo, S. J., 1998, Stratigraphic architecture of Lower Permian cyclic carbonate reservoirs (Chase Group) in the Mid-Continent, USA, based on outcrop studies, AAPG Bulletin, v. 82, p. 464-483.

Meissner, F. 1978, Petroleum geology of the Bakken Formation, Williston Basin, North Dakota and Montana, in. Williston Basin Proceedings 1978, Montana Geological Society, Billings, pp. 207-227.

Montgomery, S. L., 1998, Thirtyone Formation, Permian Basin, Texas: structural and lithologic heterogeneity in a Lower Devonian chert reservoir, AAPG Bulletin, v. 82, p. 1–24.

Pawlewicz, M. and H. Mitchell, 2006, 1-D Burial history modeling in the Permian Basin, in M. A. Raines, ed. , Resource Plays in the Permian Basin: Resource to Reserves, Fall Symposium, October 25 -27, 2006, West Texas Geological Society, Publication #06 -117, 87p.

Pawlewicz, M., C. E., Barker, S. McDonald, 2005, Vitrinite reflectance data for the Permian Basin, West Texas and Southeast New Mexico, USGS Open-File Report, 2005-1171

Peters, K. E. and Cassa, M. R., 1994, Applied source rock geochemistry, in Magoon, L. B. and Dow, W., G., eds., The Petroleum System: From Source to Trap, AAPG Memoir 60, p. 93-120.

Pratsch, J. C., 1983, Gasfields, NW German basin: secondary gas migration as a major geologic parameter, Journal of Petroleum Geology, v. 5, p. 229-244.

Price, L. C., 1980, Utilization and documentation of vertical oil migration in deep basins, Journal of Petroleum Geology, v. 2, p. 353-387.

Ruppel, S. C., and Barnaby, R. J., 2001, Contrasting styles of reservoir development in proximal and distal chert facies: Devonian Thirtyone Formation, Texas, AAPG Bulletin, v. 84, p. 7–34.

Ruppel, S. C., R. H. Jones, C. L. Breton, and J. A. Kane, 2005, Preparation of maps depicting the geothermal gradient and Precambrian structure in the Permian Basin, Contract report to the U.S. Geological Survey Order no. 04CRSA0834 and requisition no. 04CRPR01474.

Ruppel, S. C., and Hovorka, S. D., 1995, Controls on reservoir development in Devonian chert: Permian Basin, Texas, AAPG Bulletin, v. 79, p. 1757–1785.

Saller, A. H., Ball, B., Robertson, S., McPherson, B., Wene, C., Nims, R., and Gogas, J., 2001, Reservoir characteristics of Devonian cherts and their control on oil recovery: Dollarhide Field, west Texas, AAPG Bulletin, v. 85, p. 35–50.

Saller, A. H., Dickson, J. A. D., and Matsuda, F., 1999, Evolution and distribution of porosity associated with subaerial exposure in upper Paleozoic platform limestones, West Texas, AAPG Bulletin, v. 83, p. 1835–1854.

Saller, A. H., Van Horn, D., Miller, J. A., and Guy, B. T., 1991, Reservoir geology of Devonian carbonates and chert—implications for tertiary recovery, Dollarhide Field, Andrews County, Texas: AAPG Bulletin, v. 75, p. 86–107.

Salvador, A., 1985, chronostratigraphic and geochronometric scales in COSUNA stratigraphic correlation charts of the United States, AAPG Bulletin, v. 69, p. 181-189.

Schmoker, J. W., 1994, Volumetric calculations of hydrocarbons generated, in Magoon, L. B. and W. G. Dow, eds., The Petroleum System: From Source to Trap, AAPG Memoir 60, p. 323-326.

Schlumberger, 2002, Introduction to PetroMod® training and exercise guide, Schlumberger Aachen Technology Center, Ritterstraβe 23, 52072 Aachen, Germany.

Schlumberger, 2002, PetroMod (2012 release), Schlumberger Aachen Technology Center, Ritterstraβe 23, 52072 Aachen, Germany.

Shumaker, R. C., 1992, Paleozoic structure of the central basin uplift and adjacent Delaware basin, West Texas, AAPG Bulletin, v. 76, p. 1804-1824.

Silver, B. A., and Todd, R. G., 1969, Permian cyclic strata, northern Midland and Delaware Basins, west Texas and southeastern New Mexico, AAPG Bulletin, v. 53, p. 2223–2251.

Sluijk, D. and M. H. Nederlof, 1984, A worldwide geological experience as a systematic basis for prospect appraisal, in G. Demaison and J. R. Morris, eds., Petroleum Geochemistry and Basin Analysis: AAPG Memoir 35, p. 15-26.

Sweeney, J. J. and A. K. Burnham, 1990, Evaluation of a simple model of vitrinite reflectance based on chemical kinetics, AAPG Bulletin, v. 74, p. 1559-1570.

Tissot, B.P., R. Pelet, and P. Ungerer, 1987, Thermal history of sedimentary basins, maturation indices, and kinetics of oil and gas generation, AAPG Bulletin, v. 71, p. 1445-1466.

Tissot, B. P., and D. H. Welte, 1984, Petroleum Formation and Occurrence: Springer-Verlag, New York, 699p.

Tyler, N., and Banta, N. J., 1989, Oil and gas resources remaining in the Permian Basin: targets for additional hydrocarbon recovery: The University of Texas at Austin, Bureau of Economic Geology, Geological Circular 89-4, 20 p.

USGS, 2012, United States Geological Survey (USGS), Permian Basin Geospatial data http://energy.usgs.gov/OilGas/AssessmentsData/NationalOilGasAssessment/USBasinSummaries.aspx?theTab=dataTab&provcode=5044, web accessed in January, 02, 2012.

Waples, D. W., 1985, Geochemistry in Petroleum Exploration: Boston, Mass., International Human Resources Development Corporation, 585 Boylston St, Boston, MA 02116,

232p.

Welte, D. H., B. Horsfield and D. R. Barker eds, 1997, Petroleum and Basin evolution: New York, Springer-Verlag, 535p.

Wright, W. F., 1979, Petroleum geology of the Permian Basin: West Texas Geological Society Publication 79-71, 98p.

Wygrala, B. P. 1989, An integrated study of an oil field in the southern Po Basin, Northern Italy. PhD Thesis, University of Cologne, Germany.

5.0 GENERAL CONCLUSIONS

Using geochemical inversion, chemometric analysis of oils, and source rocks and thermal maturity analysis/modeling in the Permian Basin, it is demonstrated that five petroleum systems exist between Ordovician and Leonardian in the Permian Basin. The petroleum systems involve the organic-rich, type II to II/III shales of the Simpson, Woodford, Barnett, Wolfcamp, and a marl, inferred to be of Bone Spring. Of significance is the geological segregation of petroleum systems, with very limited cross-stratigraphic migration due to the presence of pervasive seals, which also double as source rocks between reservoirs. The five petroleum systems can conveniently be divided into two broad categories, that is, the pre-Pennsylvanian and the post-Pennsylvanian. Entrapment in the Pre-Pennsylvanian systems is dominantly structural and migration is vertical, both up and downwards against buoyancy. Oils in these petroleum systems are highly thermally mature, and are enhanced by in-reservoir maturation due to downward migration (Woodford and Simpson). Post-Pennsylvanian petroleum systems are relatively low in maturity, and migration and entrapment is lateral and largely stratigraphic.

The key aspects of the Permian Basin petroleum systems studied include good to excellent organic richness, high-quality kerogen, and adequate thermal maturity (large pods of active source rocks). These factors played important roles in making large volumes of oil available for expulsion and migration to reservoirs. The segregation of petroleum systems, especially the areas of the Midland and Delaware Basins occasioned by pervasive seals/source rocks implies short distance migration with minimum migration loses and by inference excellent seal integrity, keeping the oils trapped for long periods

of time. Timing of petroleum generation and expulsion relative to trap formation for all the petroleum systems was such that traps formed well in advance of generation/expulsion, ensuring a perfect accumulation of most of the generated hydrocarbons.

The oils of the Simpson petroleum system, sourced from the Simpson shales, migrated downwards and are reservoired in the Simpson sandstones and Ellenberger carbonates in the Central Basin Platform and in the western margins of the Midland Basin. Thermal and generation modeling indicates adequate thermal maturity, beyond the oil window for most of the Simpson shales in the Central Basin Platform and that generation begun during the Triassic, after traps had long formed. Adequate organic richness, good to excellent quality source rock character and the well packaged petroleum systems elements that provided high seal integrity and allowed for short distance migration are key features of this petroleum system. There is currently no active generation from a large portion of the Simpson in the Central Basin Platform. Depending on the physical attributes of the shales, unconventional gas may be recoverable from this source rock. The Simpson petroleum system is geographically located within the Central Basin Platform and stratigraphically covers the Simpson Group cratonic sandstones (reservoirs) and shale, and the underlying karst-modified dolomite of the Ellenberger (reservoir). Generation and expulsion from the Simpson source rock is up to 1.2 Bbbl. Most of the Simpson in the Central Basin Platform is within late oil-window to condensate zone.

Oils from the Woodford Shale migrated and are reservoired in a large stratigraphic extent ranging from Ordovician to Pennsylvanian, with a possibility of oils being in the Permian

reservoirs as well, especially over the Central Basin Platform. The Woodford petroleum system is geographically distributed throughout the Permian Basin. Excellent organic richness, excellent kerogen quality and adequate thermal maturity through most of the Woodford Shale, are the key features of the Woodford source rock that spell extreme expulsion and migration efficiencies for this petroleum system. In addition, downward migration, occasioned by the well-packaged petroleum system elements that allowed for short distance migration, largely occasioned by the high integrity of the overlying seals/source rock. Generation and expulsion, which occurred in Early-Mid Permian in most parts, occurred after traps had long formed during the Pennsylvanian. The Woodford in the Delaware Basin is coked, and there is no exploration significance. In the Central Basin Platform and Midland Basin however, there is active hydrocarbon generation, with some patched thermally immature zones. This will still provide adequate conventional oils to reservoirs. Within the study area, the Woodford shale has generated and expelled 13.3 Bbbl, which is far beyond the STOOIP of the entire Permian.

The Barnett petroleum system oils are reservoired mainly in the Pennsylvanian and Permian strata in the Central Basin Platform, demonstrating true buoyancy unlike its pre-Pennsylvanian counterparts where migration took a downward direction against buoyancy. Despite the poor constraint due to a limited number of samples, excellent organic richness, excellent kerogen quality and adequate thermal maturity are attributes of the Barnett shale source rock. With a large portion of the shale at adequate maturity beyond the oil window, and generation and expulsion occurring during Mid-Permian to Late Permian, most of the hydrocarbons from this source rock must have been trapped as

traps had long formed by this time. The Barnett shale is coked in the Delaware Basin, and therefore has no exploration significance. In the Central Basin Platform and Midland Basin however, there is active hydrocarbon generation, with thermally immature zones. This will still provide adequate conventional oil to reservoirs. To date, it has generated and expelled up to 80.9 Bbbl of bulk petroleum.

The Wolfcamp (Early Permian) shale generated oils are reservoired within the Wolfcampian, mainly in carbonate aprons encased in the Wolfcamp shale in slope and basin areas and in adjoining Wolfcampian carbonates in the shelf regions. In essence, the source, the reservoir, migration route and the seal are all Wolfcampian, a juxtaposition, which, without doubt, implies shorter migration distances. The Wolfcampian is adequately thermally mature in the Delaware Basin and the southern Midland Basin. Although not overly organic-rich as the superior Woodford, its thickness, together with the source-reservoir juxtaposition makes it one of the most important petroleum systems in the Permian Basin. The Wolfcamp in the Delaware Basin is between the floor of liquid hydrocarbon generation and the dry gas zone, indicating significant unconventional potential in the form of shale gas if other physical parameters allow. In most of the Midland Basin, the Wolfcamp is actually immature to early mature, especially in the northern portions. This will provide the adjoining reservoirs with adequate hydrocarbons for a long time to come. Generation and expulsion from this system begun during Late Permian to Triassic and is still actively generating throughout the Permian Basin. Todate, up to 73.9 Bbbl has been generated and expelled by this source rock.

The Spraberry source rock is at incipient stages of hydrocarbon generation in the south, with most of it actually still immature with respect to petroleum generation. Volumetrically, this is the least important petroleum systems among the petroleum systems studied.

The oils inferred to be from the Bone Spring marl source rock are located mainly in Central Basin Platform and Midland Basin, and denote lateral migration albeit with vertical component due to the incline associated with the major structural make-up of the Delaware Basin relative to the Central Basin Platform and Midland Basins. The source rock of this petroleum is inferred to have been deposited under extremely reducing or anoxic conditions and could imply adequate organic richness and kerogen quality. The maturity is however; low, just about the mid-oil window, approximately 1%R_o. Therefore, much of the generation potential hasn't been realized, consequently only limited oil has charged reservoirs.

As revealed by this study, the source rocks are highly variable in organofacies, and the oils are extremely mature. Characterization and especially correlation of such oils with source rocks using biomarker data alone is extremely challenging. It is recommended that adequate approaches compatible with high thermal maturity be sought to adequately evaluate oils.

Adequate source rock characterization (source rock screening) of individual source rocks throughout the basin is recommended, especially the Wolfcamp, Barnett, and Simpson (especially in areas outside the Central Basin Platform). A need to sample immature

source rocks wherever possible. Wherever possible, sampling should be as close as possible to circumvent the highly varied organofacies.

APPENDICES

Appendix 1: Petroleum systems play combinations based on similar genetic geochemical characteristics. Play definitions from Dutton et al. (2004; 2005)

Petroleum System I (Group I)

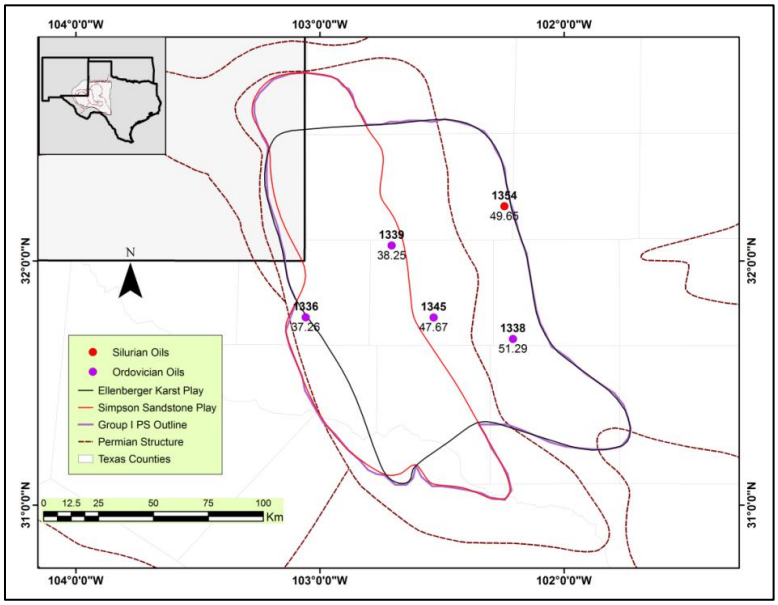

Petroleum System II/III (Group II/III)

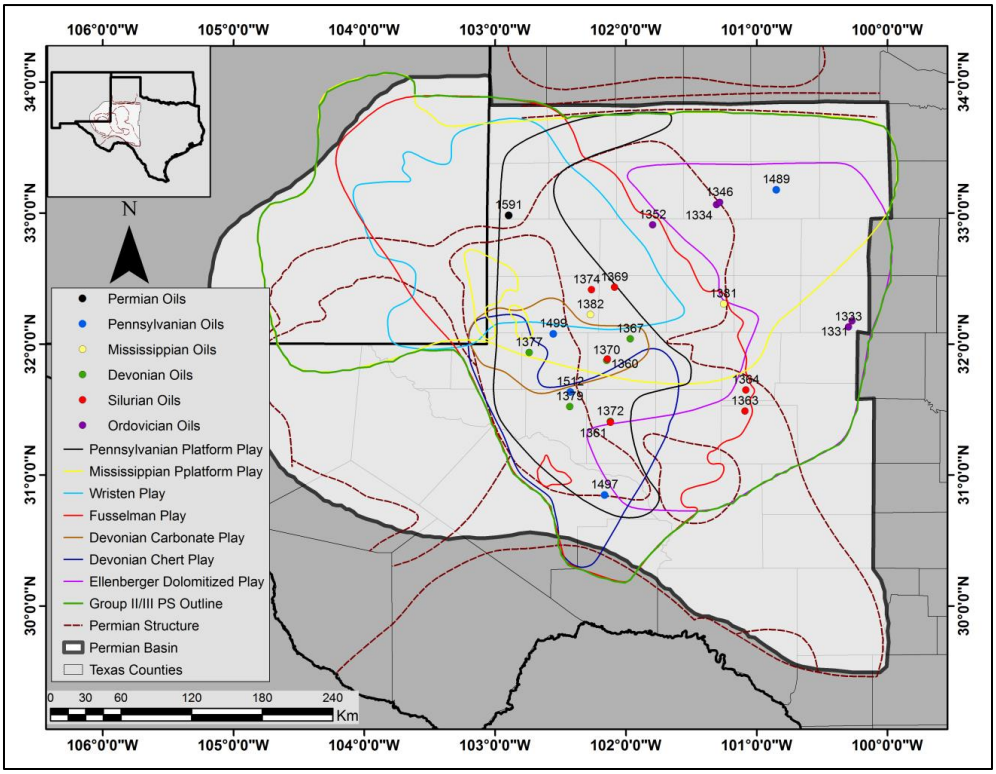

Petroleum System IV (Group IV)

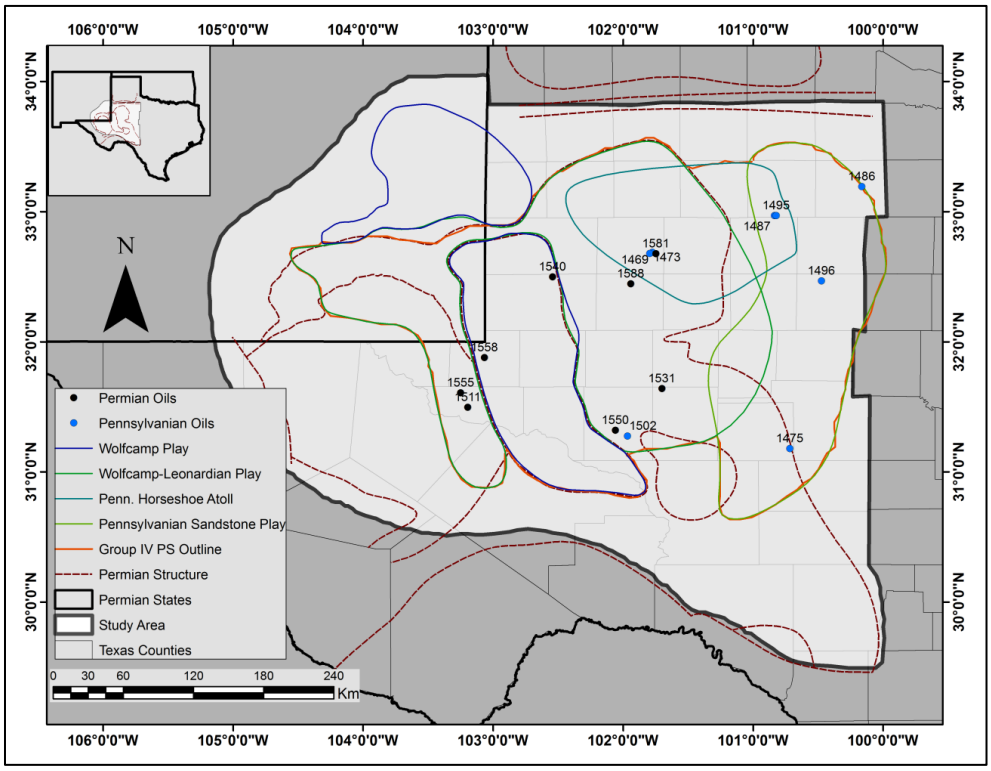

Petroleum System IV (Group IV)

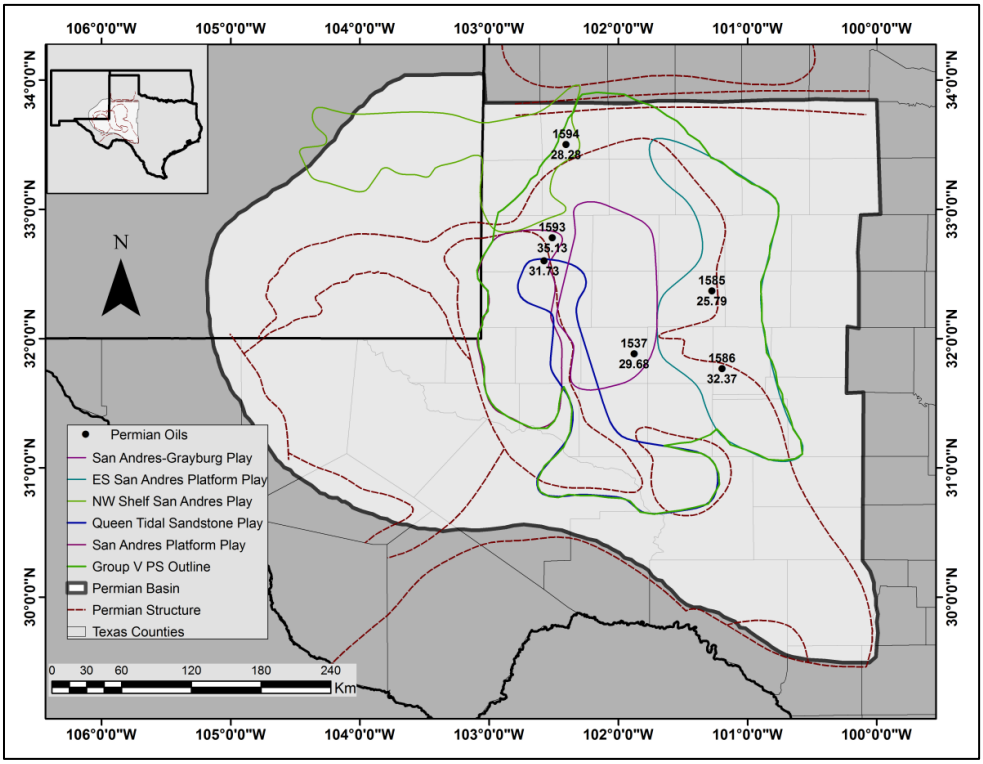

Appendix 2: Oil sample identification and locations

Sample Id.	Reservoir Age	Top Depth(ft)	Well Name	Api Number	Latitude	Longitude	County
1336	Ordovician		SM Halley #165	42-495-	31.76881	-103.05913	Winkler
1338	Ordovician	13200	Midland R Fee	42-329-	31.68022	-102.21075	Midland
1339	Ordovician		JE Cowden #8	42-135-	32.0624	-102.7074	Ector
1345	Ordovician		Ector Fee Unit #4	42-135-	31.76799	-102.53526	Ector
1354	Ordovician	12800	Mabee A NCT-1	42-003-	32.22315	-102.24524	Andrews
1334	Ordovician	8100	Kirkpatrick #1	42-169-	33.06418	-101.30804	Garza
1346	Ordovician	8110	Stoker K 939 Dp	42-169-	33.0804	-101.2849	Garza
1331	Ordovician	5835	B Hanks #20	42-353-	32.17547	-100.27128	Nolan
1333	Ordovician	6305	CM Whitaker #5	42-353-	32.12956	-100.29835	Nolan
1352	Ordovician	10381	CL Rodgers #1	42-115-	32.90987	-101.79684	Dawson
1360	Silurian	12450	Scharbauer	42-329-	31.88492	-102.14201	Midland
1361	Silurian	11650	J H Graf #1	42-461-	31.40209	-102.11819	Upton
1363	Silurian	8664	McGill AB	42-235-	31.48724	-101.09019	Irion
1364	Silurian	8651	Foster, Ethyl #2	42-431-	31.64864	-101.0829	Sterling
1369	Silurian	12237	State of Tx AH	42-317-	32.41983	-102.20066	Martin
1374	Silurian	12510	State of Tx AE	42-003-	32.3973	-102.38092	Andrews
1367	Devonian	11600	RJ Sandefur #1	42-329-	32.03836	-101.96799	Midland
1370	Devonian	11850	Bryant G Unit #7	42-329-	31.87507	-102.1475	Midland
1372	Devonian	11200	JH Graf NCT-1	42-461-	31.40914	-102.12051	Upton
1377	Devonian		Thomas A NCT-	42-135-	31.93423	-102.74127	Ector
1379	Devonian		State of Tx DV	42-103-	31.52215	-102.43104	Crane
1381	Mississippian	8640	Howard F Fee #3	42-227-	32.30667	-101.25321	Howard
1382	Mississippian	11200	Mabee A NCT1	42-003-	32.22474	-102.27292	Andrews
1469	Pennsylvanian	8195	LB Vaughn #1	42-115-	32.68609	-101.77578	Dawson
1473	Pennsylvanian	8080	MJ Peterson #2	42-115-	32.67784	-101.79664	Dawson
1475	Pennsylvanian	6327	JM	42-235-	31.17952	-100.71849	Irion
1486	Pennsylvanian	4795	TA Upshaw A	42-433-	33.1918	-100.16457	Stonewa
1487	Pennsylvanian	6790	Fuller NCT1	42-263-	32.96996	-100.83641	Kent
1495	Pennsylvanian	6900	Fuller NCT3	42-263-	32.96922	-100.8228	Kent
1496	Pennsylvanian	6250	Rowan & Hope	42-353-	32.468	-100.47564	Nolan
1499	Pennsylvanian	8936	Holt OB TB 1	42-135-	32.07693	-102.55539	Andrews
1502	Pennsylvanian	9999	Christy JD #1	42-461-	31.27425	-101.96692	Upton
1489	Pennsylvanian	6630	Atkins Unit #1	42-263-	33.17689	-100.85033	Kent
1497	Pennsylvanian	7759	Zimmerman AB	42-371-	30.84701	-102.16349	Pecos
1512	Pennsylvanian	9012	Crane Fee H #1	42-103-	31.63282	-102.42612	Crane
1511	Permian	6151	Avary GQ #2	42-475-	31.49647	-103.19581	Ward
1531	Permian	8126	Wilde EG #7	42-383-	31.63935	-101.70249	Reagan
1550	Permian	9522	Mann AT #1	42-461-	31.32013	-102.0599	Upton
1555	Permian	11227	Univ. 11-18-A #2	42-475-	31.60731	-103.25141	Ward
1540	Permian	9010	Westbrook oil	42-003-	32.49775	-102.54375	Andrews
1558	Permian	5112	Seth Campbell	42-495-	31.87724	-103.06803	Winkler
1581	Permian	7033	CW Shafer #12	42-115-	32.67633	-101.74802	Dawson
1591	Permian	8274	Annie Miller A	42-501-	32.9808	-102.8974	Yoakum
1588	Permian	7953	Slaughter Elma	42-317-	32.44563	-101.94288	Martin
1537	Permian	5951	Robertson JB #67	42-165-	32.58213	-102.70617	Gaines
1585	Permian	4555	Read HN F #1	42-227-	32.36872	-101.27766	Horward
1586	Permian	5052	Sterling E Fee #4	42-431-	31.76687	-101.19854	Sterling
1593	Permian	5540	GMK Unit #702	42-165-	32.7785013	-102.5126305	Gaines
1538	Permian	9219	Foster T NCT-2	42-165-	32.60027	-102.57544	Gaines
1594	Permian	7178	Pace CT #2	42-219-	33.49998	-102.40679	Hockley

Appendix 3: Location of wells from which source rock samples were recovered. Sample Id represents composite samples of one source rock from a given well as detailed in Appendices 4.3 and 4.4.

Id	Source Rock	Well Name	County	Api	Longitude	Latitude
Sp1	**Spraberry**	Proctor #1	Reagan		-101.66758	31.5135
Sp2		Bedwell, R.T JR #1	Dawson	4211530575	-102.03127	32.7389
Sp3		Dean Ranch #1-A	Dawson	4211530450	-101.76363	32.7795
WF1	**Wolfcamp**	Robinson, Walter #1	Howard	4222732622	-101.38191	32.2778
WF2		Thompson Thad Estate #1	Scheileche	4241300837	-100.72200	30.8903
WF3		Hughes#1-E	Reagan		-101.54500	31.4604
WF4		Fasken David #1	Andrews	4200332474	-102.26188	32.1214
WF5		Means, J.S #1-E	Andrews	4200335611	-102.52027	32.3847
WF6		McDowell Estate #1	Borden		-102.16798	33.3594
WF7		Garupa #1	Pecos	4237131816	-103.01081	31.0474
B2	**Barnett**	Burleson #1	Gaines		-102.47200	32.6839
B3		Midland Farms #1	Midland		-101.94700	31.6839
B5		Elwood, W.L. Estate #1	Mitchell		-102.11500	32.4220
W1	**Woodford**	Walker Paul #1	Cochran	4207910254	-102.82100	33.5168
W2		Porter #1	Borden		-101.60300	32.8301
W3		Butler L.L #2	Andrews		-101.29200	32.6034
W4		Good Clara E #1	Borden	4203310054	-102.62700	32.2535
W5		Scharbauer C. NCT-1 #7-B	Midland		-102.05000	31.8000
W6		Federal Elliot #1	Lea	3002501885	-103.26800	32.6293
Sm1	**Simpson**	University #1	Andrews		-102.84400	32.1844
Sm2		Fasken, Inez #1	Midland		-102.24100	31.9879
Sm3		Fasken, Inez #1	Midland		-102.24100	31.9879
Sm4		Mccrea, Celia A #1	Andrews		-102.87800	32.3675
Sm5		Canon C.C #17	Pecos		-103.14900	30.9802
Sm6		Moore Wayne #6	Pecos		-103.05400	31.2042
Sm7		Trigg Mary #1	Reagan		-101.71700	31.2449

Appendix 4: Listing of all source rock samples showing the composite sample combinations

Lab. Id	Composite Id	County	Well Name	Long-itude	Lati-tude	Api	Depth (ft)
Sp1	**Sp1**	Reagan	Proctor #1	-101.6676	31.5136		7,705
Sp2	**Sp2**	Dawson	Bedwell, R.T JR #1	-102.0313	32.7389	4211530575	7,950
Sp3	**Sp3**	Dawson	Dean Ranch #1-A	-101.7636	32.7796	4211530450	7,550.5
Wf1	**WF1**	Howard	Robinson, Walter #1	-101.3819	32.2779	4222732622	7,531
Wf2		Howard	Robinson, Walter #1				7,587
Wf3	**WF2**	Scheilecher	Thompson Thad Estate #1	-100.7220	30.8903	4241300837	6,215
Wf4		Scheilecher	Thompson Thad Estate #1				6,235
Wf5	**WF3**	Reagan	Hughes#1-E	-101.5450	31.4604		7,704
Wf6		Reagan	Hughes#1-E				7,822
Wf7		Reagan	Hughes#1-E				7,870
Wf8		Reagan	Hughes#1-E				7,899
Wf9	**WF4**	Andrews	Fasken David #1	-102.2619	32.1214	4200332474	10,900
Wf10		Andrews	Fasken David #1				11,042
Wf11		Andrews	Fasken David #1				11,092
Wfc1	**WF5**	Andrews	Means, J.S #1-E	-102.5203	32.3847	4200335611	8,000-8,010
Wfc2		Andrews	Means, J.S #1-E				8,090-8,130
Wfc3		Andrews	Means, J.S #1-E				8,150-8,190
Wfc4		Andrews	Means, J.S #1-E				8,210-8,220
Wfc5		Andrews	Means, J.S #1-E				8,450-8,460
Wfc6	**WF6**	Borden	McDowell Estate #1	-102.1680	33.3595		4,500-4,710
Wfc7		Borden	McDowell Estate #1				4,810-5,010
Wfc8		Borden	McDowell Estate #1				5,600-5,610
Wfc9		Borden	McDowell Estate #1				6,000-6,010
Wfc10		Borden	McDowell Estate #1				6,500-6,510
WF7A	**WF7**	Pecos	Garupa #1	-103.0108	31.0475	4237131816	11,623
WF7B		Pecos	Garupa #1				11639
WF7C		Pecos	Garupa #1				11,654
B5A	**B2**	Gaines	Burleson #1	-102.4720	32.6839		8,425
B5B		Gaines	Burleson #1				11,057
B5C		Gaines	Burleson #1				11,057

Bc8	**B3**	Midland	Midland Farms #1	-101.9470	31.6839		6,610-6,620
Bc9		Midland	Midland Farms #1				6,390-6,400
Bc10		Midland	Midland Farms #1				6,790-6,800
Bc11		Midland	Midland Farms #1				6,900-7,035
Bc12		Midland	Midland Farms #1				7,120-7,125
Bc3	**B5**	Mitchell	Elwood, W.L. Estate #1	-102.1150	32.4220		4,810-4,820
Bc4		Mitchell	Elwood, W.L. Estate #1				5,030-5,040
Bc5		Mitchell	Elwood, W.L. Estate #1				5,220-5,230
Bc6		Mitchell	Elwood, W.L. Estate #1				5,570-5,730
Bc7		Mitchell	Elwood, W.L. Estate #1				5,860-5,870
w1		Cochran	Walker Paul #1	-102.8210	33.5168	4207910254	11,609
w2			Walker Paul #1				11,631
w3	**W1**		Walker Paul #1				11,639
w4			Walker Paul #1				11,674
w5			Walker Paul #1				11,685
w6	**W2**	Borden	Porter #1	-101.603	32.8301		9,793
w7			Porter #1				9,800
w8			Porter #1				9,820
Wc1		Andrews	Butler L.L #2	-101.2920	32.6034		12,250-12260
Wc2	**W3**		Butler L.L #2				12,335-12340
Wc3		Andrews	Butler L.L #2				12,400-12405
Wc4			Butler L.L #2				12,465-12470
Wc5	**W4**		Good Clara E #1	-102.6270	32.2535	4203310054	5,400-5410
Wc6			Good Clara E #1				5,500-5510
Wc7			Good Clara E #1				5,600-5610
Wc8		Borden	Good Clara E #1				5,700-5710
Wc9			Good Clara E #1				5,800-5810
Wc10			Good Clara E #1				5,900-5910
Wc11	**W5**		Scharbauer C. NCT-1 #7-B	-102.0500	31.8000		11,600-11610
Wc12			Scharbauer C. NCT-1 #7-B				11,700-11710
Wc13		Midland	Scharbauer C. NCT-1 #7-B				11,900-11910
Wc14			Scharbauer C. NCT-1 #7-B				12,000-12010
Wc15			Scharbauer C. NCT-1 #7-B				12,400-12410
Wc16			Scharbauer C. NCT-1 #7-B				12,900-12910
W6A	**W6**		Federal Elliot #1	-103.2680	32.6293	3002501885	14,613
W6B		Lea	Federal Elliot #1				14,631

W6C			Federal Elliot #1			14,632
Sc7	**Sm1**	Andrews	University #1	-102.8440	32.1844	12380-12500 (Sh.)
Sc8						12380-12500 (Carb.)
Sc9						12620-12630
Sc10						12740-12750
Sc11						12980-12990
Sc12						13000-13010
Sc13		Midland	Fasken, Inez #1	-102.2410	31.9879	12460-12470
Sc14	**Sm2**					12260-12270 (Sh)
Sc15						12260-12270 (Carb.)
Sc16						12320-12330 (Sh)
Sc17						12320-12330 (Carb.)
Sc18						12360-12370 (Sh.)
Sc19						12360-12370 (Carbonate)
Sc20	**Sm3**					12580-12590 (Sh)
Sc21						12580-12590 (Carb.)
Sc22						12690-12700 (Sh.)
Sc23						12690-12700 (Carb.)
Sc24						12810-12820
Sc25						12930-12940
Sc2	**Sm4**	Andrews	Mccrea, Celia A #1	-102.8780	32.3675	9,920-9,925
Sc3						10,040-10,125
Sc4						10,225-10,310
Sc5						10,380-10,385
Sc6						10,456-10,457
S5A	**Sm5**	Pecos	Canon C.C #17	-103.1490	30.9802	8,480
S5B						8,498
S5C						8,503
s1	**Sm6**	Pecos	Moore Wayne #6	-103.054	31.2042	16,865
s2						16,897
s3						16,906
s4						16,910
s5						16,920
s6						13,840-13,890

S4A	**Sm7**	Reagan	Trigg Mary #1	-101.7170	31.2449	10,253
S4B						10,256
S4C						10,259
S4D						10,261

Sh. = Shale; Carb. Carbonate. All carbonate samples from the Simpson had less than 1% total organic carbon content, therefore not part of the composite.

Appendix 5: Interpreted geochemical logs showing composite samples

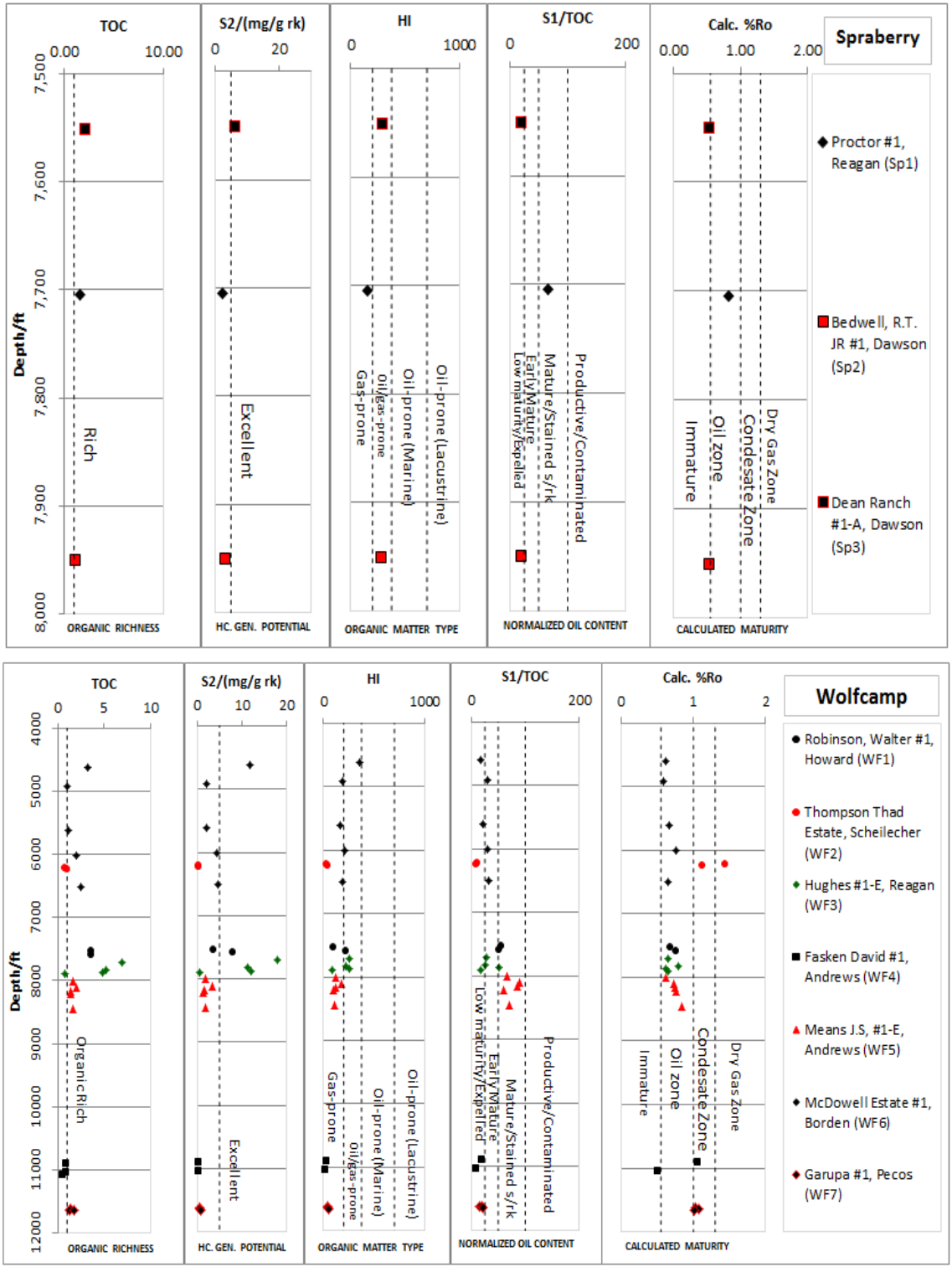

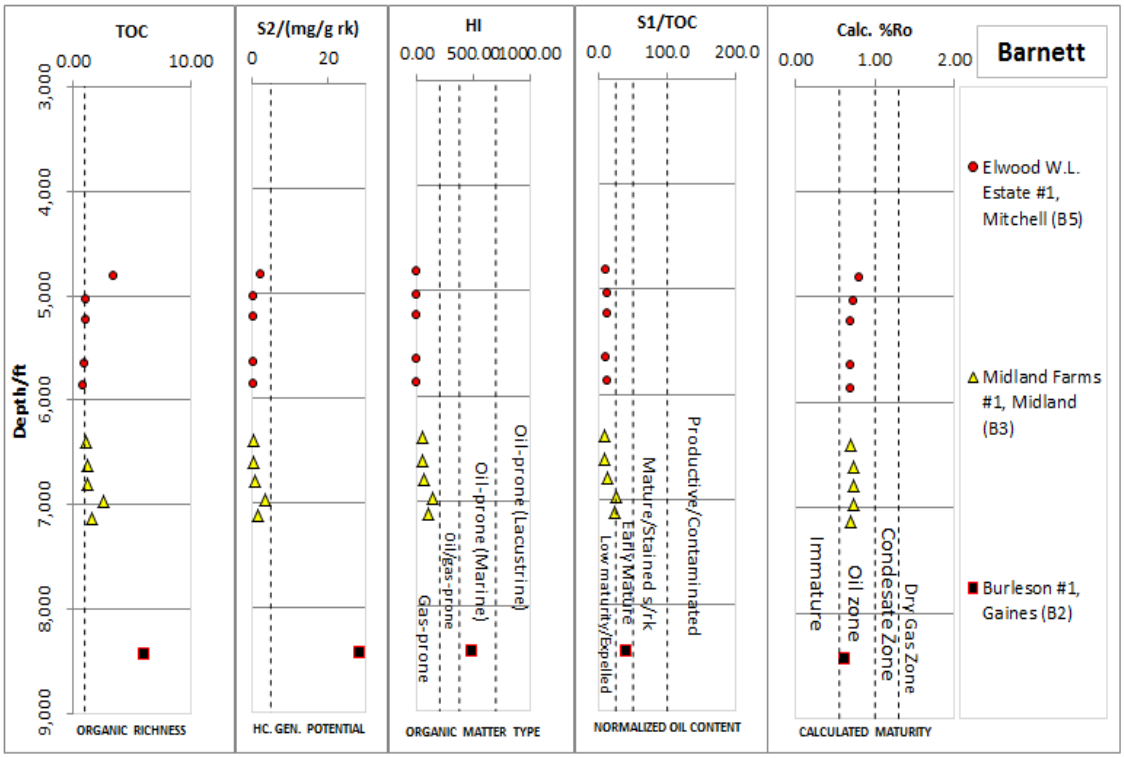
Barnett
TOC
0.00
10.00
S2/(mg/g rk)
0
20
HI
0.00
500.00
1000.00
S1/TOC
0.0
100.0
200.0
Calc. %Ro
0.00
1.00
2.00
Depth/ft
3,000
4,000
5,000
6,000
7,000
8,000
9,000
Oil-prone (Lacustrine)
Oil-prone (Marine)
Oil/gas-prone
Gas-prone
Productive/Contaminated
Mature/Stained s/rk
Early Mature
Low maturity/Expelled
Immature
Oil zone
Condesate Zone
Dry Gas Zone
ORGANIC RICHNESS
HC. GEN. POTENTIAL
ORGANIC MATTER TYPE
NORMALIZED OIL CONTENT
CALCULATED MATURITY
Elwood W.L. Estate #1, Mitchell (B5)
Midland Farms #1, Midland (B3)
Burleson #1, Gaines (B2)

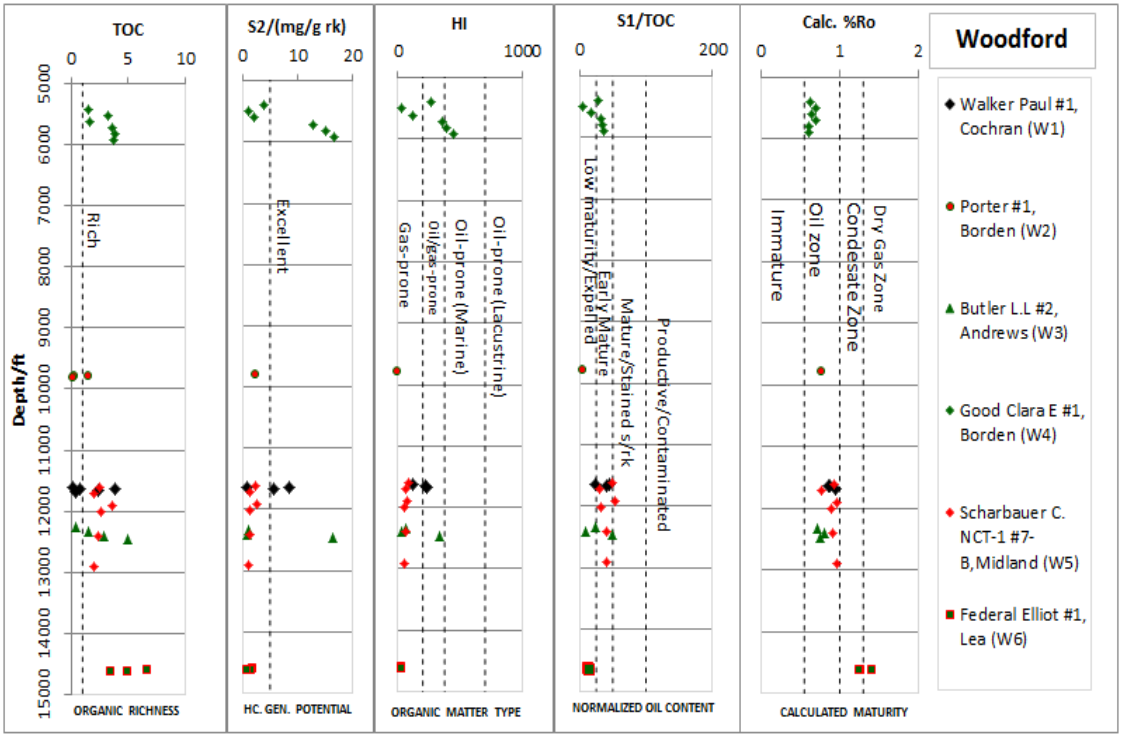
Woodford
TOC
0
5
10
S2/(mg/g rk)
0
10
20
HI
0
1000
S1/TOC
0
200
Calc. %Ro
0
1
2
Depth/ft
5000
6000
7000
8000
9000
10000
11000
12000
13000
14000
15000
Rich
Excellent
Oil-prone (Lacustrine)
Oil-prone (Marine)
Oil/gas-prone
Gas-prone
Productive/Contaminated
Mature/Stained s/rk
Early Mature
Low maturity/Expelled
Immature
Oil zone
Condesate Zone
Dry Gas Zone
ORGANIC RICHNESS
HC. GEN. POTENTIAL
ORGANIC MATTER TYPE
NORMALIZED OIL CONTENT
CALCULATED MATURITY
Walker Paul #1, Cochran (W1)
Porter #1, Borden (W2)
Butler L.L #2, Andrews (W3)
Good Clara E #1, Borden (W4)
Scharbauer C. NCT-1 #7-B,Midland (W5)
Federal Elliot #1, Lea (W6)

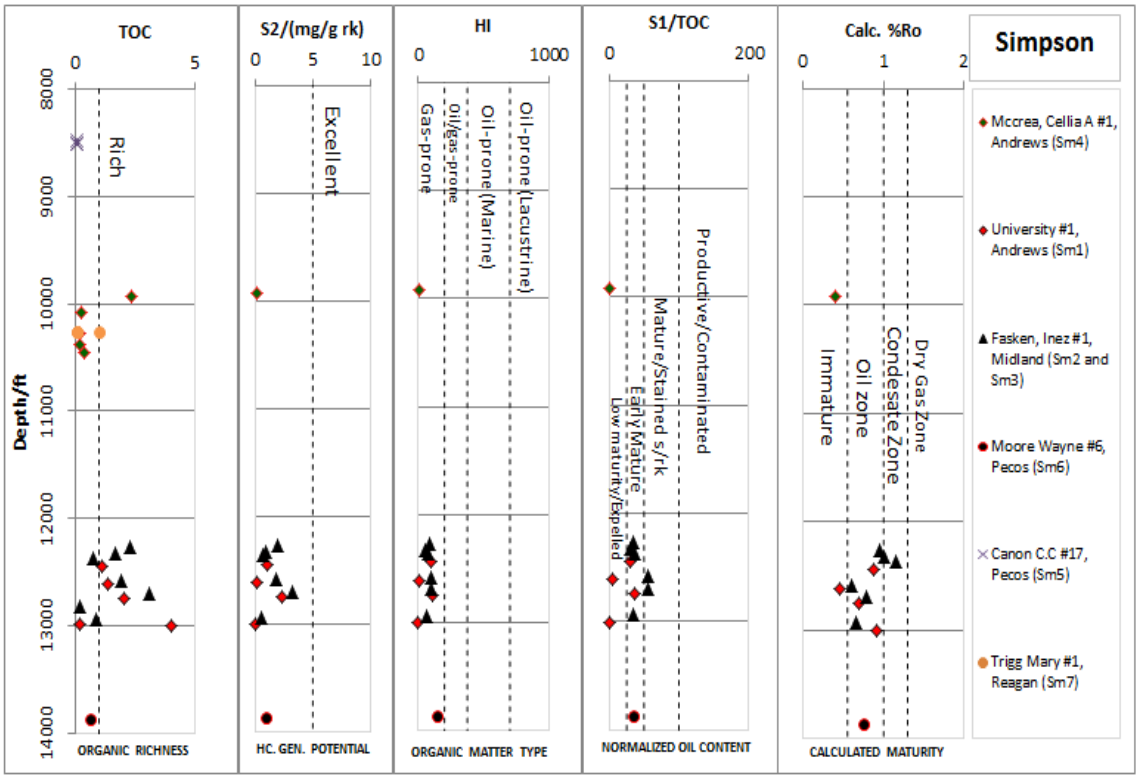
TOC
0
5
Rich
ORGANIC RICHNESS
S2/(mg/g rk)
0
5
10
Excellent
HC. GEN. POTENTIAL
HI
0
1000
Gas-prone
Oil/gas-prone
Oil-prone(Marine)
Oil-prone(Lacustrine)
ORGANIC MATTER TYPE
S1/TOC
0
200
Productive/Contaminated
Mature/Stained s/rk
Early Mature
Low maturity/Expelled
NORMALIZED OIL CONTENT
Calc. %Ro
0
1
2
Immature
Oil zone
Condesate Zone
Dry Gas Zone
CALCULATED MATURITY
Depth/ft
8000
9000
10000
11000
12000
13000
14000
Simpson
Mccrea, Cellia A #1, Andrews (Sm4)
University #1, Andrews (Sm1)
Fasken, Inez #1, Midland (Sm2 and Sm3)
Moore Wayne #6, Pecos (Sm6)
Canon C.C #17, Pecos (Sm5)
Trigg Mary #1, Reagan (Sm7)

Appendix 6: Detailed listing of parameters used in modeling (DLW-1; MLD-2, MLD-3 and CBP-1)

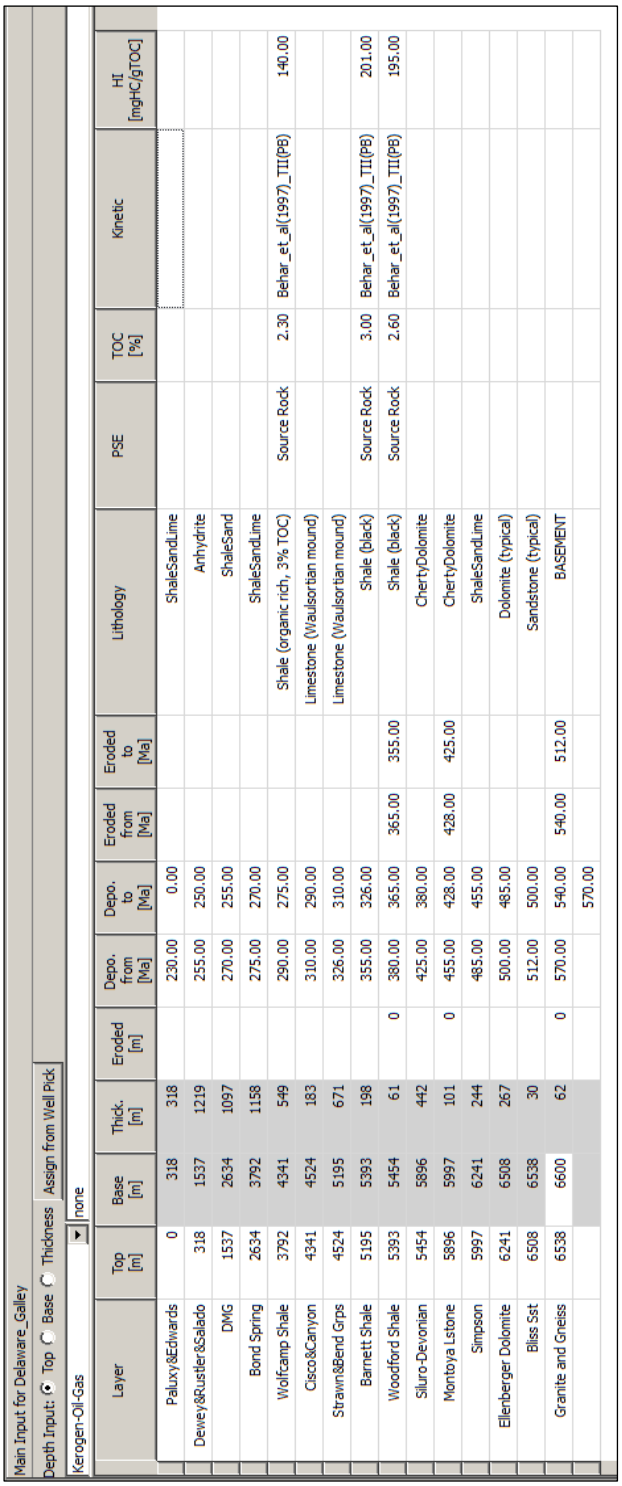

Main Input for Delaware_Galley

Depth Input: Top Base Thickness | Assign from Well Pick

Kerogen-Oil-Gas | none

Layer	Top [m]	Base [m]	Thick. [m]	Eroded [m]	Depo. from [Ma]	Depo. to [Ma]	Eroded from [Ma]	Eroded to [Ma]	Lithology	PSE	TOC [%]	Kinetic	HI [mgHC/gTOC]
Paluxy&Edwards	0	318	318		230.00	0.00			ShaleSandLime				
Dewey&Rustler&Salado	318	1537	1219		255.00	250.00			Anhydrite				
DMG	1537	2634	1097		270.00	255.00			ShaleSand				
Bond Spring	2634	3792	1158		275.00	270.00			ShaleSandLime				
Wolfcamp Shale	3792	4341	549		290.00	275.00			Shale (organic rich, 3% TOC)	Source Rock	2.30	Behar_et_al(1997)_TII(PB)	140.00
Cisco&Canyon	4341	4524	183		310.00	290.00			Limestone (Waulsortian mound)				
Strawn&Bend Grps	4524	5195	671		326.00	310.00			Limestone (Waulsortian mound)				
Barnett Shale	5195	5393	198		355.00	326.00			Shale (black)	Source Rock	3.00	Behar_et_al(1997)_TII(PB)	201.00
Woodford Shale	5393	5454	61	0	380.00	365.00	365.00	355.00	Shale (black)	Source Rock	2.60	Behar_et_al(1997)_TII(PB)	195.00
Siluro-Devonian	5454	5896	442		425.00	380.00			Cherty Dolomite				
Montoya Lstone	5896	5997	101	0	455.00	428.00	428.00	425.00	Cherty Dolomite				
Simpson	5997	6241	244		485.00	455.00			ShaleSandLime				
Ellenberger Dolomite	6241	6508	267		500.00	485.00			Dolomite (typical)				
Bliss Sst	6508	6538	30		512.00	500.00			Sandstone (typical)				
Granite and Gneiss	6538	6600	62	0	570.00	540.00	540.00	512.00	BASEMENT				
						570.00							

Input Parameters for Model DLW-1 (Delaware Basin)

Main Input for CBP_1

Depth Input: Top Base Thickness | Assign from Well Pick

Kerogen-Oil-Gas | none

Layer	Top [m]	Base [m]	Thick. [m]	Eroded [m]	Depo. from [Ma]	Depo. to [Ma]	Eroded from [Ma]	Eroded to [Ma]	Lithology	PSE	TOC [%]	Kinetic	HI [mgHC/gTOC]
Judkins/Monahans sands	0	35	35		1.00	0.00			Sandstone (typical)	Overburden Rock			
Ogalla Grp	35	65	30		5.30	2.80			Conglomerate (typical)	Overburden Rock			
Edwards	65	70	5		105.00	101.00			Limestone (micrite)	Overburden Rock			
Paluxy	70	80	10		109.00	105.00			Sandstone (typical)	Overburden Rock			
Dockum	80	460	380		235.00	220.00			ShaleSand	Overburden Rock			
Dewey Lake Fm	460	490	30		251.00	250.00			Sandstone (typical)	Overburden Rock			
Rustler Fm	490	590	100		252.00	251.00			Anhydrite	Overburden Rock			
Salado Fm	590	840	250		254.00	252.00			Anhydrite	Overburden Rock			
Artesia	840	1480	640	0	262.50	255.00	255.00	254.00	Sandstone (typical)	Overburden Rock			
San Andres	1480	1930	450	0	269.00	263.00	263.00	262.50	Dolomite (typical)	Overburden Rock			
Glorieta	1930	1940	10		270.00	269.00			Sandstone (typical)	Overburden Rock			
Clear Fork Grp	1940	2240	300		275.00	270.00			Dolomite (organic lean, sandy)	Overburden Rock			
Wolfcamp	2240	2490	250		290.00	275.00			ShaleSandLime	Overburden Rock			
Cisco	2490	2500	10		300.00	290.00			Limestone (Waulsortian mound)	Overburden Rock			
Canyon	2500	2520	20		310.00	300.00			Limestone (Waulsortian mound)	Overburden Rock			
Strawn	2520	2580	60		312.00	310.00			Shalecarbonate	Overburden Rock			
Mississippian	2580	2702	122	100	361.00	340.00	340.00	312.00	Limestone (micrite)	Overburden Rock			
Woodford	2702	2782	80	100	380.00	365.00	365.00	361.00	Shale (black)	Overburden Rock	2.60	Behar_et_al(1997)_TII(PB)	195.00
Thirtyone Fm	2782	3082	300	0	405.00	385.00	385.00	380.00	Dolomite (typical)	Overburden Rock			
Wristen Fm	3082	3142	60		422.00	405.00			Dolomite (typical)	Overburden Rock			
Fussellman	3142	3212	70		425.00	422.00			Dolomite (typical)	Overburden Rock			
Montoya	3212	3282	70	50	443.00	435.00	435.00	425.00	Dolomite (typical)	Overburden Rock			
Bromide	3282	3432	150		456.00	455.00			Limestone (shaly)	Seal Rock			
Tulip Creek Fm	3432	3532	100		458.00	456.00			ShaleSandLime	Reservoir Rock			
McLish Fm	3532	3632	100		460.00	458.00			ShaleSandLime	Source Rock	1.73	Behar_et_al(1997)_TII(PB)	110.00
Oil Creek Fm	3632	3682	50		475.00	460.00			ShaleSandLime	Source Rock	1.73	Behar_et_al(1997)_TII(PB)	110.00
Joins Fm	3682	3697	15		485.00	475.00			Limestone (shaly)	Underburden Rock			
Ellenberger	3697	4097	400		507.00	485.00			Dolomite (typical)	Reservoir Rock			
Granite/Aren. schists	4097	4200	103		542.00	507.00			BASEMENT	Underburden Rock			
						542.00							

Input Parameters for Model CBP-1 (Central Basin Platform)

Main Input for Midland_Galley_South

Depth Input: (•) Top ( ) Base ( ) Thickness [Assign from Well Pick]

Kerogen-Oil-Gas | none

Layer	Top [m]	Base [m]	Thick. [m]	Eroded [m]	Depo. from [Ma]	Depo. to [Ma]	Eroded from [Ma]	Eroded to [Ma]	Lithology	PSE	TOC [%]	Kinetic	HI [mgHC/gTOC]
Paluxy&Edwards	0	151	151		235.00	0.00			ShaleSandLime				
Dewey&Rustler&Salado	151	395	244		255.00	250.00			Anhydrite				
Artesia Grp	395	852	457		264.00	257.00			SandDolomiteAnhydrite				
San Andres	852	1157	305		270.00	264.00			Sand&Carbonate				
Dean&Spraberry&Clear Fork	1157	1767	610		275.00	270.00			ShaleSandLime	Source Rock			
Wolfcamp Shale	1767	2377	610		290.00	275.00			Shalecarbonate	Source Rock	2.30	Behar_et_al(1997)_TII(PB)	140.00
Cisco&Canyon	2377	2682	305	100	310.00	300.00	300.00	290.00	Limestone (Waulsortian mound)				
Strawn&Bend Grps	2682	2834	152	100	315.00	312.00	312.00	310.00	Limestone (Waulsortian mound)				
Barnett Shale	2834	2924	90	0	357.00	330.00	330.00	315.00	Shalecarbonate	Source Rock	3.00	Behar_et_al(1997)_TII(PB)	201.00
Woodford Shale	2924	2946	22	0	380.00	363.00	363.00	357.00	Shale (black)	Source Rock	2.60	Behar_et_al(1997)_TII(PB)	195.00
Siluro-Devonian	2946	3113	167	0	428.00	400.00	400.00	380.00	ChertyDolomite				
Ellenberger Dolomite	3113	3593	480	0	507.00	485.00	485.00	428.00	Dolomite (typical)				
Granite and Gneiss	3593	3653	60		540.00	507.00			BASEMENT				
						540.00							

Input Parameters for Model MLD-2 (Midland Basin)

Main Input for Midland_3

Depth Input: Top Base Thickness | Assign from Well Pick

Kerogen-Oil-Gas | none

Layer	Top [m]	Base [m]	Thick. [m]	Eroded [m]	Depo. from [Ma]	Depo. to [Ma]	Eroded from [Ma]	Eroded to [Ma]	Lithology	PSE	TOC [%]	Kinetic	HI [mgHC/gTOC]
Dewey Lake Fm	665	738	73		252.00	250.00			Sandstone (typical)	Overburden Rock			
Rustler	738	768	30		254.00	252.00			Anhydrite	Seal Rock			
Salado	768	983	215		255.00	254.00			Anhydrite	Seal Rock			
Artesia Grp	983	1467	484	0	264.00	257.00	257.00	255.00	SandDolomiteAnhydrite	Overburden Rock			
San Andres	1467	1787	320		270.00	264.00			SandDolomiteAnhydrite	Overburden Rock			
Clear Fork Grp	1787	2047	260		272.00	270.00			Sand&Carbonate	Overburden Rock			
Dean and Spraberry	2047	2351	304		275.00	272.00			ShaleSand	Overburden Rock			
Wolfcamp Shale	2351	2909	558	0	290.00	280.00	280.00	275.00	Shale (typical)	Source Rock	2.30	Behar_et_al(1997)_TII(PB)	140.00
Penn. shales & Carbonates	2909	3814	905	3000	315.00	300.00	300.00	290.00	Shalecarbonate	Reservoir Rock			
Barnett	3814	3964	150	0	339.00	330.00	330.00	315.00	BanettMix	Source Rock	3.00	Behar_et_al(1997)_TII(PB)	201.00
Mississippian Lstone	3964	3994	30		355.00	339.00			Limestone (micrite)	Seal Rock			
Kinderhook	3994	4009	15	0	360.00	356.00	356.00	355.00	Dolomite (typical)	none			
Woodford	4009	4039	30	0	380.00	365.00	365.00	360.00	Shale (black)	Source Rock	2.60	Behar_et_al(1997)_TII(PB)	195.00
Thirtyone Fm	4039	4161	122	0	405.00	400.00	400.00	380.00	ChertyDolomite	Reservoir Rock			
Wristen Fm	4161	4221	60		415.00	405.00			ChertyDolomite	Reservoir Rock			
Fussellman	4221	4266	45	0	425.00	422.00	422.00	415.00	ChertyDolomite	Reservoir Rock			
Sylvan	4266	4281	15		428.00	425.00			Shale (typical)	Underburden Rock			
Montoya	4281	4327	46	0	443.00	436.00	436.00	428.00	ChertyDolomite	Underburden Rock			
Bromide	4327	4342	15	0	456.00	455.00	455.00	443.00	ChertyDolomite	Underburden Rock			
Tulip Creek Fm	4342	4367	25		458.00	456.00			Limestone (shaly)	Underburden Rock			
McLish Fm	4367	4417	50		460.00	458.00			Limestone (shaly)	Underburden Rock			
Oil Creek Fm	4417	4447	30		475.00	460.00			Limestone (shaly)	Underburden Rock			
Joins Fm	4447	4462	15		480.00	475.00			Limestone (micrite)	Underburden Rock			
Ellenberger	4462	4712	250	200	507.00	485.00	485.00	480.00	Dolomite (typical)	Reservoir Rock			
Granite and Gneiss	4712	4762	50		542.00	507.00			BASEMENT	Underburden Rock			
						542.00							

Input Parameters for Model MLD-3 (Midland Basin)

Boundary Conditions used in all the models as illustrated by MLD-2

Boundary Conditions for Midland_Galley_South

Sort Tables | Auto SWIT | McKenzie HF ... | PWD

290.00

Age [Ma]	PWD [m]
0.00	0
235.00	0
255.00	0
264.00	40
270.00	50
275.00	60
290.00	50
310.00	50
315.00	0
357.00	100
380.00	160
428.00	120
507.00	60

Age [Ma]	SWIT [°C]
0.00	20.00
235.00	30.00
255.00	25.84
264.00	23.83
270.00	22.05
275.00	21.54
290.00	21.61
310.00	23.00
315.00	25.00
357.00	22.00
380.00	22.00
428.00	22.00
507.00	23.00

275.00

Age [Ma]	HF [mW/m^2]
0.00	46.00
235.00	46.00
255.00	46.00
264.00	46.00
270.00	46.00
275.00	46.00
290.00	46.00
310.00	46.00
315.00	46.00
357.00	46.00
380.00	46.00
428.00	46.00
507.00	46.00